University of Nevada, Reno

Advanced Signal Control Strategies and Analysis Methodologies for Diverging Diamond Interchanges

A dissertation submitted in partial fulfillment of the
requirements for the degree of Doctor of Philosophy in
Civil Engineering

by

Peifeng Hu

Dr. Zong Tian/Dissertation Advisor

May, 2013

University of Nevada, Reno
Statewide · Worldwide

THE GRADUATE SCHOOL

We recommend that the dissertation
prepared under our supervision by

PEIFENG HU

entitled

Advanced Signal Control Strategies And Analysis Methodologies For Diverging Diamond Interchanges

be accepted in partial fulfillment of the
requirements for the degree of

DOCTOR OF PHILOSOPHY

Zong Z. Tian, Advisor

Adrain R. Gibby, Committee Member

Gokhan Pekcan, Committee Member

Yantao Shen, Committee Member

Shunfeng Song, Graduate School Representative

Marsha H. Read, Ph. D., Dean, Graduate School

May, 2013

ABSTRACT

This dissertation introduces three new methodologies to improve traffic signal operations of Diverging Diamond Interchanges (DDIs). Methodology one applies to a DDI without signals for left-turns from the freeway off-ramp. This methodology combines Webster's method and the specific characteristics of a DDI to determine traffic signal operation parameters such as cycle length, phasing splits, and phasing sequence. Comparing to methodology one, methodology two can handle more general and complex cases. Both methodologies can be implemented at a DDI by one traffic controller and operate successfully for a variety of controller types including pre-timed, fully actuated, and coordinated actuated control. Methodology three, also called proposed operation 3, combines Genetic Algorithm and a professional simulation tool such as VISSIM to search for the optimal operations for DDIs based on the phasing scheme of methodology 1 or 2.

As a case study, methodology two is comprehensively studied based on a proposed DDI located at Moana Lane and U.S. 395, in Reno, Nevada. Through testing in a hardware-in-the-loop platform, this methodology can operate successfully for pre-timed, fully actuated, and coordinated actuated traffic signal controls.

Microscopic simulation models were developed to evaluate the traffic signal operation of each scenario. The simulation results revealed that proposed methodology 2 reduces average delay by 17% in the morning (AM) peak hour and 28% in the afternoon (PM) peak hour at the Moana DDI, when compared to the methodology presented by staff from

the City of Reno, NV. The average total delays of different cycle lengths show that the optimal cycle length changes with the variation of saturation flow ratios at this DDI. The simulations illustrated that the performances of the same traffic signal operation varied when it was applied to a variety of traffic volume distributions among routes. Therefore, developing a traffic signal operation for a DDI based on its traffic volume distributions on routes, instead of turning movement volumes, is necessary. The results also indicate that the range of signal operation performance on a variety of traffic volume distributions on routes reduces when the space between the two crossovers intersections of a DDI increases.

ACKNOWLEDGMENTS

I would like to express my sincere gratitude to my advisor, Dr. Zong Z. Tian. Dr. Tian provided me such a valuable opportunity to study at the University of Nevada, Reno and guided me on traffic engineering research. Dr. Tian taught me methods and strictly disciplinary attitudes to be engaged in traffic research and cared for me like my parents. Without Dr. Tian's guidance and tremendous support, the completion of this dissertation research would have been extremely difficult. I really appreciate Dr. Tian's wife and his two daughters as they accepted me as a member of their family during the past five years.

I also appreciate my other advisory committee members: Dr. Adrain Reed Gibby, Dr. Gokhan Pekcan, Dr. Shunfeng Song, and Dr. Yantao Shen. All of them gave me helpful suggestions and comments on my dissertation research.

My colleagues, the transportation research group members, and all friends helped me so much in these years, either in my studies or in life. They have all been so important in making my life impressive and meaningful. I will not forget these enjoyable moments with them and sincerely thank them for all the support.

Finally, all my appreciation goes to my family. My parents and my younger brother always gave me their love and steady support no matter what difficulties happened with me.

TABLE OF CONTENTS

LIST OF FIGURES

LIST OF TABLES

CHAPTER 1. INTRODUCTION

1.1 BACKGROUND

A diverging diamond interchange (DDI), also called a double crossover diamond interchange (DCD), is a new type of diamond interchange. This interchange guides the two directions of traffic on the arterial to drive on the opposite side of the roadway. After passing over or under the freeway, traffic on the arterial can either make a free left turn to the freeway on-ramp or switch back to the normal side of the road at the second crossover and continue on the arterial.

Prior to 2009, the communities of Versailles, Le Perreux-sur-Marne, and Seclin in France had the only known DDIs in existence. The DDI concept was introduced to the United States in 2003 by Gilbert Chlewicki, in a paper submitted to the 2nd Urban Street Symposium held in Anaheim, California; however, it was 2009 before the first U.S. DDI was constructed in Springfield, Missouri. Several field and simulation studies have shown that DDI has many advantages compared to conventional diamond interchanges (CDIs). As a result, six states (Missouri, Utah, Georgia, Kentucky, Maryland, and New York) have constructed DDIs with demonstrated operational improvements. More than 18 states, including Nevada, are constructing DDIs.

1.2 PROBLEM STATEMENT

Most current studies on DDIs can be categorized into two groups: one group primarily involves signal control strategies with field implementation and evaluation, and the other

group involves comparison with CDIs, Single-point urban interchanges (SPUIs), or other interchange types through microscopic simulation.

As the DDI concept is relatively new in the U.S., research on its modeling, analysis, and signal control strategies is still in preliminary stages. All the existing studies applied pre-timed traffic signal operations to control DDIs as their methodologies did not research other control types such as fully actuated control, and coordinated actuated control. In addition, most studies found in the literature only provided some basic phasing schemes which are not the most efficient. An example is the lack of using overlaps as in the case of conventional diamond interchanges.

Up to now, a commonly accepted analysis methodology is not yet available. For example, the Highway Capacity Manual 2010 (HCM 2010) does not have any materials related to DDI. Currently, professionals are relying on empirical based methods to analyze DDI operations and to generate signal timing plans for operating DDIs. The lack of a well-established methodology does not guarantee the optimal operational solution.

Moreover, most studies neither included traffic volume distributions (also called route distributions) nor researched the performance differences under a variety of distributions when comparing with other interchange types.

Therefore, research on this subject has drawn a significant interest from researchers around the nation. The success of this research will enhance the knowledge of analyzing and operating DDIs, thus it is of significance to both academic scholars and practical engineers.

1.3 RESEARCH GOALS AND OBJECTIVES

The main goal of this study is to develop efficient signal operation and analysis methodologies for DDIs. While a few studies have been conducted mostly through evaluation of field observations, no commonly acceptable methodologies exist for analyzing and operating DDIs. The following objectives are identified in order to accomplish the above stated research goal:

- Develop optimization methodologies for signal control and signal timing parameters pertinent to innovative phasing schemes;
- Develop control and operational strategies for achieving the best performance of DDIs;
- Test/evaluate the methodologies and strategies using real-world cases and advanced simulation techniques; and
- Develop practical guidelines for implementing and operating DDIs.

1.4 ORGANIZATION OF THE DISSERTATION

This dissertation consists of seven chapters. Chapter 1 provides an overview of this study as presented above. Chapter 2 provides a comprehensive literature review pertinent to DDIs. The basic parameters and concepts related to traffic signal control are explained in Chapter 3. This chapter also provides a review on research in related subjects such as methodologies and tools for conventional diamond interchanges. Chapter 4 introduces the mathematical models for solving traffic signal operation problems. Chapter 5 compares the available traffic signal operations and presents new operational methodologies on

DDIs. The application of one recommended methodology using an actual DDI case is presented in Chapter 6. This chapter also comprehensively tests three control types such as pre-timed control, fully actuated control, and coordinated actuated control at the DDI. In addition, this chapter studies the relationship between cycle length and saturation flow ratios of the DDI. Furthermore, chapter 5 researches the performance differences under a variety of traffic volume distributions. The last chapter provides a summary and offers conclusions based on this research.

CHAPTER 2. PREVIOUS STUDIES ON DIVERGING DIAMOND INTERCHANGES

2.1 INTRODUCTION

This chapter reviews existing design guidelines and operational analysis studies of Diverging Diamond Interchanges (DDIs). This chapter also summarizes the advantages and disadvantages of DDIs according to the previous studies. The limited available literature indicates that a comprehensive study on DDIs is necessary.

2.2 EXISTING DESIGN GUIDELINES

Currently, DDIs have been considered as an alternative interchange design to improve intersection capacity, minimize congestion, and promote intersection safety. However, no design standards currently exist for DDIs. The Missouri Department of Transportation (MoDOT) is the only state that has released a document providing both an overview as well as guidance on some aspects based on designs already completed or under construction within the state of Missouri *(1)*. MoDOT stated that closely spaced right-in/right-out or left-in driveway accesses do not bring about a greater operational challenge for DDIs compared to other interchange types. MoDOT also recommended that the desirable speed for regular passenger vehicles to proceed through a DDI is at 20-30 mph; but turning movements to and from all ramps should be made at 15 mph. The recommended minimum crossing angle of each crossover intersection should be 40 degrees. In addition, MoDOT presented their suggestions on horizontal crossover

geometrics, lane width, shoulders, sign distance, acceleration and deceleration lanes, clear zones, pedestrians, and bicycle accommodations, etc. The report also noted that MoDOT's Engineering Policy Guide had been updated to include detailed information on Diverging Diamond Interchanges in the light of their knowledge gained and experiences with deployment of DDIs. The Federal Highway Administration (FHWA) preferred to use turning radii at the crossover junction in the 150 to 300 feet range according to its experience at the same DDI located in Springfield, MO *(2)*. In a drivers' evaluation, Bared et al. also found out that the mean speed at the DDI's crossovers was about 23.2 mph (37.3 km/h) which is less than the 34.4 mph (55.4 km/h) mean speed found at a conventional diverging diamond (CDI) *(3)*.

The Utah Department of Transportation (UDOT) completed construction of three DDIs by October of 2011. UDOT preferred to separate the crossover intersections by 800 to 1000 feet, as this space was a good rule of thumb for providing sufficient room for queue storage and ability to move traffic through system. UDOT also recommended the approach angle for the crossover intersections of a DDI should be 30 degrees or greater *(4)*. Other states, including Tennessee, Rhode Island, New York, Maryland, Kentucky, and Georgia, completed their DDIs between 2010 and 2012, but without having developed new design recommendations.

2.3 OPERATIONAL ANALYSIS STUDIES

2.3.1 Comparing DDIs to Other Interchange Designs

A few published studies compared the operation of DDIs to other interchanges like CDIs and single point urban interchanges (SPUIs). In these studies, researchers needed to develop signal timing plans to evaluate a DDI's effectiveness. Most studies sought signal timing plans manually, or used Synchro traffic optimization software to generate an optimum timing plan for each traffic scenario. Since Synchro does not have a specific function for finding optimal timing solutions for DDIs, these studies interpreted the two crossover intersections of DDIs as two separate intersections operated by two controllers. These operations were evaluated through several runs in VISSIM, a microscopic simulation software.

Several professionals had concluded that their DDI outperforms the other interchange designs either in terms of delay, number of stops, queue length, or capacity. Chlewicki concluded that the total delay, stop delay, and total stops for the whole road network are about 2.9 times, 4.2 times, and 2.0 times worse, respectively, for the CDI when comparing to the DDI *(5)*. The results of the FHWA's research also showed 15%-60% reduction of intersection delay for the DDI in comparison to the conventional interchange under different traffic volume scenarios. Based on the FHWA's simulation results, a DDI processed approximately 6,000 veh/h with a six-lane bridge, while a CDI needed an eight-lane bridge; similarly, a DDI processed approximately 3,700 veh/h with a four-lane bridge, while a CDI needed a six-lane bridge *(6)*. The capacity of each turning movement was higher with a DDI than the CDI; in particular, the capacity of left-turn movements was nearly twice that of the corresponding CDI left-turn capacity *(7)*. Sharma et al. indicated that the performance of DDI was better than CDI with lower delays of critical

movements, lower travel time, and lower maximum queues in each traffic scenario. The DDI increased capacity of the critical movements, particularly the left-turns, compared to the CDI for most scenarios *(8)*.

In addition to CDIs, some professionals also compared the operation of DDIs to SPUIs. Siromaskul and Speth concluded that with running protected only phasing; the DDI outperformed the CDI under all of the scenarios, and the SPUI while with protected-permitted phasing in volume scenarios 3 to 5. The SPUI operated slightly better than the DDI under scenarios 1 and 2. The cycle length for DDI in this study was also selected manually and they were running only two phases for the DDI without exclusively using overlapping phases *(9)*. Siromaskul found that the DDI greatly outperformed SPUI in three trials with four total traffic volume scenarios. The DDI received only 50% of average delays experienced by the SPUI *(10)*.

2.3.2 Considering a DDI as an Alternative Design for Existing CDIs

DDIs usually offer substantial improvements in operation over other interchange types. But it may not be most efficient under all traffic conditions. A DDI does not perform well when ramp traffic is low and through volumes are high. Siromaskul and Speth concluded that the least beneficial condition of a DDI is when the arterial volumes are heavy and ramp traffic is low *(9)*. Chlewicki also knew that the DDI cannot coordinate all traffic movements effectively if they are all equally heavy. The design would perform efficiently when left-turn movements are the heaviest *(5)*. Similarly, a report prepared for I-15 Utah County Corridor (CORE) expressed that the DDI design would typically be well suited for locations with high demands from the freeway or high demand across the

freeway with low left-turn existing volume from the freeway *(4)*. Sharma and Chatterjee came to the conclusion that the DDI would be efficient when the heavier left-turn traffic are opposed by the heavier through movements *(8)*. As Chilukuri et al. indicated, the DDI is suitable for heavier traffic demands but underperforms the CDI when traffic demand is low *(11)*. However, these studies did not provide quantitative guidelines for decision makers to select the best alternative according to the traffic demand and geometric configurations. Most of them generally suggested applying a DDI as an alternative interchange design when on-ramp left-turns are heavy, through volumes on bridge approaches are moderate or unbalanced, or off-ramp left-turn traffic is moderate to heavy.

2.4 ADVANTAGES AND DISADVANTEGES

While DDIs have several advantages that make it an attractive design alternative under a variety of traffic conditions compared to CDIs, their disadvantages cannot be neglected. A number of published studies discussed above assessed the operational efficiency of DDIs as well as safety benefits and drawbacks. The generally discussed advantages and disadvantages of the DDI in these studies are summarized below:

Advantages of DDIs

- Allow two-phase signals with short cycle lengths that can significantly reduce delay;
- Increases the capacity of turning movements to and from the ramps, and thereby the capacity of the entire interchange;

- May potentially reduce the number of lanes on the crossroad and minimize right of way requirements;
- Substantially reduces the number of conflict points, thus theoretically improving safety as shown in Figure 2-1, Figure 2-2, and Table 2-1; and
- Improves pedestrian safety, theoretically.

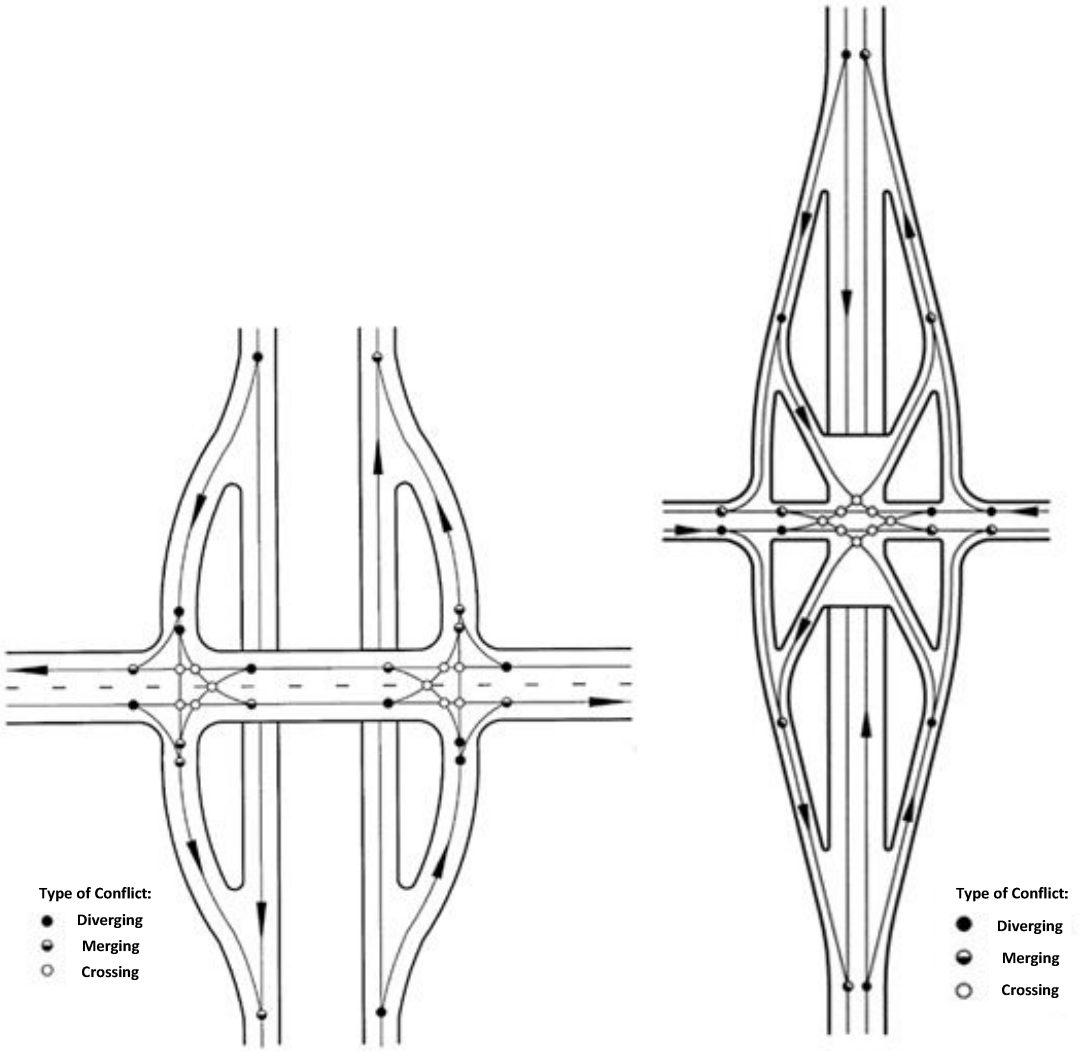

Figure 2-1 Points of Conflict on Traditional Interchanges: CDI (left) and SPUI (right) *(1)*

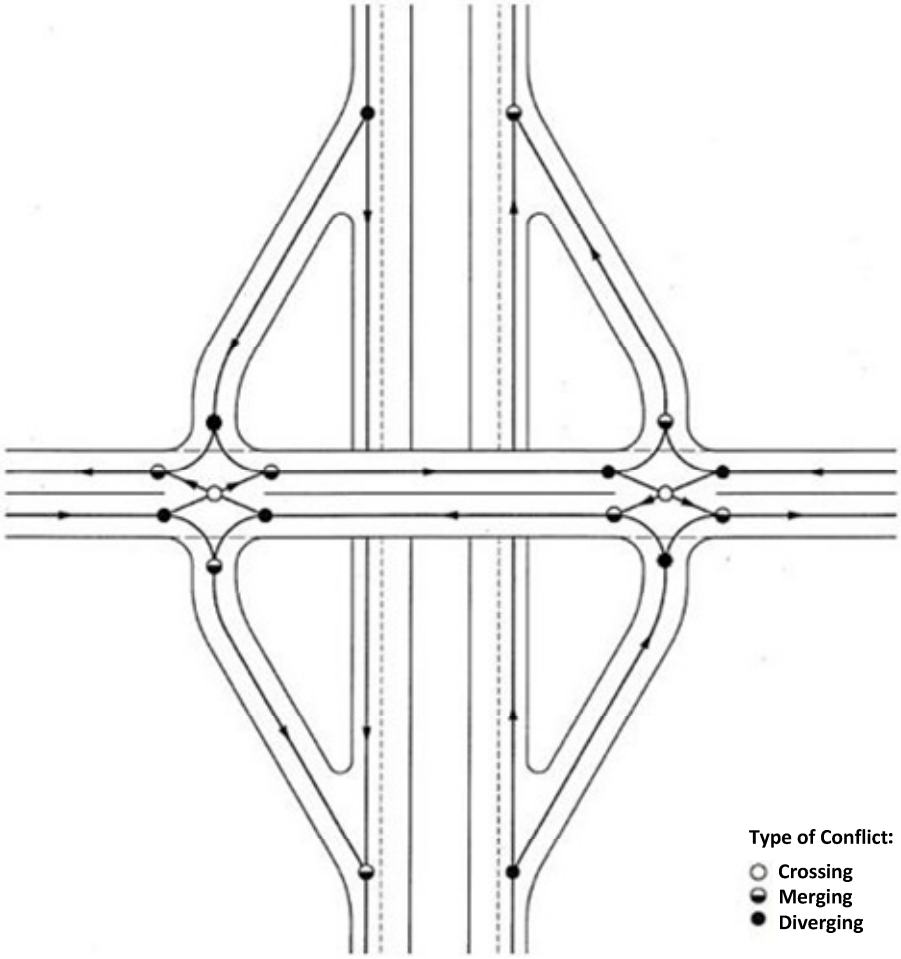

Figure 2-2 Conflict Diagram for a DDI *(1)*

Table 2-1 Conflict Points *(1)*

Type	Diamond	SPUI	DDI
Diverging	10	8	8
Merging	10	8	8
Crossing	10	8	2
Total	30	24	18

Disadvantages of DDIs

- The interchange may initially be confusing to most drivers who merge along the left side of the roadway or the reversed flow of traffic;
- Free-flowing traffic for through movements in both directions is impossible, as the signals cannot guarantee that both directions' traffic pass through the two crossover intersections simultaneously;
- Exiting traffic cannot reenter the freeway in the same direction without leaving the interchange;
- Pedestrians would be required to cross free-flowing traffic on freeway ramps. This could be mitigated by signalizing all movements without impacting the two-phase nature of the interchange signals.

2.5 SUMMARY

This chapter reviews the previous studies and practical experiences of DDIs. Based on these studies, DDIs have outstanding advantages over CDIs in most conditions, especially when left-turn traffic is heavy. All of them are only suitable for pre-timed traffic signal operations. In fact, most of these studies could further improve their traffic signal operation efficiency by thoroughly applying overlapping phases and other traffic signal controller types such as fully actuated control and coordinated actuated control. In addition, no quantitative guidelines can be used for traffic engineers to select DDIs or CDIs according to the results of these studies.

CHAPTER 3. TRAFFIC SIGNAL CONTROL ELEMENTS AND METHODS

3.1 INTRODUCTION

Traffic signal control is one of the most popular ways to ensure that traffic moves as smoothly and safely as possible. In 1868, the first recorded illuminated traffic signal with green and yellow colors was installed in London near the Houses of Parliament *(12, 13)*. In 1909, the U.S. patents for traffic control devices were acquired including semaphores, arrows to direct traffic, illumination sources, and lens systems. Now, a variety of traffic control devices, methods, and systems have been implemented around the world, ranging from actuated, coordinated, to sophisticated adaptive control systems *(14)*.

This chapter introduces the major elements of traffic control systems and reviews the related studies and strategies. The contents of the chapter include: traffic signal control elements, traffic signal control performance indices, traffic signal control methods, existing optimization methods, micro simulation tools, and summary.

3.2 TRAFFIC SIGNAL CONTROL ELEMENTS

3.2.1 Cycle length

A cycle length is the total time for a signal to complete one cycle, as shown in Figure 3-1. A cycle length is the sum of green interval, yellow interval, and red interval. In 1958, Webster introduced an equation for calculating the optimal cycle length that seeks to minimize the average delay at an intersection. This optimal cycle length is calculated by

Equation (3-1) *(15)*. The Highway Capacity Manual 2010 (HCM 2010) modified Webster's equation and proposed a similar formula to calculate optimal cycle length on the basis of intersection geometry features, traffic volume characteristics, and the intersection's location. The cycle length generated from these equations must be checked to see whether it falls within a reasonable range. The cycle length can not be too low (i.e. less than 60 s) to ensure pedestrians cross intersection safely, but also not too high such that it increases the average delay for vehicles (i.e. greater than 150 s). Studies have found that the average delay of vehicles will decrease first and then increase as cycle length increases. Figure 3-2 shows this relationship between the average delay and cycle length for an intersection *(16, 17)*.

$$C_o = \frac{1.5*L+5}{1.0-\sum_{i=1}^{i=N} Y_i} \quad (3\text{-}1)$$

where

C_o: optimal cycle length for minimizing delay (s);

L: total lost time of a cycle (s);

Y_i: flow ratio of critical lane group i; and

N: number of critical lane groups.

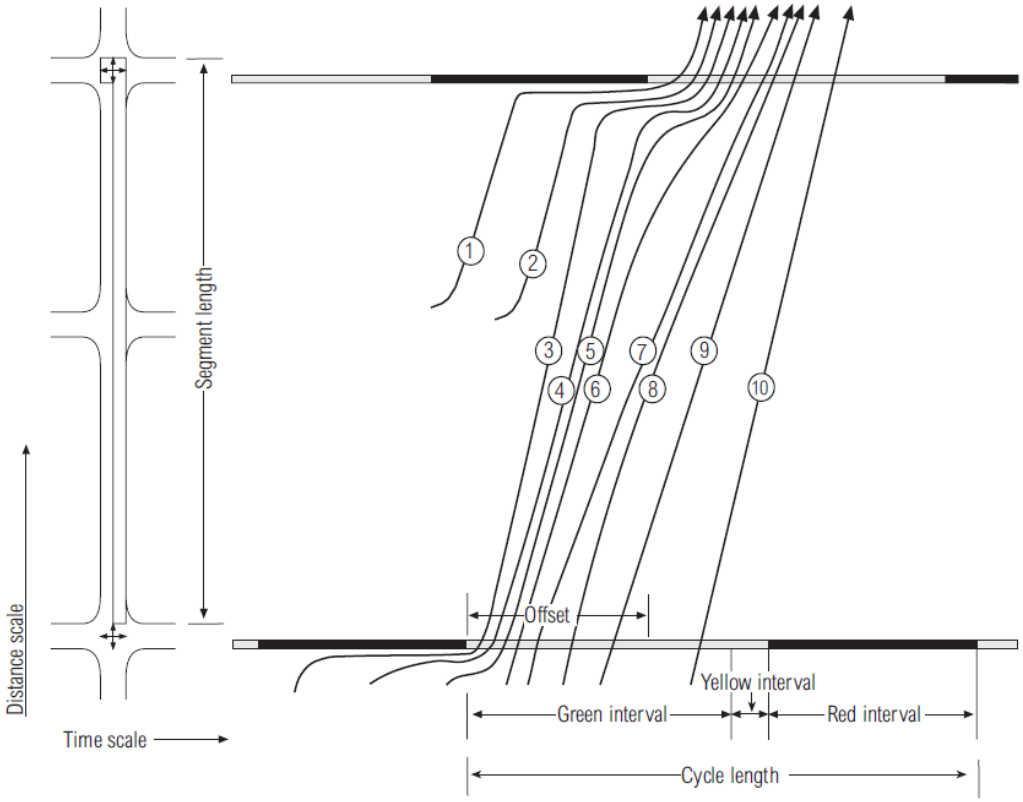

Figure 3-1 Typical Speed Profiles of Vehicles on Urban Streets *(16)*

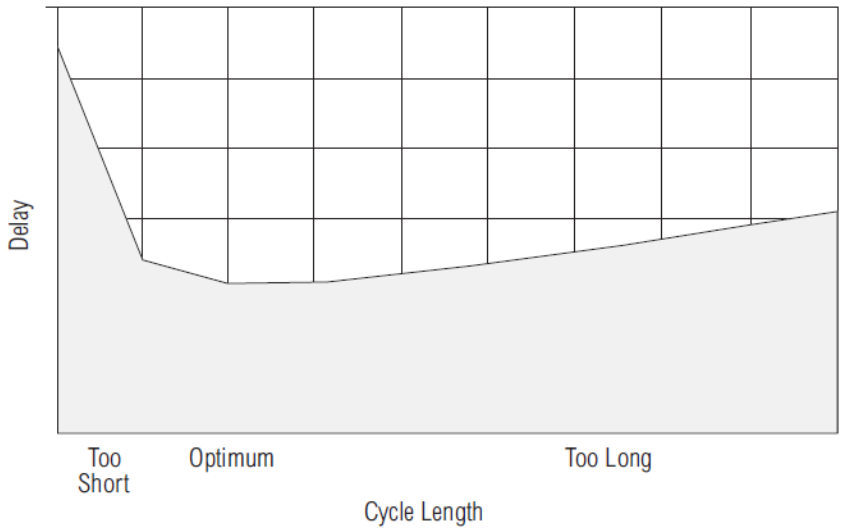

Figure 3-2 The Relationship Between Delay and Cycle Length *(16)*

3.2.2 Traffic Signal Phase

A traffic signal phase is the green, yellow, and red interval in a cycle assigned to a specific traffic movement(s). Traffic signal phase consists of two categories: pedestrian phase and vehicular phase. A pedestrian phase is an interval of time for allowing pedestrians to across an intersection. The interval of a pedestrian phase is determined by the width of an intersection and pedestrians' average walking speed. The definition of vehicular phase has some been met with some confusion in traffic signal timing circles. Some studies have defined a vehicular phase to be the interval of time to allow one or more vehicular traffic movements to pass through an intersection *(17)*. As illustrated in Figure 3-3, the westbound left-turn and through vehicular movements are named as phase 2. The southbound and northbound vehicular movements are defined as phase 3. Alternately, many agencies have defined a traffic vehicular phase as the part of cycle length given to an individual movement or combination of non-conflicting of movements *(18–20)*. Following this definition, the National Electrical Manufacturers Association (NEMA) has developed a standard eight-phase signal scheme at a four-leg intersection, as shown in Figure 3-4. In this figure, a dual ring control is used to avoid operating conflicting movements at the same time and a "barrier" is used to separate the east-west movements from north-south movements. The NEMA definition of vehicular phase is selected for use in this research.

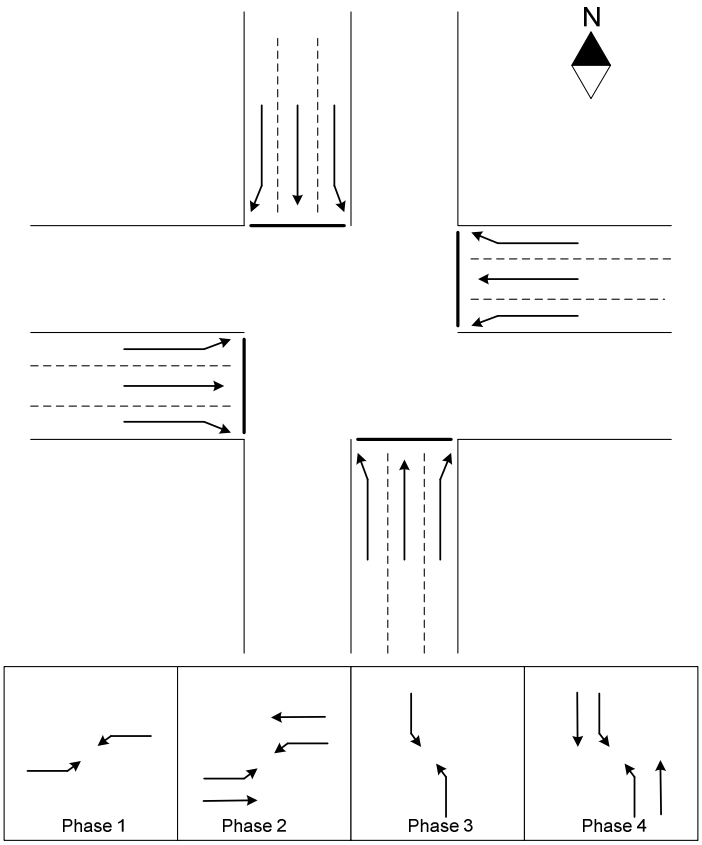

Figure 3-3 An Example of Four-Phase Control

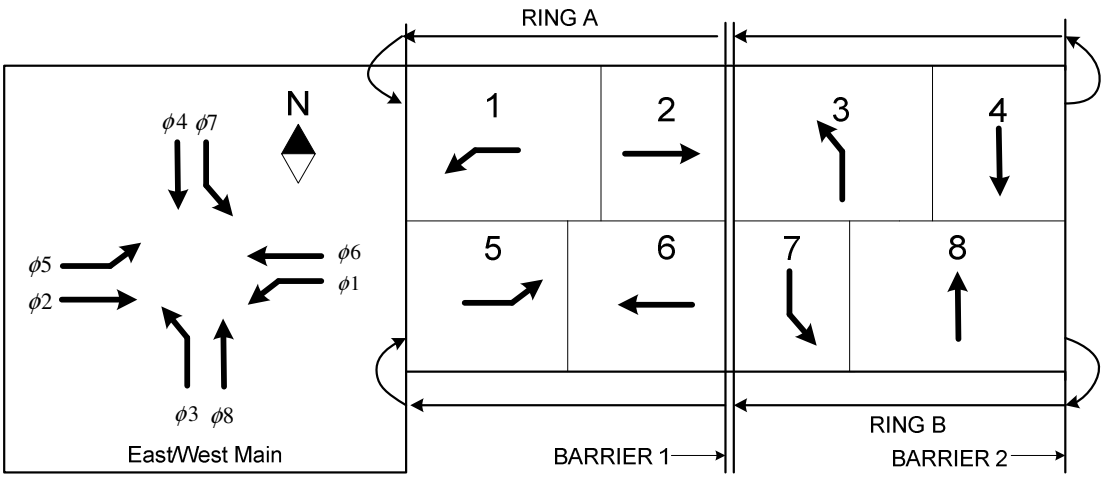

Figure 3-4 Eight Standard NEMA Phases and Dual Ring Concept

3.2.3 Phase Split

A phase split is the interval of green time, yellow time, and red time in a cycle assigned to specified traffic movement(s). A pedestrian phase split can be calculated by Equation (3-2) *(16)*.

$$T_p = T_w + \frac{D_w}{S_w} \tag{3-2}$$

where

T_p: pedestrian phase time (s);

T_w: walk interval (s);

D_w: walking (crossing) distance (ft); and

S_w: average walking speed in ft/s (typically 3.5 to 4 ft/s).

Before allocating green time to each vehicular phase, the total lost time in one cycle must be subtracted first. The remaining time will be allocated appropriately for each phase on the principle of equalizing the degree of saturation for the movement(s). The phase split for vehicles can be computed by Equation (3-3) *(16)*.

$$g_i = (C - L) * \frac{v_i}{V} \tag{3-3}$$

where

g_i: green phase split (s);

C: cycle length (s);

L: total lost time per cycle (s);

v_i: traffic volumes of movement i (veh/h); and

V: total traffic volumes of critical movements (veh/h).

3.2.4 Phasing Sequence

Phasing sequence is the order of phases in each ring. In Figure 3-4, the phasing sequence is 1-2-3-4, and 5-6-7-8. Phasing sequence is an important factor to improve traffic signal coordination. The first two phases within a ring barrier are considered phase partners. Only phase partners can exchange their sequences. For instance, phase 1 can follow phase 2, and phase 8 can start earlier than phase 7. Phases 1, 2, 5, and 6 of the main street in Figure 3-4 can have four phasing sequences shown in Figure 3-5 *(21)*.

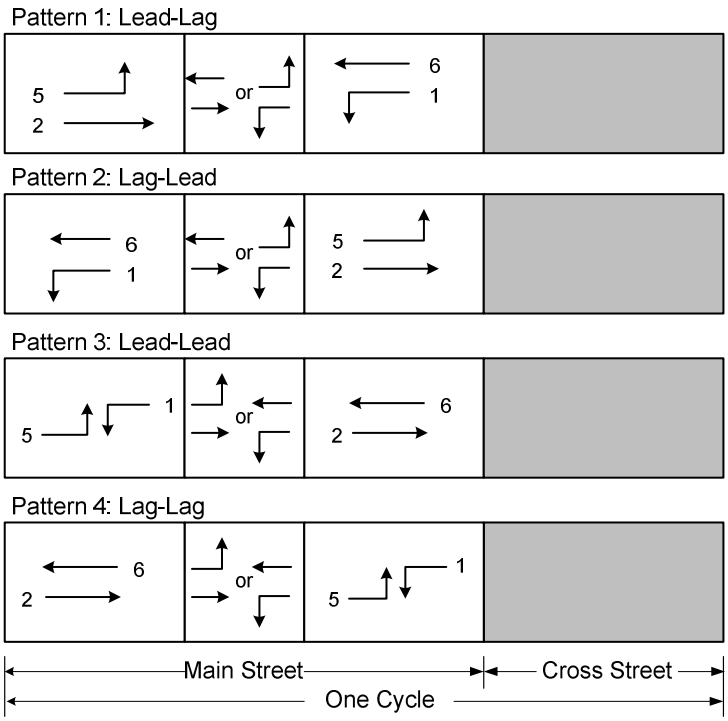

Figure 3-5 Four Possible Phasing Sequence Patterns with Overlapping Phases

3.2.5 Offset

The term offset is used to adjust the start time of a set of recurring signal phases later in signal cycle. The offset ranges from 1 to the cycle length (or from 0 to the value of cycle length minus 1) of the signalized intersection. The offset reference point refers to that position in a set of signal phases that the offset time refers to; this can be beginning of the green interval, end of red time, etc. Each intersection in a coordinated system has both a reference point and an offset. Taking the end of red time of main street as a reference point, the offset at each intersection is indicated in Figure 3-6 *(21)*.

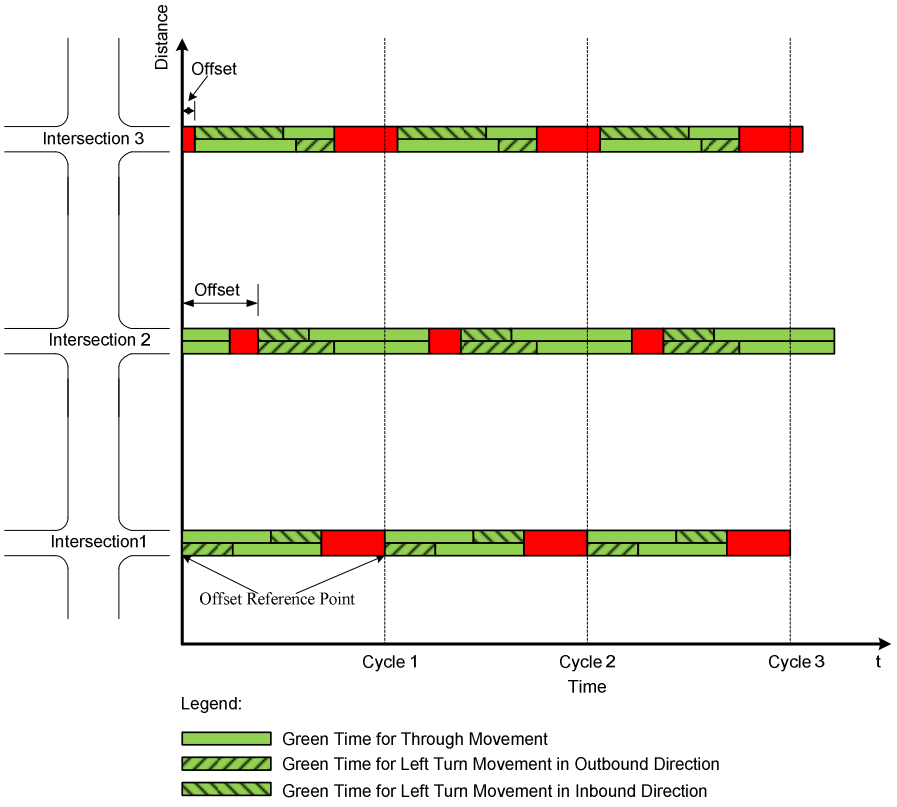

Figure 3-6 Offset Reference Points and Offsets

3.3 TRAFFIC SIGNAL CONTROL PERFORMANCE INDICES

When optimizing a traffic signal control plan, an objective function is used to evaluate the performance of each operation. This objective function is called the Performance Index (PI). The PI of an arterial and a network can include delay, queue length, stops, travel time, the percentage of progression efficiency, fuel consumption, progression opportunities, or any combinations among these measures, and depends on the desired operational characters of the system under consideration.

3.3.1 Delay

Most studies and software packages apply the HCM delay model for assessing a signal timing plan *(22–24)*. The model includes initial deceleration delay, queue move-up time, stopped delay, and queue acceleration delay. The equation for modeling delay, as shown below, contains three main items *(16)*:

$$d = d_1 * PF + d_2 + d_3 \tag{3-4}$$

where

d: control delay per vehicle (s/veh);

d_1: uniform control delay, assuming uniform arrivals (s/veh);

PF: progression adjustment factor, which accounts for effects of signal progression;

d_2: incremental delay per vehicle, to account for effects of random arrivals and oversaturation queues (s/veh); and

d_3: initial queue delay per vehicle, which accounts for delay to all vehicles due to initial queue at the start of analysis period (s/veh).

3.3.2 Queue Length

The maximum backup of queue (vehicles) at under-saturated conditions is presented in Figure 3-7. The maximum queue (number of vehicles) can be found with the following equation *(19)*:

$$Q = \frac{v}{(1-{}^{v}/_{s})*3600} * R \quad (3\text{-}5)$$

where

v: arrival rate of vehicles (veh/h);

s: saturation flow rate (veh/h); and

R: red time (s).

Not all simulation software follow a uniform definition of queue length. Synchro does not exactly follow this equation to calculate the queue length (vehicles) since some vehicles at the end of queue only slow down but not fully stop. Synchro only considers vehicle delay more than six sec to be part of the queue, which is Q_2 in Figure 3-7 *(19)*. CROSIM, PASSER II-90, and SIGNAL 94 use Q_1 in Figure 3-7 as their queue length (vehicles) *(25–27)*. TRANSYT-7F calculates the maximum queue which is Q in the same figure *(24)*. VISSIM collects the maximum queue according to its micro simulation model.

The queue length (feet) is the product of queue length (vehicles) and the sum of average length of vehicles (feet) and the interval between successive vehicles.

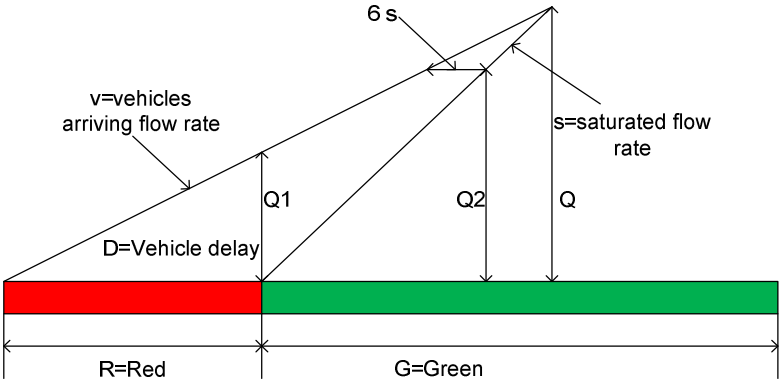

Figure 3-7 Arrival Departure Diagram

3.3.3 Stops

The stops are calculated in the same manner as to the queue length (vehicles). The vehicle stops in one cycle under unsaturated conditions are the same value of Q, Q_1, or Q_2 in Figure 3-7. However, the numbers of vehicles assumed as stopped were adjusted in most agencies based on their own studies *(19, 26)*.

3.3.4 The Percentage of Progression Efficiency

The percentage of progression efficiency was first applied as traffic signal coordination performance index by Bleyl in 1967 *(28)*. The optimal traffic signal coordination plan is selected if its percentage of progression efficiency is the greatest. The percentage of progression efficiency of a progression solution for a give cycle length is defined as:

$$E_c = \frac{B_I + B_O}{2 * C} * 100\% \tag{3-6}$$

where

E_c: percentage of progression efficiency;

B_I: inbound bandwidth (s);

B_O: outbound bandwidth (s); and

C: cycle length (s).

3.3.5 Vehicular Emissions

The vehicular emissions can be estimated by many ways. Most methods are similar and the total emissions resulting from a traffic signal timing plan are calculated based on travel speeds, stopped delay, stops, and simplified emission rates. Carbon monoxide , volatile organic compounds , and oxides of nitrogen are three major types of vehicular emissions *(19, 24, 26, 29)*.

3.3.6 Progression Opportunities

Progression opportunities were first introduced in release 7 of the TRANSYT-7F software. Forward progression opportunities are defined as the ability that the vehicles in a platoon can pass two successive intersections during green time. Each such opportunity during a given period is recorded as a progression opportunity. All the progression opportunities in both directions along the main street over all the periods were summed to be aggregate progression opportunities *(30)*.

3.3.7 Combinations

A variety of performance indices are generated by combining some of the above basic measures. Synchro combines the total delay and vehicle stops as its performance index to choose the cycle length, phasing sequence, phase split, and offsets *(19)*. TRANSYT-7F

users have a great deal of options to define their PIs by combining the basic measures in searching for optimal traffic signal timing plans *(24)*. VISSIM also provides a variance of optional PIs for users to evaluate their traffic signal operations *(29)*.

3.4 TRAFFIC SIGNAL CONTROL METHODS

Traffic signal control methods mainly include pre-timed, semi-actuated control, fully-actuated control, coordinated actuated control, and coordinated pre-timed control. Each control type has specific attributes which are discussed fully in the following sections.

3.4.1 Pre-timed Traffic Signal Control

A pre-timed signal control is a signal control in which the cycle length, phasing plan, and phase splits are preset to repeat continuously. Pre-timed control does not need data collectors or detectors equipped at the intersection, thus reducing agencies' installation and maintenance costs. Pre-timed control is beneficial to install at intersections with constant traffic volumes in certain periods, but may not serve drivers efficiently when traffic volumes fluctuate due to the fixed time assigned to each phase. Time-of-day pre-timed controls are composed of several pre-timed control plans to satisfy the various traffic volumes during different periods of the day. The pre-timed control can also work well at closely spaced intersections where traffic volumes and patterns are consistent on a daily or day-of-week basis *(31)*. The pre-timed control provides an alternative to traffic engineers to coordinate intersections since both the start and end of green are predictable. There are two key types of control: pre-timed traffic signal control for isolated intersections and pre-timed coordinated traffic signal control.

3.4.1.1 Pre-timed Traffic Signal Control for Isolated Intersections

The pre-timed traffic signal control for isolated intersections is simplest method for operating traffic control plans. This control method can save traffic agencies on installation and operation costs. In addition, it does not require traffic engineers and professionals with much knowledge of traffic signal control theory. It usually has lowest efficiency on a variety of traffic demands compared to other traffic control methods.

3.4.1.2 Pre-timed Coordinated Traffic Signal Control

Pre-timed coordinated control is a control when both crossing streets need to be coordinated in a network. The green time of each coordinated phase is fixed and can not change. The pre-timed coordinated control is operated in downtown areas with highly stable traffic volumes on each movement. The advantage of pre-timed coordinated control is that it can maintain traffic pattern and work more efficiently, especially when traffic volumes along each street are high. However, pre-timed coordinated control lacks the ability to adjust to serve traffic based on demand and may waste green time when there are no or few vehicles in some movements.

3.4.2 Actuated Traffic Signal Control

Actuated traffic signal control consists of semi-actuated, fully actuated, and coordinated actuated signal control. The phase green time of an actuated traffic signal will vary within the limit between initial green time and maximum green time based on traffic demand volume at the turning movement. A phase will likely be skipped entirely when there is no demand.

3.4.2.1 Semi-Actuated Traffic Signal Control

Semi-actuated control is a type of actuated traffic signal control in which the designated major movement receives green unless there is a call for service on a minor movement phase. Vehicle detectors are only provided for the minor movements, and may be placed on the major movement if dilemma zone protection is desired.

Semi-actuated control is suitable for application at intersections in coordinated systems. It is also suitable for isolated intersections with low-speed main road and light traffic on side streets.

The primary advantage of semi-actuated control is that it can be effectively used in coordinated arterial systems. Another advantage is that semi-actuated control can reduce delay of both the main street and side street of an intersection compared to pre-timed control. The major disadvantage of semi-actuated control is that heavy traffic on a side street can cause excessive delay to the traffic on the major road *(32)*.

3.4.2.2 Fully-Actuated Traffic Signal Control

Fully-actuated control is an actuated traffic signal control in which vehicle detectors are placed at each approach of the intersection to control the occurrence of green phases and length of green time of each movement.

Fully-actuated control performs well at intersections where traffic volumes vary widely during the day. It can also be operated instead of coordinated control during off-peak periods when traffic flow is low in coordinated signal systems *(33, 34)*.

The major advantage of fully-actuated control is that it can reduce delay significantly more than pre-timed control, since it can be highly responsive to the traffic demand of each movement. Fully-actuated control can also allow phases to be skipped if there are no calls of some movements. The key disadvantage of fully-actuated control is that it is more expensive to install and maintain than pre-timed or semi-actuated control, due to the extra detection equipment required.

3.4.2.3 Coordinated Actuated Traffic Signal Control

Coordinated actuated traffic signal control can be considered a hybrid of semi-actuated and fully actuated signal control. The cycle length and the end of green time for coordinated main street phases are fixed. The side street phases are controlled by actuated mode and the green can terminate early if there is little demand for the phase. The remaining green time of side street phases are added back to the coordinated phases on main streets.

The coordinated actuated control is widely applied in coordinated signal systems. The major advantage of coordinated actuated control is that it can guarantee a fixed cycle length and minimum green times for coordinated phases. It can also allow more vehicles to travel smoothly along the main street without causing too much delay for vehicles on side streets. Vehicles on side streets arriving at an intersection during main street green time must stop and wait for the end of coordinated phases in main roads. This may cause complaints from side street users especially when there are no vehicles on main streets.

3.4.3 Adaptive Traffic Signal Control

Adaptive traffic signal control is a method that can adjust signal settings of each intersection on the basis of real-time traffic information from traffic detectors. Adaptive traffic signal control is a dynamic, real-time, on-line approach to reducing traffic congestion by continuously measuring changing traffic patterns and demands. Since the 1970s, several well-known adaptive traffic signal controls have been developed around the world. Some of these control systems are briefly introduced in the following subsections.

3.4.3.1 Split, Cycle, and Offset Optimization Technique (SCOOT)

SCOOT is "a tool for managing and controlling traffic signals in urban areas. It is an adaptive system that responds automatically to fluctuations in traffic flow through the use of on-street detectors embedded in the road *(35)*."

In 1973, the UK Transport and Road Research Laboratory (TRRL) first started to research a vehicle-responsive method of signal control called SCOOT (split, cycle and offset optimization technique). TRRL and the Ferranti, GEC and Plessey traffic companies carried out a full-scale trial of the developed system in Coventry in 1980. Based on their results, SCOOT reduced vehicle delay by an average of about 12 percent during the working day *(35)*. SCOOT places intersections into many sub-areas and operates at a common cycle length for signal controllers in each sub-area. According to actual traffic flow variations, SCOOT makes frequent and small changes to signal control parameters such as cycle length, phase split, and offset from a pre-timed plan *(36)*.

3.4.3.2 Sydney Coordinated Adaptive Traffic System (SCATS)

SCATS is an adaptive transportation system developed in Sydney, Australia by the Roads and Traffic Authority in the 1970s *(37, 38)*. SCATS does not have an individual traffic signal control plan optimizer and selects the best signal timing plans from some pre-timed plans imbedded in advance. SCATS has two levels of control: strategic and tactical. Strategic control is used to determinate suitable signal timings for areas and sub-areas based on average prevailing traffic conditions. Tactical control takes over the local signal controller at each intersection using exactly the same operational techniques as the isolated operation within the constraints imposed by the regional computers' strategic control settings. Luk found that SCATS reduced travel time by 23% in comparison with uncoordinated operations in 1984 *(39)*. Dutta et al. tested SCATS in a field demonstration project at 28 intersections in the city of Troy in Oakland County, Michigan in 1992 and found that SCATS outperformed pre-timed signal timing plans *(40)*. However, Hu et al. developed pre-timed coordinated signal timing plans on Boulder Highway in the Las Vegas urban area in 2009 and found their pre-timed plans had better performance than SCATS *(41)*. The results of Hu et al.'s study supported a conclusion drawn from Petrella and Lappin's prior work that a well-designed coordinated plan should always provide equal or better performance than adaptive signal control systems under predictable traffic conditions *(42)*.

3.4.3.3 Optimized Policies for Adaptive Control (OPAC)

OPAC is a real-time traffic control system which was originally developed at the University of Massachusetts, Lowell *(43, 44)*. It is a distributed control strategy with a

dynamic optimization algorithm to minimize the total delay and stops. OPAC has the following features:

The Virtual Fixed Cycle (VFC) was first introduced and implemented in traffic signal control in version 4 of OPAC, designated as OPAC-4. VFC has fixed virtual cycle length ranges from fixed yield point to next virtual cycle's yield point. This VFC allows the synchronization phases to terminate early or extend later to better serve dynamic traffic demands without being out of coordination. OPAC-4 has a three-layer control architecture as shown in Figure 3-8. The synchronization layer optimizes the VFC of all intersections. The coordination control layer calculates offsets subject to VFC constraints from the synchronization and the local control layer optimizes the phase sequence subjects to the VFC and offset constraints from the synchronization and coordination layers *(45)*.

OPAC shows improved performance with travel time data collected in before and after studies along Reston Parkway in Reston, Virginia. However, OPAC is not widely used around the world due to its low communication speed between control center and local intersections *(46)*.

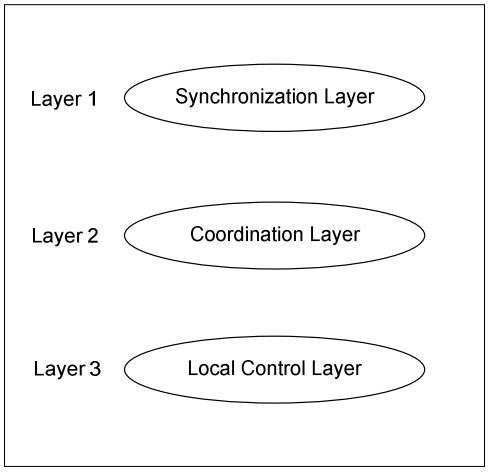

Figure 3-8 Control Architecture in OPAC-4

3.4.3.4 Real-Time Hierarchical Optimized Distributed Effective System (RHODES)

RHODES is a Real-time Hierarchical Optimized Distributed Effective System for traffic control. It was first developed for the city of Tucson, Arizona by the University of Arizona in 1992 *(47)*.

There are three levels of hierarchical architecture within RHODES: network load control, network flow control, and intersection control. The network load control is the highest level that is used to capture the slowly varying characteristics of traffic. The network flow control is the middle level of control that allocates green time for each different demand pattern and each phase. A model called REALBAND is used to optimize the movement of observed platoons in this level of network by minimizing delays and stops *(48, 49)*. The intersection control is the lowest level, which can select the appropriate phase splits based on predicted and observed arrivals of individual vehicles at each

intersection. At this level, RHODES uses a dynamic programming-based algorithm called Controlled Optimization of Phases *(50)*.

3.5 EXISTING OPTIMIZATION METHODS

Although many traffic signal control methods are being applied around the world, the core parts for these signal control methods are optimization approaches and tools. This section introduces the main existing optimization approaches and tools, including Webster's method, MAXBAND, PASSER II, MULTIBAND, TRANSYT-7F, and others.

3.5.1 Webster's Method

Webster first introduced his signal optimization method through conducting a series of experiments on pre-timed isolated intersection operations in 1958 *(51)*. The optimal cycle length can be determined by minimizing the total delay when arrival traffic is random, as calculated by Equation (3-1). The critical phases have equal degrees of saturation for the given cycle length and calculated by Equation (3-3).

Webster's method has emerged as the basic method for optimizing signals, as most of the analytical tools developed for cycle length selection since then focus on under-saturated flow and assume intersections operate as isolated intersections. As an example, the HCM traffic signal analysis method was developed based on the theories in Webster's method. For an isolated intersection, however, Webster's method provides meaningless cycle length when the degree of saturation of lane groups approaches 1.0 *(52)*.

3.5.2 MAXBAND

MAXBAND is an optimization model that finds the best signal timing plan with maximum bandwidth on arterials and triangular networks. The first effort on MAXBAND was Brooks, who utilized a computer program to maximize progression bandwidth assuming only two-phase traffic signals along the arterials *(53)*. In the 1960s, Little et al. developed a fundamental mathematical model called Multi-Integer Linear Program for MAXBAND *(54, 55)*. Little and Gartner et al. then applied MAXBAND to triangular networks to coordinate intersections *(56, 57)*. Messer et al. improved MAXBAND to deal with four-phase signals and applied this method on grid networks in 1970s *(58–60)*.

The performance index of MAXBAND is the weighted sum of bandwidths in both directions. MAXBAND can be used to determine offsets along each arterial, the splits of green time at each intersection of the network, and the common cycle length of the controlled area.

MAXBAND has following advantages:

1. Compared to delay and stops, the bandwidth can be more easily calculated and understood by traffic engineers; and
2. The efficiency of MAXBAND to obtain the optimal solution is relatively high since it needs only a few inputs and calculations.

MAXBAND has disadvantages summarized as below:

1. The maximum bandwidth does not guarantee a minimum delay and number of stops. Thus, the optimal signal timing plan may not be the best plan with minimum delay and stops;
2. MAXBAND cannot generate the best phase splits, when compared to other methods such as TRANSYT-7F; and
3. MAXBAND only gets maximum bandwidth along the through movement of a main street without considering the left-turn traffic on the main street or traffic on the side streets.

3.5.3 PASSER

PASSER was first developed by Messer et al. based on Little and Brook's bandwidth-based program from 1970s *(58, 61)*. PASSER II applied Webster's model for calculating phase splits. Then, a hill-climbing approach was used to adjust phase splits to minimize delay. PASSER II used exhaustive search methods to obtain the best cycle length *(62)*. PASSER III employed a delay-based exhaustive optimization method to determine the variables including cycle length, splits, phasing sequence, and offsets. PASSER III can produce accurate results for traffic engineers in under-saturated traffic conditions and can be applied to diamond interchanges with or without U-turn lanes using three or four phase signal operations *(63, 64)*. PASSER IV can maximize arterial progression in arterial and multi-arterial signal networks *(26)*. PASSER V is the latest version of the PASSER family of signal timing optimization programs developed by the Texas Transportation Institute (TTI) *(65)*. In PASSER V, genetic algorithms (GA) were

introduced to develop signal timings for minimizing delay or for maximizing arterial progression *(66)*.

PASSER still has some disadvantages as noted below:

1. PASSER timings may cause additional delays for vehicles on side streets when it reduces the delays and stops on arterials; and
2. PASSER has limited ability to provide optimal signal timing plans for large closed road networks.

3.5.4 SYNCHRO

Synchro is a delay-based macroscopic analysis tool to analyze and optimize traffic signal timing plans. It uses an exhaustive search method for finding optimal timing plans. To reduce the number of traffic signal scenarios, Synchro applies the divide-and-conquer method. At each step, Synchro generates optimal signal timing plans based on the average delay of five percentile patterns of traffic flow. By far, Synchro provides a good user interface, although it has trouble generating acceptable coordinated traffic signal timing plans in most cases *(19)*.

The first version of Synchro was released in 1994. The latest version of Synchro is Synchro 8 which supports the HCM 2010 methodology for signalized intersections and roundabouts.

3.5.5 TRANSYT-7F

TRANSYT-7F is a widely used model for analyzing and optimizing signal timings on arterials and networks. The original TRANSYT-7F model was originally developed by Dr. Dennis I. Robertson in the Transport Research Laboratory in the United Kingdom in 1967 *(67)*. The Federal Highway Administration (FHWA) bought the copyright of TRANSYT-7F in the 1970s. Then, the TRANSYT-7F program and the original TRANSYT-7F manual were developed for FHWA under the National Signal Timing Optimization Project by the University of Florida Transportation Research Center. In 1978, TRANSYT-7F was formally built up and it significantly reduced data preparation and run time by changing optimization processes *(68)*. TRANSYT-7F continued to be further improved and maintained by the University of Florida's McTrans Center. TRANSYT-7F release 11 is the latest version and is now available in HCS 2010 and TSIS+T7F.

TRANSYT-7F has many advantages including:

1. Explicates optimization of progression opportunities;
2. Replaces the random delay estimation by the delay model from HCM;
3. Applies GA and Hill-Climbing Method to search for optimal signal timing plans; and
4. Provides traffic flow profile for each link and calculates delay and stops more accurately than MAXBAND and PASSER under most conditions.

TRANSYT-7F has an obvious shortcoming on description of traffic flow features in microscopic simulation comparing to other simulation tools such as VISSIM, CORSIM etc.

3.6 MICRO SIMULATION TOOLS

Many micro simulation tools are currently being applied in the world. Table 3-1 summarizes the basic information of the six main simulation software packages. Only VISSIM and CORSIM will be introduced briefly in this section.

Table 3-1 Micro Simulation Software

Name	Software Developer	Year	Country
VISSIM	PTV Planung Transport Verkehr AG	1992	Germany
TSIS-CORSIM	Federal Highway Administration	1998	USA
SimTraffic	Trafficware Corporation	1993	USA
TransModeler	Caliper Corporation	2007	USA
AIMSUN2	TSS - Transport Simulation Systems	1998	Spain
PARAMICS	The Edinburgh Parallel Computing Centre and Quadstone Ltd.	1990s	UK

3.6.1 VISSIM

VISSIM is a microscopic, time step, and behavior-based multi-mode software to simulate urban traffic, public transport, and pedestrian flows. It was developed by PTV Planung Transport Verkehr AG in Karlsruhe, Germany in 1992. VISSIM employs the psycho-physical driver behavior model developed by Wiedemann in 1974. This model can replicate the drivers' iterative process of acceleration and deceleration. VISSIM simulates traffic flow by moving "driver-vehicle-units" through a network. Every driver with his or her specific behavior characteristics is assigned to a specific vehicle *(29)*.

VISSIM also provides a variety of evaluation types including travel times, delay, data collection, queue length, emission, etc. It develops a specific procedure for simulating a road network according to either static or dynamic assignment method for traffic distribution. It is widely used in simulating complex traffic systems around the world. These applications mainly include:

1. Simulation of traffic signal control;
2. Evaluation of public transportation strategy;
3. Calculation of capacity of toll collection stations;
4. Calculation of capacity of lane merge areas;
5. Evaluation of the performance of vehicles and pedestrians in a traffic system; and
6. Evaluation of the effects of toll collection policy or dynamic information signs.

The main shortcomings of VISSIM contain:

1. Considerable time and effort needed to adjust traffic signal operation plans;
2. Time consuming to simulate each traffic operation plan especially for large networks. This will limit its ability to search for the optimal signal timing plans; and
3. Unable to provide the optimal traffic signal control plans very efficiently. VISSIM 5.40, the latest version, provides such functions only for stage based operations. In addition, it can only optimize a few intersections for its very time consuming exhaustive algorithms and complexity of traffic signal control.

3.6.2 TSIS-CORSIM

TSIS-CORSIM, first publicly released in the 1990s, is a microscopic traffic simulation software package developed by the Federal Highway Administration (FHWA). TSIS-CORSIM is combination of TSIS (Traffic Software Integrated System) and CORSIM. TSIS enables users to conduct traffic operations analysis and allow users to define and manage traffic analysis projects, create traffic networks and inputs for traffic simulation analysis, execute traffic simulation models, and interpret the results of those models. CORSIM consists of two main components: NETSIM, and FRESIM. NETSIM was originally developed under the name "Urban Traffic Control System" in the early 1970s and can simulate traffic on urban streets. FRESIM was developed for simulating highways and freeways.

TSIS-CORSIM has most similar functions provided by VISSIM. TSIS-CORSIM also has its advanced vehicle following model and lane changing model. The minimum simulation step size is 1 second, which means all the simulation features and data can be updated in every second. However, TSIS-CORSIM cannot provide 3D simulation animation and has no dynamic assignment packages. These disadvantages cause the limited abilities of TSIS-CORSIM to evaluate ramp controlling strategy, lanes merging process, incident management strategy, and traveler navigation systems *(24)*.

3.7 SUMMARY

This section briefly reviewed traffic signal control elements, traffic signal control performance indices, traffic signal control methods, existing optimization methods and

tools, and micro simulation software. After this review section, it will be easier to understand the concepts, terminologies, and algorithms in following sections related to traffic signal control at Diverging Diamond Interchanges.

CHAPTER 4. MATHEMATICAL OPTIMIZATION ALGORITHMS

4.1 INTRODUCTION

Traffic signal control has been widely studied since the 1960s, as it plays an essential role in traffic management. A well-developed signal plan can enhance traffic flow, reduce delay, and minimize pollution.

Computer technology has provided a solution to solve traffic signal control problems in the past few decades. With the assistance of computer technology, traffic signal control methods have been developed from isolated pre-timed control to coordinated control and adaptive traffic signal control systems. A variety of optimal traffic signal tools have been applied in practice. Mathematical optimization algorithms play an important role in these optimization tools. A suitable mathematical optimization algorithm can not only help traffic engineers obtain better control plans, but also spend less time in doing so.

This chapter presents an overview of several mathematical optimization algorithms and briefly introduces the optimization algorithms applied in traffic signal control. The genetic algorithm is explained more thoroughly, since it is the potential optimization algorithm used for generating optimal traffic signal control plans in the future.

4.2 OVERVIEW

4.2.1 The Definition of Optimization Algorithm

In mathematics and computational science, mathematical optimization refers to the selection of a group of best elements from some sets of available alternatives to minimize or maximize an objective function.

In general, an optimization problem can be represented in the following way.

Minimize or maximize: $f(x)$

Subject to: $x \in X$ (4-1)

The function $f(x)$ is the objective function that should be minimized or maximized given any element x in set X. The x is a vector of n independent variables, that is $= [x_1, x_2, \dots x_n]^T \in R^n$. The variables $x_1, x_2, \dots x_n$ are referred to as decision variables. The "T" here means transposition process. R refers to the real value. The X is a subset of R^n, called the feasible set. If an element x^* in X such that $f(x^*) \leq f(x)$ for all x in X, the x^* is the optimal solution that can minimize the objective function. Or if an element x^* in X such that $f(x^*) \geq f(x)$ for all x in X, the x^* is the optimal solution that can maximize the objective function.

Such a formulation is called an optimization problem, which is a general framework of many real-world and theoretical problems. The main categories of optimization problems include linear programming, integer programming *(69)*, quadratic programming *(70)*, nonlinear programming *(71)*, stochastic programming *(72)*, dynamic programming *(73)*, combinatorial optimization *(72)*, and infinite dimensional optimization *(74)*. Generally, there may be several local minima and maxima when the feasible region or the objective function of the problem does not present convexity. Although there are a large number of

algorithms proposed for solving non-convex problems, most of them are not capable of making a distinction between local optimal solutions and rigorous optimal solutions.

There are more than 81 categories of popular optimization algorithms currently. These optimization algorithms can be grouped into different types of optimization algorithms based on algorithms features or the problems themselves characters. Four main types of optimization algorithms are summarized in this section according to their algorithm features. The types of optimization algorithms are trial and error, optimization algorithms, iterative methods, and heuristics.

4.2.2 Trial and Error

Trial and error, or trial by error, is a general method of problem solving by trying each possible solution *(75)*. This method is called "generate and test" in the field of computer science, and is better known as "guess and check" in elementary algebra.

Trial and error makes no attempt to discover why a solution works, generally finding a solution through trying again and again. Trial and error provides a problem-specific solution. The advantage of trial and error is that it is simple and requires little mathematical knowledge related to problems. Trial and error is successful in computer science in many aspects, especially for simple problems and discrete problems with limited solutions. However, trial and error still experiences a time consuming issue in many problem areas, even though computer technology can operate extremely fast. For example, according to Ashby's study, the perfectionist all-or-nothing method, with no attempt at holding partial successes, would be expected to take more than 10^{301} sec, that

is $3.5 * 10^{291}$ centuries *(76)*. This tremendous time consuming issue is also discussed in Traill's research *(77)*. In traffic signal control area, Hu et al. spent around 32,767 sec to obtain the optimal signal timing plans by the step size of 10 sec on an arterial consisting of six intersections *(78)*. Despite these limitations, the latest version of VISSIM (VISSIM 5.40) released their new functions for searching the optimal traffic signal coordination timing plans by trial and error method due to its simplicity *(29)*.

4.2.3 Optimization Algorithms

Optimization algorithms mainly refer to the algorithms use to solve linear programming, linear-fractional programming, network optimization problems, and combinational optimization problems. There are many optimization algorithms that can solve these kinds of problems. Take linear programming as an example, Dantzig developed a popular algorithm for linear programming called simplex algorithm (or simplex method) *(79)*. Some other methods have been developed for solving linear programming problems, such as criss-cross algorithm, Khachiyan's ellipsoidal algorithm, Karmarkar's projective algorithm, and path-following algorithms *(80)*. Network optimization problems have their own optimization methods to search for optimal solutions, including Constructal Theory, Ford-Fulkerson Algorithm, Flow (computer networking), Max-flow Min-cut Theorem, Oriented Matroid, and Shortest Path Problem *(81)*. MAXBAND and PASSER have applied linear programming methods in traffic signal coordination control to search the maximum bandwidth *(82)*.

4.2.4 Iterative Methods

Iterative methods are mainly used to solve non-linear programming. These methods primarily include Gradient Descent method, Newton's method, Quasi-Newton method, Finite difference, Approximation theory, and Numerical analysis. Although there are some differences between these methods, the common characteristic is that it takes steps to find optimal solutions. Take Gradient Descent method and Newton's method as examples, Gradient Decent method is a first-order optimization algorithm that finds a local minimum or maximum value of a function using gradient decent. The gradient descent can take many iterations to compute a local minimum or maximum with a required accuracy *(83)*. Search methods based on Newton's method's gradient techniques can be faster than Gradient descent method, but the cost of every iteration are higher since they consist of calculating every step in a matrix by which the gradient vector is multiplied to go into a "better" direction *(84)*. TRANSYT-7F applied hill-climbing search method, which is an iterative Gradient search algorithm, to find the optimal traffic signal control solutions *(24)*.

4.2.5 Heuristics

A heuristic is a technique designed to solve a problem that ignores whether the problem can be solved by above methods or not, but which usually produces a good or acceptable solution for either simple or more complex problems.

Heuristics are intended to gain feasible solutions, but they are conceptually simple. In the application of computer science, Simon and Newell indicated the Heuristic Search

Hypothesis: a physical symbol system will repeatedly generate and modify known symbol structures until the created structure matches the solution structure *(85)*. It indicates that a heuristic method's each successive iteration depends upon the step before it. Thus, the heuristic search learns what roads to pursue and which solutions to disregard by measuring how close the current iteration is to the optimal solution.

A heuristic method can accomplish its task by using various search methods. The good search methods applied can generate approximate solutions faster than others *(86)*. There are several heuristic methods, such as Mimetic Algorithm, Differential Evolution, Dynamic Relaxation, Genetic Algorithms (GA), Nelder-Mead Simplified Heuristic, Particle Swarm Optimization, Simulated Annealing, and Tabu Search. GA is the most popular used method in traffic signal coordination control. TRANSYT-7F applied GA to generate the optimal traffic signal coordination timing plans *(24)*.

This research will briefly introduce GA in searching for feasible solutions for signal timing at DDIs. Thus, the concept of GA is introduced fully in the remainder of this chapter.

4.3 GENETIC ALGRITHM

4.3.1 History

In the 1960s, Ingo Rechenberg and Hans-Paul Schwefel started to try a randomized method that may be regarded as the simplest algorithm driven by mutation and selection. And in early 1970s, Rechenberg's group could solve complex engineering problems through evolution strategies *(87)*.

John Holland became known as the father of genetic algorithms when he popularized the concept in his 1975 book *Adaptation in Natural and Artificial Systems (88)*. Holland and his students developed genetic algorithm originally from their studies of cellular automata at the University of Michigan. Holland's Schema Theorem became a formalized framework for predicting the quality of the next generation during that period. Until the mid-1980s, full theories of GA were built up. The First International Conference on GA was held in Pittsburgh, Pennsylvania in July 1985.

As academic interest grew in the 1980s, the applications of GA based on computer technology became increasingly popular. General Electric started selling a mainframe-based GA toolkit for industrial processes that became the world's first genetic algorithm product in the late 1980s. In 1989, Axcelis, Inc. released the world's first commercial GA product for desktop computers, named Evolver *(89)*.

4.3.2 Methodology

A GA is a heuristic search method that mimics the process of natural evolution. GA is used to generate useful solutions for a problem and search solutions like any other optimization algorithm, by defining the optimization parameters, the cost function, and constraints. However, GA belongs to the class of evolutionary algorithms (EA), which generate solutions to optimization problems using techniques inspired by natural evolution, such as initial population, natural selection, paring, mating, and mutations.

In a GA, the variables are represented by genes of a chromosome. The objective function generates an output from a chromosome (a set of input parameters). The objective

function can have a variety of forms such as a mathematical function, an experiment, and a game. GA can generate an acceptable optimization solution through following basic steps *(90)*:

Step 1. Build a model for a problem. This model includes the objective function, parameters, and constraints;

Step 2. Convert parameters into a chromosome or several chromosomes;

Step 3. Randomly generate an initial solution (a chromosome or a group of chromosomes) within the feasible solution space of the problem which is controlled by the parameters' constraints;

Step 4. Select best chromosomes by natural selection principle. Generate new chromosomes through paring, mating, and mutations among these best chromosomes;

Step 5. Update old chromosomes by newly generated chromosomes; and

Step 6. Terminate the algorithm if a fixed number of generations are up or the convergence requirement is satisfied. Otherwise, go back to step 3 and keep searching for the best solution.

A path through the components of GA is shown in Figure 4-1. Each part of this overview is discussed in detail in this chapter.

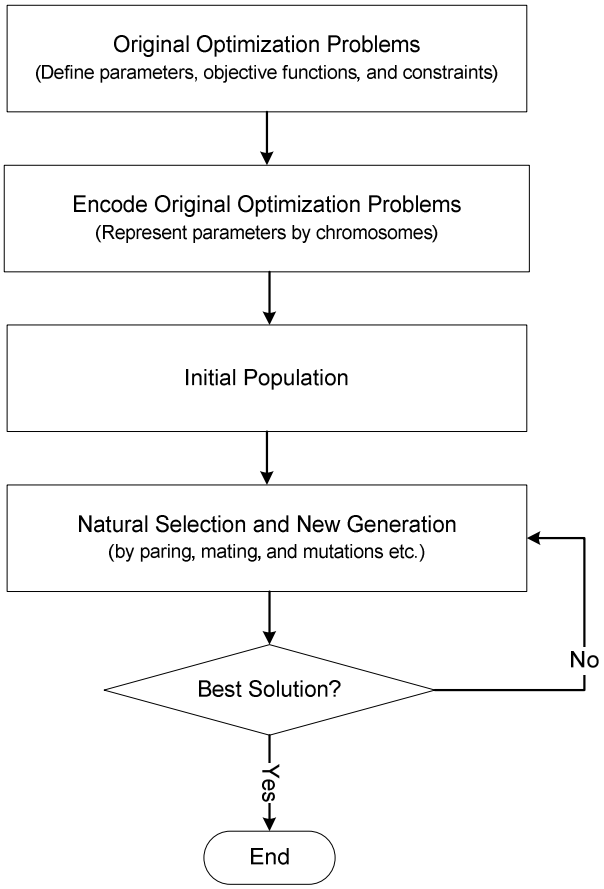

Figure 4-1 Overview of Genetic Algorithm

4.3.2.1 Original Optimization Problem

GA can find optimal solutions in bioinformatics, phylogenetics, computational science, engineering, economics, chemistry, manufacturing, mathematics, physics, and other fields. The optimization problems can be a variety of forms. To apply GA in these fields, the optimization problems need have two features: parameter feasible solution domain (constraints of parameters), and an objective function to evaluate the solutions among all feasible solutions.

The original optimization problems can be generally expressed as Formula (4-1) shown in the beginning of this chapter. The objective function and parameters indicate different meanings based on the fields of problems. Thus, building up a suitable original optimization model for a problem can fundamentally improve GA's accuracy and efficiency.

4.3.2.2 Encode and Decode

Encoding original optimization problems is a process to transfer an original problem to a GA's model. Every variable can be encoded to a string of "0 or 1" bits within a certain range of error. A chromosome can represent all unknown variables by combining the "0 or 1" strings. For example, the variable $x_1 = 21$ can be expressed $[10101]$ in binary version; the variable $x_2 = 11$ can be expressed $[01011]$ in binary version. A chromosome represents variable x_1 and x_2 can be:

$$chromosome_{1,2} = [1010101011] \tag{4-2}$$

The length of this chromosome is 10.

For a continuous variable with range $[U_1, U_2]$, each variable can be approximately encoded by K binary values of "0" and "1" in the following ways. The greater K is, the more accurate it is to represent each variable by a string of binary values. The value of K is determined by the requirement of accuracy on variables. For example, if variable x_i in the range of $[U_1, U_2]$ needs to keep its accuracy within four decimal places. The value of K for this case is determined by the following formula.

$$2^{K-1} < (U_2 - U_1) * 10^4 \leq 2^K - 1 \tag{4-3}$$

The mathematic formulas for the binary encoding of a variable x_i within $[U_1, U_2]$ are given by:

$$x_{i,norm} = \frac{x_i - U_1}{U_2 - U_1} \tag{4-4}$$

$$x_{i,K,B} = [b_{i,K} b_{i,K-1} \cdots b_{i,2} b_{i,1}], if \left| \frac{\sum_{j=1}^{K} b_{i,j} * 2^{j-1}}{2^K - 1} - x_{norm} \right| is\ the\ least. \tag{4-5}$$

where

$x_{i,norm}$: normalized variable, $0 \leq x_{i,norm} \leq 1$;

$x_{i,K,B}$: variable x_i's binary version value with K bits of "0" or "1"; and

$b_{i,j}$: jth binary value of variable x_i , $b_{i,j}$ equals 0 or 1.

The genetic algorithms work with the binary values, but most objective functions often require continuous parameters. Before calculating the objective functions, the binary values need to first be decoded into continuous variables. A continuous variable x_i can be decoded from a binary version value $x_{i,K,B} = [b_{i,K} b_{i,K-1} \cdots b_{i,2} b_{i,1}]$ through the following two formulas:

$$x_{i,norm} = \frac{\sum_{j=1}^{K} b_{i,j} * 2^{j-1}}{2^K - 1} \tag{4-6}$$

$$x_i = U_1 + x_{i,norm} * (U_2 - U_1) \tag{4-7}$$

4.3.2.3 Initial Population

A GA usually starts with a large number of chromosomes known as initial population. A large initial population provides the GA with ample and diversified selections in its searching space. The general initial population can be created by Formula (4-8),

assuming N chromosomes are generated by a random function with only values of "0" or "1."

$$CR_{IP} = \begin{bmatrix} cr_1 \\ cr_2 \\ \vdots \\ cr_N \end{bmatrix} = \begin{bmatrix} x_{1,1,K,B} & x_{1,2,K,B} & \cdots & x_{1,M,K,B} \\ x_{2,1,K,B} & x_{2,2,K,B} & \cdots & x_{2,M,K,B} \\ \vdots & \vdots & \vdots & \vdots \\ x_{N,1,K,B} & x_{N,2,K,B} & \cdots & x_{N,M,K,B} \end{bmatrix}$$

$$= \begin{bmatrix} b_{1,1,K}b_{1,1,K-1}\cdots b_{1,1,2}b_{1,1,1} & b_{1,2,K}b_{1,2,K-1}\cdots b_{1,2,2}b_{1,2,1} & \cdots & b_{1,M,K}b_{1,M,K-1}\cdots b_{1,M,2}b_{1,M,1} \\ b_{2,1,K}b_{2,1,K-1}\cdots b_{2,1,2}b_{2,1,1} & b_{2,2,K}b_{2,2,K-1}\cdots b_{2,2,2}b_{2,2,1} & \cdots & b_{2,M,K}b_{2,M,K-1}\cdots b_{2,M,2}b_{2,M,1} \\ \vdots & \vdots & \vdots & \vdots \\ b_{N,1,K}b_{N,1,K-1}\cdots b_{N,1,2}b_{N,1,1} & b_{N,2,K}b_{N,2,K-1}\cdots b_{N,2,2}b_{N,2,1} & \cdots & b_{N,M,K}b_{N,M,K-1}\cdots b_{N,M,2}b_{N,M,1} \end{bmatrix}$$

(4-8)

where

CR_{IP}: initial population;

cr_i: chromosome i, $1 \le i \le N$;

N: total initial chromosomes;

M: total variables (unknown parameters);

$x_{i,j,K,B}$: original variables, $1 \le i \le N$, $1 \le j \le M$; and

$b_{i,j,k}$: 0-1 binary variables, $b_{i,j,K}$=0 or 1, $1 \le i \le N$, $1 \le j \le M$, $1 \le k \le K$.

The population size often affects the accuracy of a GA and the number of generations needed to converge. The population size should not be greater than its initial population size. Based on Gotshall and Rylander's study, the optimal population for a given problem is the crossing point where the benefit of quick convergence is offset by increasing

inaccuracy *(91)*. Several studies provided equations to calculate optimal initial population size *(92–94)*.

4.3.2.4 Natural Selection

The initial population is too large to generate better offspring in the iterative steps of a GA. Thus, most bad chromosomes are discarded and good ones will be kept to generate offspring. Natural selection occurs in each generation or iteration of a GA. A GA will quickly terminate if few good chromosomes are selected in each step. But the GA will extremely slowly find the optimal individual when few bad chromosomes are discarded in each iteration. Haupt indicated that scholars often keep 50% of parents in the natural selection *(95)*. Up to now, many natural selection methods have been developed, such as Roulette Wheel Selection *(96)*, Stochastic Tournament *(97)*, Expected Value Selection *(98, 99)*, and Thresholding *(100)*, and others. Roulette Wheel Selection was chosen to be a natural selection example and introduced in this study.

The Roulette Wheel Selection gives each chromosome a chance to become a parent in proportion to its fitness. The chromosomes with the largest fitness (slot sizes) have more chance of being chosen. The potential problem of Roulette Wheel Selection is that one or a few members can dominate all the others and be selected in a high proportion. The Roulette Wheel Selection contains the following steps *(101)*.

Step 1: Get each chromosome's fitness value and sum of all chromosomes' fitness values

In a GA, fitness is used to evaluate the goodness of the individuals in the population. Individuals with higher fitness value will have higher probability of being selected as

candidates for further examination and generating offspring. Most GAs require that the fitness function should be non-negative. There are three commonly used basic fitness functions:

(1) Fitness functions type 1

The fitness functions can be derived from objective functions by,

$$F(x) = \begin{cases} f(x), & if\ objective\ function\ is\ maximazing \\ -f(x), & if\ objective\ function\ is\ minimizing \end{cases} \quad (4\text{-}9)$$

This type of fitness function is simple and intuitive. But negative values of some fitness functions make Roulette Wheel Selection out of work.

(2) Fitness functions type 2

For minimization problems, the fitness function can be defined as,

$$F(x) = \begin{cases} C_{max} - f(x), & if\ f(x) < C_{max} \\ 0, & otherwise \end{cases} \quad (4\text{-}10)$$

where

C_{max}: maximum estimation of $f(x)$ to guarantee $F(x)$ is not less than 0 for any x in the domain.

For maximization problems, the type 2 fitness function is,

$$F(x) = \begin{cases} f(x) - C_{min}, & if\ f(x) > C_{min} \\ 0, & otherwise \end{cases} \quad (4\text{-}11)$$

where

C_{min}: minimum estimation of $f(x)$ to guarantee $F(x)$ is not less than 0 for any x in the domain.

(3) Fitness functions type 3

For minimization problems, the fitness function is defined as,

$$F(x) = \frac{1}{1+c+f(x)}, c \geq 0, c + f(x) \geq 0 \quad (4\text{-}12)$$

For maximization problems, the fitness function is,

$$F(x) = \frac{1}{1+c-f(x)}, c \geq 0, c - f(x) \geq 0 \quad (4\text{-}13)$$

Step 2: Calculate the probability of individual being selected

The probability of each individual chromosome being selected is,

$$P_i = \frac{F(x_i)}{\sum_{i=1}^{K} F(x_i)} \quad (4\text{-}14)$$

where

P_i: probability assigned to chromosome i.

Step 3: Calculate the cumulative probability of individuals being selected

The cumulative probability of each individual chromosome is,

$$CP_i = \sum_{j=1}^{i} P_j \quad (4\text{-}15)$$

where

CP_i: cumulative probability assigned to chromosome i.

Step 4: Select chromosome

First, generate a random number r from [0,1].

Second, select chromosome 1 if $r < CP_1$, otherwise select chromosome j if it satisfies the following requirement.

$$CP_{j-1} \leq r \leq CP_j \tag{4-16}$$

Finally, repeat the above two processes for the total number of chromosomes.

4.3.2.5 New Generation

The new generation can be created by crossover and mutation. Besides these two main genetic operators, some other operators such as regrouping, colonization-extinction, or migration in genetic algorithms, are also provided *(102)*. Through these genetic operators, each new "child" solution is created from the previously selected "parent" chromosomes. A new "child" solution usually contains the most of characteristics of its "parent". Crossover and mutation operators are briefly introduced in this section.

(1) Crossover

In genetic algorithms, crossover is a genetic operator used to vary the genes of chromosomes from parent generation to offspring generation. There are four main crossover methods: one-point crossover, two-point crossover, cut and splice, and uniform crossover and half uniform crossover. Only one-point crossover and two-point crossover methods are explained as examples below.

One-point crossover is the simplest crossover method. All genes, after a randomly chosen point, are swapped between the two parent chromosomes. Figure 4-2 shows this crossover processing.

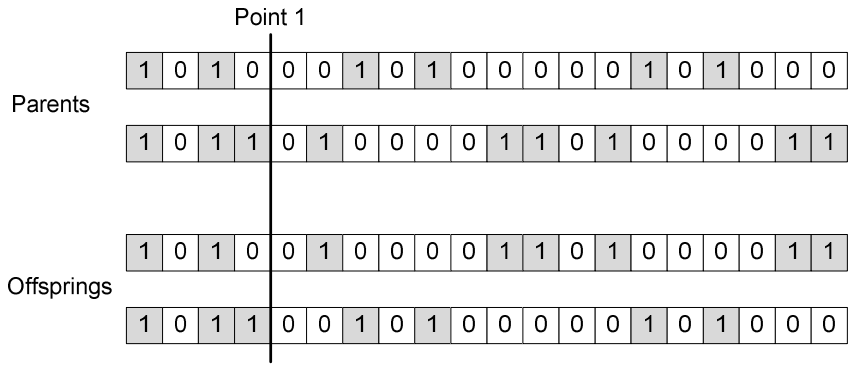

Figure 4-2 One-Point Crossover

Two-point crossover has two randomly chosen points. All the genes between these two points in the parental chromosomes are swapped and other genes are kept same to reproduce two new chromosomes. Children chromosomes are generated this way; this process is illustrated in Figure 4-3.

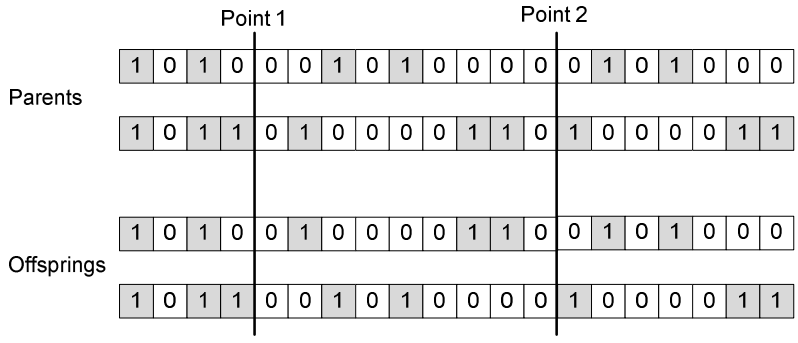

Figure 4-3 Two-Point Crossover

(2) Mutation

Mutation is a genetic operator used to maintain genetic diversity from one generation and prevent all solutions in the population becoming trapped in the local optimum of the problem. A common method of implementing the mutation operator is to generate a random variable for the genes in an offspring chromosome. Most mutations decrease the fitness of a chromosome. Occasionally, some mutations can increase the fitness values of the chromosomes and increase the ability of searching for the global optimum solution. This random variable tells whether or not a particular gene will be modified. The reference mutation probability of a gene is $1/L$, where $L \geq 1$, is the length of the chromosome. Take the child chromosomes in Figure 4-3 as an example; the reference mutation probability of each gene is $1/20 = 0.05$. A random number generator will determine the position of a chromosome that needs to be modified. A user-defined mutation probability can determine whether mutation occurs or not. The mutation probability should be set low to avoid replacing the existing good chromosomes, but not too low to lose its diversity ability to search global optimal solutions. Figure 4-4 illustrates a mutation process.

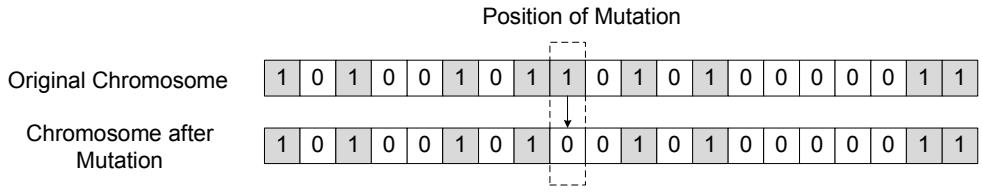

Figure 4-4 Mutation Process

4.3.2.6 Termination

There are two main ways to terminate a GA: maximum number of generations and convergence. A fixed number of generations are defined at the beginning of a GA. When this number is reached, the GA must stop. Convergence means that an acceptable solution has been found or successive iterations no longer produce better results than current solution with required speed. A GA can terminate when the convergence condition has been satisfied even if the maximum number of generations is not yet exceeded.

4.3.3 Advantages and Disadvantages of GA

The representative advantages of GA include *(90, 101, 103)*:

- GA is a very easy to understand method and does not require users to have a strong mathematical background;
- GA can solve a variety of problems including multi-dimensional, non-differential, non-continuous, and even non-parametrical problems;
- GA can find acceptable optimal solutions very quickly, especially for large-scale optimization problems;
- GA can provide global optimal solutions; and
- GA has extensibility to mix other algorithms to solve complex problems.

The primary disadvantages of GA are *(90, 101, 103)*:

- GA has relative low efficiency to solve some specific problems in comparison to other optimization methods;
- GA cannot find the real global optimal solutions in most cases. It can only provide some acceptable solutions; and
- GA requires a large number of fitness function calculations. This will increase a GA's running time for large-scale and complex problems.

4.4 SUMMARY

This chapter mainly overviewed the history of evolutionary methods applied in optimization problems, and introduced the key steps to GA. In addition, this chapter provided the fundamental theoretical support for potential applications of GAs at DDIs.

CHAPTER 5. TRAFFIC SIGNAL OPERATIONS AT DDIs

5.1 INTRODUCTION

Chapter 2 through Chapter 4 reviewed previous studies on Diverging Diamond Interchanges, as well as the concepts, technical tools, and some optimization methods related to traffic signal control. This chapter concentrates on traffic signal operations for DDIs. As stated previously, a DDI can outperform a CDI in most situations for its specific design and operational approach. Better traffic signal operations can further improve a DDI's efficiency and reduce its delay. Therefore, this chapter presents three major methods to improve a DDI's operational performance.

This chapter first reviews five current traffic signal operations for DDIs and summarizes their advantages and disadvantages succinctly. The following section presents two major traffic signal operational improvements for DDIs. This section also introduces the third method of how to apply genetic algorithm (GA) for determining traffic signal parameters based on the proposed operations. Finally, the third section summarizes the contributions of this chapter.

5.2 CURRENT SIGNAL OPERATIONS

The literature review in Chapter 2 revealed several traffic control operations that have been implemented at or proposed for operating DDIs. These studies disclosed that each traffic control operation is unique and has its applicable conditions. Therefore, this

section starts with the descriptions of the five typical operations and ends by a summary of their advantages and disadvantages.

5.2.1 Current Operation 1

The Federal Highway Administration (FHWA) recommended a simple DDI traffic operation that consists of two phases as shown in Figure 5-1 and Figure 5-2 *(2)*. This operation is applicable when the off-ramps are "yield" controlled. The arterial traffic passing through the first signal during the earlier part of the phase is guaranteed to pass through the second signal without stopping, but the traffic in the later part of the phase will have to stop at the second signal.

Figure 5-1 Phase and Ring Diagram for the Two-phase Scheme

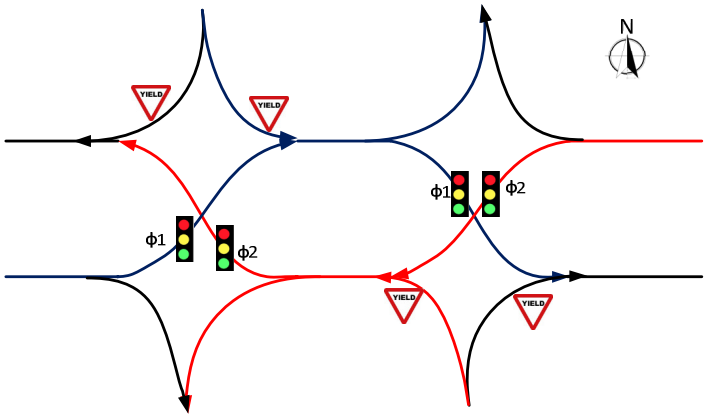

Figure 5-2 Phase Designation Diagram for the Two-phase Scheme

5.2.2 *Current Operation 2*

The Missouri Department of Transportation (MoDOT) was the first in the United States to implement a DDI at the intersection of I-44 and MO-13 in Springfield, Missouri. MoDOT presented two DDI phasing schemes *(1)*. The simpler traffic operation is shown in Figure 5-3. As can be seen, the right-turn movements at the off-ramps are signal controlled while the left-turn movements are yield controlled.

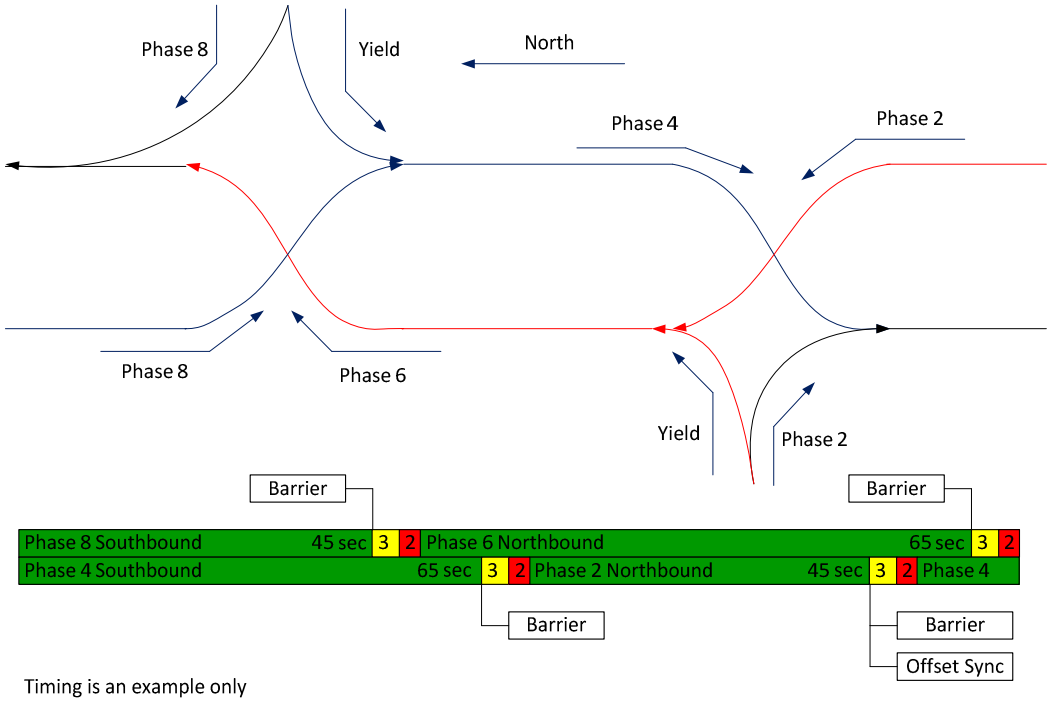

Figure 5-3 Traffic Signal Operation Proposed by MoDOT – Option 1

5.2.3 *Current Operation 3*

MoDOT provided a more complex DDI phasing operation as shown in Figure 5-4. As concluded by MoDOT, this operation could clear the space between the crossovers, but the left-turn traffic from the off-ramps will occupy the space whether signalized or not.

Furthermore, this signal operation needs two controllers and optimizes traffic signal operations manually.

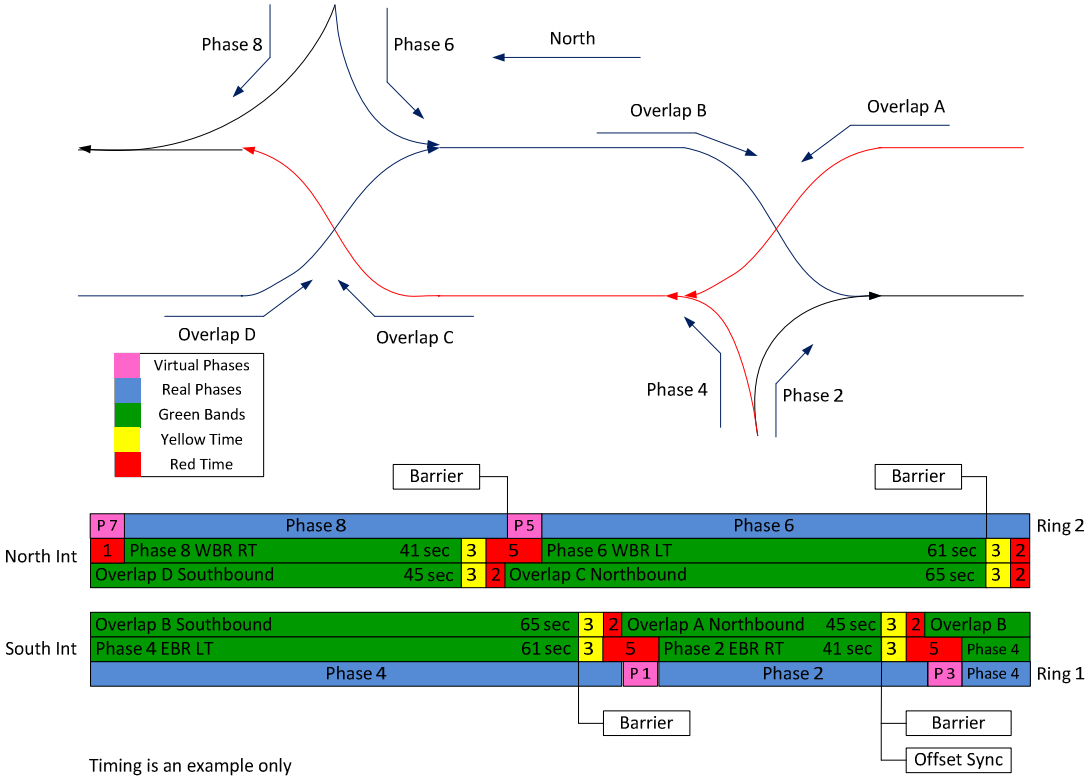

Figure 5-4 Traffic Signal Operation Proposed by MoDOT – Option 2

5.2.4 Current Operation 4

Edara et al. proposed a traffic operation shown in Figure 5-5 and tested in a VISSIM simulation model *(7)*. This phasing scheme was only tested based on fixed-time operation. It applied overlaps to control the DDI for reducing its traffic delay. The phase numbering also appears to be inconsistent to the National Electrical Manufacturers Association (NEMA) designations. For example, Phases 1 and 5 appear to be conflicting movements in the diagram of this study.

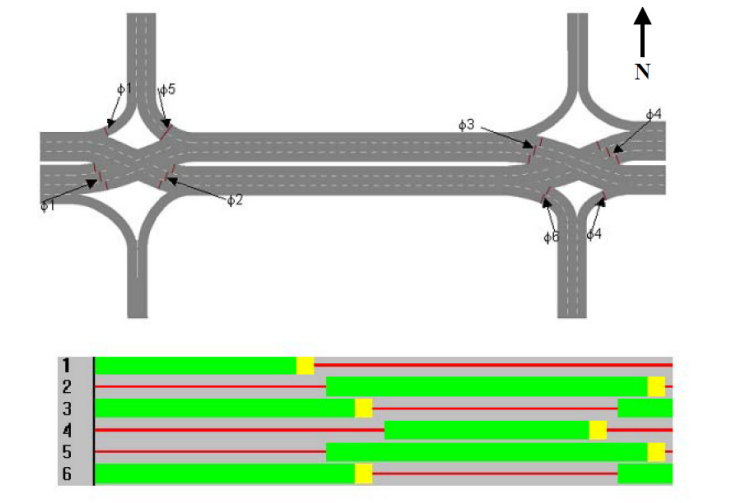

Figure 5-5 A DDI Phasing Scheme in VISSIM Developed by Edara et al.

5.2.5 Current Operation 5

This operational scheme was developed by John Baker from the City of Reno in 2012. It is a simple operation for a traffic engineer to grasp. This operation is suitable for a DDI that involves a heavy right-turn movement at the southbound off-ramp, which no-turn-on-red is allowed due to the dual-lane geometry. This right-turn movement needs to be on a protected phase. This scheme has been successfully tested in a hardware-in-the-loop platform in September, 2012 (Appendix A).

This initial phasing scheme has two overlaps: one overlap consists of phases 2 and 3; the other contains phases 4 and 6. For purposes of this research, this phasing scheme was modified by adding phase 1 into the overlap of phases 4 and 6 as shown in Figure 5-6 and Figure 5-7. This phasing scheme consists of five phases (phase 1, 2, 3, 4, and 6). The phase 4 (eastbound through) and phase 2 (northbound left) movements are guaranteed not to stop between the signals; however, the southbound left-turn movement and the

westbound through movement will experience some stops in the later part of the phases. In general, the phase 4's duration should be sufficient to handle the southbound off-ramp right-turn movement demand without phase 1. The consequence of including phase 1 is a slightly longer cycle length during coordination; however, it does not appear to cause too many delays when cycle length is great.

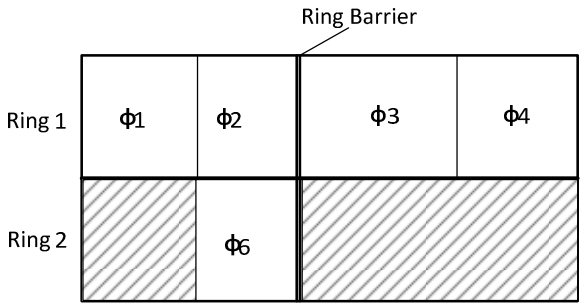

Figure 5-6 Phase, Ring, and Barrier Diagram by City of Reno

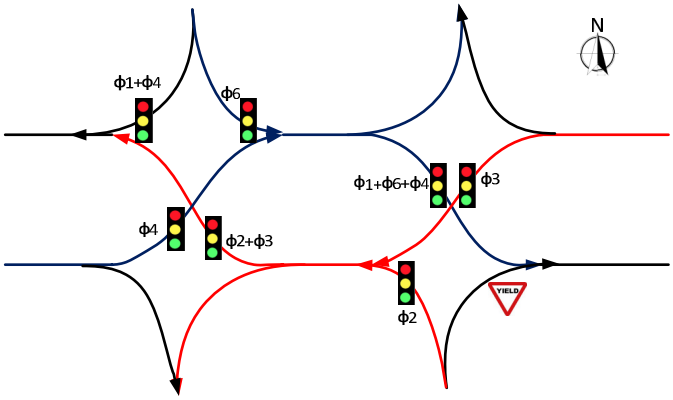

Figure 5-7 Phase Designation Diagram by City of Reno

5.2.6 Summary

Table 5-1 briefly summarizes each the advantages and disadvantages of the above DDI traffic signal operations schemes.

Table 5-1 Advantages and Disadvantages of Different DDI Phasing Schemes

Signal Operations	**Control Type(s) Allowed**	**Overlap(s) Applied**	**Advantages**	**Disadvantages**
Operation 1	• Pre-Timed • Fully Actuated • Semi-Actuated • Coordinated Actuated	No	• Simple • Short cycle length • Short lost time • Suitable for many traffic control types	• Does not apply if off-ramp is signalized • Cannot avoid vehicle stopping between the two crossovers
Operation 2	• Only Pre-Timed being Applied and Tested	Yes	• Simple and low loss time • Efficient by using overlaps • Clears the through traffic between the crossovers	• Is not applicable when off-ramp left-turn is signalized
Operation 3	• Only Pre-Timed being Applied and Tested	Yes	• Clears the through traffic between the crossovers • Efficient by using overlaps • Decreases off-ramp left turn delays by using overlaps	• Off-ramp left turns stop between the crossovers • Part of off-ramp left turn traffic stops twice to pass through the entire DDI
Operation 4	• Only Pre-Timed being Applied and Tested	Yes	• Reduces total delay by using overlaps • Clears the through traffic between the crossovers	• Most off-ramp left turns stop twice • Only a concept tested in simulation which may not work with standard controller
Operation 5	• Pre-Timed • Fully Actuated • Semi-Actuated • Coordinated Actuated	Yes	• Reduces the total delay by using phase overlaps • Clears the through traffic in the space between the crossovers • Reduces operational costs by using a	• Phase 1 may not be necessary and can result in waste of green time, since the southbound right-turn demand can generally be accommodated by phase 4

			single traffic signal controller • Suitable for many traffic control types	• Arterial through vehicles towards the end of the phase may be stopped at the second signal • Less efficient for off-ramp left-turn movements because they cannot be released until the arterial phases terminate • Fails to consider the effects of traffic route volume on signal operations

5.3 PROPOSED SIGNAL OPERATIONS

This section introduces the three major types of proposed operations. Proposed operation 1 is a three phase signal timing scheme used for controlling the DDI left-turn off-ramps by "yield" signs. Proposed operation 2 controls DDI traffic using signal-controlled off-ramps and a signal timing scheme involving seven phases and one dummy phase. Proposed operation 3 is a GA-based methodology to optimize signal timing parameters according to the specific existing phasing schemes.

5.3.1 Proposed Operation 1

Proposed operation 1 is developed for the situations when off-ramp left-turn traffic is relatively low. Three signal phases are applied for controlling all traffic movements shown in Figure 5-8 and Figure 5-9. Unlike the pre-timed only traffic signal operation presented by MoDOT, the proposed phasing scheme can run all control types: pre-timed, semi-actuated, fully actuated, and coordinated actuated. Phase 1 is fixed, and is

approximately equal to the travel time between the two signals at nodes “8” and “7” (or between “7” and “8”) as demonstrated in Figure 5-10. Phase 1 must run in each cycle, therefore it should be set to maximum recall in a traffic signal controller. Phases 4 and 3 serve eastbound and westbound movements separately. Each split of phases 4 and 3 depends on the traffic demands and saturation flow rates of the related traffic movements. Phase 1 allows these two through movements to travel simultaneously in the space between the two crossovers. The overlap of phases 3 and 1 clears up through traffic moving to west by adding an additional travel time of phase 1 to phase 3. However, the vehicles coming in late during phase 4 can pass through node “8” but cannot get through the second node “7.” This will cause more delays for these vehicles since they have to wait for the next green signal. Therefore, the presented phasing sequence shown in Figure 5-8 services westbound traffic better than eastbound with the same phasing split. Selecting phasing sequence becomes necessary for further increasing the efficiency of proposed operation 1. Thus, this section presents a method of choosing phasing sequence for this operation as well.

Proposed operation 1 includes two major types of signal timing plans: proposed operation 1-a and proposed operation 1-b. Proposed operation 1-a, also called movement volume based proposed operation 1, allocates its green time for critical lane groups on the basis of their volume and capacity. Proposed operation 1-b, also called origin-destination (O-D) volume based proposed operation 1, allocates its green time according to the capacity of each lane group and the traffic volume on routes among O-D pairs of a DDI.

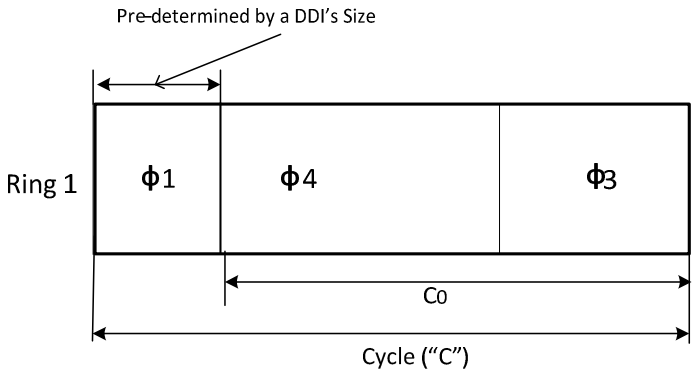

Figure 5-8 Phase Scheme for Proposed Operation 1

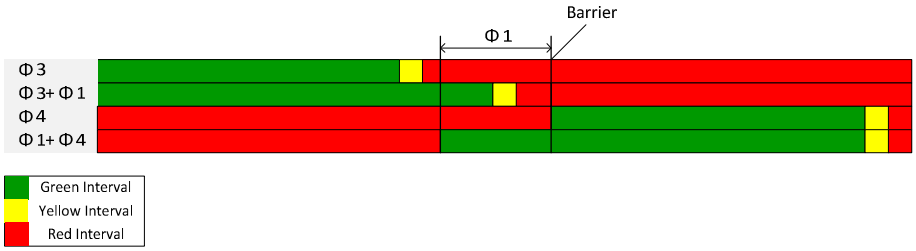

Figure 5-9 Phases and Overlaps in Traffic Signal Operation 1

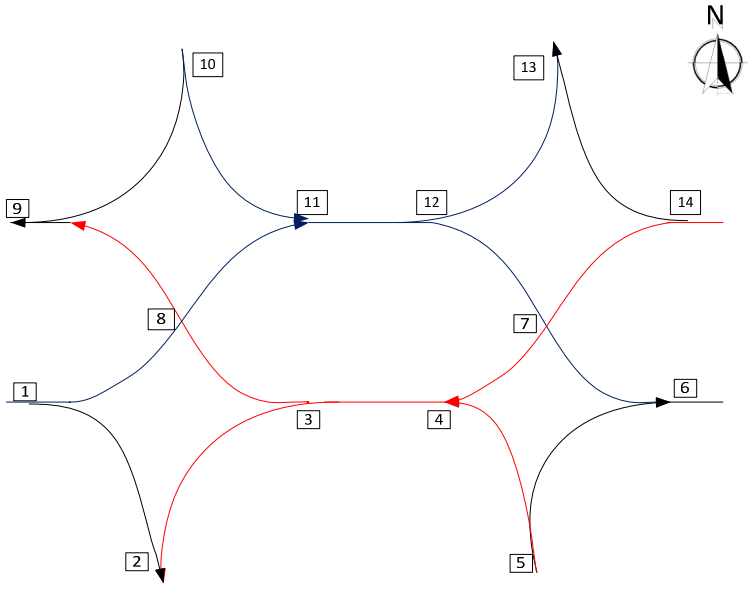

Figure 5-10 Identifications for Nodes of a DDI

5.3.1.1 Proposed Operation 1-a

Proposed operation 1-a is used for controlling two types of DDIs as shown in Figure 5-11 and Figure 5-12. The type 1 DDIs have light off-ramp left-turn and right-turn traffic. Under this condition, all traffic exiting from a freeway are controlled by yield signs shown in Figure 5-11. The type 2 DDIs, unlike the type 1 DDIs, have heavy off-ramp right-turn traffic but low left-turn traffic. Its signal timing plan is depicted in Figure 5-12. Since the phasing schemes of these two types of DDIs are similar, this research first introduces the methodology to determine the type 1 DDIs' signal timing parameters. After that, a methodology to search for type 2 DDIs' parameters is provided through minor adjustments to the type 1 methodology. The traffic signal parameters for the DDIs include cycle length as well as each phase's yellow interval, all red interval, split, and green time.

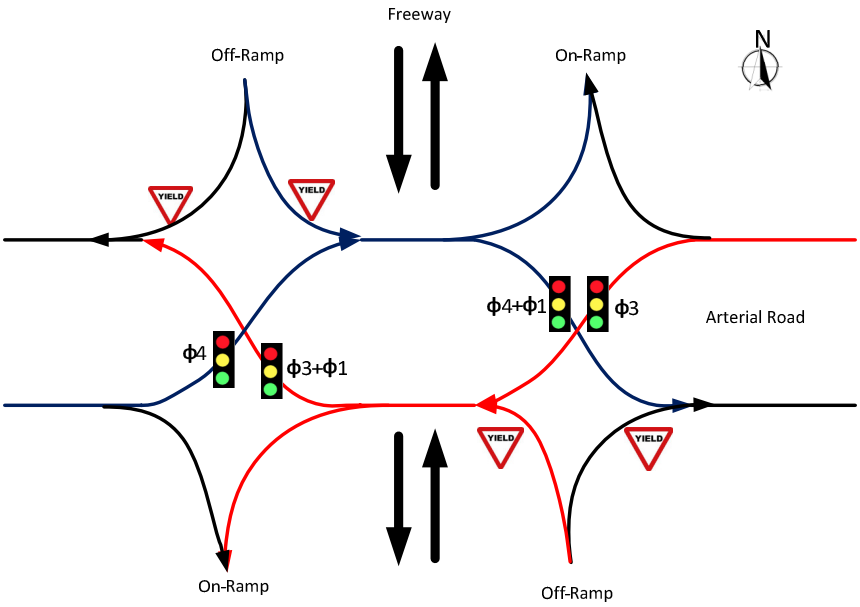

Figure 5-11 Traffic Signal Operation 1-a for a Type 1 DDI

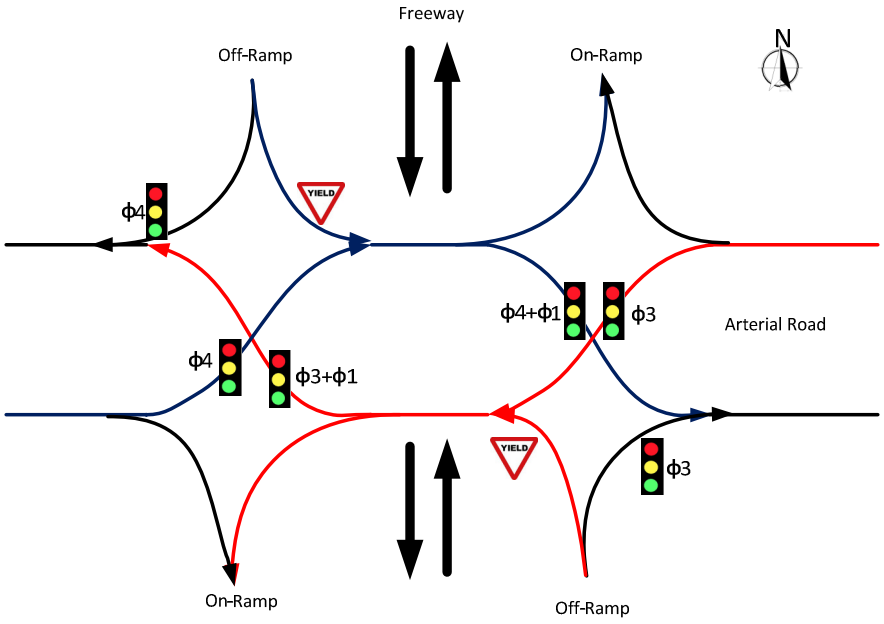

Figure 5-12 Traffic Signal Operation 1-a for a Type 2 DDI

Currently, searching for an optimal traffic signal timing plan for DDIs is complex. As mentioned above, no methodologies exist for providing optimal signal operations for DDIs. Most traffic professionals select their solutions manually. However, the proposed operation 1 is a quantitative methodology to choose traffic operation parameters based on the similar principles of Webster's methodology shown in Equation (3-1).

1) Assumptions and Principles

Like Webster's method, two major assumptions must be guaranteed when developing a reasonable signal timing plan for a pre-timed signal. One is that the volume-to-capacity (v/c) ratios for critical lane groups must be equal. Another is that the green time allocated to each phase is assumed to be in proportion to the saturation flow rate of the critical lane

group. In addition, non-critical phases are assigned with the same value of their non-conflicting critical phases.

2) Cycle Length

Based on the signal configuration and phases shown in Figure 5-8, Figure 5-9, and Figure 5-11, the traffic signal timing parameters of a DDI satisfy the relationship shown in the equation below.

$$g_3 + g_4 = C_0 + T_{8,11,12,7} + T_{7,4,3,8} - L = C_0 + 2 * T_{8,7} - L \quad (5\text{-}1)$$

where

g_3: effective green time of phase 3 (s);

g_4: effective green time of phase 4 (s);

C_0: sum of splits of phases 3 and 4 shown in Figure 5-8 (s);

$T_{8,11,12,7}$: split of phase 1, fixed and determined by the travel time between the two crossovers "8" and "7" through the nodes "8," "11," "12," and "7" as shown in Figure 5-10 (s);

$T_{7,4,3,8}$: split of phase 1, fixed and determined by the travel time between the two crossovers "7" and "8" through the nodes "7," "4," "3," and "8" as shown in Figure 5-10 (s);

$T_{8,7}$: split of phase 1, fixed and determined by the travel time between the two crossovers "7" and "8", usually equal to $T_{8,11,12,7}$ and $T_{7,4,3,8}$ (s); and

L: lost time per cycle (s).

Phase capacity for each critical lane group can be obtained by the following formula:

$$c_i = s_i * \frac{g_i}{C_e} \tag{5-2}$$

where

i: number of critical phases;

c_i: phase capacity (veh/h);

s_i: saturation flow rate for lane group i (veh/h); and

C_e: effective cycle length for all critical lane groups (s).

Volume to capacity ratio for each critical lane group is calculated by the following equation :

$$x_i = \frac{v_i}{c_i} = \frac{v_i}{s_i * (\frac{g_i}{C_e})} = \frac{v_i}{s_i} * \frac{C_e}{g_i} \tag{5-3}$$

Then

$$g_i = \frac{v_i}{s_i} * \frac{C_e}{x_i} \tag{5-4}$$

For this type of DDI, theoretical effective cycle length for the two critical lane groups (eastbound and westbound) satisfy the following relationship with C_0:

$$C_e = C_0 + 2 * T_{8,7} \tag{5-5}$$

Replace the g_3, g_4, and C_0 in Equation (5-1) by Equations (5-4) and (5-5), and it comes to:

$$\sum_i^N \frac{v_i}{s_i} * \frac{C_e}{x_i} = C_e - L \tag{5-6}$$

Then, based on the assumption, $X = x_i = x_j$ for $i \neq j$, the effective cycle length is:

$$C_e = \frac{L}{1-\frac{\sum_i^N \frac{v_i}{s_i}}{X}} = \frac{L}{1-\frac{\sum_i^N y_i}{X}} = \frac{L}{1-\frac{Y}{X}} \tag{5-7}$$

where

y_i: flow ratio for critical lane group y_i; and

Y: sum of flow ratios.

For this traffic signal timing plan, the total lost time is:

$$L = \sum_{i=3}^{N=4} l_i \tag{5-8}$$

$$l_i = l_{s,i} + l_{c,i} = l_{s,i} + Y_i + AR_i - e_i \tag{5-9}$$

where

l_i: lost time of critical lane group i (s);

$l_{s,i}$: start-up lost time of critical lane group i (s);

$l_{c,i}$: clearance lost time of critical lane group i (s);

Y_i: yellow interval of critical lane group i (s);

AR_i: all-red interval of critical lane group i (s); and

e_i: extension of effective green time of critical lane group i (s).

Figure 5-13 illustrates the relationship among actual green, lost-time elements, extension of effective green, and all-red interval. Messer et al. had found the start-up lost time and

extension of effective green time are nearly identical, and typically 2 sec *(16)*. Thus, the relationship shown in Equation (5-9) can be modified to the following equation:

$$l_i = l_{s,i} + Y_i + AR_i - e_i = 2 + Y_i + R_i - 2 = Y_i + AR_i \quad (5\text{-}10)$$

When the total lost time (L), the sum of flow ratios of critical lane groups (Y), and expected v/c ratio for all critical lane groups (X, usually pre-determined based on traffic professionals' expectations) are obtained, the cycle length of this DDI can be determined by the relationship shown in Equation (5-7).

The real cycle length shown in Figure 5-8 can also be found through subtracting the effective cycle length by phase split 1, and expressed as:

$$C = C_e - T_{8,7} = \frac{L}{1-\frac{Y}{X}} - T_{8,7} \quad (5\text{-}11)$$

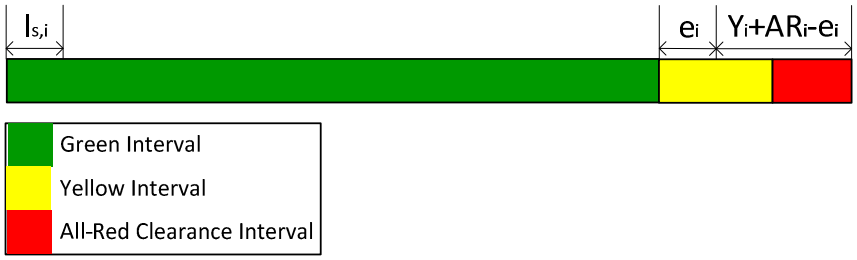

Figure 5-13 Relationship among Actual Green, Lost-Time, Extension of Effective Green, and All-Red

3) Effective Green Times and Phase Splits

Effective green times of phases 3 and 4 can be calculated by:

$$g_i = \frac{y_i}{\sum_i^N y_i} * (C_e - L) \quad (5\text{-}12)$$

The phase 1 green time is:

$$g_1 = \emptyset_1 - Y_1 - AR_1 \tag{5-13}$$

where

$\emptyset_1$: equals to $T_{8,7}$ (s).

The green times of phases 3 and 4without including phase 1 in each of them illustrated in Figure 5-8 can be obtained by:

$$g_i' = g_i - \emptyset_1 \tag{5-14}$$

where

g_i': green time for phase i without including phase 1 ($i = 3, 4$).

The phase splits 3 and 4 without including phase 1 in each of them are:

$$\emptyset_i = g_i + Y_i + AR_i \tag{5-15}$$

The above equations can also be used for determining the traffic signal timing parameters for DDIs shown in Figure 5-12. The critical phase 3 should be determined by two traffic lane groups: the westbound through lane group at crossover "7" and the northbound right-turn lane group at node "6." The critical flow ratio of phase 4 must be subjected to the larger of the two lane groups: the eastbound through lane group at crossover "8" and the southbound right-turn lane group at node "9." The y_i in Equation (5-7) can be replaced by:

$$y_3 = max\{\frac{v_{3,14,7}}{s_{3,14,7}}, \frac{v_{3,5,6}}{s_{3,5,6}}\} \tag{5-16}$$

$$y_4 = max\{\frac{v_{4,1,8}}{s_{4,1,8}}, \frac{v_{4,10,9}}{s_{4,10,9}}\} \quad (5\text{-}17)$$

where

$v_{3,14,7}$: traffic volume of lane group between nodes "14" and "7" (veh/h);

$s_{3,14,7}$: saturation flow rate of lane group between nodes "14" and "7" (veh/h);

$v_{3,5,6}$: traffic volume of lane group between nodes "5" and "6" (veh/h);

$s_{3,5,6}$: saturation flow rate of lane group between nodes "5" and "6" (veh/h);

$v_{4,1,8}$: traffic volume of lane group between nodes "1" and "8" (veh/h);

$s_{4,1,8}$: saturation flow rate of lane group between nodes "1" and "8" (veh/h);

$v_{4,10,9}$: traffic volume of lane group between nodes "10" and "9" (veh/h); and

$s_{4,10,9}$: saturation flow rate of lane group between nodes "10" and "9" (veh/h).

Following Equations (5-11) through (5-15), all the traffic signal timing parameters can be found similarly for this type of DDI.

5.3.1.2 Proposed Operation 1-b

The above methods are based on the traffic volume of critical lane groups. However, they do not include the traffic volume of critical routes. For an example, the DDI depicted in Figure 5-14 shows one scenario where 80% of eastbound traffic passes through crossover node "8" and turns to the northbound on-ramp while only 20% of the remaining eastbound traffic continues through the second crossover intersection to the east. The scenario shown in Figure 5-15 presents a similar condition to Figure 5-14, except that

20% of eastbound traffic passing through crossover node "8" turns left to enter the freeway while the remaining 80% travels through crossover node "7" to continue east. According to proposed operation 1-a, the traffic signal timing plans between these two scenarios would have no differences, as critical movement volumes do not change. In fact, the traffic signal timing plans for these two scenarios should be different. Therefore, the traffic signal timing plan based on critical routes is presented specifically for DDIs to distinguish the volume scenarios shown in Figure 5-14 and Figure 5-15.

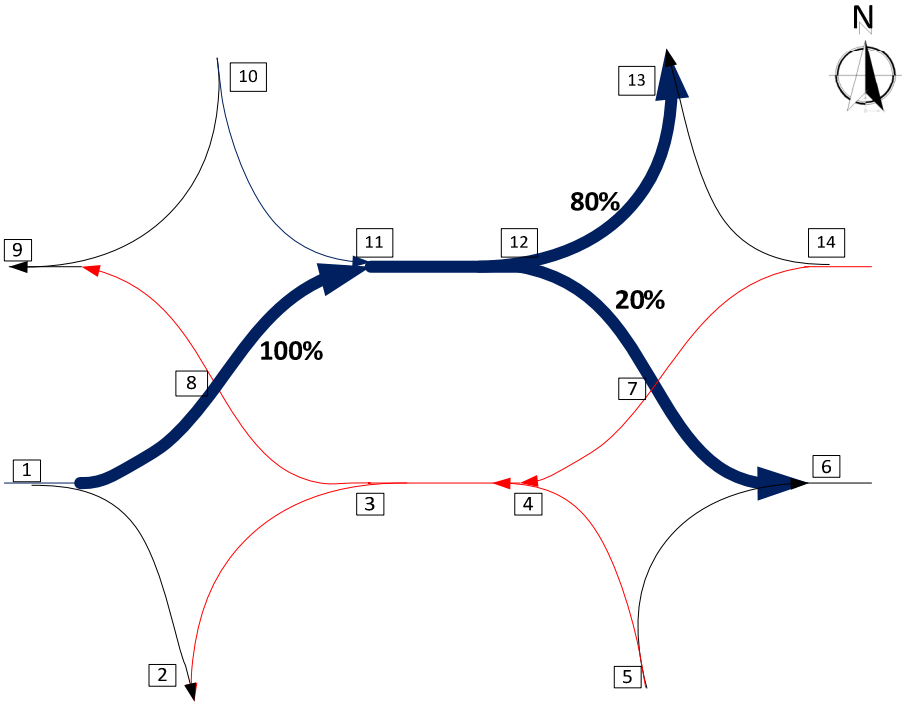

Figure 5-14 Traffic Distribution Scenario 1

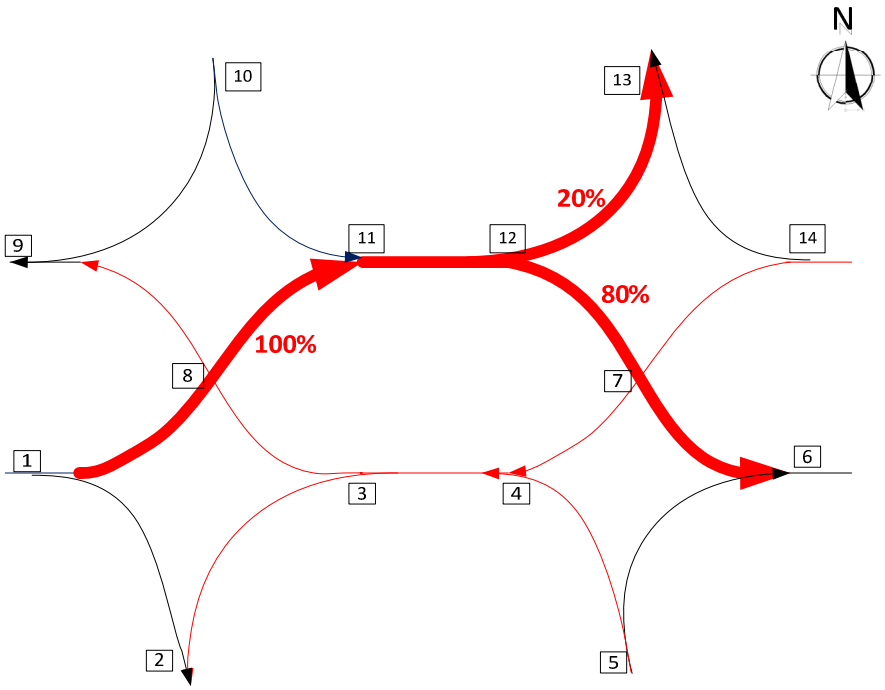

Figure 5-15 Traffic Distribution Scenario 2

This signal timing development process consists of two major steps: the traffic signal timing without considering the critical routes and the green extensions for traffic demand based on critical routes.

1. Traffic Signal Timing Without Considering the Critical Routes

The traffic signal timing without considering the critical routes is exactly same as proposed operation 1-a. Assume the traffic cycle length, phase splits, and green times have been found through the above processes. Unlike typical four-leg intersections, DDIs have greater space between two crossover intersections, so that the signal cycle length found through Equation (5-11) is possibly less than the signal cycle length required in practice.

2. Extensions According to the Traffic Volumes of Critical Routes

An additional green extension should be added for serving the through traffic, to allow as much as possible to pass through the two crossovers. However, the exact extension is difficult to determine since traffic is a non-linear and dynamic process of many factors, such as the capacity of critical lane groups, the traffic volume of each route, the space between two crossovers, cycle length, and green times. This study introduces a linear method for determining the extension. This method contains such factors as the space between the two crossovers, traffic flow ratio of critical lane groups, and the traffic counts of several critical routes.

1) The Length of Total Extension

An extension based on traffic distribution scenario 2 (shown in Figure 5-15) should be greater than an extension based on traffic distribution scenario 1 (shown in Figure 5-14), since scenario 2 has a greater proportion of eastbound through traffic. The extension should also increase when the westbound through traffic rises. Therefore, the total extension is expressed as:

$$E = T_{8,11,12,7} * max\left\{1, \frac{s_{1,8}}{s_{12,7}}\right\} * \frac{v_{8,11,12,7}}{v_{1,8}} + T_{7,4,3,8} * max\left\{1, \frac{s_{14,7}}{s_{3,8}}\right\} * \frac{v_{7,4,3,8}}{v_{14,7}} \quad (5\text{-}18)$$

where

$s_{1,8}$: saturation flow rate of lane group between nodes "1" and "8" (veh/h);

$s_{12,7}$: saturation flow rate of lane group between nodes "12" and "7" (veh/h);

$v_{8,11,12,7}$: traffic counts on the route passing through "8," "11," "12," and "7" (veh/h);

$v_{1,8}$: traffic counts on the routes passing through "1" and "8" (veh/h);

$s_{14,7}$: saturation flow rate of lane group between nodes "14"and "7" (veh/h);

$s_{3,8}$: saturation flow rate of lane group between nodes "3" and "8" (veh/h);

$v_{7,4,3,8}$: traffic counts on the route passing through "7," "4," "3," and "8" (veh/h); and

$v_{14,7}$: traffic counts on the routes passing through "14" and "7" (veh/h).

2) Extension for Each Phase

The extension for phase 4 relies on the flow ratio of the critical lane group between nodes "1" and "8;" and the percentage of through traffic on the route passing nodes "8," "11," "12," and "7." In addition, the same factors in the opposite direction can affect the extension for phase 4. The phase 4 extension can be determined by the following formula:

$$E_4 = E * \left(\frac{\frac{y_4}{\sum_{i=3}^{N=4} y_i} * T_{8,11,12,7} * \max\left\{1, \frac{s_{1,8}}{s_{12,7}}\right\} * \frac{v_{8,11,12,7}}{v_{1,8}}}{\frac{y_4}{\sum_{i=3}^{N=4} y_i} * T_{8,11,12,7} * \max\left\{1, \frac{s_{1,8}}{s_{12,7}}\right\} * \frac{v_{8,11,12,7}}{v_{1,8}} + \frac{y_3}{\sum_{i=3}^{N=4} y_i} * T_{7,4,3,8} * \max\left\{1, \frac{s_{14,7}}{s_{3,8}}\right\} * \frac{v_{7,4,3,8}}{v_{14,7}}} \right) \quad (5\text{-}19)$$

Similarly, the phase 3 extension can be calculated through the following equation:

$$E_3 = E * \left(\frac{\frac{y_3}{\sum_{i=3}^{N=4} y_i} * T_{7,4,3,8} * \max\left\{1, \frac{s_{14,7}}{s_{3,8}}\right\} * \frac{v_{7,4,3,8}}{v_{14,7}}}{\frac{y_4}{\sum_{i=3}^{N=4} y_i} * T_{8,11,12,7} * \max\left\{1, \frac{s_{1,8}}{s_{12,7}}\right\} * \frac{v_{8,11,12,7}}{v_{1,8}} + \frac{y_3}{\sum_{i=3}^{N=4} y_i} * T_{7,4,3,8} * \max\left\{1, \frac{s_{14,7}}{s_{3,8}}\right\} * \frac{v_{7,4,3,8}}{v_{14,7}}} \right) \quad (5\text{-}20)$$

or

$$E_3 = E - E_4 \tag{5-21}$$

5.3.1.3 Optimal Phasing Sequence

The above processes present the methodologies for determining the traffic signal timing parameters, including cycle length and phase splits, for a DDI. In fact, phasing sequence is also one of the major parameters for traffic signal operation. According to the phasing scheme characteristics in proposed operation 1, two kinds of phasing sequences are "phases 1+4 -> +1" (shown in Figure 5-8) and "phases 1+3 -> 4+1" (shown in Figure 5-16). Under "phases 1+4 -> 3+1," phases 1 and 4 serve the eastbound traffic (traffic from node "1" through nodes "8," "11," and "12" to "7" and "13"); phases 3 and 1 serve the westbound traffic (traffic from node "14" through nodes "7," "4," and "3" to "8" and "2") shown in Figure 5-10. Since phase 1 starts before phase 4, the vehicles coming in late during the phase 4 at the first crossover cannot pass through the following crossover since they have to travel at least $T_{8,11,12,7}$ s before approaching at this crossover. Therefore, these vehicles have to stop in front of the second crossover and wait for the next green. However, the westbound traffic from node "14" can pass through nodes "7," "4," and "8" smoothly to node "9" for the additional phase 1 following phase 3. The phasing sequence "1+3->4+1" has the opposite effect of the phasing sequence "1+4->3+1". Given these sequences, this study introduces a methodology for selecting a phase sequence for traffic signal timing plan at DDIs with three phase of operation: phases 1, 3, and 4. A flowchart describing this methodology is shown in Figure 5-17. If $PSM > 1.0$,

select phasing sequence "1+4 -> 3+1" as shown in Figure 5-16; otherwise select phasing sequence "1+3 -> 4+1" as shown in Figure 5-8.

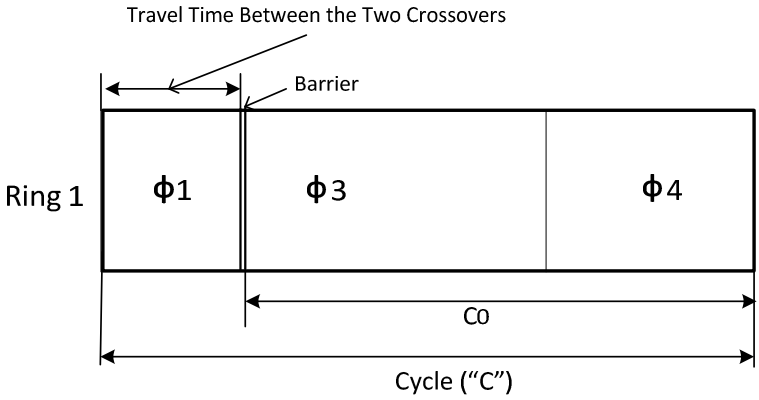

Figure 5-16 Phase sequence 1+3 -> 4+1

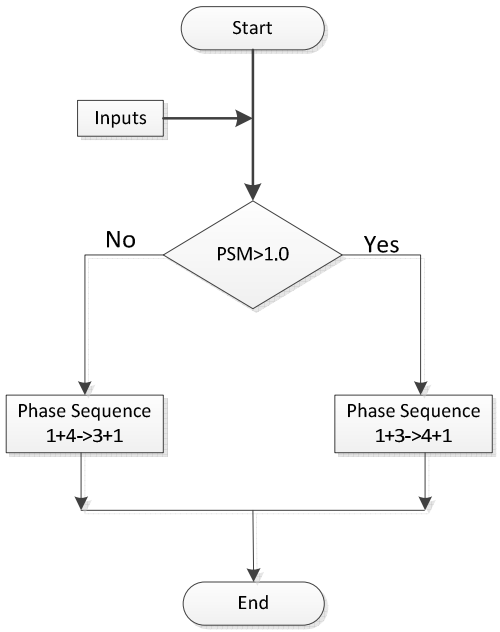

Figure 5-17 Process of phase sequence for three phase operation of DDIs

The lagging phase 1 in the overlaps can serve the heavier traffic demand on the second crossover. The phase selection methodology is based on the following calculations:

$$PSM = \frac{c_{1,8} * Pert_{8,11,12,7} * s_{12,7}}{c_{14,7} * Pert_{14,7,4,3,8} * s_{3,8}} \quad (5\text{-}22)$$

$$Pert_{8,11,12,7} = \frac{v_{8,11,12,7}}{v_{1,8}} \quad (5\text{-}23)$$

$$Pert_{14,7,4,3,8} = \frac{v_{7,4,3,8}}{v_{14,7}} \quad (5\text{-}24)$$

$$c_{1,8} = \frac{s_{1,8} * g_{1,8}}{C_e} = \frac{s_{1,8} * y_{1,8} * \frac{C_e}{X_{CI}}}{C_e} = \frac{s_{1,8} * y_{1,8}}{X_{CI}} = \frac{v_{1,8}}{X_{CI}} \quad (5\text{-}25)$$

$$c_{14,7} = \frac{s_{14,7} * g_{14,7}}{C_e} = \frac{s_{14,7} * y_{14,7} * \frac{C_e}{X_{CI}}}{C_e} = \frac{s_{14,7} * y_{14,7}}{X_{CI}} = \frac{v_{14,7}}{X_{CI}} \quad (5\text{-}26)$$

where

$c_{1,8}$: capacity of lane group from nodes "1" to "8" (veh/h);

$c_{14,7}$: capacity of lane group from nodes "14" to "7" (veh/h);

$y_{1,8}$: flow ratio of lane group from nodes "1" to "8";

$y_{14,7}$: flow ratio of lane group from nodes "14" to "7";

Thus, Equation (5-22) can be expressed in a simple way:

$$PSM = \frac{v_{8,11,12,7} * s_{12,7}}{v_{7,4,3,8} * s_{3,8}} \quad (5\text{-}27)$$

Equation (5-27) reveals that the phasing sequence of proposed operations 1-a and 1-b is determined by the eastbound traffic volume $v_{8,11,12,7}$ and westbound traffic volume $v_{7,4,3,8}$ as well as saturation flow rates $s_{12,7}$ and $s_{3,8}$. It has no relationship with other parameters such as cycle length and phase splits.

5.3.1.4 Route Traffic Counts

Since traffic counts on each route are one of the inputs for the traffic signal timing plans of DDIs, a practical way to collect traffic route counts becomes important. However, traffic counts on routes in a road network are usually much harder and more time consuming to collect than traffic turning volumes of each intersection. Fortunately, the traffic counts on every route of a DDI can be exactly determined when the traffic turning volumes are collected in the field.

5.3.1.4.1 Relationship between Route Traffic Counts and Turning Volumes

In general, routes between origins and destinations in a roadway network are not unique, even when the traffic counts of each turning movement at every intersection are fixed. For any given intersection, it is not easy to determine the proportion of traffic that came from an upstream intersection and where these vehicles are going to at the next downstream intersection. For example, the eastbound traffic at an intersection can come from the right-turn movement, or the through-movement, or the left-turn movement of its upstream intersection. However, most current traffic signal timing tools consider each intersection individually by using turning volumes. This may not cause large errors in common situations, since the turning traffic in the adjacent intersections varies slightly and does not have a large impact on overall operations as the through traffic dominates the timing However, there are many cases in which turning traffic may vary extremely even for two closely-spaced intersections. For some areas including freeway interchanges, such as CDIs and DDIs, it is much more critical than at other intersections to consider right-turn and left-turn vehicles. Under such conditions, traffic signal timing plans based

on turning volumes seems ill-suited to conduct analyses compared to using route traffic volumes.

Traffic signal timing based on O-D route traffic counts can overcome the weaknesses of the popular traffic signal timing tools. PTV AG, in its latest release VISSIM 5.40, is starting to provide optimized traffic signal timing plans based on O-D route distributions in a road network. PTV AG is simply applying the exhaustive searching methods to obtain the cycle length, offsets, phase splits, and phase sequences on the basis of its micro-simulation software VISSIM and VISSIG *(29)*. However, this function is limited to stage-based signal timing operations applications, and is not for National Electrical Manufacturers Association (NEMA) based operations. Furthermore, this tool does not have ability to optimize traffic signal operations for DDIs.

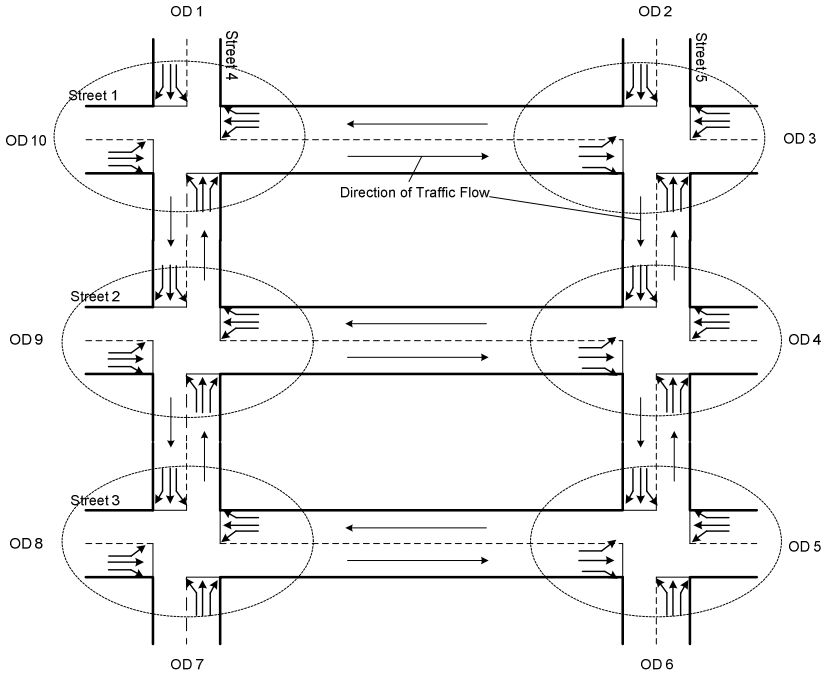

Figure 5-18 Traffic Turning Volumes as Inputs

Traffic system is a dynamic and stochastic process so that traffic route distributions are also a dynamic and stochastic process. Therefore, the exact description of traffic route distributions is beyond the scope of this study. In order to focus on the topic of this study, the following necessary assumptions are declared in this research:

1. Traffic route distributions are static;
2. No mid-segment entrances or exits exist in the road network; and
3. No loop routes in a road network.

Assume a road network has M horizontal streets and N vertical streets. The total O-D nodes are $D_{OD,M,N} = (M + N) \times 2$ and each node is denoted by $OD_{h,i,j}$ or $OD_{v,k,l}$ which will be explained below. The total intersections are $I_{M,N} = M \times N$ and each intersection is represented by $I_{m,n}$. The total number of one-direction links is determined by the following equation:

$$N_{L,M,N} = ((M + 1) * N + (N + 1) * M) * 2 = 2 * (M + N + 2 * M * N) \quad (5\text{-}28)$$

Assume O-D point $OD_{h,i,j}$ is connected with $OD_{v,k,l}$ by t routes in the network. Each route is determined by a succession of one-direction links with positive traffic counts. The t routes between point $OD_{h,i,j}$ and $OD_{v,k,l}$ can be expressed by the matrix as below;

$$T_{t,h,i,j,v,k,l,M,N} = \begin{bmatrix} f_{1,1} & \cdots & f_{1,p} & \cdots & f_{1,N_{L,M,N}} \\ f_{2,1} & \cdots & f_{2,p} & \cdots & f_{2,N_{LM,N}} \\ \vdots & \vdots & \vdots & \vdots & \vdots \\ f_{q,1} & \cdots & f_{q,p} & \cdots & f_{q,N_{L,M,N}} \\ \vdots & \vdots & \vdots & \vdots & \vdots \\ f_{t,1} & \cdots & f_{t,p} & \cdots & f_{t,N_{L,M,N}} \end{bmatrix} \quad (5\text{-}29)$$

where

$T_{t,h,i,j,v,k,l,M,N}$: volume matrix of one-direction links for t routes between points $OD_{h,i,j}$ and $OD_{v,k,l}$ assuming M horizontal streets and N vertical streets;

$OD_{h,i,j}$: O-D point which is determined by its subscript $h, i,$ and j;

h: 0-1 indicator of horizontal and vertical direction, $h = 0$ means the O-D point is at the horizontal streets, and $h = 1$ indicates the O-D point is at the vertical streets;

i: identification number of an O-D point in the street;

j: the 0-1 indicator of the position of the O-D point on the street, $j = 0$ means the O-D point is at the left end of the street when it is a horizontal street; and $j = 1$ indicates the O-D point is at the right end of the street when it is a horizontal street, $j = 0$ means the O-D point is at the top end of the street when they it is a vertical street, and $j = 1$ indicates the O-D point is at the bottom end of the street when it is a vertical street;

v: same as h;

k: same as i;

l: same as j; and

$f_{q,p}$: traffic counts at link p in the route q, $f_{q,p} \geq 0$, $1 \leq q \leq t$, and $4 \leq p \leq N_{L,M,N}$.

In theory, the total origin and destination pairs are:

$$N_{OD,M,N} = 4 * (M + N)^2 \tag{5-30}$$

The total origin and destination routes can be expressed by the following equation:

$$T_{N_{OD,M,N}} = \left[T_{t_1} \quad T_{t_2} \quad \cdots \quad T_{t_a} \quad \cdots \quad T_{t_{N_{OD,M,N}}}\right] \tag{5-31}$$

where

T_{t_a} : the a^{th} O-D pair routes which are expressed by Equation (5-29).

Thus, the $T_{N_{OD,M,N}}$ is a 2 dimensional matrix with $t_{max} \times (N_{OD,M,N} \times N_{L,M,N})$ elements entirely.

where

$$t_{max} = \max\{t_1, \cdots t_{N_{OD,M,N}}\} \tag{5-32}$$

Figure 5-19 shows a 3×2 road network as an example. Based on the above analysis, the total end nodes should be 10 (10=(3+2)*2) and the total intersections are 6 (6=3*2). The total one-direction links are:

$$N_{L,M,N} = 2 * (M + N + 2 * M * N) = 2 * (3 + 2 + 2 * 3 * 2) = 34 \tag{5-33}$$

The maximum origin and destination pairs are:

$$N_{OD,M,N} = 4 * (M + N)^2 = 100 \tag{5-34}$$

Table 5-2 demonstrates an example of the relationship between the southbound through movement at intersection $I_{1,1}$ with its route counts between the origin $OD_{1,1,0}$ and

destinations $OD_{0,2,0}$, $OD_{0,3,0}$, $OD_{1,1,1}$, $OD_{1,2,1}$, $OD_{0,3,1}$, and $OD_{0,2,1}$ as shown in Figure 5-19.

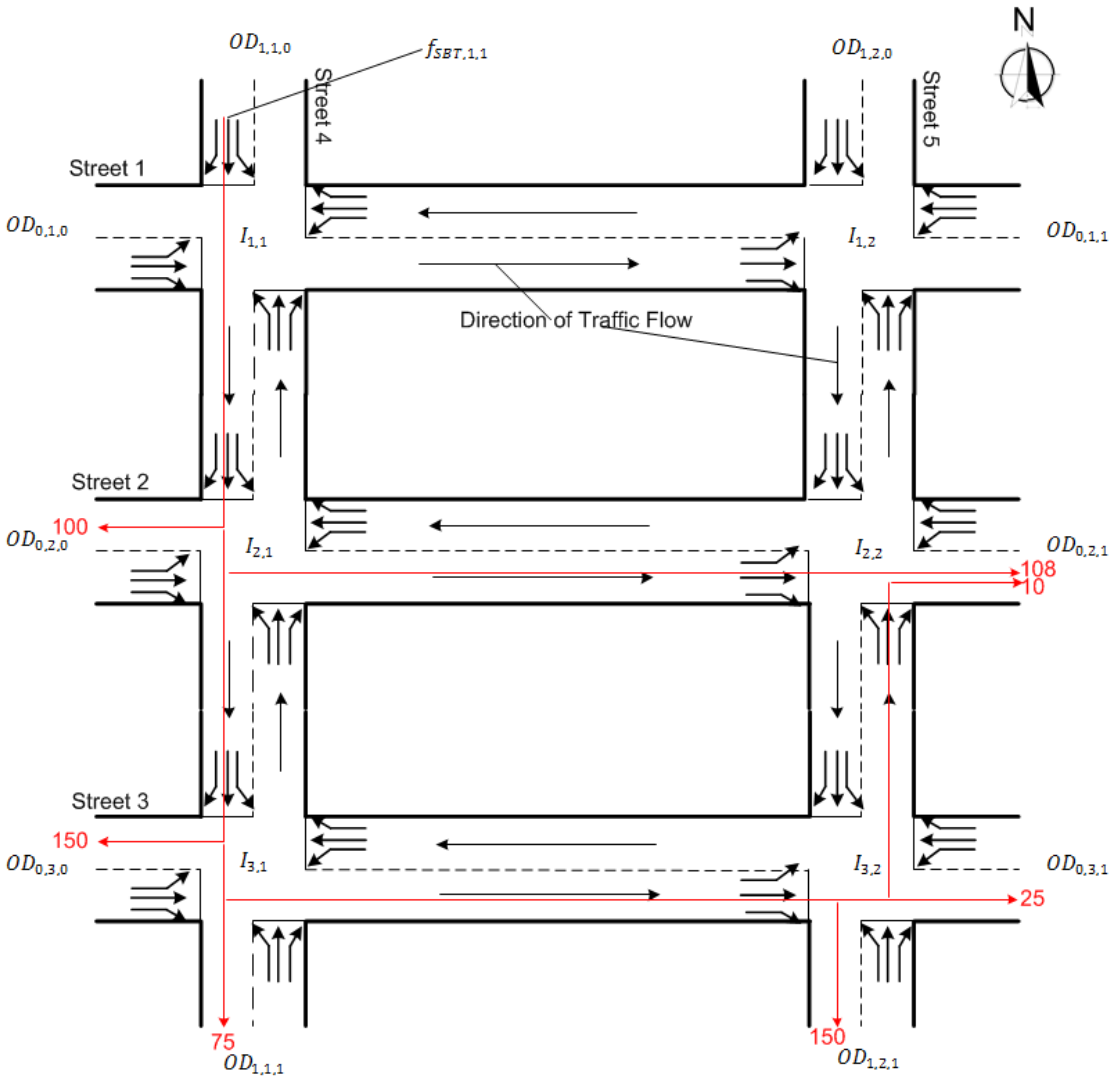

Figure 5-19 One Example of the Relationship between Turning Volume and Route Counts

Table 5-2 One Example of the Relationship between Turing Volume and Route Counts

Route ID	Origin	Destination	Route	Traffic Flow Rate (veh/hour)
1	$OD_{1,1,0}$	$OD_{0,2,0}$	$OD_{1,1,0}, I_{1,1}, I_{2,1}, OD_{0,2,0}$	100
2	$OD_{1,1,0}$	$OD_{0,3,0}$	$OD_{1,1,0}, I_{1,1}, I_{2,1}, I_{3,1}, OD_{0,3,0}$	150
3	$OD_{1,1,0}$	$OD_{1,1,1}$	$OD_{1,1,0}, I_{1,1}, I_{2,1}, I_{3,1}, OD_{1,1,1}$	75
4	$OD_{1,1,0}$	$OD_{1,2,1}$	$OD_{1,1,0}, I_{1,1}, I_{2,1}, I_{3,1}, I_{3,2}, OD_{1,2,1}$	150
5	$OD_{1,1,0}$	$OD_{0,3,1}$	$OD_{1,1,0}, I_{1,1}, I_{2,1}, I_{3,1}, I_{3,2}, OD_{0,3,1}$	25
6	$OD_{1,1,0}$	$OD_{0,2,1}$	$OD_{1,1,0}, I_{1,1}, I_{2,1}, I_{3,1}, I_{3,2}, I_{2,2}, OD_{0,2,1}$	10
7	$OD_{1,1,0}$	$OD_{0,2,1}$	$OD_{1,1,0}, I_{1,1}, I_{2,1}, I_{2,2}, OD_{0,2,1}$	108
The southbound through movement traffic flow rate $f_{SBT,1,1}$:				618

As the network with M horizontal streets and N vertical streets, the possible unknown traffic routes are between $N_{OD,M,N}$ and $t_{max} \times N_{OD,M,N}$, or between $4 * (M+N)^2$ and $t_{max} \times 4 * (M+N)^2$. The total turning movements can be collected is:

$$N_{TMF} = \sum_{i=1,j=1}^{i=M,j=N} N_{i,j} \tag{5-35}$$

where

N_{TMF}: total turning movements in a $M \times N$ road network;

$N_{i,j}$: total turning movements at intersection $I_{i,j}$ which is the crossing section of street i and street j;

The traffic volumes for each movement are the sum of traffic counts on each route which passes through the movement. The relationship between traffic movement volumes and traffic route counts can be expressed by the following equation.

$$f_{t,d,i,j} = \sum_{n=1}^{n=N_{OD,M,N}} \delta_n * f_n \quad (5\text{-}36)$$

where,

$f_{t,d,i,j}$: traffic movement volumes for type t, of d approach, at intersection (i,j), $t = 0$ means left-turn movement, $t = 1$ means through movement, $t = 2$ means right-turn movement, and $t = 3$ means U-turn movement; $d = 0$ indicates westbound approach, $d = 1$ indicates eastbound approach, $d = 2$ indicates southbound approach, and $d = 3$ indicatess northbound approach;

δ_n: δ_n=1 if route n passes through the movement, 0 otherwise; and

f_n: traffic flow rate at route n, $f_n \geq 0$.

According to Equations (5-31), (5-35), and (5-36), the total unknown variables (traffic route counts), noted as $N_{r,M,N}$ (between $4 * (M+N)^2$ and $t_{max} \times 4 * (M+N)^2$), have N_{TMF} linear constraints in mathematic view. Based on linear equation theory, there will be infinite route traffic count scenarios when the following condition is satisfied:

$$N_{r,M,N} > N_{TMF} \quad (5\text{-}37)$$

Otherwise, the route traffic counts can be uniquely determined by the traffic movement volumes, which can be easily collected in the field.

5.3.1.4.2 Traffic Count Collection for DDIs' O-D Routes

For the DDI shown in Figure 5-20, the total traffic turning movements (N_{TMF}) is 12 and the total unknown traffic routes $N_{r,M,N}$ is also 12. Based on the above analysis, the traffic route counts can be obtained exactly by all the traffic turning movements as highlighted in Figure 5-20. In other words, it is not necessary to collect traffic route counts directly for this DDI. Instead, traffic volumes can be gathered at the 12 turning movements shown in Table 5-3 and then linear equation methodology can be applied to solve the traffic route counts for each O-D pair shown in Table 5-4.

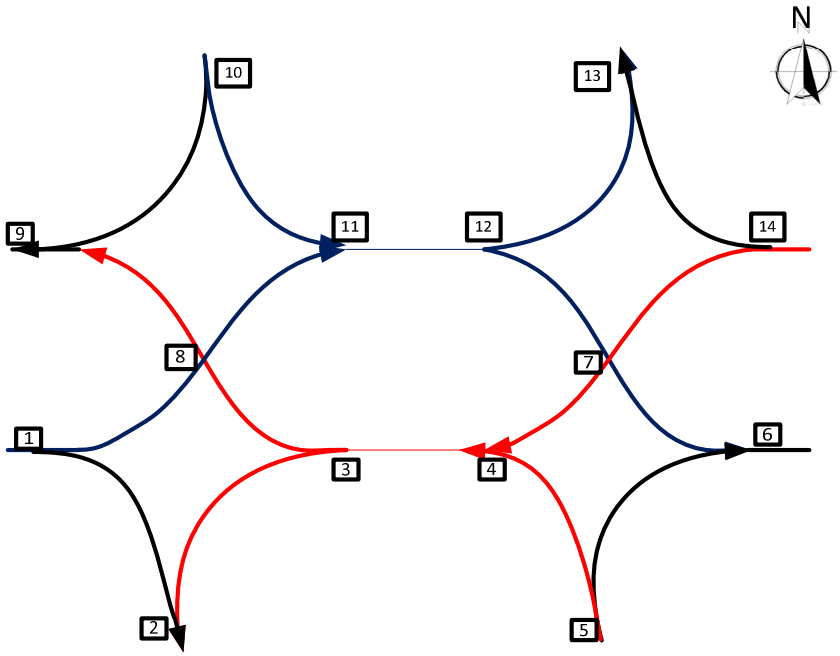

Figure 5-20 Traffic Turning Movements for Data Collection

Table 5-3 Turning Movements Needing to Volume Collection of a DDI

Traffic Movement ID	Origin	Destination
1	10	9
2	10	11
3	1	8
4	1	2
5	3	8
6	3	2
7	5	4
8	5	6
9	14	7
10	14	13
11	12	13
12	12	7

Table 5-4 Traffic Routes among all O-D Pairs of a DDI

Route ID	Origin	Via Nodes	Destination
1	10		9
2	10	11, 12	13
3	10	11, 12, 7	14
4	1	11, 12	13
5	1	11, 12, 7	14
6	1		2
7	5	4, 3, 8	9
8	5	4, 3,	2
9	5		6
10	14		13
11	14	4, 3, 8	9
12	14	4, 3,	2

5.3.2 Proposed Operation 2

5.3.2.1 Phasing Scheme

Proposed operation 1 discusses the traffic signal timing plans for DDIs without signalization of the left-turn traffic on the off-ramp. Proposed operation 2 illustrates a

general methodology of the traffic signal timing plans for DDIs with off-ramp left-turn traffic controlled by a signal.

Proposed operation 2 includes eight signal phases, as shown in Figure 5-21. Phases 1 and 5 have the same split that is approximately equal to the travel time ($T_{11,12,7}$ sec) between the two signals at locations "11" and "7" (or between "4" and "8") as depicted in Figure 5-10. Phases 1 and 5 should start and terminate at the same time; therefore both should be set to maximum recall with the same "Max 1" or "phase splits" in the controller settings. Using these two phases allows the southbound (SB) off-ramp to be released earlier by $T_{11,12,7}$ sec while still maintaining no stops at the next signal. This treatment adds an additional $T_{11,12,7}$ sec of green to the SB off-ramp. Phase 7 serves as the green extension for phase 2, which allows the vehicles entering late in phase 2 to pass through location "5" and get to location "8". These vehicles can then be served when phase 3 comes on, resulting in reduced delays for the northbound (NB) off-ramp traffic. In addition, Phase 7 is set to "Max Recall" for safety and its duration must be less than the minimum green of phase 4, which is set to be "Min Recall" in the controller. Phase 4 alone serves the southbound right-turn traffic. Other signal timing parameters will be discussed in the following section. Although Phase 8 does not specifically control any of the movements, having phase 8 with a "Min Recall" ensures phases 3 and 7 not to come on at the same as they are actually conflicting phases. Figure 5-22 shows the locations of phases in proposed operation 2 for a DDI. The SB off-ramp right turn traffic and the NB off-ramp right turn traffic are controlled by "yield" type. Figure 5-23 through Figure 5-27 demonstrates the active movements and their pertinent phases.

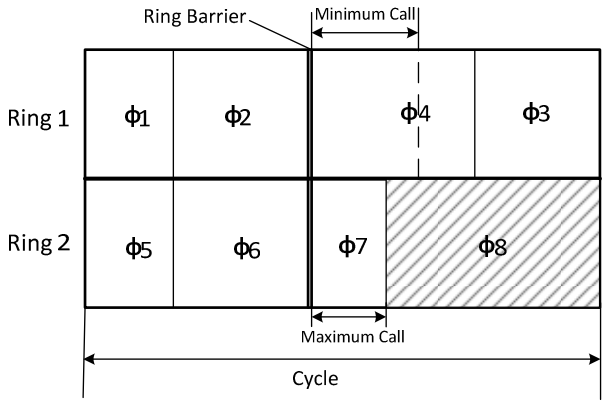

Figure 5-21 Phases, Rings, and Barrier for Proposed Operation 2

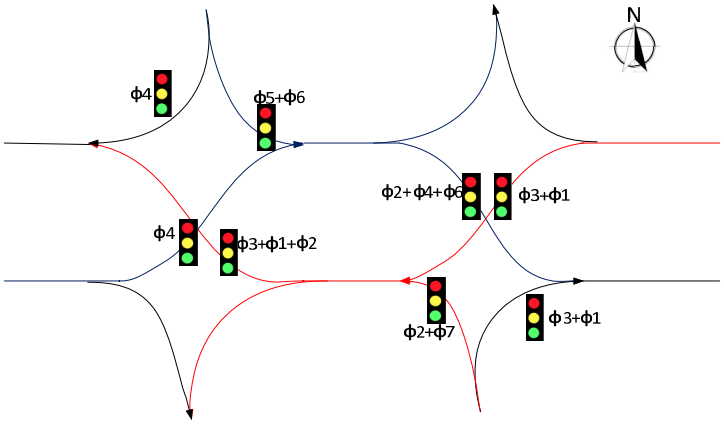

Figure 5-22 Phase Location Diagramfor Proposed Operation 2

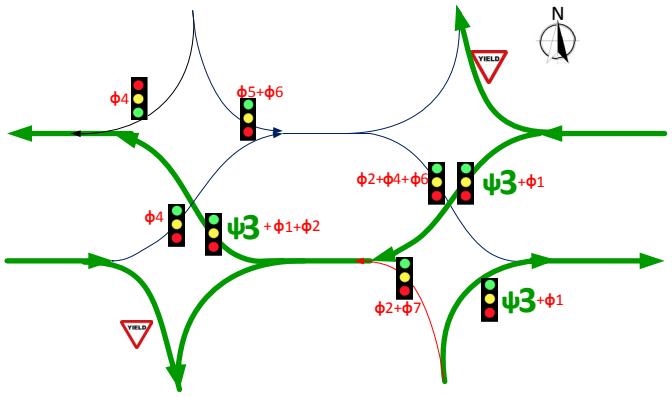

Figure 5-23 Active Traffic Movements at Phase 3

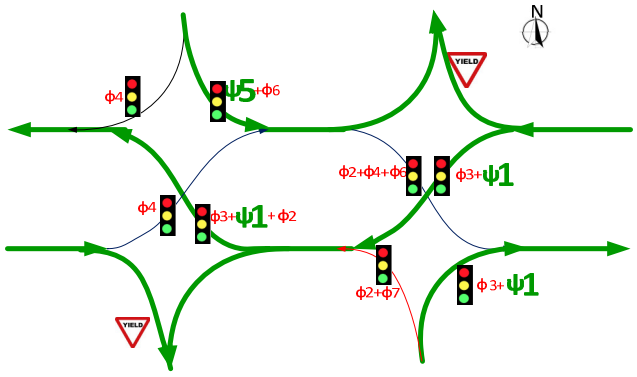

Figure 5-24 Active Movements during Phases 1 and 5

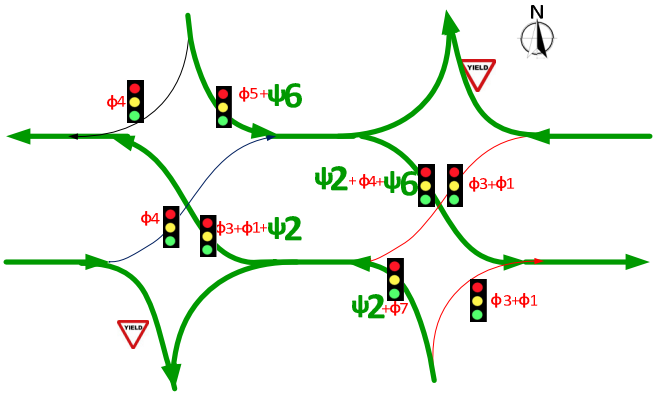

Figure 5-25 Active Movements during Phases 2 and 6

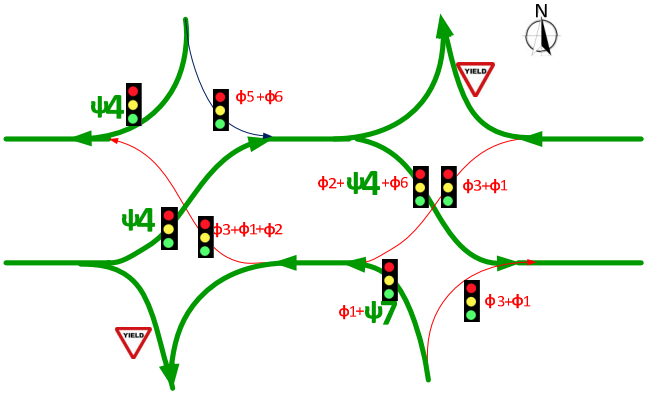

Figure 5-26 Active Movements during Phases 4 and 7

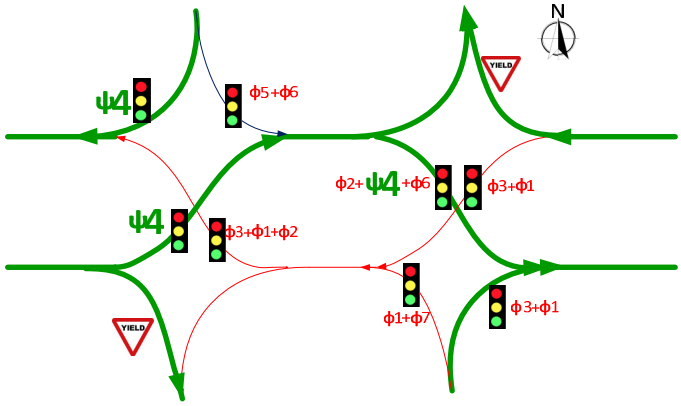

Figure 5-27 Active Movements during Phase 4

5.3.2.2 Proposed Operation 2-a

1. Assumptions and Basic Strategies

Similarly to proposed operation 1, proposed operation 2 assumes that the v/c ratios for critical lane groups must be equal, and that the green times allocated to critical lane groups are assumed to be proportional to their saturation flow rates.

Proposed operation 2 introduces phases 2 and 6 in the traffic signal timing scheme. Two major differing traffic signal timing schemes apply for these types of DDIs. One scheme is that phase 6 is the critical phase; the other is that phase 2 is the critical phase. Phases 3 and 4 are also critical phases in either condition. The flow chart in Figure 5-28 indicates the basic steps needed to develop traffic signal timing plans for these types of DDIs. Finally, the extension time is added to these phases based on route traffic volumes.

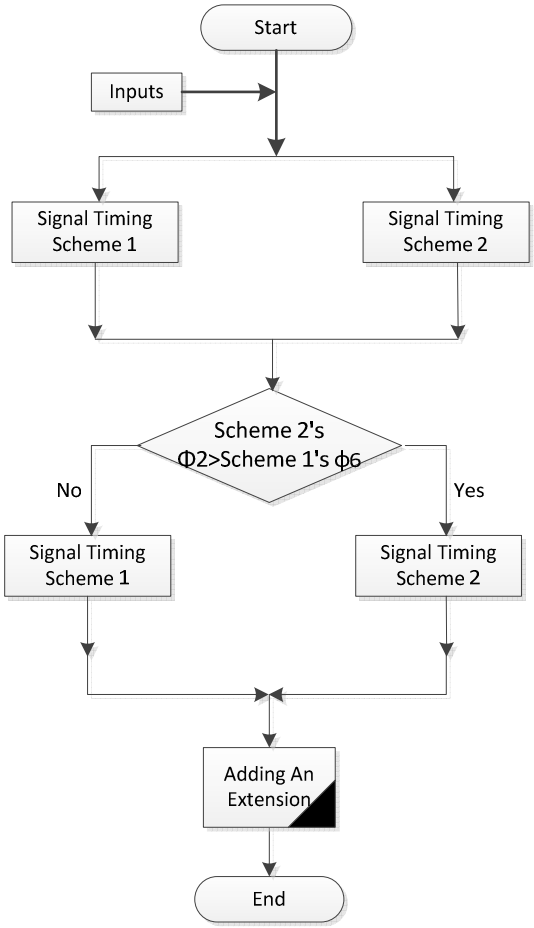

Figure 5-28 Signal Timing Plans Overview for Proposed Operation 2

2. Signal timing scheme 1 (Proposed operation 2-a-1)

Signal timing scheme 1, also called proposed operation 2-a-1, deals with the traffic signal timing plan when phases 6, 4, and 3 are critical phases. Assume the phasing sequence is as indicated in Figure 5-21. Phase 1 is predetermined by the travel time of $T_{11,12,7}$ sec. Phase 1 can serve southbound left-turn (SBL) off-ramp traffic by combining with phase 6. Phase 1 can also add to the westbound through (WBT) traffic by the end of phase 3 for

serving this movement. For other assumptions and strategies of the proposed operation 2-1, they are similar to those of proposed operation 1.

1) Cycle Length

For the traffic signal operation shown in Figure 5-22, the DDI traffic signal timing parameters must satisfy the relationship in the following equation:

$$g_3 + g_4 + g_6 = C_0 + T_{11,12,7} + T_{11,12,7} - L = C_0 + 2 * T_{11,12,7} - L \quad (5\text{-}38)$$

where

g_3: effective green time of phase 3 (s);

g_4: effective green time of phase 4 (s);

g_6: effective green time of phase 6 (s);

C_0: sum of splits of phases 3, 4, and 6 shown in Figure 5-21 (s);

$T_{11,12,7}$: split of phase 1, fixed and determined by the travel time between the two signals "11" and "7" through nodes "11," "12," and "7" shown in Figure 5-10; and

L: total lost time per cycle (s);

For this kind of DDIs, the effective cycle length for the three critical lane groups (SBL, eastbound (EB), and westbound (WB)) satisfy the following relationship with C_0:

$$C_e = C_0 + 2 * T_{11,12,7} \quad (5\text{-}39)$$

Replacing g_3, g_4, g_6 and C_0 in Equations (5-38) and (5-39) yields:

$$\sum_i^N \frac{v_i}{s_i} * \frac{C_e}{x_i} = C_e - L \quad (5\text{-}40)$$

Then, based on the assumption, $X = x_i = x_j$ for $\neq j$, the effective cycle length is:

$$C_e = \frac{L}{1-\frac{\sum_i^N \frac{v_i}{s_i}}{X}} = \frac{L}{1-\frac{\sum_i^N y_i}{X}} = \frac{L}{1-\frac{Y}{X}} \quad (5\text{-}41)$$

where

y_i: flow ratio for critical lane group y_i; and

Y: sum of all critical lane groups.

For this traffic signal timing plan, the total lost time is:

$$L = l_3 + l_4 + l_6 \quad (5\text{-}42)$$

$$l_i = l_{s,i} + l_{c,i} = l_{s,i} + Y_i + AR_i - e_i \quad (5\text{-}43)$$

where

l_i: lost time of critical lane group i ($i = 4\ and\ 6$) (s);

$l_{s,i}$: start-up lost time of critical lane group i ($i = 4\ and\ 6$) (s);

$l_{c,i}$: clearance lost time of critical lane group i ($i = 4\ and\ 6$) (s);

Y_i: yellow interval of critical lane group i ($i = 4\ and\ 6$) (s);

AR_i: all-red interval of critical lane group i ($i = 4\ and\ 6$) (s); and

e_i: extension of effective green time of critical lane group i ($i = 4\ and\ 6$) (s).

$$l_3 = l_{s,3} = 2 \quad (5\text{-}44)$$

The lost time of phase 3 is 2 sec, since it is overlapped by phase 1. Phase 1 is overlapped by phase 2. Therefore, the westbound through traffic has start-up lost time of 2 sec only as shown in Equation (5-44).

The real cycle length is computed by:

$$C = C_e - L - T_{11,12,7} = \frac{L}{1-\frac{Y}{X}} - L - T_{11,12,7} \quad (5\text{-}45)$$

2) Effective Green Times and Phase Splits

Effective green times can be calculated by:

$$g_i' = \frac{y_i}{\sum_i^N y_i} * (C_e - L) \quad (5\text{-}46)$$

where

g_i': effective green time for phase i ($i = 3, 4, 6$).

The actual green time illustrated in Figure 5-21 can be obtained by:

$$g_1 = \emptyset_1 - Y_1 - AR_1 \quad (5\text{-}47)$$

$$g_3 = g_3' - \emptyset_1 \quad (5\text{-}48)$$

$$g_4 = g_4' \quad (5\text{-}49)$$

$$g_2 = g_6 = g_6' - \emptyset_1 \quad (5\text{-}50)$$

where

$\emptyset_1$: is equal to $T_{11,12,7}$ (s).

The phase splits 3, 4, and 6 are:

$$\emptyset_i = g_i + Y_i + AR_i \tag{5-51}$$

The y_i in Equation (5-41) can be replaced by:

$$y_3 = max\{\frac{v_{3,14,7}}{s_{3,14,7}}, \frac{v_{3,5,6}}{s_{3,5,6}}\} \tag{5-52}$$

$$y_4 = max\{\frac{v_{4,1,8}}{s_{4,1,8}}, \frac{v_{4,10,9}}{s_{4,10,9}}\} \tag{5-53}$$

where

$v_{3,14,7}$: traffic volumes of lane group between nodes "14" and "7" (veh/h);

$s_{3,14,7}$: saturation flow rate of lane group between nodes "14" and "7" (veh/h);

$v_{3,5,6}$: traffic volumes of lane group between nodes "5" and "6" (veh/h);

$s_{3,5,6}$: saturation flow rate of lane group between nodes "5" and "6" (veh/h);

$v_{4,1,8}$: traffic volumes of lane group between nodes "1" and "8" (veh/h);

$s_{4,1,8}$: saturation flow rate of lane group between nodes "1" and "8" (veh/h);

$v_{4,10,9}$: traffic volumes of lane group between nodes "10" and "9" (veh/h); and

$s_{4,10,9}$: saturation flow rate of lane group between nodes "10" and "9" (veh/h).

3. Signal timing scheme 2 (Proposed operation 2-a-2)

Unlike proposed operation 1-a, signal timing scheme 2, also called proposed operation 2-a-2, deals with the traffic signal timing plan when phases 2, 3, and 4 are critical phases. As the phasing sequence indicated in Figure 5-21, Phase 1 is predetermined by the travel time of $T_{11,12,7}$ sec. Phase 1 can serve SBL off-ramp traffic by combining with phase 6.

Phase 1 can also add to the WBT through traffic by the end of phase 3 to serve this lane group. However, phase 1 cannot serve NB off-ramp left-turn traffic with phase 2. Thus, the proposed operation 2-2 is different from proposed operation 2-1. In order to develop a signal timing plan for the worst condition, phase 7 is neglected when developing signal timing plans for proposed operation 2-1 although it can add an additional travel time for northbound (NB) off-ramp left-turn traffic following phase 2.

1) Cycle Length

For the traffic signal operation shown in Figure 5-22, the DDI traffic signal timing parameters should satisfy the relationship in the equation below:

$$g_2 + g_3 + g_4 = C_0 + T_{11,12,7} - L = C_0 + T_{11,12,7} - L \quad (5\text{-}54)$$

where

g_2: effective green time of phase 2 (s);

g_3: effective green time of phase 3 (s);

g_4: effective green time of phase 4 (s);

C_0: sum of splits of phases 2, 3, and 4 shown in Figure 5-21 (s);

$T_{11,12,7}$: split of phase 1, fixed and determined by the travel time between the two signals "11" and "7" through the nodes "11," "12," and "7" shown in Figure 5-10; and

L: total lost time per cycle (s).

Under this condition, the effective cycle length for the three critical lane groups (NBL, EB, and WB) satisfy the following relationship with C_0:

$$C_e = C_0 + T_{11,12,7} \tag{5-55}$$

Replacing g_2, g_3, g_4 and C_0 in Equations (5-54) and (5-55) yields:

$$\sum_i^N \frac{v_i}{s_i} * \frac{C_e}{x_i} = C_e - L \tag{5-56}$$

Then, based on the assumption, $X = x_i = x_j$ for $i \neq j$, the effective cycle length is:

$$C_e = \frac{L}{1-\frac{\sum_i^N \frac{v_i}{s_i}}{X}} = \frac{L}{1-\frac{\sum_i^N y_i}{X}} = \frac{L}{1-\frac{Y}{X}} \tag{5-57}$$

where

y_i: flow ratio for critical lane group y_i; and

Y: sum of all critical lane groups.

The real cycle length is calculated as:

$$C = C_e - L = \frac{L}{1-\frac{Y}{X}} - L \tag{5-58}$$

For this traffic signal timing plan, the total lost time is:

$$L = l_2 + l_3 + l_4 \tag{5-59}$$

$$l_i = l_{s,i} + l_{c,i} = l_{s,i} + Y_i + AR_i - e_i \tag{5-60}$$

where

l_i: lost time of critical lane group i ($i = 4\ and\ 2$) (s);

$l_{s,i}$: start-up lost time of critical lane group i ($i = 4\ and\ 2$) (s);

$l_{c,i}$: clearance lost time of critical lane group i ($i = 4\ and\ 2$) (s);

Y_i: yellow interval of critical lane group i ($i = 4\ and\ 2$) (s);

AR_i: all-red interval of critical lane group i ($i = 4\ and\ 2$) (s); and

e_i: extension of effective green time of critical lane group i ($i = 4\ and\ 2$) (s).

$$l_3 = l_{s,3} = 2 \tag{5-61}$$

The lost time of phase 3 is only 2 sec, since it is overlapped by phase 1. Phase 1 is overlapped by phase 2. Therefore, the westbound through traffic has start-up lost time of 2 sec only as shown in Equation (5-61).

2) Effective green times and phase splits

Effective green times can be calculated by:

$$g_i' = \frac{y_i}{\sum_i^N y_i} * (C_e - L) \tag{5-62}$$

where

g_i': effective green time for phase i ($i = 2, 3, and\ 4$).

The actual green time illustrated in Figure 5-21 can be obtained by:

$$g_1 = \emptyset_1 - Y_1 - AR_1 \tag{5-63}$$

$$g_6 = g_2 = g_2' \tag{5-64}$$

$$g_3 = g_3' - \emptyset_1 \tag{5-65}$$

$$g_4 = g_4' \tag{5-66}$$

where

$\emptyset_1$: is equal to $T_{11,12,7}$ (s).

The phase splits 2, 3, and 4 are:

$$\emptyset_i = g_i + Y_i + AR_i \tag{5-67}$$

The y_i in Equation (5-41) can be replaced by:

$$y_3 = max\{\frac{v_{3,14,7}}{s_{3,14,7}}, \frac{v_{3,5,6}}{s_{3,5,6}}\} \tag{5-68}$$

$$y_4 = max\{\frac{v_{4,1,8}}{s_{4,1,8}}, \frac{v_{4,10,9}}{s_{4,10,9}}\} \tag{5-69}$$

5.3.2.3 Proposed Operation 2-b

The real green time of phase 6 in proposed operation 2-a-2 is different from the real green time of phase 2 in proposed operation 2-a-1. The criteria for selecting the right signal timing scheme is based on the value of green time of phases 6 and 2 by these two schemes respectively. If the real green time of phase 2 based on proposed operation 2-a-2 is greater than the real green time of phase 6 based on proposed operation 2-a-1, proposed operation 2-a-2 will be applied for developing traffic signal timing plans for the DDI. Then the phase 6 must be allocated the same phase split as phase 2 in the proposed operation 2-a-2. Assume proposed operation 2-a-1 or 2-a-2 is selected to calculate traffic signal timing plans in this study. An extension may need to be added to the cycle length C_e for the same reason explained for proposed operation 1. The proposed operation 2

with adding an additional extension is called proposed operation 2-b. The ways to determine the extensions for phases 2, 3, and 4 are decided by the following process.

$$E = T_{8,11,12,7} * max\left\{1, \frac{s_{1,8}}{s_{12,7}}\right\} * \frac{v_{8,11,12,7}}{v_{1,8}} + T_{4,3,8} * max\left\{1, \frac{s_{5,4}}{s_{3,8}}\right\} * \frac{v_{5,4,3,8}}{v_{5,4}} \quad (5\text{-}70)$$

where

$T_{8,11,12,7}$: travel time from nodes "8" to "7" through nodes "11" and "12" (s);

$T_{4,3,8}$: travel time from nodes "4" to "8" through node "3" (s);

$s_{5,4}$: saturation flow rate of lane group between nodes "5"and "4" (veh/h);

$v_{5,4,3,8}$: traffic counts on the route passing through "5," "4," "3," and "8" (veh/h); and

$v_{5,4}$: traffic counts on the routes passing through "5" and "4" (veh/h).

The extension for phase 4 is affected by the flow ratio of the critical lane group between nodes "1" and "8;" and its percentage of through traffic in the route passing through nodes "8," "11," "12," and "7." In addition, the same factors in the other directions can affect the extension for phase 4. Therefore, phase 4's extension can be allocated by the following formula:

$$E_2 = E * \left(\frac{\frac{y_2}{\sum_{i=2}^{N=4} y_i} * T_{4,3,8} * \max\left\{1, \frac{s_{5,4}}{s_{3,8}}\right\} * \frac{v_{5,4,3,8}}{v_{5,4}}}{\frac{y_4}{\sum_{i=2}^{N=4} y_i} * T_{8,11,12,7} * \max\left\{1, \frac{s_{1,8}}{s_{12,7}}\right\} * \frac{v_{8,11,12,7}}{v_{1,8}} + \frac{y_2}{\sum_{i=2}^{N=4} y_i} * T_{4,3,8} * \max\left\{1, \frac{s_{5,4}}{s_{3,8}}\right\} * \frac{v_{5,4,3,8}}{v_{5,4}} + e_3'} \right) \quad (5\text{-}71)$$

$$E_4 = E * \left(\frac{\frac{y_4}{\sum_{i=2}^{N=4} y_i} * T_{8,11,12,7} * \max\left\{1, \frac{s_{1,8}}{s_{12,7}}\right\} * \frac{v_{8,11,12,7}}{v_{1,8}}}{\frac{y_4}{\sum_{i=2}^{N=4} y_i} * T_{8,11,12,7} * \max\left\{1, \frac{s_{1,8}}{s_{12,7}}\right\} * \frac{v_{8,11,12,7}}{v_{1,8}} + \frac{y_2}{\sum_{i=2}^{N=4} y_i} * T_{4,3,8} * \max\left\{1, \frac{s_{5,4}}{s_{3,8}}\right\} * \frac{v_{5,4,3,8}}{v_{5,4}} + e_3'} \right) \quad (5\text{-}72)$$

$$E_3 = E - E_2 - E_4 \tag{5-73}$$

$$e_3' = \min\{\max\{g_3 - T_{7,4,3,8}, \alpha * T_{7,4,3,8}\}, T_{7,4,3,8}\} \tag{5-74}$$

$$\alpha = \frac{1}{2} * \left(\frac{v_{8,11,12,7}}{v_{1,8}} + \frac{v_{5,4,3,8}}{v_{5,4}}\right) \tag{5-75}$$

where

$T_{7,4,3,8}$: travel time between the two signals "7" and "8" through the nodes "4" and "3," usually $T_{7,4,3,8} = T_{8,11,12,7}$ (s);

5.3.2.4 Optimal Phasing Sequence

The phase sequence can be decided by applying the same methodology presented for proposed operation 1 on the basis of route traffic volumes. The route traffic volumes are exactly determined by traffic movement volumes discussed for proposed operation 1.

5.3.2.5 Bandwidth

Bandwidth is a direct way to illustrate the traffic progression through several intersections. Proposed operations 1 and 2 have great bandwidths for each traffic movement. Taking proposed operation 2 as an example, the bandwidths for its major movements are summarized in Table 5-5 and depicted among Figure 5-29 to Figure 5-32. Based on this table and these figures, the bandwidth will reduce when the space between the two crossovers is increased, as illustrated in Figure 5-33. Since other conditions do not change, the optimal cycle length based on conventional methods, such as Webster's method, will not change. However, the effective bandwidths decrease as the space

between these two crossovers increases. This is another explanation for adding an extension to the optimal cycle length in proposed operations 1 and 2.

Table 5-5 Four Movements' Bandwidths of Proposed Operation 2 at a DDI

First Location (Node ID)	Movement	Second Location (Node ID)	Movement	Bandwidth (s)
11	SBL	7	EBT	Φ1+Φ2
4	NBL	8	WBT	Φ2-$T_{4,3,8}$
8	EBT	7	EBT	Φ4-$T_{8,11,12,7}$
7	WBT	8	WBT	Φ3

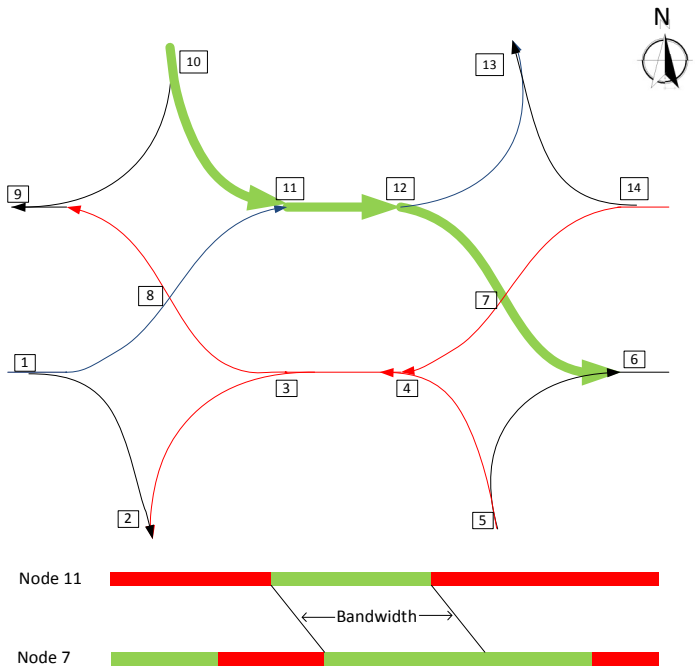

Figure 5-29 SBL Bandwidth

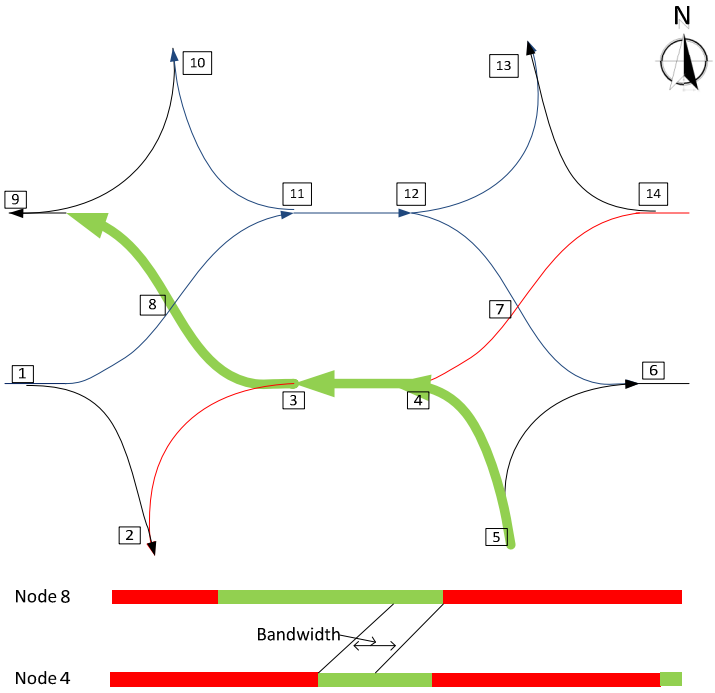

Figure 5-30 NBL Bandwidth

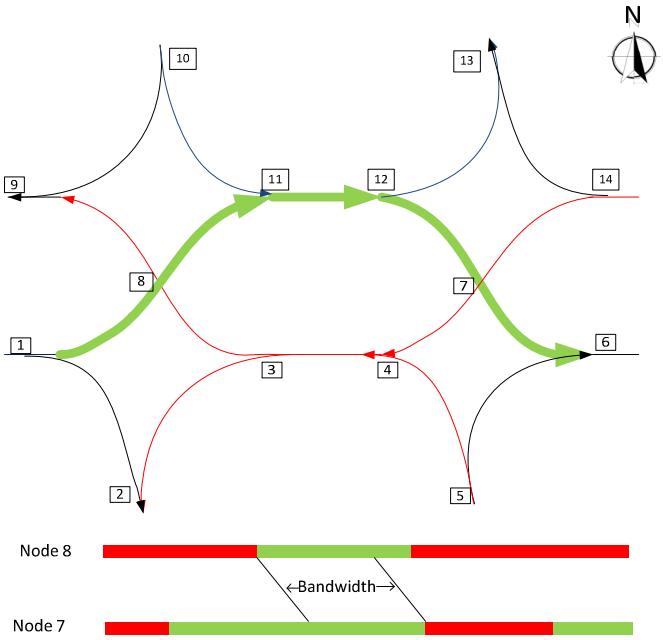

Figure 5-31 EBT Bandwidth

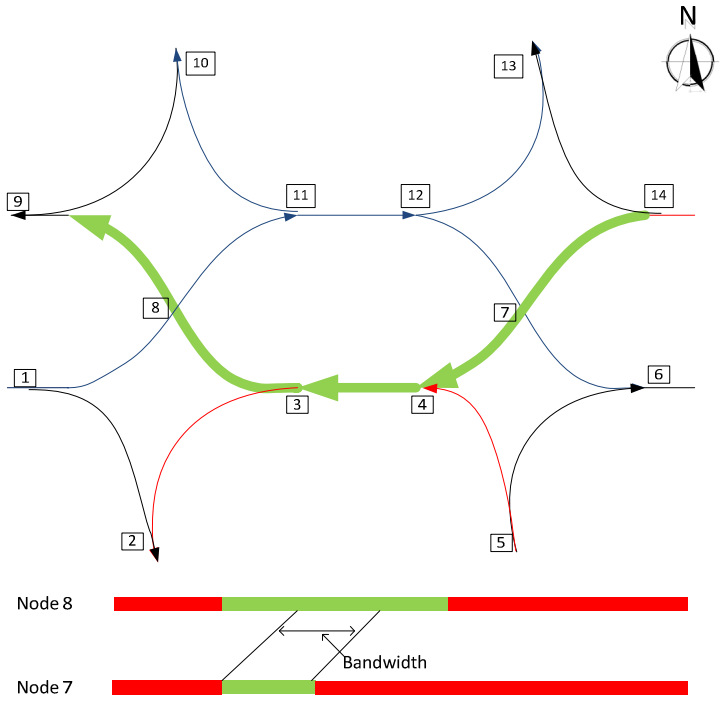

Figure 5-32 WBT Bandwidth

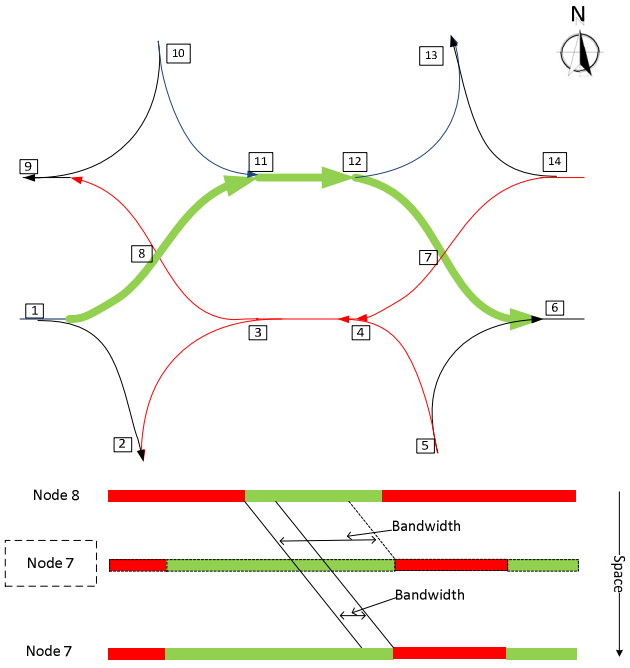

Figure 5-33 WBT Bandwidths Before and After the Space's Increase

5.3.3 Proposed Operation 3

Traffic is a dynamic and nonlinear system. Any analytical methodology cannot describe the traffic process perfectly. Traffic micro simulation is an appropriate method to mimic the traffic system. However, all the current micro simulation tools cannot optimize traffic signal control very well for one reason: the comparatively long time it takes to run each simulation. For example, a DDI simulation model in VISSIM 5.40 takes more than 3 minutes to complete one simulation of 3600 sec. In addition, most simulation tools only allow users to adjust some parameters by accessing specific files through other programming software such as C++ and MATLAB. Therefore, it is not practical for the majority of traffic professionals to search for optimal solutions by simulation tools. Although GA has been applied by some traffic professionals seeking optimal signal timing plans, it cannot be applied in practice regularly for the above reasons. This study will discuss the potential application of GA in optimizing traffic signal timing plans of DDIs. However, this study does not provide case studies for combining GA and simulation tools due to the time consuming and technical restraints on software parameter access. This research only focuses on the theoretical methodology of GA applications on traffic signal operations at DDIs. The GA optimization module based on proposed operation 2 is presented for explaining its major components and process, assuming a fixed timing scheme is implemented at a DDI and its traffic model has been created in a professional simulation tool. All the following recommendations are based on previous experiences applying GA to traffic signal control.

5.3.3.1 GA OPTIMIZATION MODULE OVERVIEW

5.3.3.1.1 Overview

A flow chart of the specific GA module for obtaining optimal traffic signal timing plans is shown in Figure 5-34. Figure 5-35 shows the main organization and relationship between GA optimization and performance estimation module. Detailed introductions to these components are presented in the following parts of this chapter.

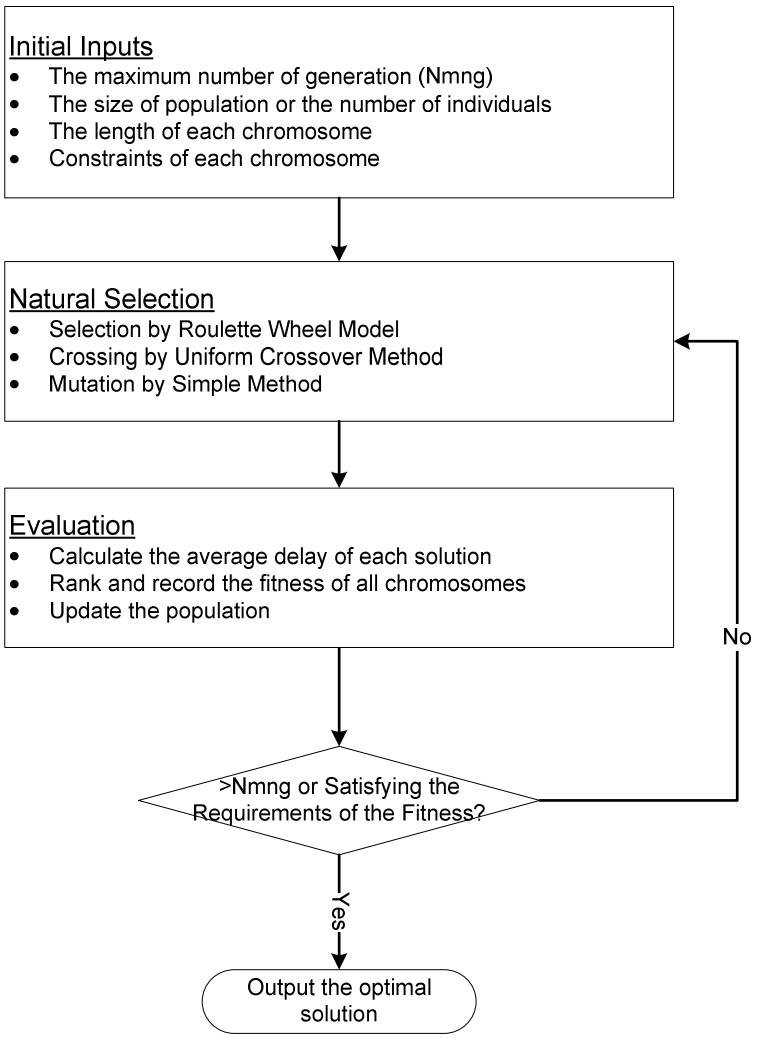

Figure 5-34 Overview of GA

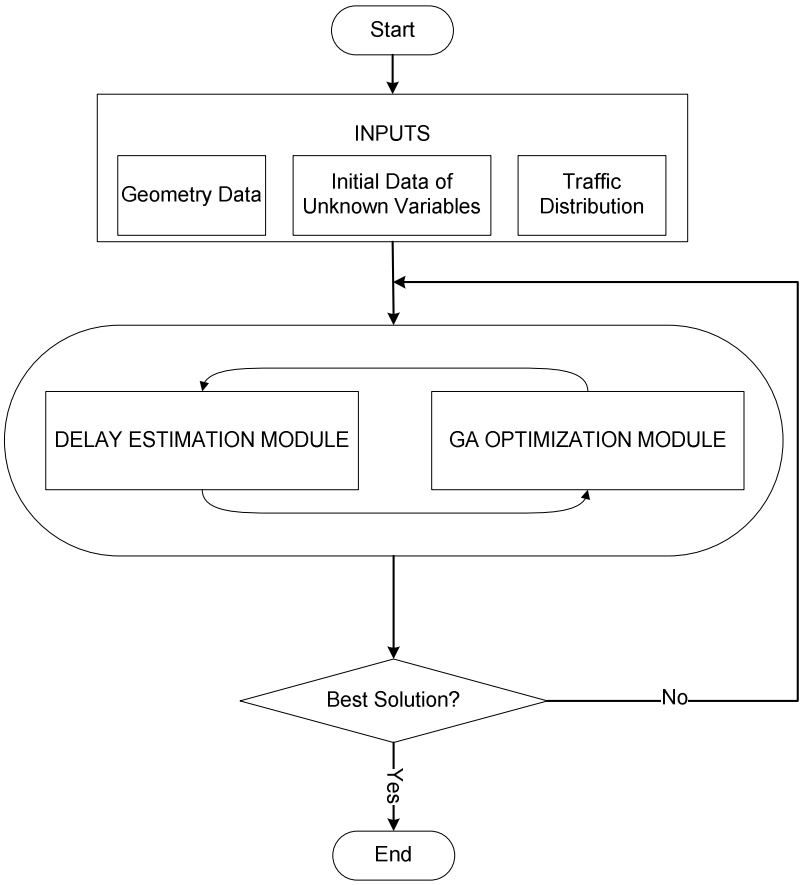

Figure 5-35 Overview of GA Applied for DDIs

5.3.3.1.2 Performance Index

There are many performance indices to evaluate traffic signal operations: delay, number of stops, average speed, fuel consumption, bandwidth, etc. However, all these performance indexes are relevant. This study prefers to search the optimal solutions on the basis of average total delay. As a performance index, average total delay for all the vehicles in a network is expressed by the following equation:

$$PI = \frac{\sum_{i=1}^{M}\sum_{j=1}^{N}\sum_{e=1}^{E}\sum_{k=1}^{K} D_{k,e,i,j}(T_s)}{\sum_{j=1}^{N}\sum_{e=1}^{E}\sum_{k=1}^{K} F_{k,e,i,j}(T_s)} \quad (5\text{-}76)$$

where

PI: performance index;

T_s: length of one simulation periods (s);

$D_{k,e,i,j}(T_s)$: total delay for the vehicles of traffic movement k, on approach e, at intersection (i, j), during a simulation period of T_s sec (s);

K: maximum number of movements on an approach of one intersection;

E: maximum number of approaches of one intersection;

N: maximum number of vertical streets in the road network;

M: maximum number of horizontal streets in the road network; and

$F_{k,e,i,j}(T_s)$: total traffic flow counts of traffic movement k, on approach e of intersection (i, j) during a simulation period of T_s (s) sec (veh).

5.3.3.2 Initial inputs

5.3.3.2.1 The maximum number of generations

This study selects a fixed maximum number of generations and fitness convergence index to terminate the GA module. If the number of iterations reaches the fixed number, the GA module will terminate its search for additional solutions. Since there are no standards on selecting a maximum number of generations, the number varies in different fields and problems. The fixed maximum number of generations is not randomly chosen, but

selected considering other factors including the fitness values, the size of population, the computation time, and the problem characteristics. The maximum number of generations to terminate the GA module is denoted by N^{MNG}. Or if the difference between the fitness value of the highest ranking solution and the successive iterations' fitness is less than the pre-defined fitness convergence index, the GA module will also terminate.

5.3.3.2.2 The size of population

The size of population varies in different application areas. There is no standard formula to determine the size of an optimal population. The population size of genetic algorithm applied in this study is denoted by N^{PS}.

5.3.3.2.3 The length of every chromosome

The length of every chromosome depends on the number of variables and the requirements for the accuracy of unknown variables. Since the phasing sequences of proposed operation 2 are fixed, this study contains one type of unknown variables: splits. The total number of unknown variables depends on the geometrical conditions of a DDI plus the requirements and constraints of traffic control. Without losing the generality of traffic signal control, the maximum unknown variables are the splits of phases 2, 3, and 4 on the basis of traffic signal scheme is shown in Figure 5-21.

The maximum number of unknown phase splits for a DDI is three. Each phase split can be exclusively determined by a string of pertinent genes. According to the GA, every variable can be encoded to a string of "0 or 1" bits. A chromosome can represent all variables by combining all these "0 or 1" strings. One simple way to build up a

chromosome for all parameters of a DDI's traffic signal operation is shown in Figure 5-36. The chromosome of each phase split, as a part of entire chromosome shown in the figure, can be generated by the following equation:

$$2^{K-1} < (U_{max} - U_{min}) * 10^{A} \leq 2^{K} - 1 \quad (5\text{-}77)$$

where

K: number of binary values of 0 and 1;

A: number of decimals;

U_{max}: maximum decimal value of variables; and

U_{min}: minimum normalized value of variables.

The mathematic formulas for the binary encoding of a variable x_i within $[U_{max}, U_{min}]$ are given by:

$$x_{norm} = \frac{x_i - U_{min}}{U_{max} - U_{min}} \quad (5\text{-}78)$$

$$x_{i,K,B} = [b_{i,K} b_{i,K-1} \cdots b_{i,2} b_{i,1}], if \left| \frac{\sum_{j=1}^{K} b_{i,j} * 2^{j-1}}{2^{K}-1} - x_{norm} \right| is\ the\ least. \quad (5\text{-}79)$$

where

x_{norm} : normalized variable, $0 \leq x_{norm} \leq 1$;

$x_{i,K,B}$: K bits of binary version value of variable x_i ; and

$b_{i,j}$: j^{th} value of bit of variable x_i , $b_{i,j}$ equals to 0 or 1, ;

Each chromosome contains N_{chrom} bits of binary number. As an example, the number of binary bits for three critical phase splits are 6, 6, and 6.

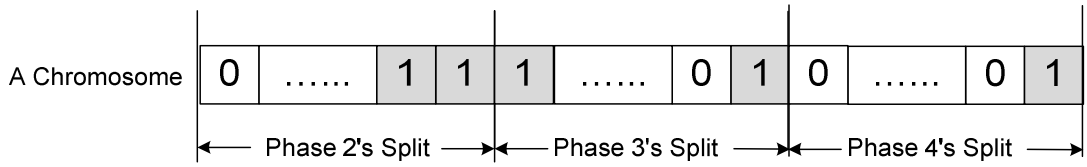

Figure 5-36 A Chromosome in Traffic Signal Control for a DDI

5.3.3.3 Natural selection

In order to provide an excellent initial sampling, the initial size of population (N_{ipop}) is often selected to be greater than than the size of the population (N_{pop}). First, the fitness values of associated chromosomes in the initial population pool are ranked. Thus, a large number of chromosomes with lower fitness values are discarded through natural selection. The remaining chromosomes with higher fitness values are kept for each iteration of the genetic algorithm. Among the N_{pop} chromosomes in each generation, only the top N_{good} chromosomes are selected to mate and propagate new offspring to replace the bottom N_{bad} chromosomes.

The value of N_{pop} is determined by experiences. N_{pop} is different in a variety of application fields. The are two popular ways to determine the value of N_{pop}: proportion method and thresholding method. Proportion method keeps the part of N_{ipop} to be N_{pop} and most of the studies choose 50% as the ratio in the natural selection process. The thresholding method keeps the chromosomes whose fitness values are less than a critical

value. This study prefers to use proportion method with the ratio of 50% so that each generation's population size can be constant.

5.3.3.3.1 Pairing by Roulette Wheel Model

In order to keep the good genes to the next generation, a pair of the good parents of chromosomes should be selected from the given population pool to produce two new offspring. The new offspring are used to replace the chromosomes with lowest performance in the past generation. There are four main methods to select each pair of chromosomes from the population pool in the current generation: pairing from the top to bottom, Random Pairing, Roulette Wheel Model, and Tournament Selection. This study recommends the Roulette Wheel Model to select the good parents to propagate the new offspring.

Roulette Wheel Model has two main approaches to assigning probabilities to the chromosomes in the mating pool: Rank Weighting and Fitness Weighting. The Rank Weighting approach simply assigns probabilities by the rank of the chromosomes without considering the effectiveness of the fitness values of chromosomes. The Fitness Weighting approach more reasonably allocates the probabilities for the chromosomes. For example, the Fitness Weighting approach weights the chromosomes evenly when all these chromosomes have approximately the same fitness values. However, the Ranking Weighting approach tends to weight much different probabilities for these chromosomes on the basis of their ranks. Formulas (4-14) to (4-16) shown in Chapter 4 are used to select the parent chromosomes of each generation.

5.3.3.3.2 Crossing by Uniform Crossover Method

This study recommends the uniform crossover method instead of one-point crossover and two-point crossover methods. The uniform crossover approach can inherit parent chromosomes in gene level rather than the segment level by the one-point crossover and two-point crossover approaches. The uniform crossover operator decides which parent chromosome will contribute how many of its gene values in the offspring chromosomes by a probability, known as a mixing ratio. The mixing ratio can be selected randomly between 0 and 1. Figure 5-37 shows the basic process of uniform crossover.

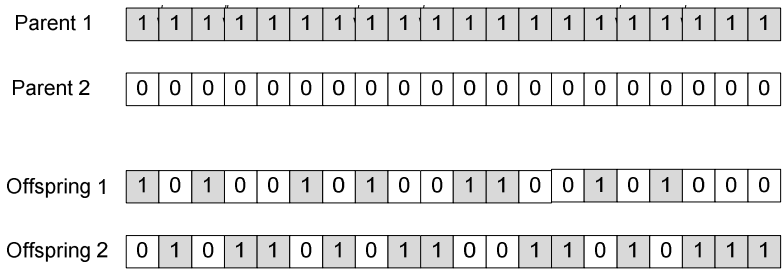

Figure 5-37 An Example of Uniform Crossover Approach

5.3.3.3.3 Mutation by Simple Method

The simple mutation method is recommended in this study. In a population pool, more than P_{mu} of chromosomes will be modified by simple mutation method. For each chromosome, every binary number has $1/N_{chrom}$ of choice to be set to its invert.

5.3.3.4 Evaluation

The chromosomes are evaluated by their fitness values. The average total delay for all vehicles in the road system is selected as the fitness of optimal chromosomes. The average delay can be obtained by a simulation tool. A lower average delay means a

higher fitness value. Thus, the chromosomes in each generation will be evaluated on the basis of their average delay generated from the traffic simulation tool.

5.3.3.5 Optimal Solution

5.3.3.5.1 Update the population

Based on the fitness values of chromosomes, the population can be updated by the pairing, crossing, and mutation processes introduced above. The total size of the population will be kept the same in each generation. The average delay for each chromosome will be ranked and recorded in every step. The best fitness of a population is used for evaluating the new population's performance. For example, if the new population's best fitness value is greater than the current generation's fitness value, the corresponding chromosomes in the new generation will replace the worst chromosomes in the current generation. Thus, the population in each generation increases their fitness values steadily.

5.3.3.5.2 Termination of algorithm

The two ways to terminate the GA are reaching the maximum generation and satisfying the requirements of fitness. This study recommends applying the maximum generation and fitness value convergence index together as the criterions to terminate the GA. For example, assuming the maximum generation denoted as N_{mg} is 10 and the fitness values convergence index is 0.05. The GA must be terminated whenever either of these two criterions is reached.

5.3.3.5.3 Output the optimal solution

After the GA terminates, the optimal solution with maximum fitness, or minimum delay, is recorded in the program as a string of binary numbers. The decoding method introduced in Chapter 4 is applied to convert the optimal chromosomes into decimal values.

Traffic professionals typically make several assumptions; in particular that assigning traffic green time proportionately for several phases is the most common way to achieve an optimal timing solution. These simple assumptions limit the performance of GA searching for optimal solutions in traffic signal coordination applications. This shortcoming cannot be eliminated fully since the unknown variables are greater than constraints. Based on mathematical theory, the unknown variables have infinite solutions given the specific chromosomes from a GA module. That is the real reason to reduce the efficiency and function of GA in traffic signal coordination control applications. Most traffic professionals applied GA on traffic signal coordination control and found their models did not work as well as GA applications in other fields without knowing this true reason. However, based on this study's proposed operations for DDIs, the splits of phases 2, 3, and 4 can be exactly determined by the chromosomes in the GA module since each phase has its independent constraints. For example, the phase 2s split is constrained by its minimum and maximum value. It is reasonable to believe that the GA can perform better in the application of searching for optimal traffic operation solutions at DDIs than its conventional application on seeking optimal traffic signal coordination plans.

5.3.3.6 Other Control Types by GA

If the traffic model created in a traffic simulation tool is running other types of traffic signal control instead of a fixed signal timing plan, GA methods can also work successfully. For example, if one DDI is operating fully-actuated control and its simulation model is connected with GA optimization model. The unknown variables are "maximum recall" instead of splits in the controller of the simulation tool. A chromosome consists of the pertinent binary bits for the maximum recalls of phases 2, 3, and 4. Furthermore, the minimum green for these phases can also be assumed to be unknown variables and be optimized by applying GA. Similarly, semi-fully actuated control and coordinated control can also be optimized by combining a traffic simulation model and the GA module. In order to reduce the randomness of outputs from a simulation model, the average total delay can be determined from the average delay of multiple runs in the simulation tool for each solution generated by the GA module. However, more simulations usually take a longer time to find out the feasible optimal solutions based on GA.

5.4 SUMMARY

This chapter reviews the existing methodologies of traffic signal timing plans for DDIs, and summarizes their strengths and drawbacks. Three proposed operations are presented for traffic signal operations of DDIs. Proposed operation 1 includes three phases: phases 1, 3, and 4. Phase 1 is pre-determined by the geometry of a DDI. Phases 3 and 4 can be determined by the traffic volumes on routes and capacities of critical traffic movements at the DDI. Proposed operation 2 adds phases 2, 5, 6, 7, and 8 into the timing scheme.

Phases 2 and 6 should start and terminate simultaneously for a pre-timed signal control type. Two timing schemes are used for generating solutions for traffic signal timing plans: one is based on the assumption that phases 6, 3, and 4 are critical phases, and another is on the basis of that phases 2, 3, and 4 are critical phases. Phases 6 and 2 generated from these two separate timing schemes are compared to each other. The timing scheme with the greater of phase 2 or phase 6 is selected as the optimal signal timing plan for the DDI. Due to the specific characteristics of DDIs, an extension adds to the cycle length of DDIs calculated by proposed operations 1 and 2. In addition, the combination of simulation tools and GA is introduced as the third proposed operation. The GA-based simulation optimization can deal with almost all traffic conditions and every type of traffic signal control for DDIs. However, for most traffic professionals, this method is not currently practical due to its time consuming nature and technical bottlenecks of the simulation tools. Figure 5-38 summarizes the traffic signal timing procedure and methodologies presented in this chapter.

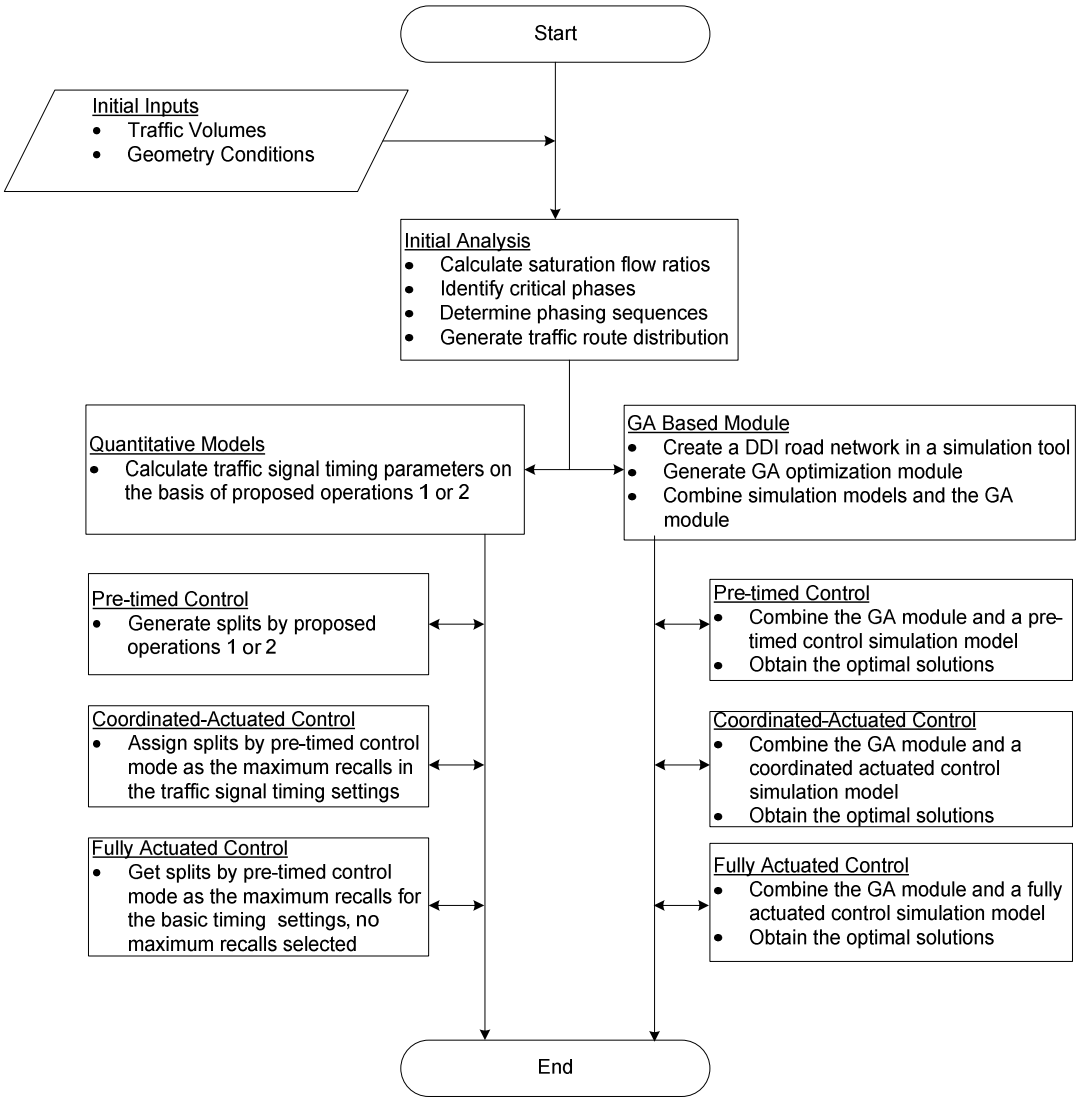

Figure 5-38 Traffic Signal Timing Procedures and Methodologies Overview

CHAPTER 6. CASE STUDY AT A DDI

6.1 INTRODUCTION

Although proposed operations can work well in theory, whether they can operate in one real traffic signal controller remains to be seen. Therefore, this chapter first focuses on testing whether proposed operation 2 can process well as one singular controller for a DDI. Then, an evaluation of the optimal cycle length generated by the proposed operation 2 is conducted. After that, the effects of traffic route distributions on signal operation is studied. Finally, the relationship between the crossover spacing and the average total delay for a DDI without adjusting other conditions is investigated.

6.2 EVALUATION AND FEASIBILITY

The Moana Lane/U.S. 395 interchange located in Reno, Nevada, is currently a standard diamond interchange and is controlled using two signal controllers. The Nevada Department of Transportation (NDOT) is planning to reconstruct this interchange into a DDI. Through my thorough testing, the proposed operation 2 can be practically applied using a real traffic signal controller. This section then presents the detailed simulation results of current operation 5 and proposed operation 2 and compares their operational performances. Finally, settings used in a real traffic signal controller for a fully actuated control based on proposed operation 2 are listed.

6.2.1 Site Description

The Moana Lane/U.S. 395 interchange (Moana DDI) is located in the City of Reno, NV. The interchange is a conventional diamond interchange as shown in Figure 6-1. However, this interchange will be replaced by the DDI illustrated in Figure 6-2.

Figure 6-1 Bird's-Eye View of the Moana Lane/U.S. 395 Interchange

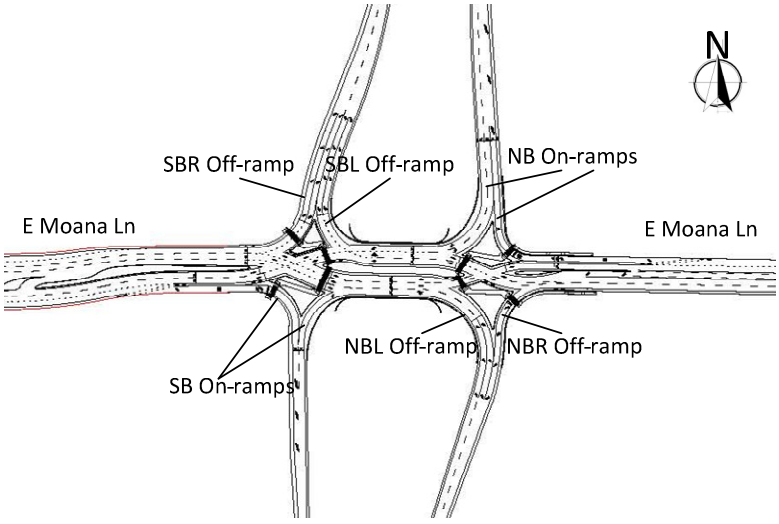

Figure 6-2 Proposed Configuration of the Moana Lane/U.S. 395 DDI

6.2.2 Traffic Demand

The traffic origins, destinations, and nodes for this DDI are depicted in Figure 6-3. The predicted peak hour demands in 2015 provided by NDOT are shown in Figure 6-4. Based on the methodologies presented in Chapter 5, the traffic origin-destination (OD) distribution in AM and PM peak hours are provided in Table 6-1 and Table 6-2. The traffic volumes on each route during 2015 peak hours are summarized in Table 6-3 and Table 6-4. The traffic volumes on each route are partial inputs of a simulation model in a professional simulation tool such as VISSIM.

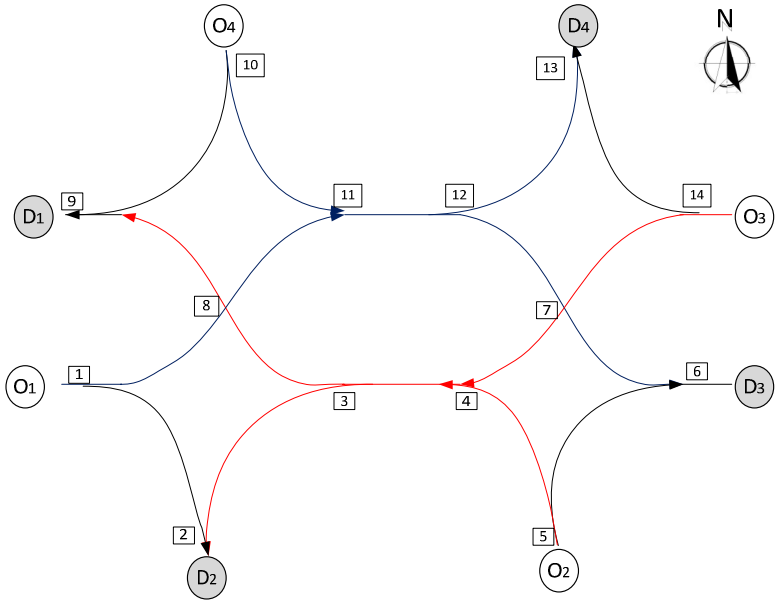

Figure 6-3 Origins, Destinations, and Nodes at Moana DDI

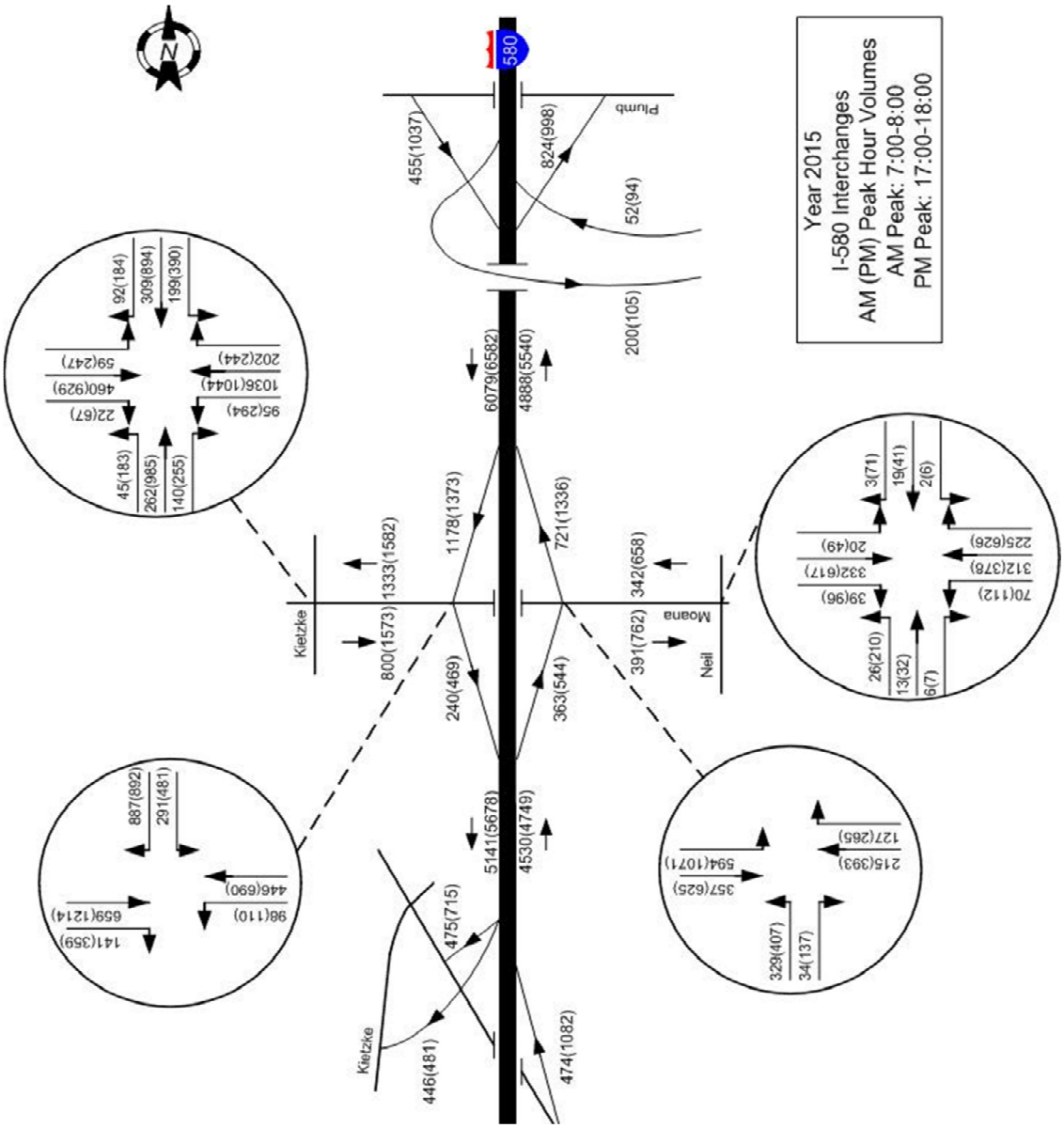

Figure 6-4 Traffic Volumes in the AM and PM Peak Hours in 2015

Table 6-1 O-D Distribution during Year 2015 AM Peak Hour (veh/h)

O-D	1	2	3	4	Total
1	0	141	66	593	800
2	329	0	34	0	363
3	117	98	0	127	342
4	887	0	291	0	1178
Total	1333	239	391	720	2683

Table 6-2 O-D Distribution during Year 2015 PM Peak Hour (veh/h)

O-D	1	2	3	4	Total
1	0	359	144	1070	1573
2	407	0	137	0	544
3	283	110	0	265	658
4	892	0	481	0	1373
Total	1582	469	762	1335	4148

Table 6-3 Traffic Volumes on Each Route during Year 2015 AM Peak Hour (veh/h)

Routes	Volumes	Routes	Volumes
1->2	141	14->7->4->3->8->9	117
1->8->11->12->7->6	66	14->7->4->3->2	98
1->8->11->12->13	593	14->13	127
5->4->3->8->9	329	10->9	887
5->4->3->2	0	10->11->12->7->6	291
5->6	34	10->11->12->13	0

Table 6-4 Traffic Volumes on Each Route during Year 2015 PM Peak Hour (veh/h)

Routes	Volumes	Routes	Volumes
1->2	359	14->7->4->3->8->9	283
1->8->11->12->7->6	144	14->7->4->3->2	110
1->8->11->12->13	1070	14->13	265
5->4->3->8->9	407	10->9	892
5->4->3->2	0	10->11->12->7->6	481
5->6	137	10->11->12->13	0

6.2.3 Traffic Signal Operations and Evaluations

6.2.3.1 Current Operation 5 Signal Parameters

Two coordination plans of current operation 5are provided that are consistent with the existing coordination plans for the adjacent signals: 110-sec cycle for AM and 130-sec cycle for PM. These plans were determined based on the 2015 traffic demands. Only cycle length, phase splits, and clearance intervals are provided in this study.

Phases 4 and 1 are not actually conflicting phases as shown in Figure 5-6. Therefore, the critical saturation flow ratio for phase 4 is the maximum of these two phases (shown in Table 6-5). There is no accurate way to determine the phase 1 split. In this study, the phase 1 split is assumed to be 10% of the cycle length. Phases 2, 3, and 4 share the remaining time in proportion to their critical saturation flow ratios. Table 6-6 illustrates each phase split in year 2015 AM and PM peak hours.

Table 6-5 Critical Saturation Flow Ratio for Phases 1 and 4

Movement	AM	PM
1->8	0.19	0.34
10->9	0.25	0.25
Critical Ratio	0.25	0.34

Table 6-6Cycle Lengths and Phase Splits for Current Operation 5

	2015 AM	2015 PM
Cycle (sec)	110	130
Phase 1 (sec)	11	13
Phase 2 (sec)	23	24
Phase 3 (sec)	23	34
Phase 4 (sec)	53	59
Phase 6 (sec)	23	24

The yellow and all-red intervals of the two coordination plans for current operation 5 used in VISSIM simulation models are provided in Table 6-7.

Table 6-7 Clearance Intervals Used in VISSIM Simulation Models for Current Operation 5

Phase	1	2	3	4	5	6	7	8
Critical Movement	10->9	3->8	3->8	12->7	None	12->7	None	None
Yellow (sec)	3.5	3.5	3.5	3.5		3.5		
Red (sec)	1.5	3.5	3.5	2.5		2.5		

6.2.3.2 Signal Parameters of Proposed Operation 2

Based on the traffic volumes shown in Table 6-1 and Table 6-2, the enhanced signal operation's cycle lengths and phase splits are summarized in Table 6-8. These splits were acquired by the methodologies for proposed operation 2 introduced in Chapter 5.

Table 6-8 Cycle Lengths and Phase Splits for Proposed Operation 2

	2015 AM	2015 PM
Cycle (sec)	110	130
Phase 1 (sec)	10	10
Phase 2 (sec)	30	29
Phase 3 (sec)	17	32
Phase 4 (sec)	53	59
Phase 5 (sec)	10	10
Phase 6 (sec)	30	29
Phase 7 (sec)	12	12
Phase 8 (sec)	58	79

This study uses the clearance intervals in VISSIM simulation models as shown in Table 6-9. These intervals are defined based on proposed operation 2 and the specific geometry conditions at the Moana DDI.

Table 6-9 Clearance Intervals Applied by Proposed Operation 2

Phase	1	2	3	4	5	6	7	8
Critical Movement	3->8	3->8	None	12->7	None	10->11	5->4	None
Yellow (sec)	3.5	3.5	3.5	3.5	3.5	3.5	3.5	3
Red (sec)	3.5	3.5	2.5	2.5	1.5	1.5	1.5	0.0

6.2.3.3 Simulation Results

Each VISSIM model ran five simulations with random seeds. The warm-up time in the simulation models was 300 sec, followed by 3600 sec of run time with data compiled and collected for each traffic movement at the Moana DDI. The average delays of five runs are presented in Table 6-10. The average maximum queues of all runs are provided in Table 6-11. The average delay of each movement for the two operations is indicated in Figure 6-5 and Figure 6-6. The average maximum queue of every movement for the two operations is listed in Figure 6-7 and Figure 6-8.

Table 6-12 illustrates the compared results of average delays shown in Table 6-10. The values in Table 6-12 are obtained by taking the difference of the average delays from proposed operation 2 and current operation 5 and then dividing by the average delay found in current operation 5. For example, the value "11%" shown in Table 6-12 is obtained by (17.9-16.1)/16.1*100%. The value "16.1" comes from the current operation 5 average delay of traffic movement "10->9" during the AM peak hour shown in Table 6-10. Similarly, the number "17.9" is the proposed operation 2 average delay of the same traffic movement in the period. Based on simulation results, proposed operation 2 brought about less average delay for most movements but greater average delay of movement "10->9" compared to the operation developed by the City of Reno for 2015

AM and PM peak hour periods. The reason for less delay of movement "10->9" by current operation 5 is that it adds phase 1 to this traffic movement compared to proposed operation 2. The average delay for all vehicles of proposed operation 2 dropped by 17% and 28% in AM and PM peak hour compared to current operation 5.

Similar to the data in Table 6-12 and Table 6-13 summarizes the compared results of average maximum queues shown in Table 6-11. The average maximum queue of movement "10->11" under proposed operation 2 decreased by 15% and 44% respectively in AM and PM peak hour compared with current operation 5. The average maximum queue of movement "5->4" in the scheme by proposed operation 2 reduced 21% in both the AM and PM peak hour over current operation 5, specifically from 222.1 to 174.8 feet in the AM peak and from 308.9 to 245.5 feet in the PM peak, . Of the other traffic movements including "1->8," "1->2," "12->7," and "14->7," proposed operation 2 performed better than current operation 5 during the peak periods. However, proposed operation 2 increased the maximum queue by 0% and 24% of movement "10->9," and increased 11% and 14% of the maximum queue of movement "3->8" " in the two peak hour periods, respectively, to 69.0 and 84.3 feet. The same reason for greater average delay of traffic movement "10->9" brought about the larger average maximum queue of this movement. The reason for longer maximum queues of movement "3->8" experienced with proposed operation 2 is that this scheme allows the release of northbound left (NBL) traffic earlier, which stops in front of node "8." The maximum queues of this movement were less than 84.3 feet. This maximum queue is acceptable for reducing the delay in front of node "4." Of the other movements, both operations

performed well with no noticeable differences for their low traffic volume, even though they seemed much different.

Table 6-10 Average Delays from VISSIM Simulation Models (sec/veh)

Peak Hours	AM		PM	
Movement	Proposed Operation 2	Current Operation 5	Proposed Operation 2	Current Operation 5
10->9	17.9	16.1	26.9	22.1
10->11	33.5	45.8	45.3	85.0
1->8	16.3	21.7	30.3	35.9
1->2	0.8	0.8	2.1	2.7
3->8	8.7	7.7	6.3	7.5
3->2	0.3	0.3	0.3	0.8
14->13	0.5	0.6	1.0	2.6
14->7	47.6	51.7	51.1	68.3
5->6	0.7	0.8	1.2	1.3
5->4	32.5	48.7	41.1	66.1
12->13	1.3	1.4	3.0	3.7
12->7	1.5	5.9	2.0	14.6
All	15.1	18.3	19.5	27.0

Table 6-11 Average Maximum Queue from Simulation Models (ft)

Peak Hours	AM		PM	
Movement	Proposed Operation 2	Current Operation 5	Proposed Operation 2	Current Operation 5
10->9	287.2	288.2	427.1	345.1
10->11	175.3	206.4	267.8	479.4
1->8	229.9	250.7	594.8	634.5
1->2	30.8	41.7	325.4	365.0
3->8	69.0	62.0	84.3	74.0
3->2	37.7	13.5	67.0	50.9
14->13	0.0	0.0	0.0	0.0
14->7	279.7	274.8	526.3	632.1
5->6	0.0	0.0	0.0	0.0
5->4	174.8	222.1	245.5	308.9
12->13	7.8	0.0	59.2	100.3
12->7	95.6	101.8	238.9	279.6

Table 6-12 Comparison of Delays between Two Operations

Peak Hour	AM	PM
Movement	Change (%)	Change (%)
10->9	11%	22%
10->11	-27%	-47%
1->8	-25%	-16%
1->2	5%	-21%
3->8	14%	-15%
3->2	-7%	-67%
14->13	-4%	-59%
14->7	-8%	-25%
5->6	-8%	-12%
5->4	-33%	-38%
12->13	-8%	-18%
12->7	-75%	-86%
All	-17%	-28%

Table 6-13 Comparison of Maximum Queues between Two Operations

Peak Hour	AM	PM
Movement	Change (%)	Change (%)
10->9	0%	24%
10->11	-15%	-44%
1->8	-8%	-6%
1->2	-26%	-11%
3->8	11%	14%
3->2	180%	32%
14->13	N.A.	N.A.
14->7	2%	-17%
5->6	N.A.	N.A.
5->4	-21%	-21%
12->13	N.A.	-41%
12->7	-6%	-15%

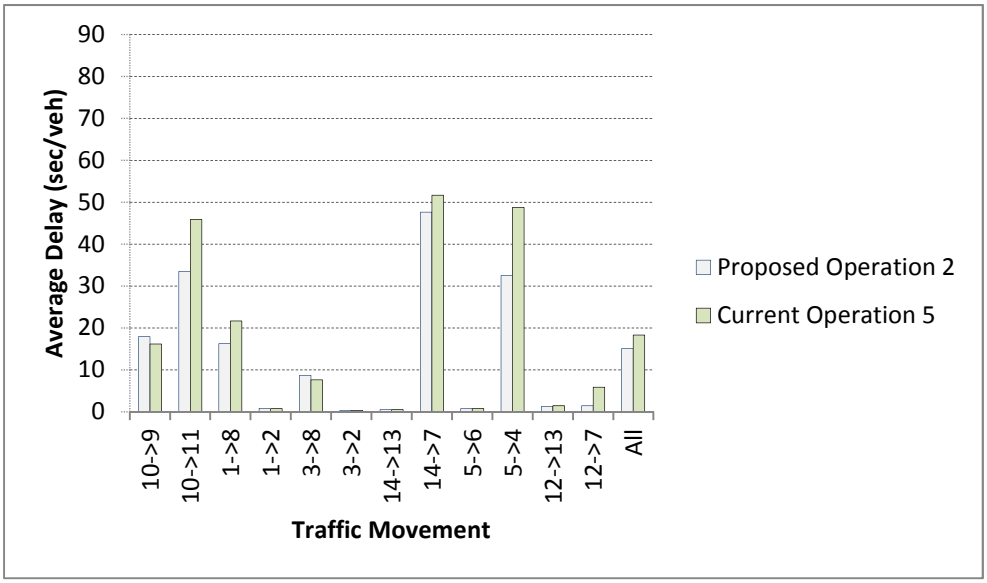

Figure 6-5 Average Delays in AM Peak Hour of Two Operations

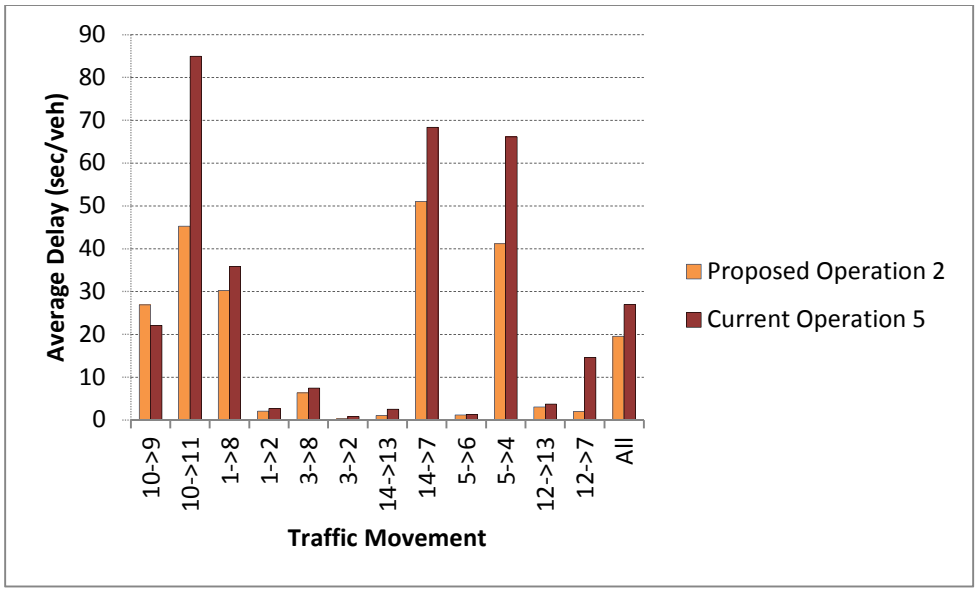

Figure 6-6 Average Delays in PM Peak Hour of Two Operations

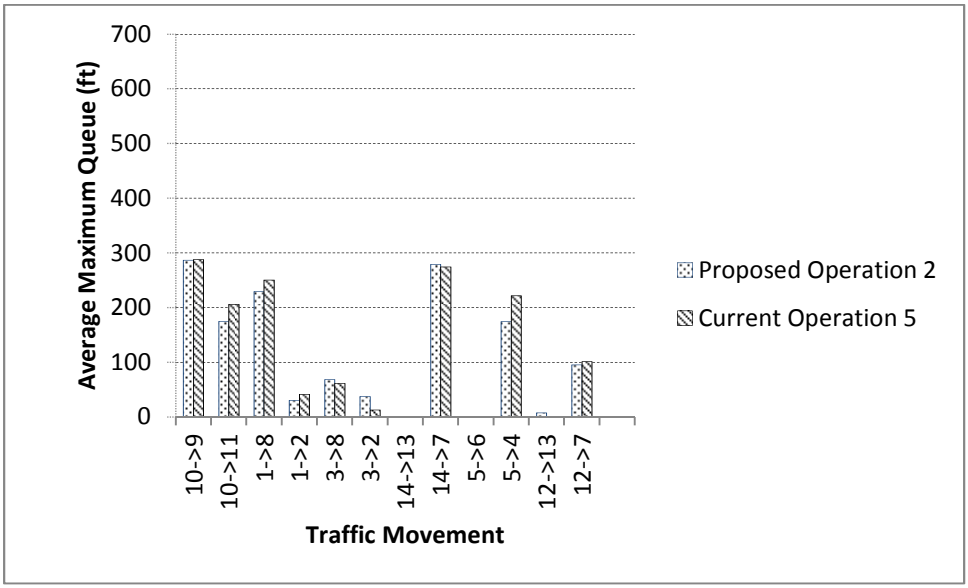

Figure 6-7 Average Maximum Queues in AM Peak Hour of Two Operations

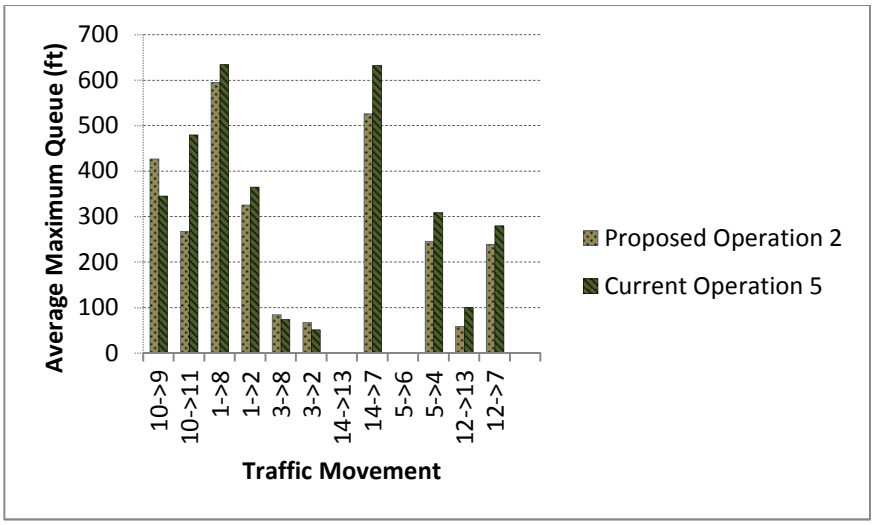

Figure 6-8 Average Maximum Queues in PM Peak Hour of Two Operations

6.2.4 Feasibility of Proposed Operation 2

A hardware-in-the-loop simulation platform, which included VISSIM simulation and a Naztec NEMA controller, shown in Figure 6-9 was established to test the feasibility of proposed operation 2.

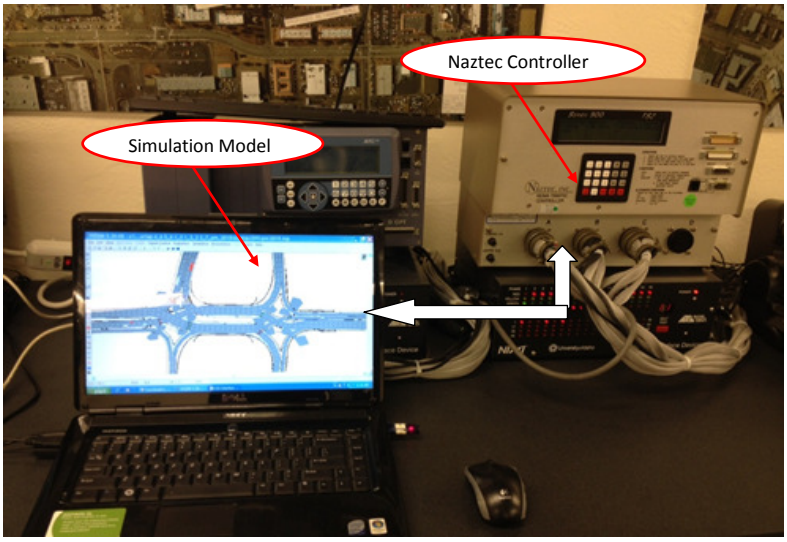

Figure 6-9 Hardware-in-the-loop Simulation Setup

Proposed operation 2 was successfully tested using the hardware-in-the-loop simulation. The controller parameters of a fully actuated control are provided in "Appendix A". All the symbols and abbreviations are consistent with terminology and labels used in the Naztec controller Manual. Through this testing, it was found that proposed operation 2 can work successfully in a real traffic signal controller.

6.3 CYCLE LENGTH

6.3.1 Introduction

Average total delay can be variable when signal control parameters (such as cycle length or v/c ratios) change. For a conventional four-leg intersection, average total delay is not sensitive until the demand levels are above 80 percent of its capacity *(16)*. Thus, an important question arises: how will average total delay of a DDI change when the cycle length and v/c ratios are increasing or decreasing? This chapter studies the sensitivity of delay to cycle length and v/c ratios based on a DDI with the same geometry conditions as the Moana DDI.

Five traffic volume scenarios were studied, as shown in Table 6-14. Scenario 1 is the base volume situation on which other scenarios are derived. Volumes of other scenarios increase in proportion to the volumes of scenario 1. For example, scenario 2's volume from origin 1 to destination 2 is 216, which is equal to 1.2 times the 180 value from scenario 1. The saturation flow rates are summarized in Table 6-15. Based on these data and geometric configurations presented at the Moana DDI, the proposed minimum greens, yellow, and all red intervals are presented in Table 6-16 for the cycle lengths ranging from 60 sec to 150 sec. The proposed maximum greens, yellow, and all red intervals are illustrated in Table 6-17. The split for each phase, found by applying the proposed operation 2-b introduced in Chapter 5, is shown in Table 6-18. The phase 3 split when cycle length is 60 sec was increased by 2 sec, since it was too small to satisfy the

requirements of the minimum green in a controller; phase 4's split was reduce simultaneously by 2 sec to maintain the 60-sec cycle length.

Table 6-14 Traffic Volume (veh/h) Scenarios

O	D	Scenario 1	Scenario 2	Scenario 3	Scenario 4	Scenario 5
1	1	0	0	0	0	0
1	2	180	216	270	306	360
1	3	200	240	300	340	400
1	4	500	600	750	850	1000
2	1	300	360	450	510	600
2	2	100	120	150	170	200
2	3	70	84	105	119	140
2	4	0	0	0	0	0
3	1	150	180	225	255	300
3	2	60	72	90	102	120
3	3	0	0	0	0	0
3	4	130	156	195	221	260
4	1	450	540	675	765	900
4	2	0	0	0	0	0
4	3	200	240	300	340	400
4	4	40	48	60	68	80

Table 6-15 Saturation Flow Rate (veh/h)

Start Node	End Node	Saturation Flow Rate
1	8	3539
5	4	3433
3	8	5085
10	9	3539
10	11	3433
12	7	3433
14	7	1863

Table 6-16 Minimum Green, Yellow, and All Red (sec)

Cycle Length	60	70	80	90	100	110	120	130	140	150	Yellow	All Red
Phase 1	3	3	3	3	3	3	3	3	3	3	3	4
Phase 2	10	10	10	10	10	10	10	10	10	10	3	4
Phase 3	3	5	5	5	5	5	5	5	5	5	3	0
Phase 4	12	12	12	12	12	12	12	12	12	12	3	4
Phase 5	5	5	5	5	5	5	5	5	5	5	3	1
Phase 6	5	5	5	5	5	5	5	5	5	5	3	1
Phase 7	5	5	5	5	5	5	5	5	5	5	3	1
Phase 8	1	1	1	1	1	1	1	1	1	1	3	0

Table 6-17 Maximum Green, Yellow, and All Red (sec)

Cycle Length	60	70	80	90	100	110	120	130	140	150	Yellow	All Red
Phase 1	3	3	3	3	3	3	3	3	3	3	3	4
Phase 2	14	17	19	22	24	27	29	32	35	37	3	4
Phase 3	0	2	5	9	12	15	17	20	23	26	3	0
Phase 4	19	24	29	32	37	41	47	51	55	60	3	4
Phase 5	6	6	6	6	6	6	6	6	6	6	3	1
Phase 6	17	20	22	25	27	30	32	35	38	40	3	1
Phase 7	8	8	8	8	8	8	8	8	8	8	3	1
Phase 8	14	21	29	36	44	51	59	66	73	81	3	0

Table 6-18 Phase Splits (sec)

Cycle Length	60	70	80	90	100	110	120	130	140	150
Phase 1	10	10	10	10	10	10	10	10	10	10
Phase 2	21	24	26	29	31	34	36	39	42	44
Phase 3	3	5	8	12	15	18	20	23	26	29
Phase 4	26	31	36	39	44	48	54	58	62	67
Phase 5	10	10	10	10	10	10	10	10	10	10
Phase 6	21	24	26	29	31	34	36	39	42	44
Phase 7	12	12	12	12	12	12	12	12	12	12
Phase 8	17	24	32	39	47	54	62	69	76	84

VISSIM 5.40 was used to evaluate the performance of each traffic scenario and output its average total delay. Figure 6-10 shows the VISSIM-based traffic simulation model. The lane configurations and speed limits in the simulation model are same as the data collected at the Moana Lane/U.S.395 interchange. Pre-timed, fully actuated, and

coordinated actuated control types were implemented in this case for each traffic scenario to study the relationship between the average total delay and signal control parameters. The basic settings for each traffic scenario in a "Ring Barrier Controller" are same among the three types of controls. Figure 6-11 displays the basic settings for one scenario with a cycle length of 60 sec. Figure 6-12 presents the additional settings for pre-timed control. Figure 6-13 demonstrates the additional settings for fully actuated control and Figure 6-14 provides the specific settings for coordinated actuated control in the simulation model. The maximum recalls for three types of control are assumed to be the same and determined based on proposed operation 2-b. The VISSIM model for each scenario ran ten simulations with random seeds. The warm-up time in the simulation models was 300 sec, followed by 900 sec (15 minutes) run time with complied data were collected for each traffic movement at Moana DDI.

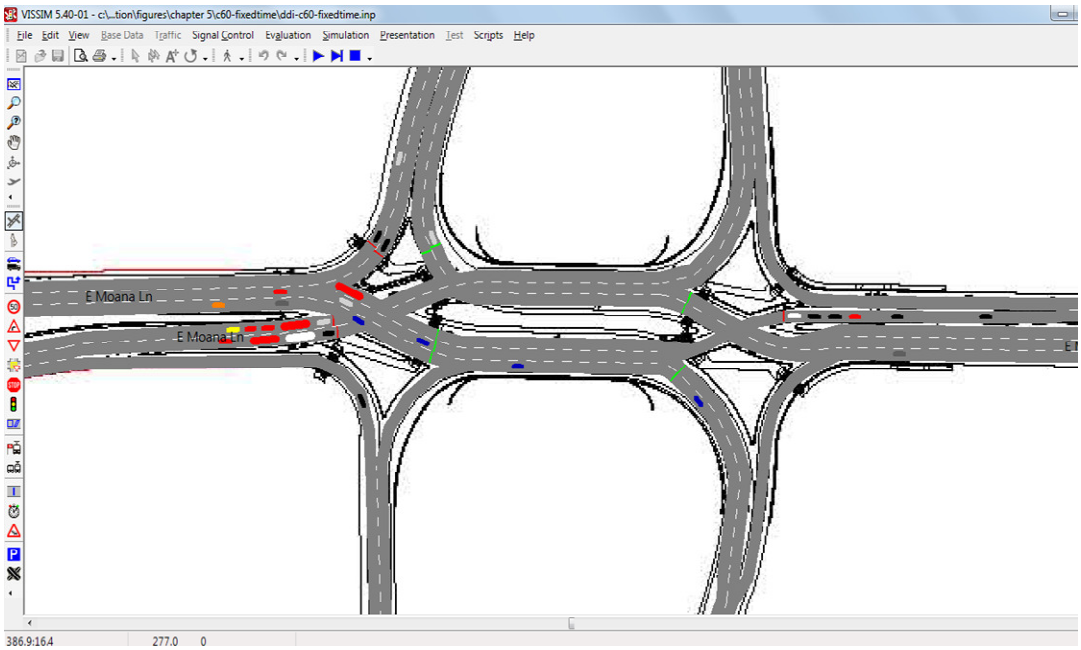

Figure 6-10 VISSIM-based Traffic Simulation Model

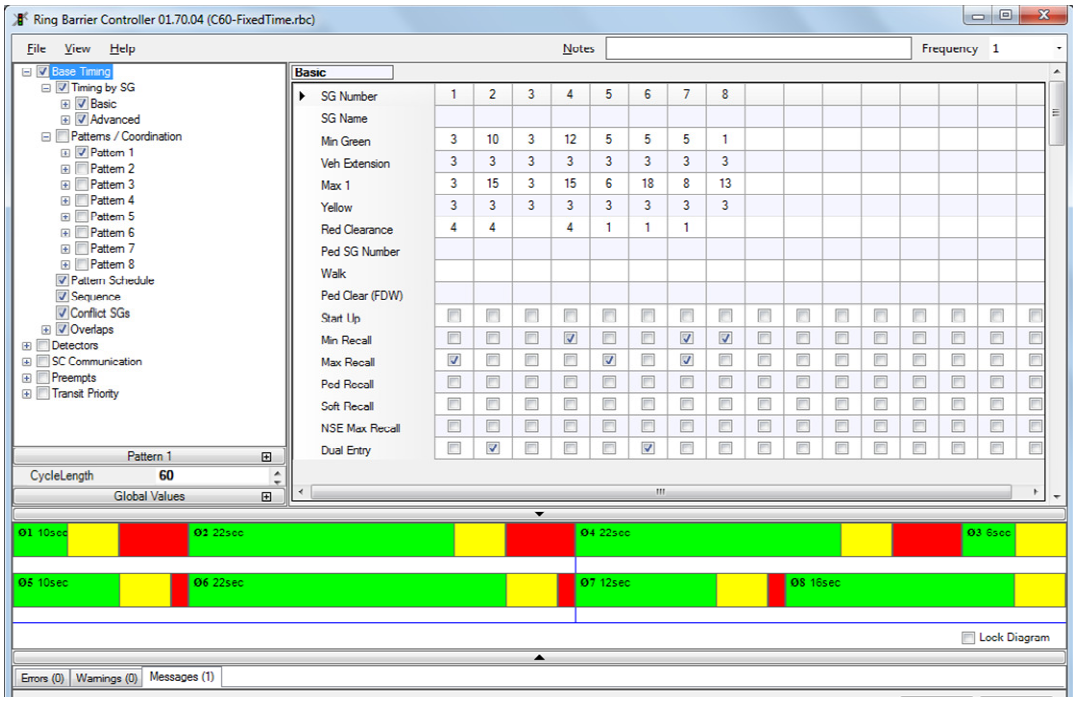

Figure 6-11 Basic Settings in "Ring Barrier Controller"

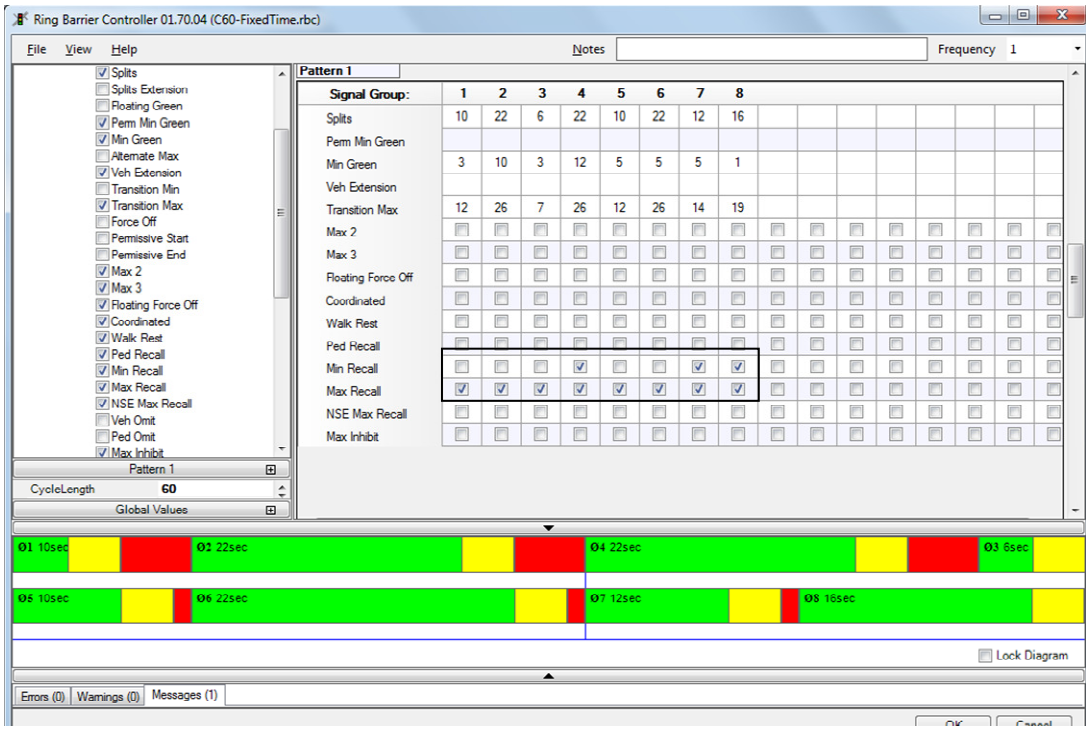

Figure 6-12 Additional Settings for Pre-timed Control

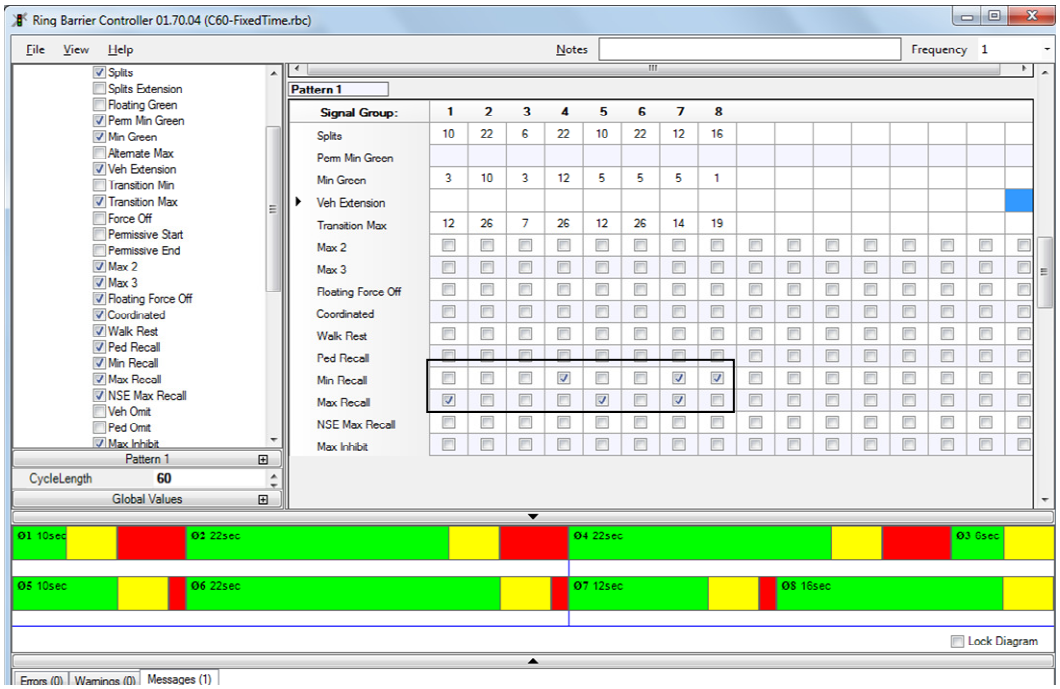

Figure 6-13 Additional Settings for Fully Actuated Control

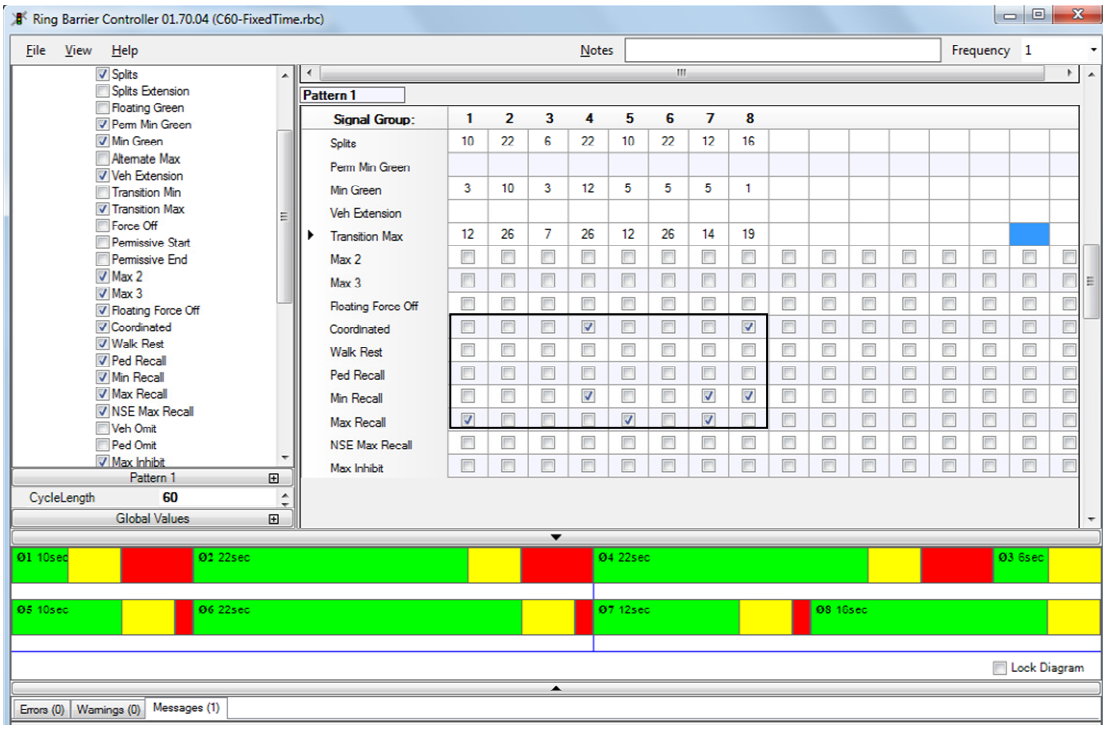

Figure 6-14 Additional Settings for Coordinated Actuated Control

6.3.2 Pre-timed Control

The simulation results for pre-timed control when cycle length ranges from 60 sec to 150 sec are presented in Figure 6-15. As can be seen in the figure, a shorter cycle length produces fewer delays when the sum of critical saturation flow ratios is less than 0.51 with the similar traffic distributions of scenarios 1 and 2. The optimal cycle length for a pre-timed control should be between 80 sec and 100 sec when the sum of critical saturation flow ratios is between 0.64 (in scenario 3) and 0.73 (in scenario 4). According to the results of scenarios 3 and 4, the average delay will initially reduce with increasing cycle length, transitions to keeping stable though increasing cycle lengths, and finally increases again with higher increasing cycle lengths. The optimal cycle length should be between around 85 sec and 130 sec in the scenario with the sum of critical saturation flow ratio of 0.85. The results also indicate that the proposed operation 2-b in Chapter 5 applies well when the sum of critical saturation flow ratios is between around 0.73 and 0.85. These results play an important role for traffic engineers and professionals in selecting optimal traffic signal timing plans in practice. The relationships between average delay of other traffic movements and cycle length are depicted in Figure 6-16 through Figure 6-22. The results show that the average delays in both directions between the two crossovers are less than 10 sec/veh. According to the average maximum queues shown in Appendix B, less than seven vehicles stopped in the middle of the DDI and will not spill back to their upstream crossover intersection by pre-timed control.

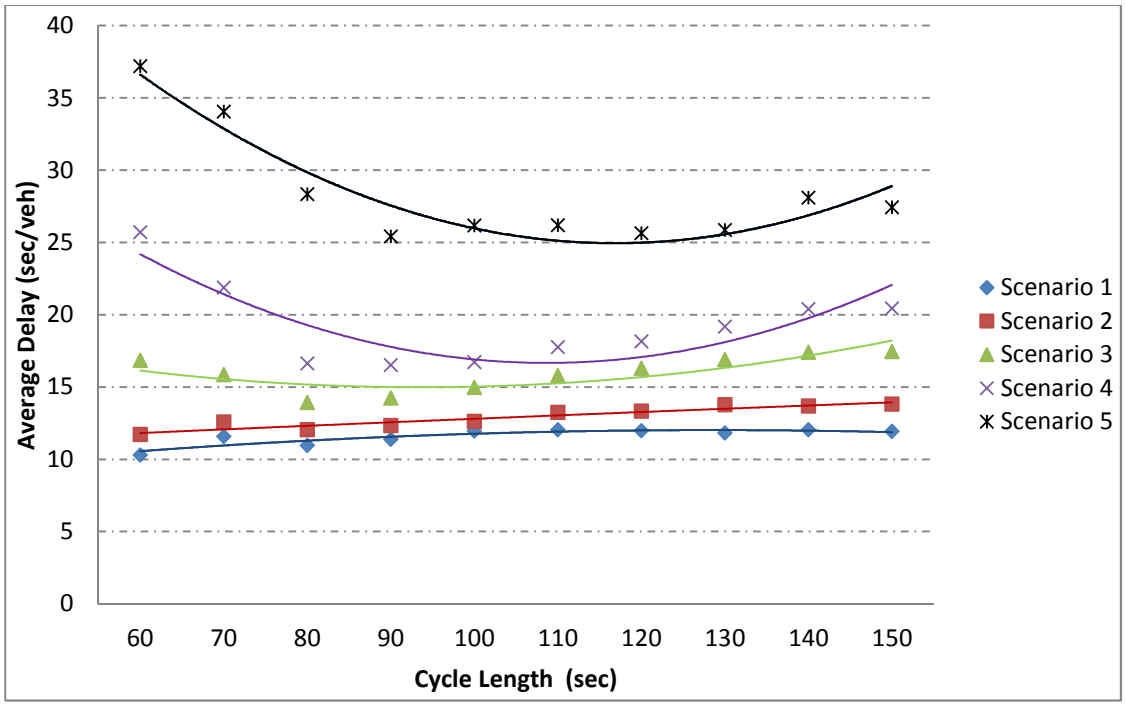

Figure 6-15 Average Delays of All Vehicles and Cycle Length

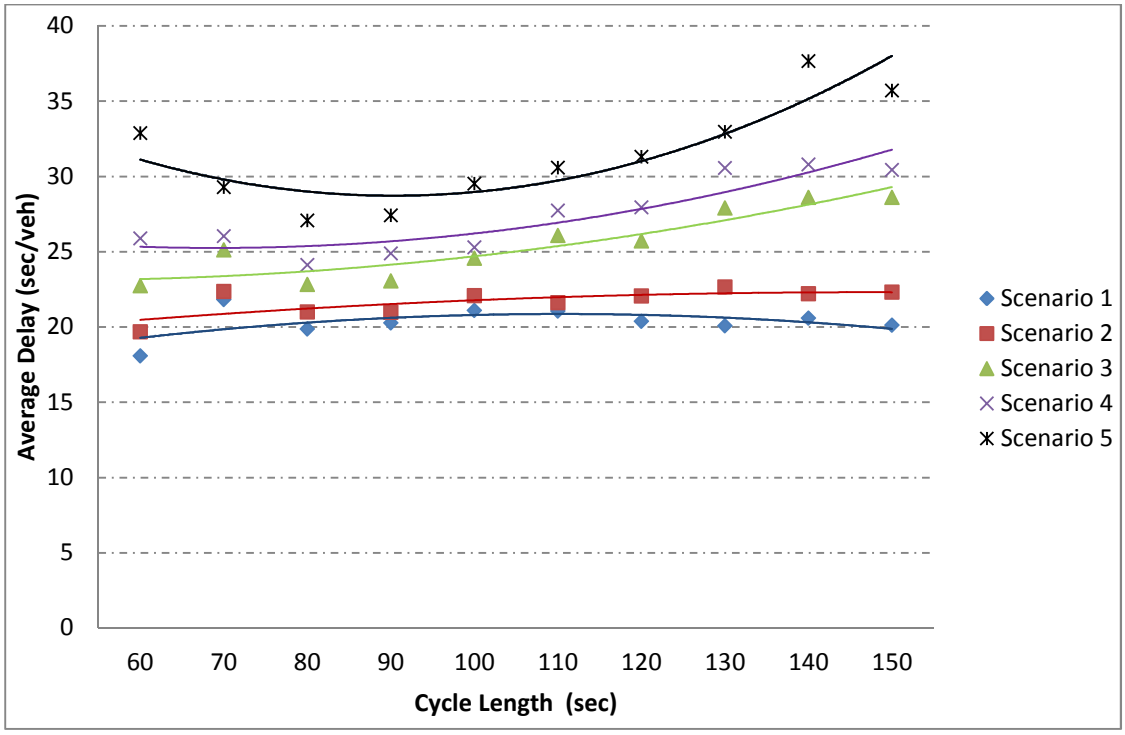

Figure 6-16 Average Delays of Vehicles of Movement "10->9" and Cycle Length

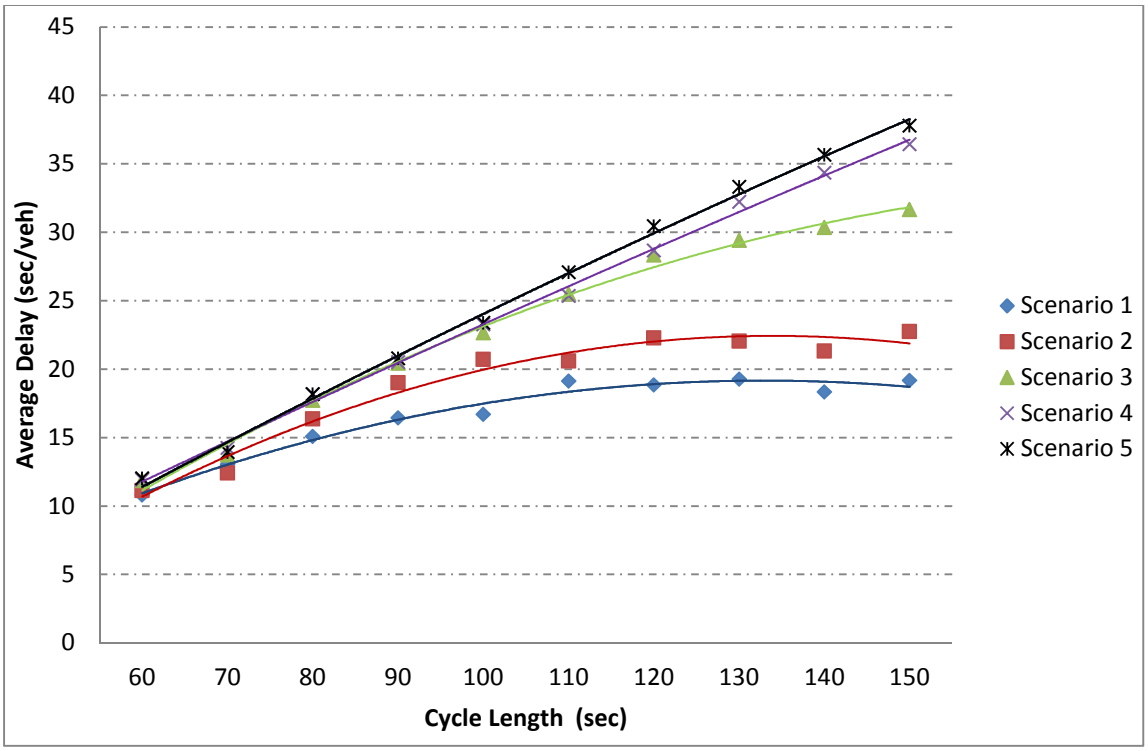

Figure 6-17 Average Delays of Vehicles of Movement "10->11" and Cycle Length

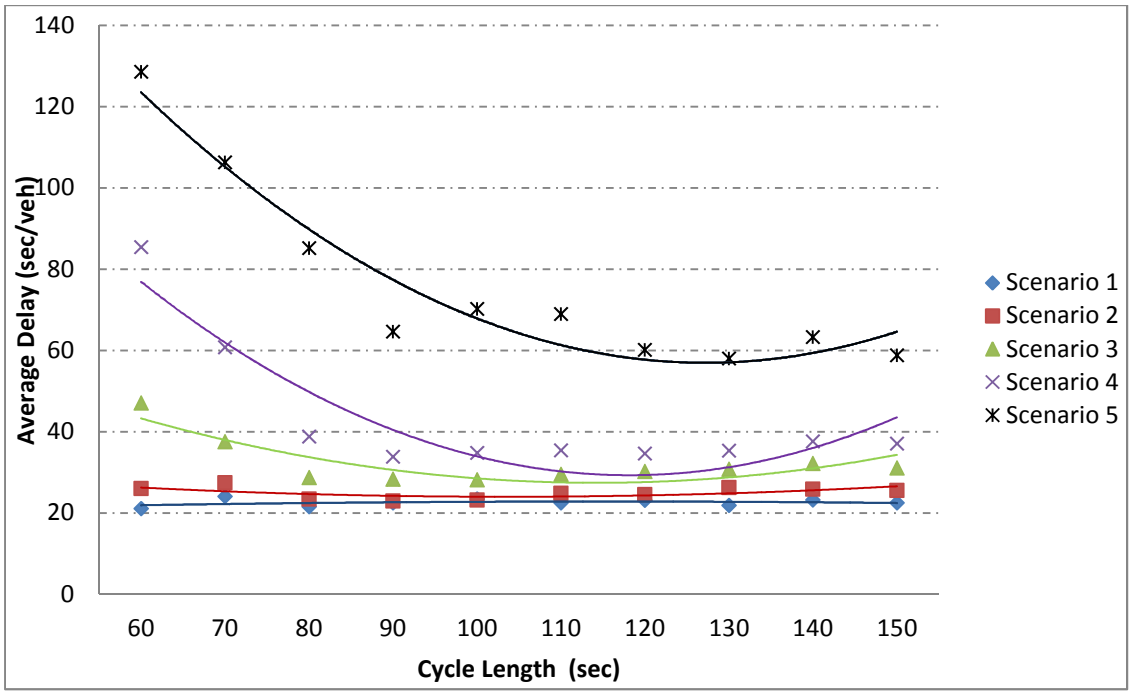

Figure 6-18 Average Delays of Vehicles of Movement "1->8" and Cycle Length

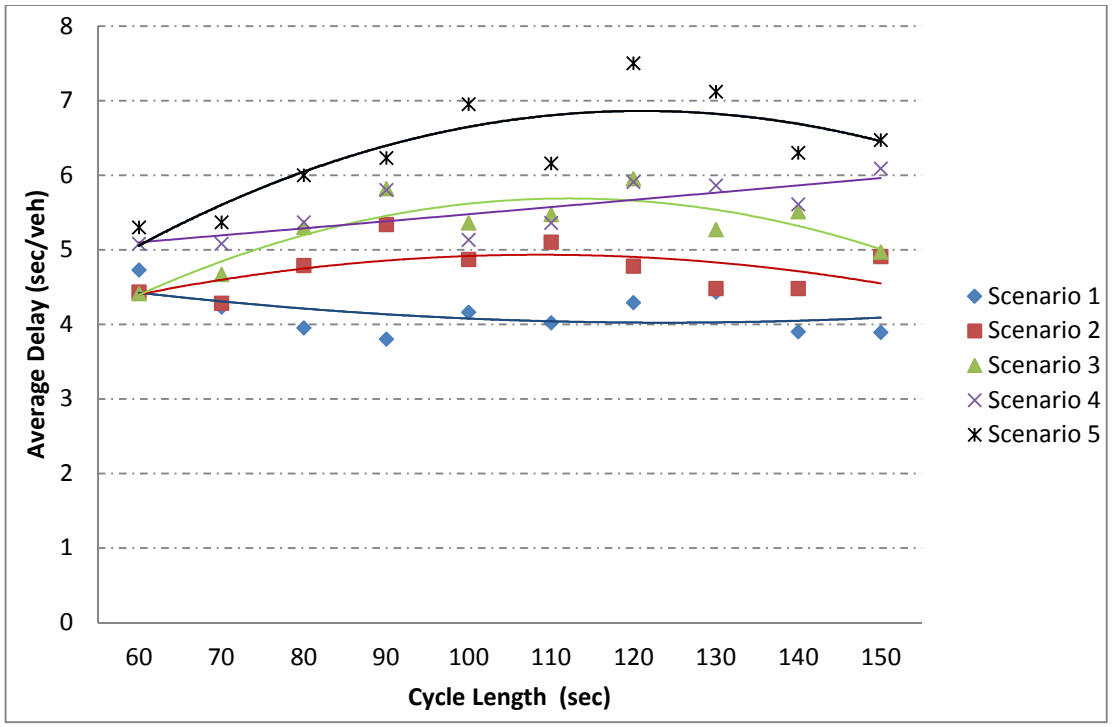

Figure 6-19 Average Delays of Vehicles of Movement "3->8" and Cycle Length

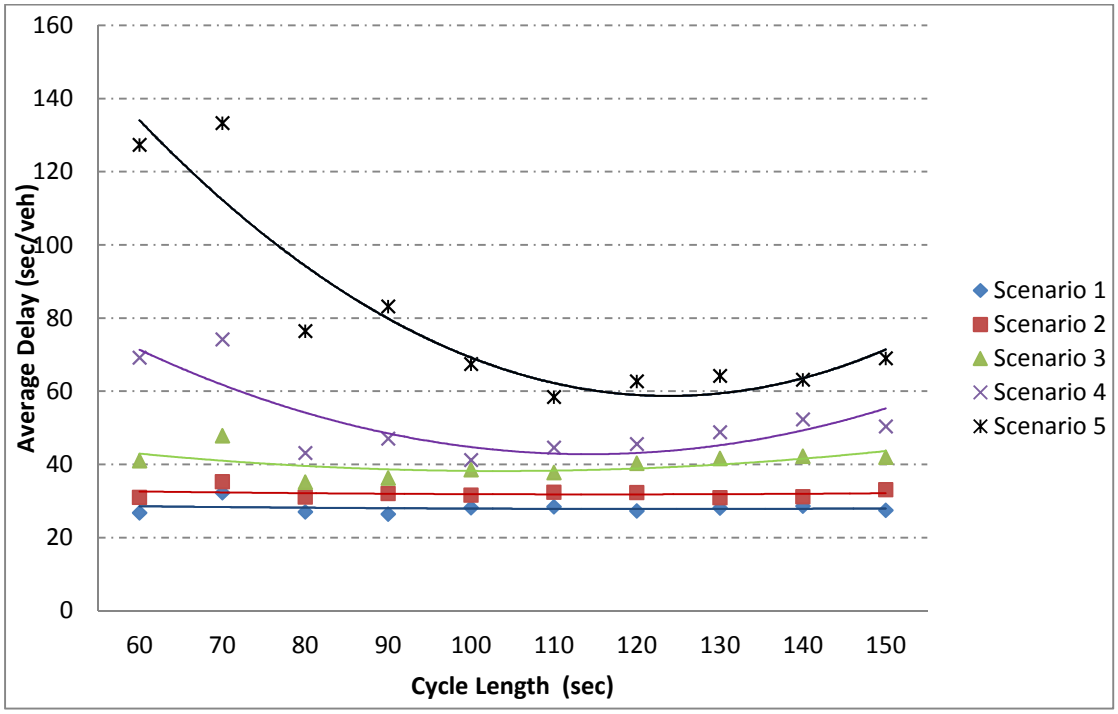

Figure 6-20 Average Delays of Vehicles of Movement "14->7" and Cycle Length

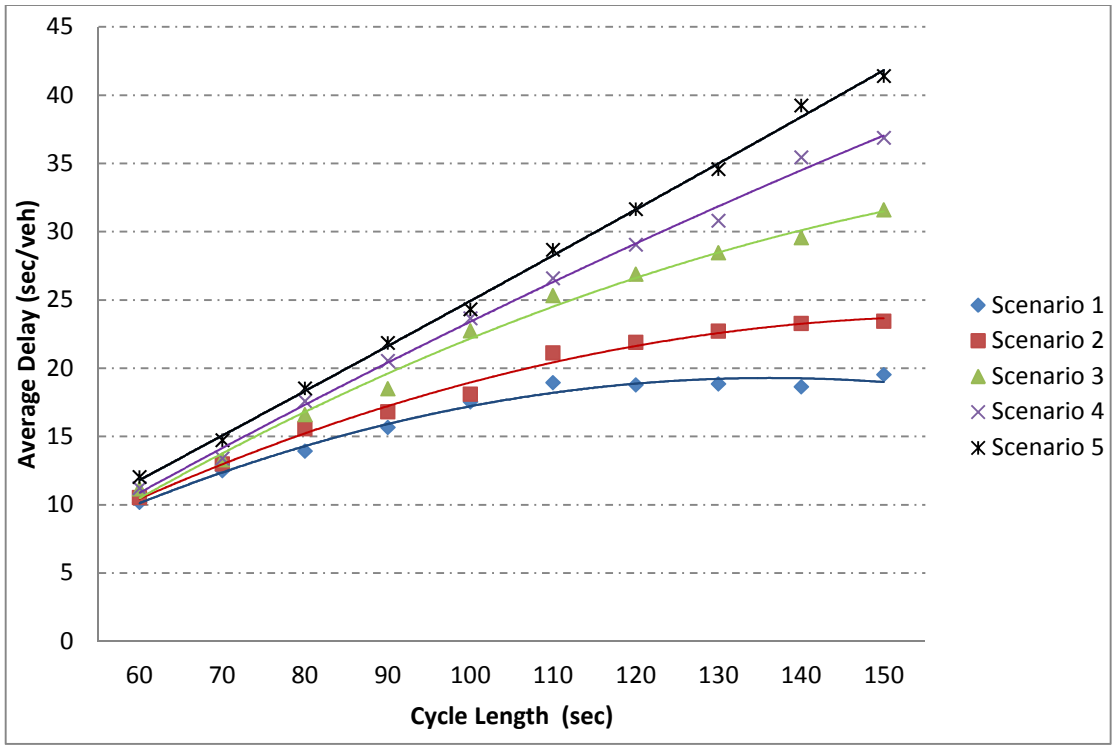

Figure 6-21 Average Delays of Vehicles of Movement "5->4" and Cycle Length

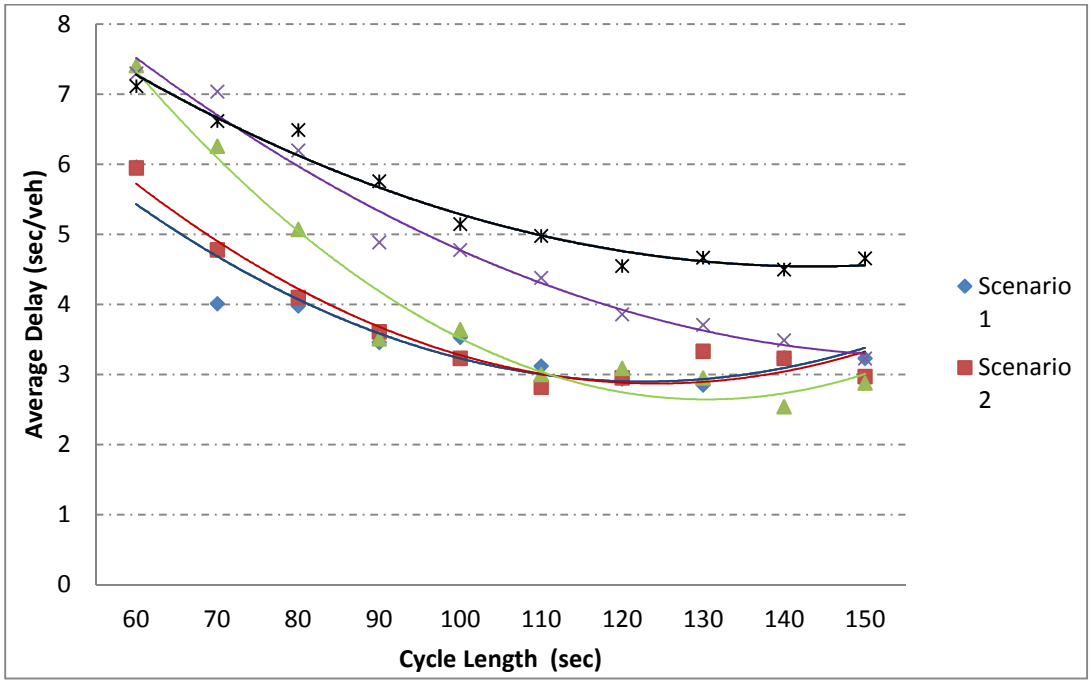

Figure 6-22 Average Delays of Vehicles of Movement "12->7" and Cycle Length

6.3.3 Fully Actuated Control

Figure 6-23 shows that fully actuated control with shorter cycle length (between 60 sec and 150 sec), which is actually the sum of critical phase maximum recall lengths, produces fewer delays when the sum of critical saturation flow ratios is less than 0.51 under scenarios 1 and 2. Except during the cycle length of 60 sec, the scenario 3 delays decrease with the decrease of its cycle length when its sum of critical saturation flow ratios is 0.64. In addition, the average delay does not change dramatically when cycle length is increasing from 60 sec to 150 sec when the sum of each scenario's critical saturation flow ratio is less than around 0.64. The optimal cycle length for fully actuated control should be between 80 sec and 110 sec when the sum of critical saturation flow ratios is between around 0.73 and 0.85. Under such conditions, either a cycle length less than 80 sec or longer than 110 sec will cause greater average total delays. All the results shown in Figure 6-23 are valuable recommendations for traffic engineers and professionals in selecting optimal traffic signal timing plans in practice. The relationships between average delay of other traffic movements and cycle length are depicted in Figure 6-24 through Figure 6-30. The results indicate that the average delays in both directions between the two crossovers are less than 10 sec/veh. According to the average maximum queues shown in Appendix B, less than seven vehicles stopped in the middle of the DDI and will not spill back to their upstream crossover intersection under fully actuated control.

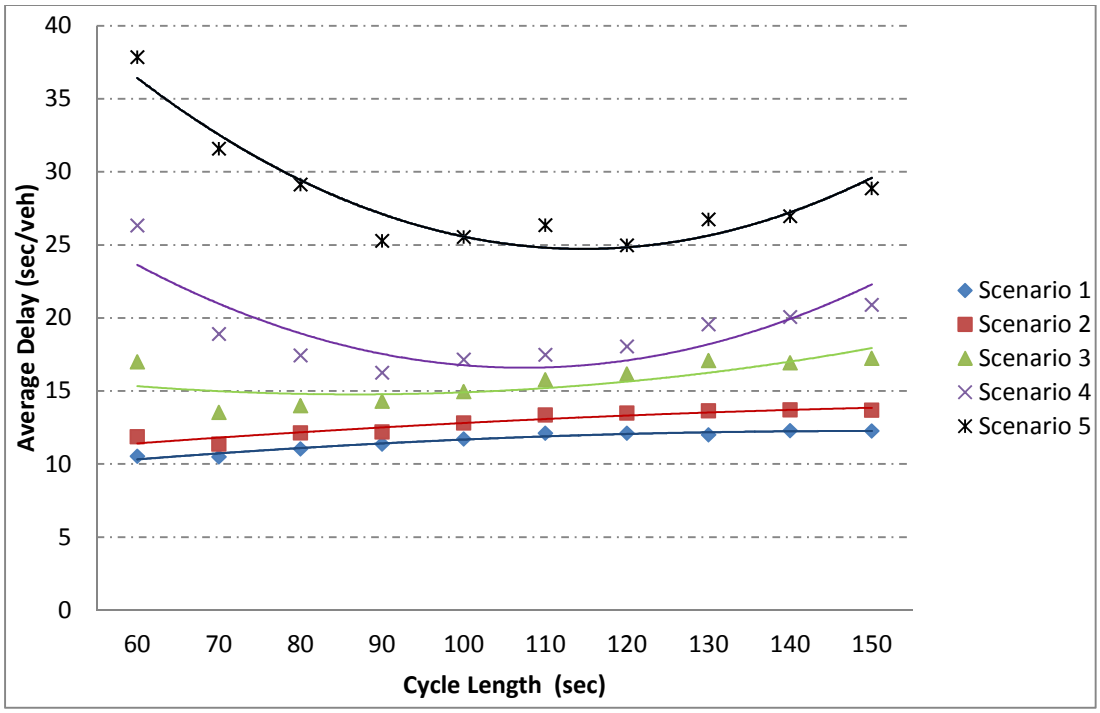

Figure 6-23 Average Delays of All Vehicles and Cycle Length

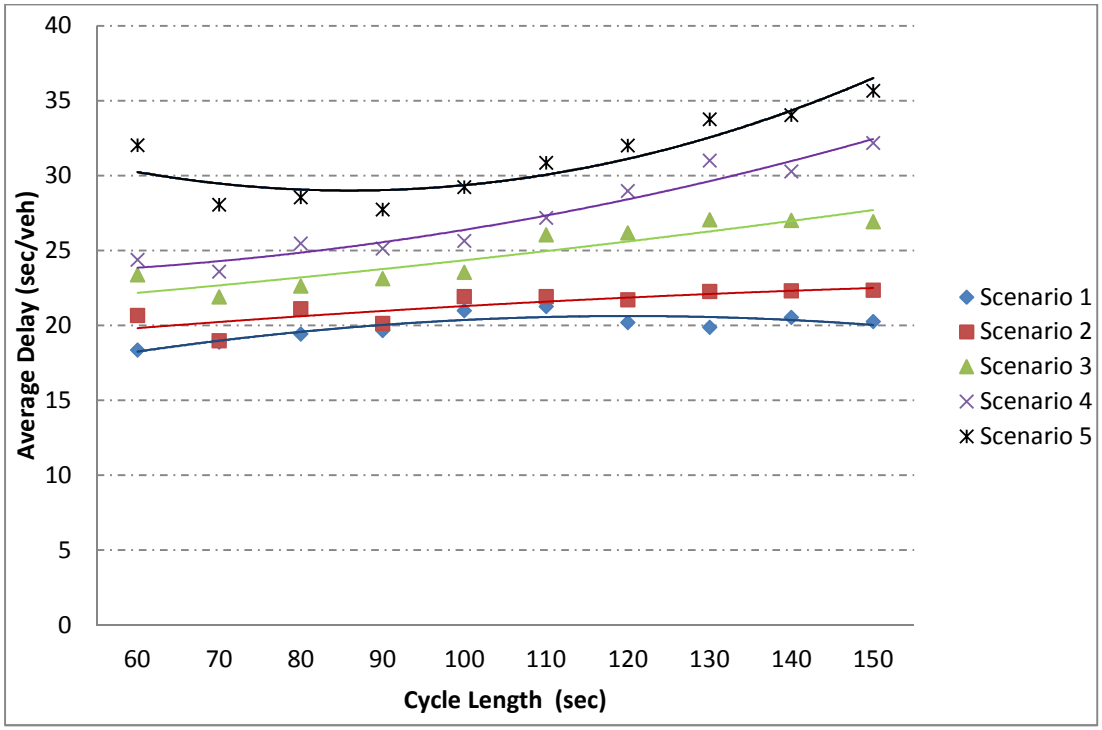

Figure 6-24 Average Delays of Vehicles of Movement "10->9" and Cycle Length

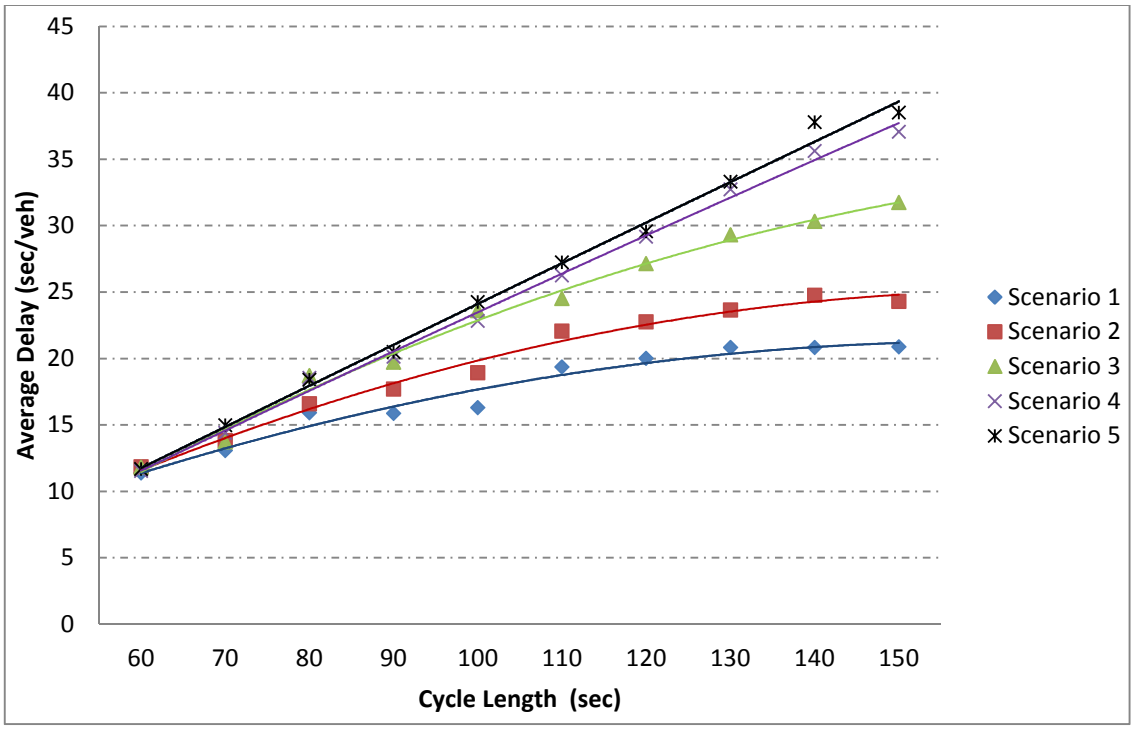

Figure 6-25 Average Delays of Vehicles of Movement "10->11" and Cycle Length

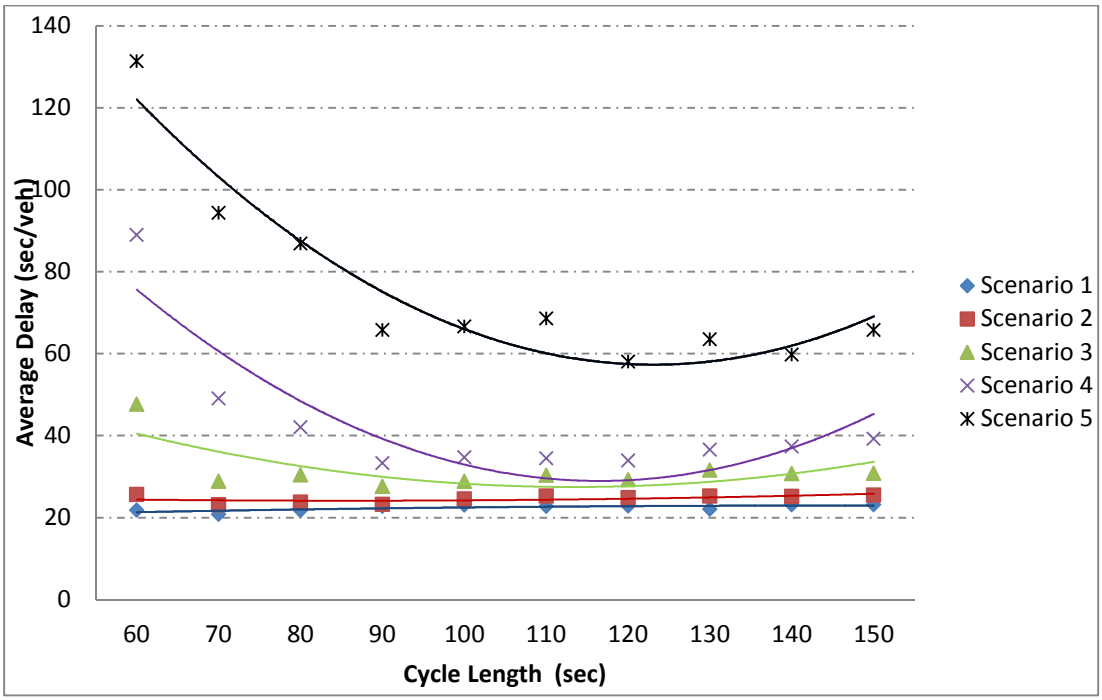

Figure 6-26 Average Delays of Vehicles of Movement "1->8" and Cycle Length

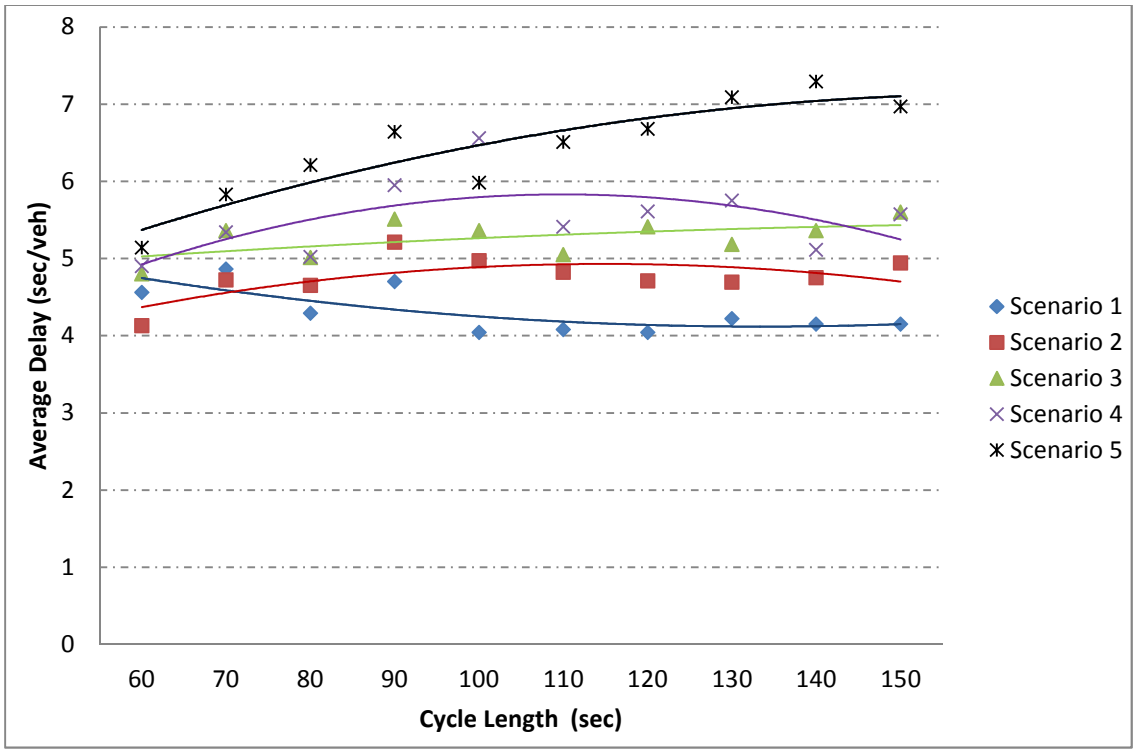

Figure 6-27 Average Delays of Vehicles of Movement "3->8" and Cycle Length

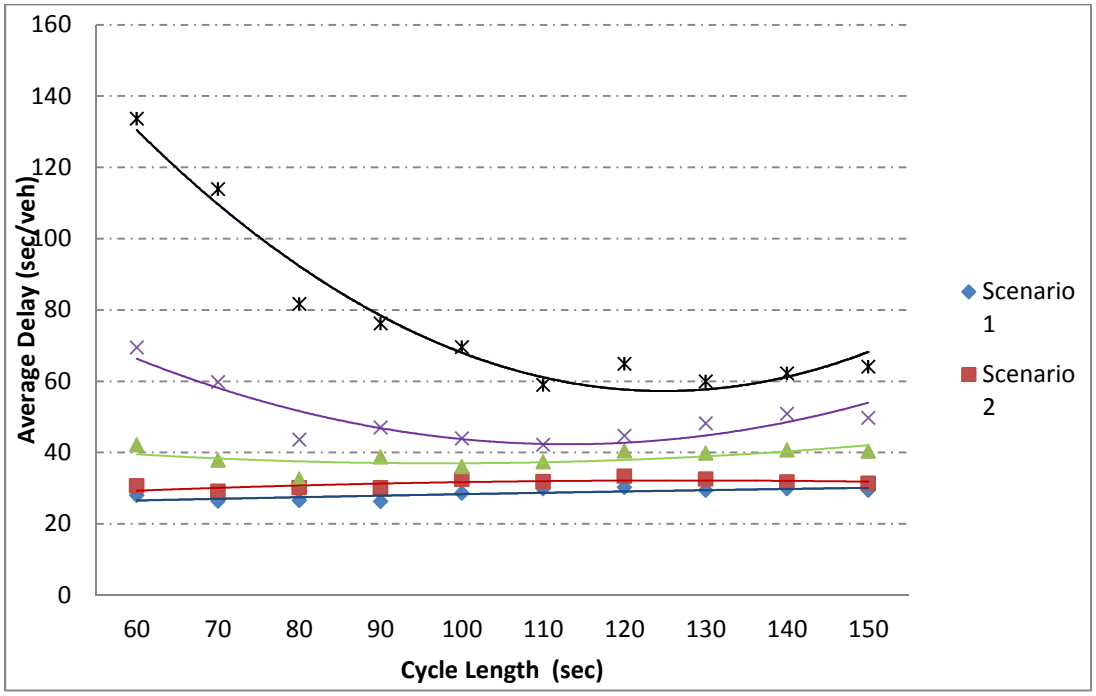

Figure 6-28 Average Delays of Vehicles of Movement "14->7" and Cycle Length

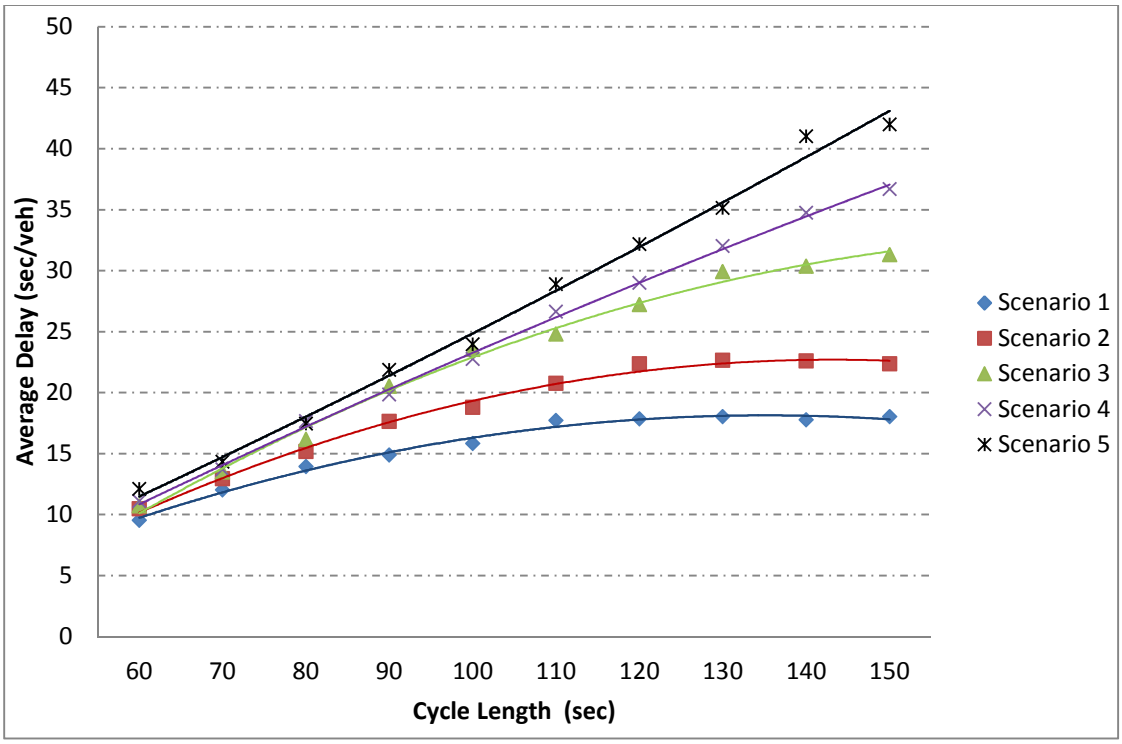

Figure 6-29 Average Delays of Vehicles of Movement "5->4" and Cycle Length

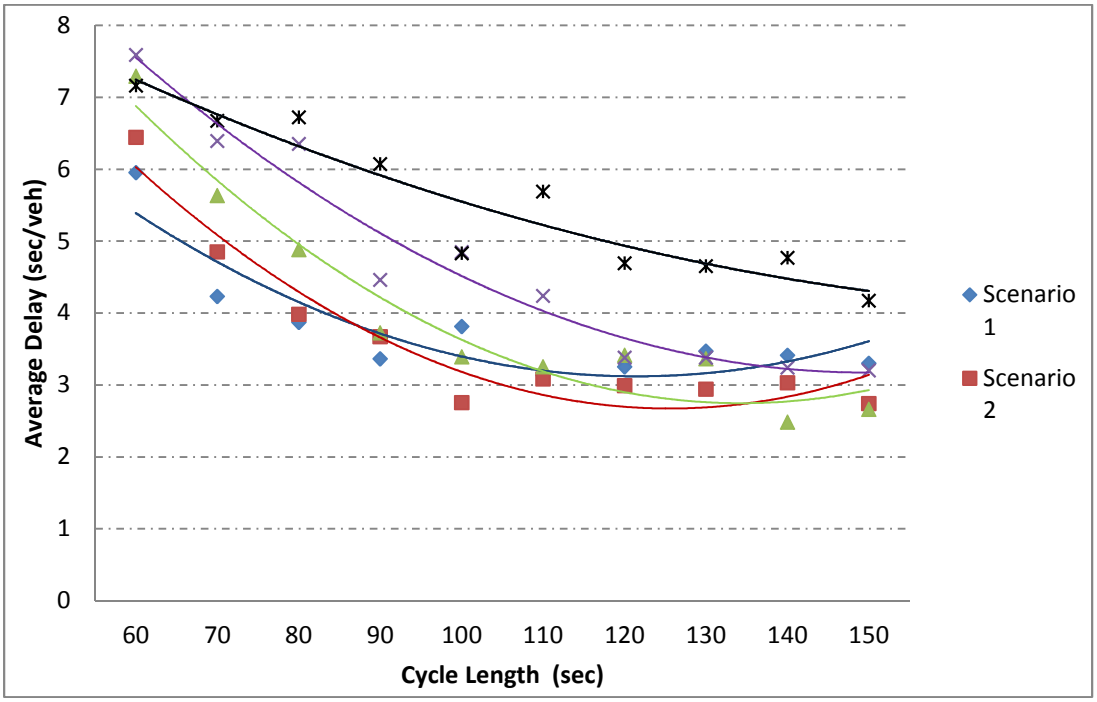

Figure 6-30 Average Delays of Vehicles of Movement "12->7" and Cycle Length

6.3.4 Coordinated Actuated Control

Figure 6-31 shows that the coordinated actuated control with shorter cycle length (between 60 sec and 150 sec) produces fewer delays when the sum of critical saturation flow ratios is less than 0.51. Except at a cycle length of 60 sec, the average total delay of this DDI rises with the increase of cycle length when the sum of critical saturation flow ratios is 0.64. The optimal cycle length for coordinated actuated control should be between 75 sec and 110 sec when the sum of critical saturation flow ratios is equal to 0.73. A cycle length shorter than 75 sec or longer than 110 sec can bring about heavy average total delay of the DDI under these conditions. The optimal cycle length ranges nearly from 85 sec to 130 sec when the sum of critical saturation flow ratios increases to 0.85. Other cycle lengths produce more serious traffic delays under the same conditions. The relationships between average delay of other traffic movements and cycle length are depicted in Figure 6-32 through Figure 6-38. The results indicate that the average delays in both directions between two crossovers are less than 12 sec/veh. In addition, less than seven vehicles stopped in the middle of the DDI and will not spill back to their upstream crossover intersection under coordinated actuated control despite the average maximum queues shown in Appendix B. These results are useful for traffic engineers and professionals to decide the optimal traffic signal timing plans in practice.

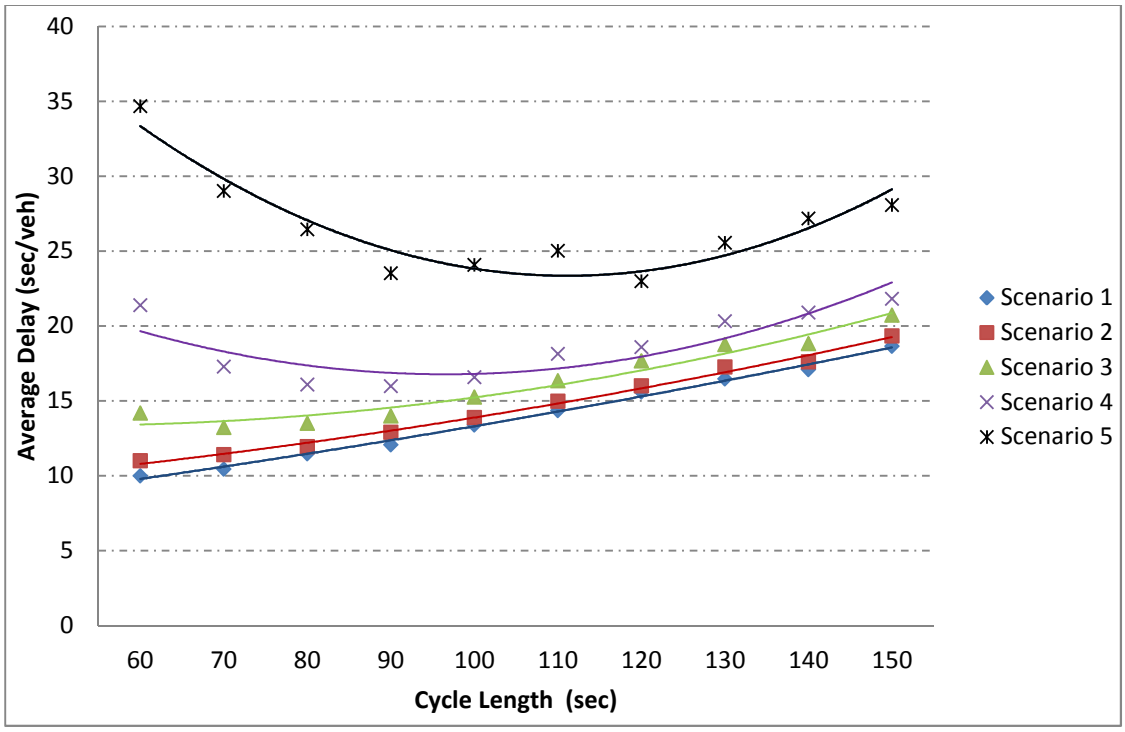

Figure 6-31 Average Delays of All Vehicles and Cycle Length

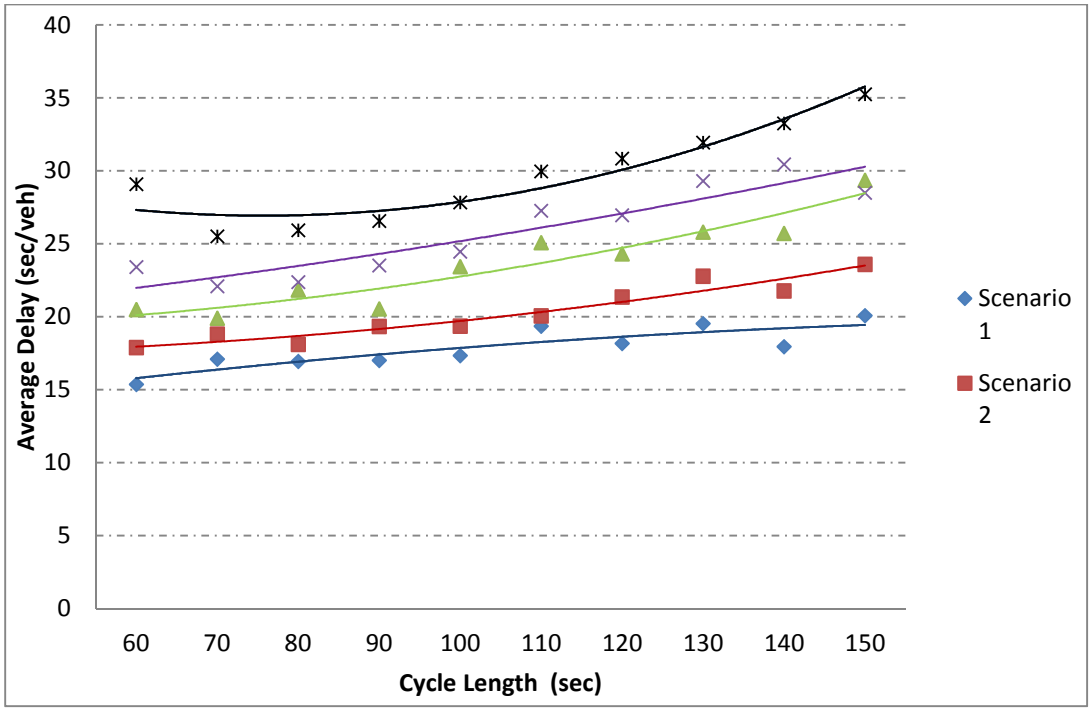

Figure 6-32 Average Delays of Vehicles of Movement "10->9" and Cycle Length

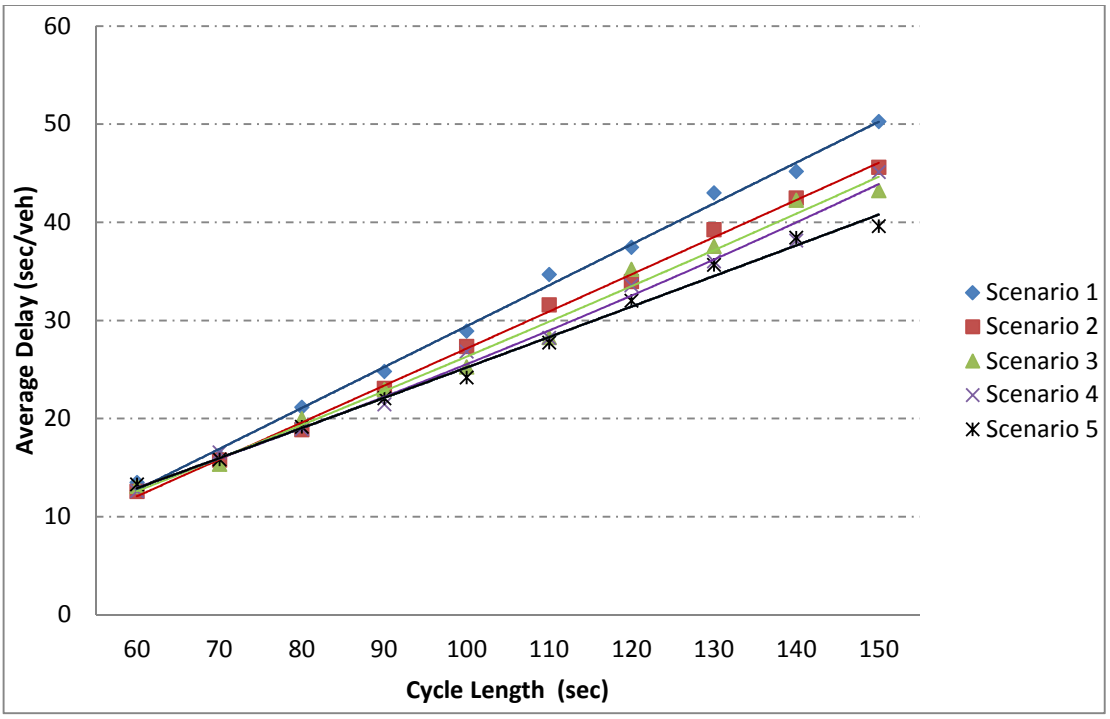

Figure 6-33 Average Delays of Vehicles of Movement "10->11" and Cycle Length

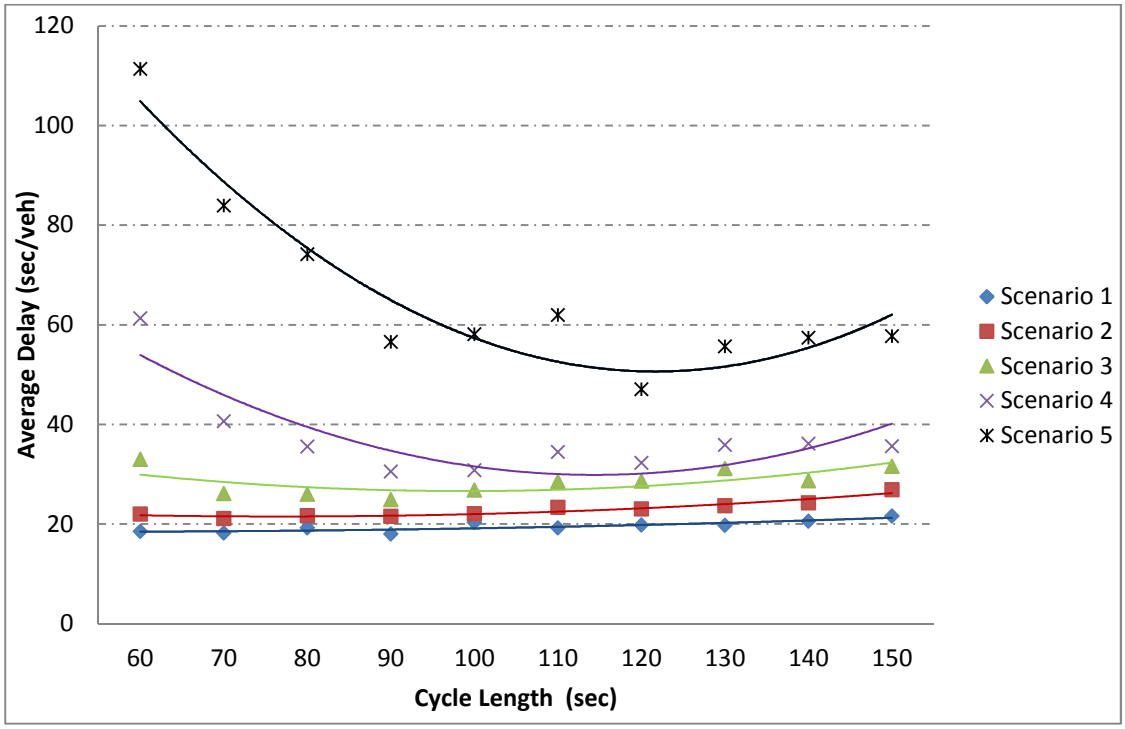

Figure 6-34 Average Delays of Vehicles of Movement "1->8" and Cycle Length

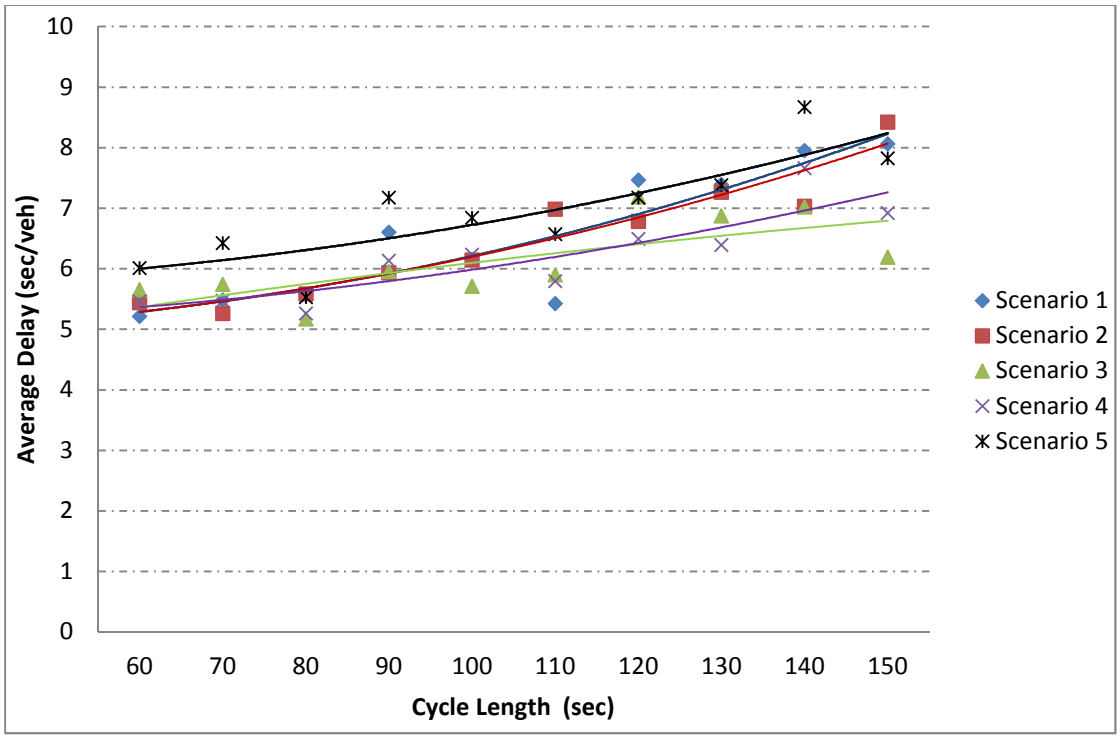

Figure 6-35 Average Delays of Vehicles of Movement "3->8" and Cycle Length

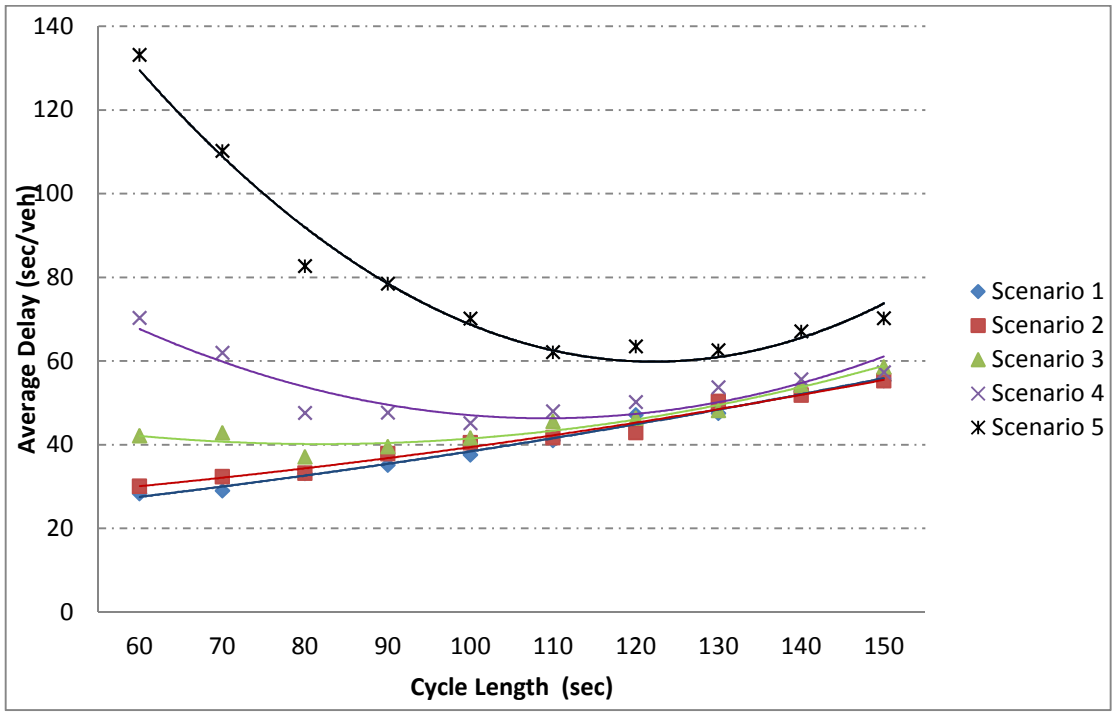

Figure 6-36 Average Delays of Vehicles of Movement "14->7" and Cycle Length

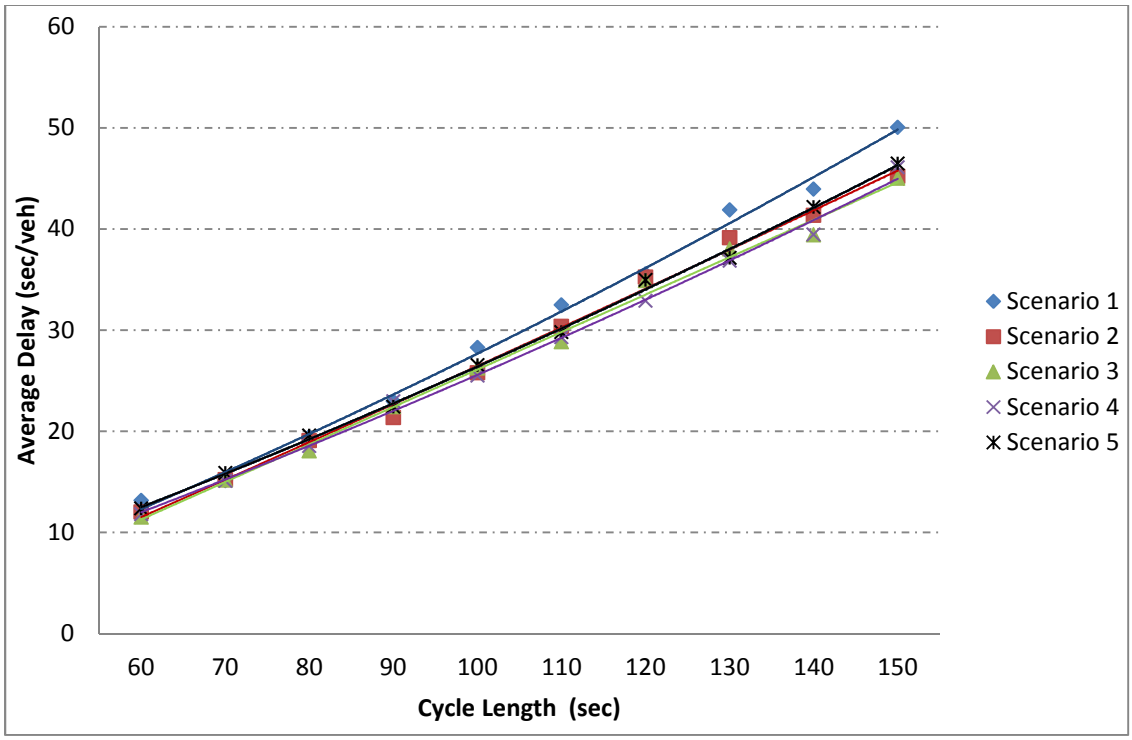

Figure 6-37 Average Delays of Vehicles of Movement "5->4" and Cycle Length

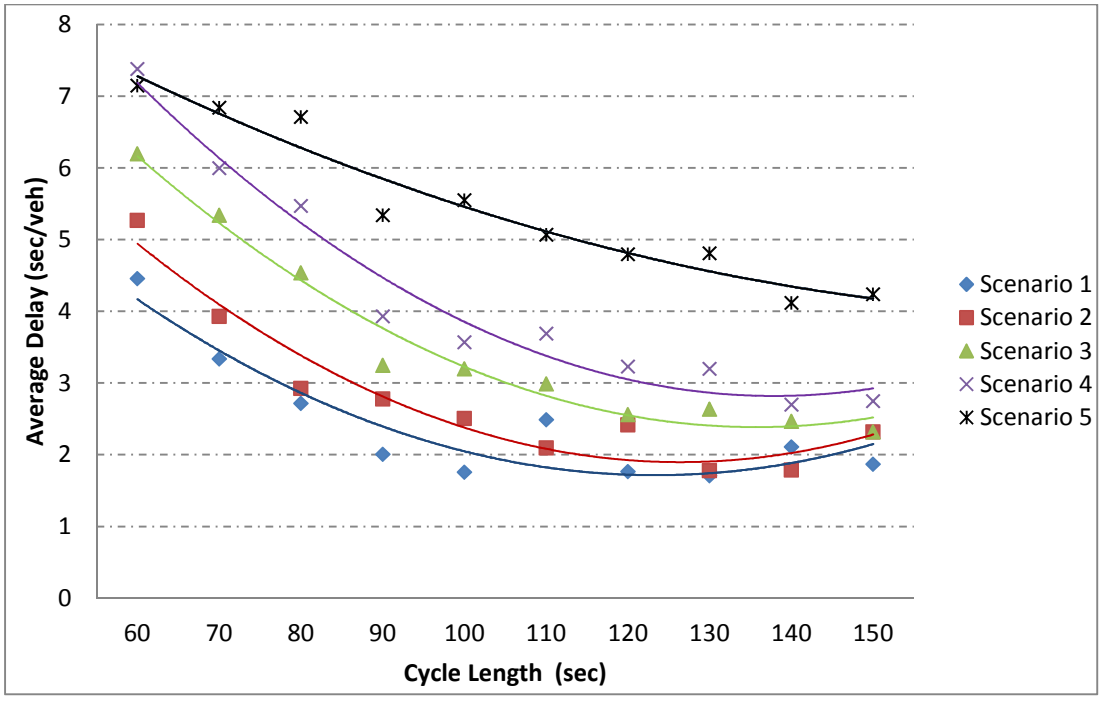

Figure 6-38 Average Delays of Vehicles of Movement "12->7" and Cycle Length

6.3.5 Summary

Figure 6-39 to Figure 6-40 shows that pre-timed control and fully actuated control operated with similar average total delays but better than coordinated actuated control in scenarios 1 and 2 for each cycle. In other words, when the sum of critical saturation flow ratios is less than 0.51 with similar traffic distribution such as scenarios 1 and 2, the pre-timed control and fully actuated control outperformed the coordinated control. The average total delay of pre-timed control and fully actuated control did not change much when the cycle length changed from 60 sec to 150 sec. However, the average total delay of this DDI increased steadily as the cycle length increased from 60 sec to 150 sec in coordinated actuated mode. Figure 6-41 illustrates that three types of controls have similar trends for average total delay as the cycle length changes from 60 sec to 150 sec when the sum of critical saturation flow ratios is 0.64. The optimal cycle length is around between 70 sec and 90 sec. Figure 6-42 shows similar trends between average total delay and cycle length under scenario 3 to those shown in Figure 6-41. However, the optimal range of cycle length is between 70 sec to 115 sec when the sum of critical saturation flow ratios is 0.73. The performances of these types of controllers are not very different. Similar conclusions are realized under scenario 5 with the sum of critical saturation flow ratios 0.85 as shown in Figure 6-43. The only evident difference is that the region of optimal cycle length is between 85 sec and 125 sec. Figure 6-44 points out that the average maximum queues in front of signal "7" between the two crossovers of the DDI ranges from 140 feet to 240 feet, which means vehicles in this segment cannot spill back to their upstream crossover intersection. Figure 6-45 indicates that the average maximum

queues at the approach of signal "8" between the two crossovers of the DDI is greater than 75 feet but less than 115 feet, so the space between crossovers can be clear at all times.

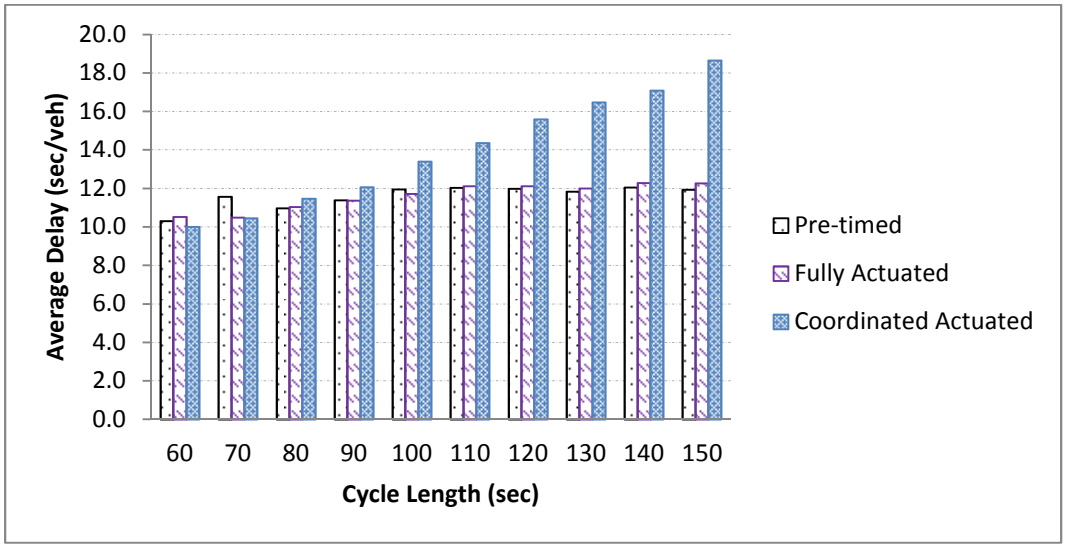

Figure 6-39 Average Delays of All Vehicles and Cycle Length in Scenario 1

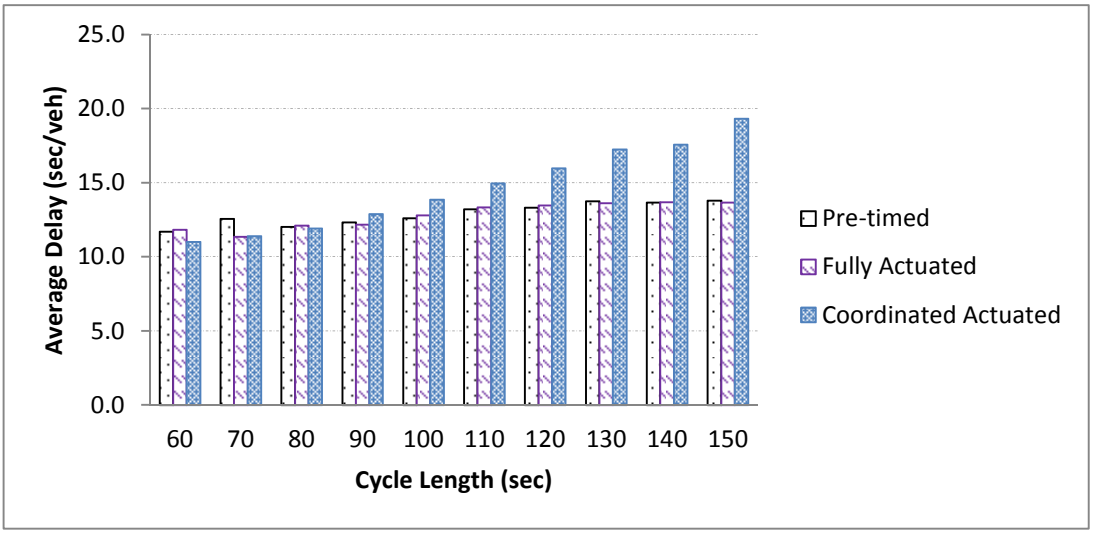

Figure 6-40 Average Delays of All Vehicles and Cycle Length in Scenario 2

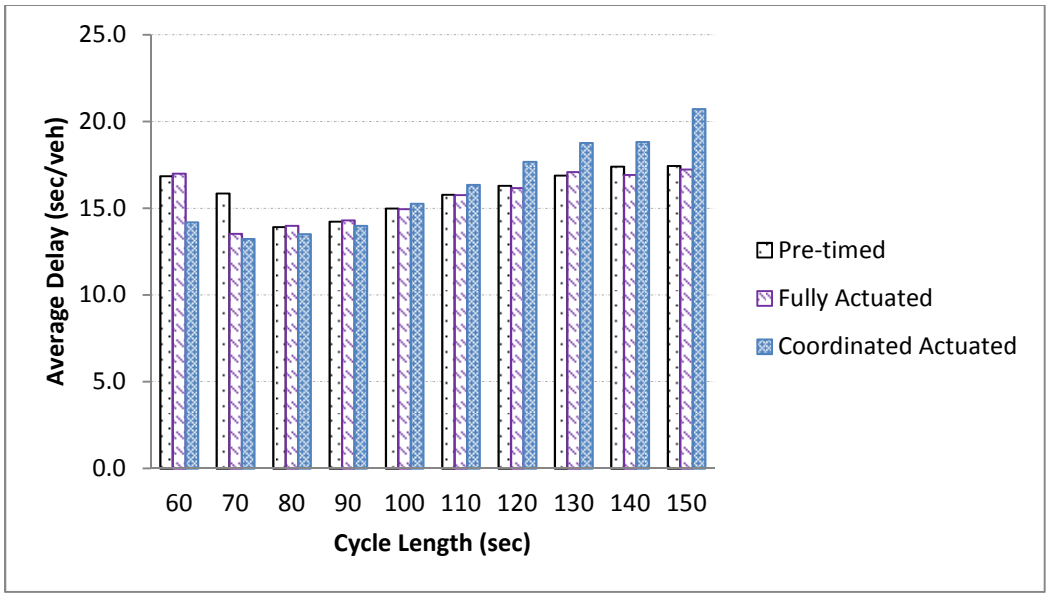

Figure 6-41 Average Delays of All Vehicles and Cycle Length in Scenario 3

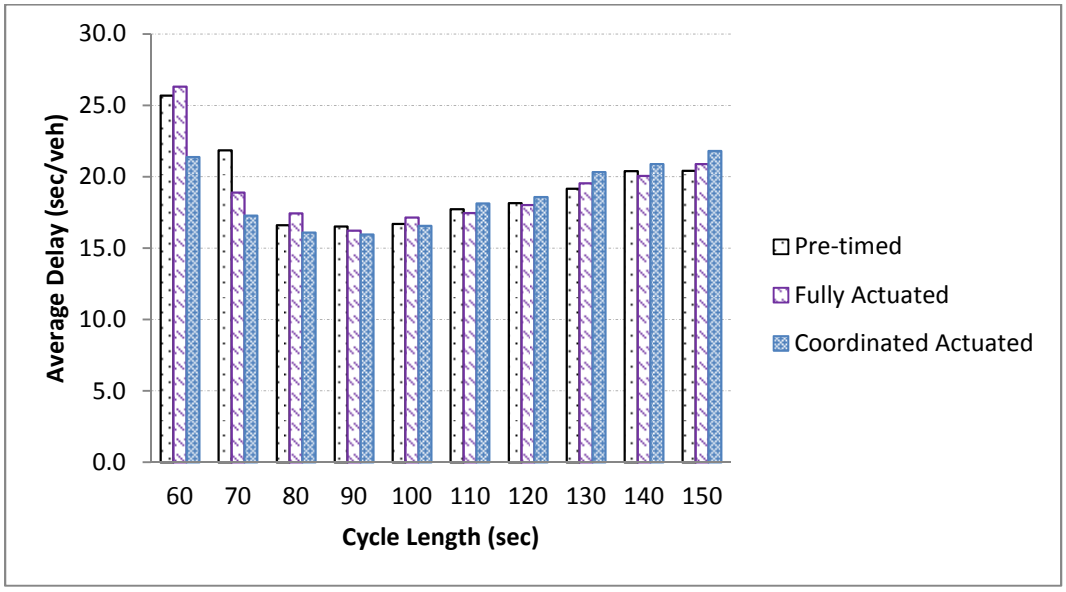

Figure 6-42 Average Delay of All Vehicles and Cycle Length in Scenario 4

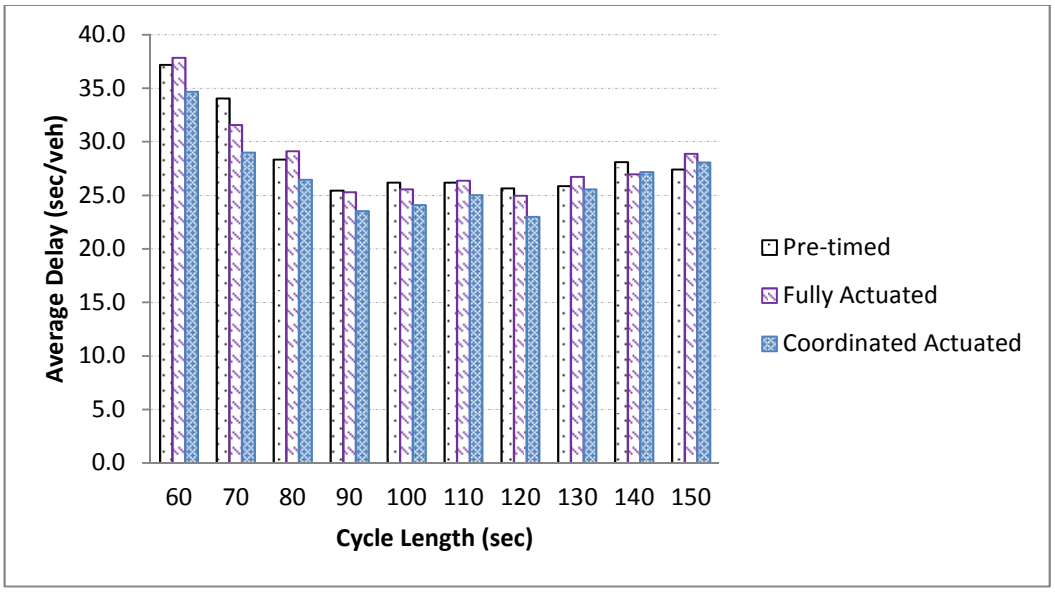

Figure 6-43 Average Delay of All Vehicles and Cycle Length in Scenario 5

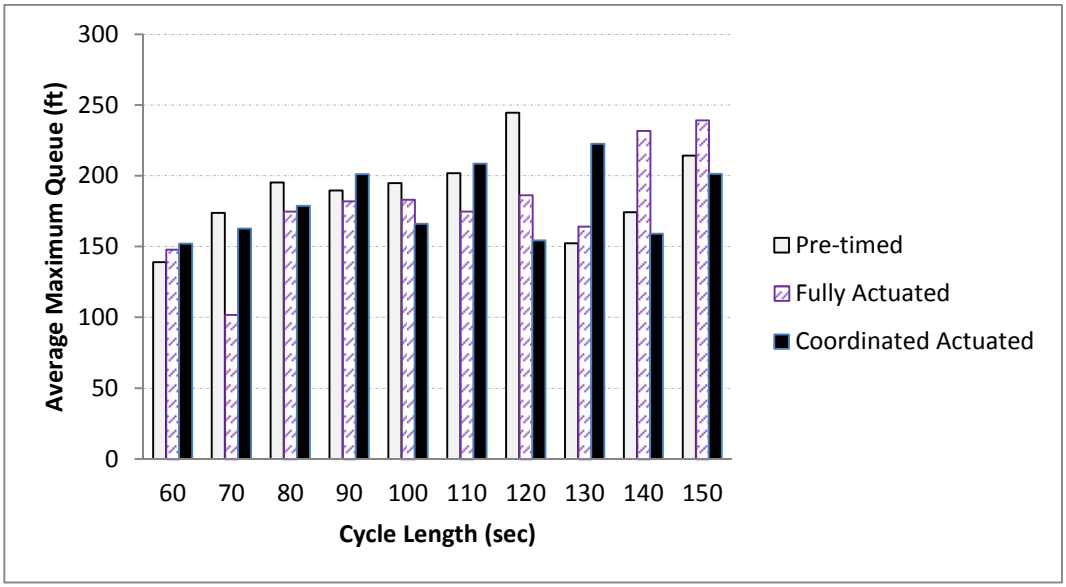

Figure 6-44 Average Maximum Queue of Movement "12->7" and Cycle Length of Scenario 5

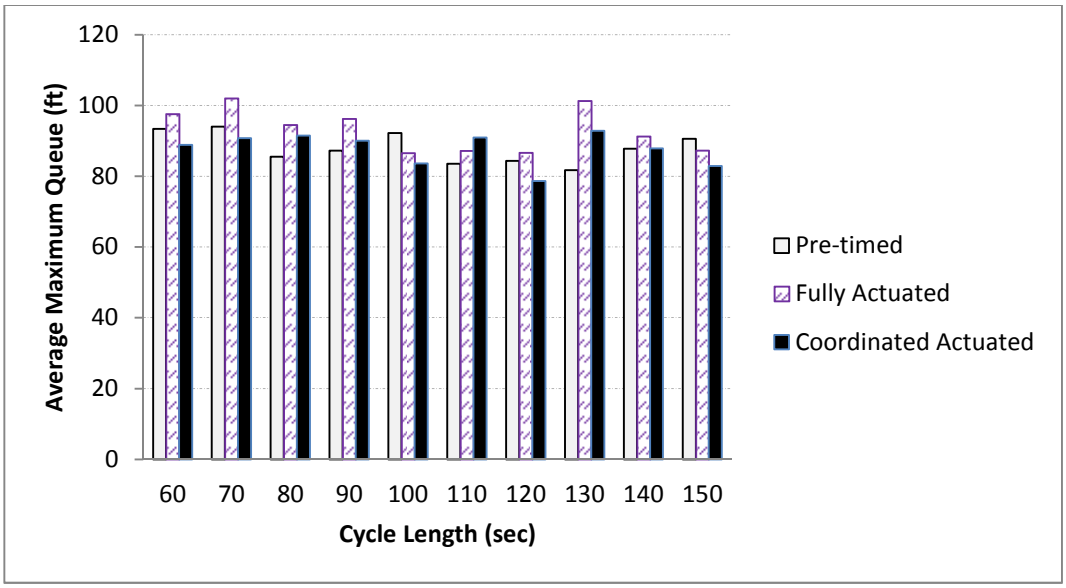

Figure 6-45 Average Maximum Queue of Movement "3->8" and Cycle Length of Scenario 5

6.4 EFFECTS OF ROUTE DISTRIBUTIONS

This section examines the effects of route distributions on traffic signal operational performance. Given traffic movement volumes on certain of major approaches, many route distribution scenarios exist. Whether the traffic signal operations should be adjusted for each route distribution scenario is tested in this section.

Fifteen route distribution scenarios were studied. Each route distribution was evaluated separately as pre-timed control and fully actuated control. In addition, every traffic operation was applied with travel time between two crossovers as both 12 sec ($T_{8,11,12,7}$=12 sec) and 22 sec ($T_{8,11,12,7}$=22 sec). For comparing the performance of the original traffic signal timing plans without adding an extensional green time (proposed operation 2-a) and adjusting traffic signal timing plans (proposed operation 2-b), each

route distribution scenario was evaluated by these two operations. Therefore, a total of 120 simulation models created in VISSIM 5.40 were evaluated as shown in Table 6-19.

Table 6-19 Total Traffic Simulation Scenarios

Operation Plans	Control Types	$T_{8,11,12,7}$=12 sec	$T_{8,11,12,7}$=22 sec
Original	Pre-timed	15	15
	Fully Actuated	15	15
Adjusted	Pre-timed	15	15
	Fully Actuated	15	15

One traffic simulation can be named as "P_1-P_2-P_3-P_4-CT."

where

P_1: $\frac{v_{8,11,12,7}}{v_{1,8}} * 100$;

P_2: $\frac{v_{5,4,3,8,9}}{v_{5,4}} * 100$;

P_3: $\frac{v_{14,7,4,3,8,9}}{v_{14,7}} * 100$;

P_4: $\frac{v_{10,11,12,7,6}}{v_{10,11}} * 100$; and

CT: controller type: pre-timed or fully actuated control.

Figure 6-46 and Figure 6-47 together illustrate the meaning of "P_1-P_2-P_3-P_4 -CT." For example, a scenario "0-50-50-100-Original" means a traffic distribution scenario with the values $P_1 = 0$, $P_2 = 50$, $P_3 = 50$, and $P_4 = 100$ and controlled by the original traffic signal timing plan.

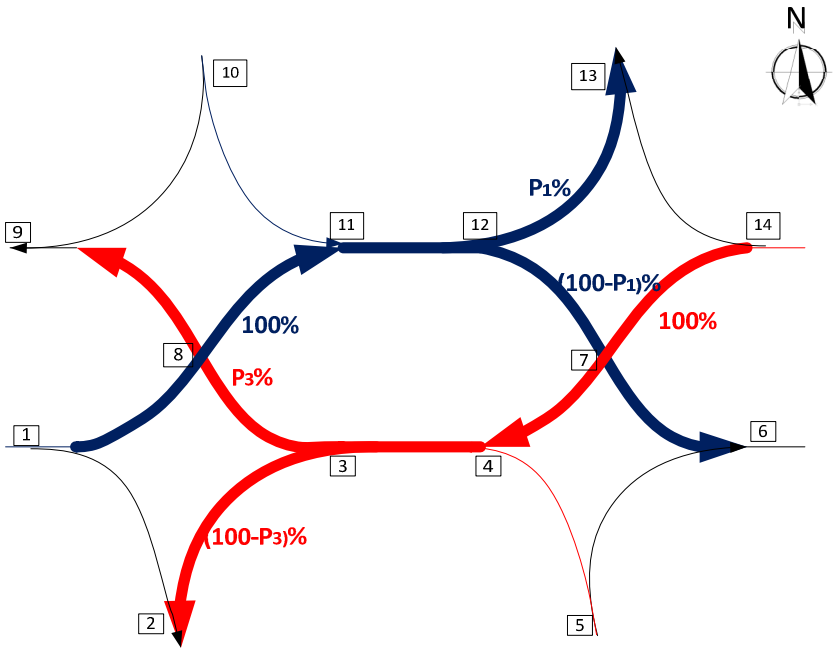

Figure 6-46 Example of Naming Route Distribution Scenario

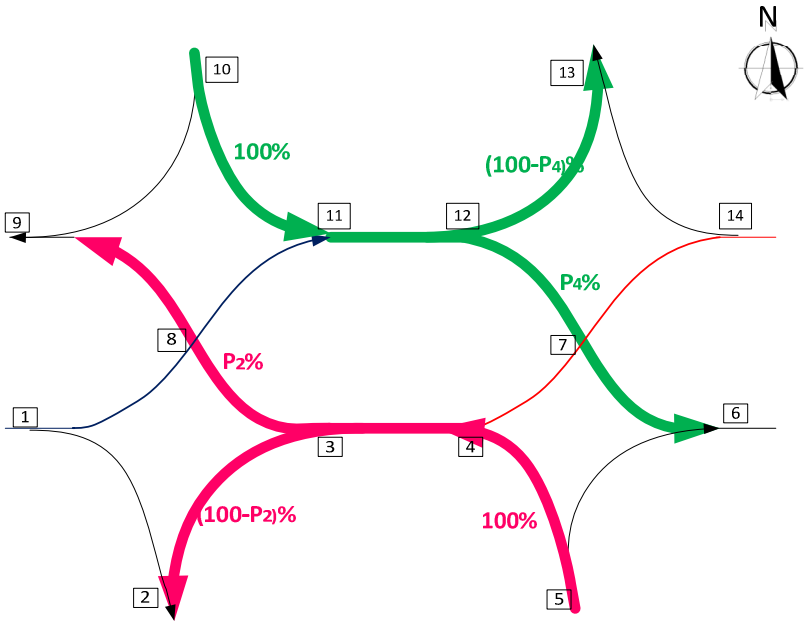

Figure 6-47 Example of Naming Route Distribution Scenario

6.4.1 Simulations When $T_{8,11,12,7}$=12 sec

The VISSIM model for each scenario was run in ten simulations with randomly generated seeds. The warm-up time in the simulation models was 300 seconds, with a continuous 900 seconds compiled simulation data collected for each traffic movement and the entire road system at the DDI. The configuration of the simulation models when $T_{8,11,12,7}$=12 sec is displayed in Figure 6 48. In Chapter 5, the traffic turning percentages at nodes 3 and 4 are not included in defining the value of an extensional green time. This manipulating methodology is not reasonable for some conditions based on the results shown in Table 6 20. The ranges of average delay of all vehicles in the network are close to 24.0% under pre-timed control and 28.8% under fully actuated control for different route distribution scenarios related to nodes 3 and 4. The major cause of dramatic differences among various scenarios is that the distance between the two crossovers is short, since the differences among various scenarios when $T_{8,11,12,7}$ =22 sec is not noticeable given other similar conditions according to the results in Table 6 24.

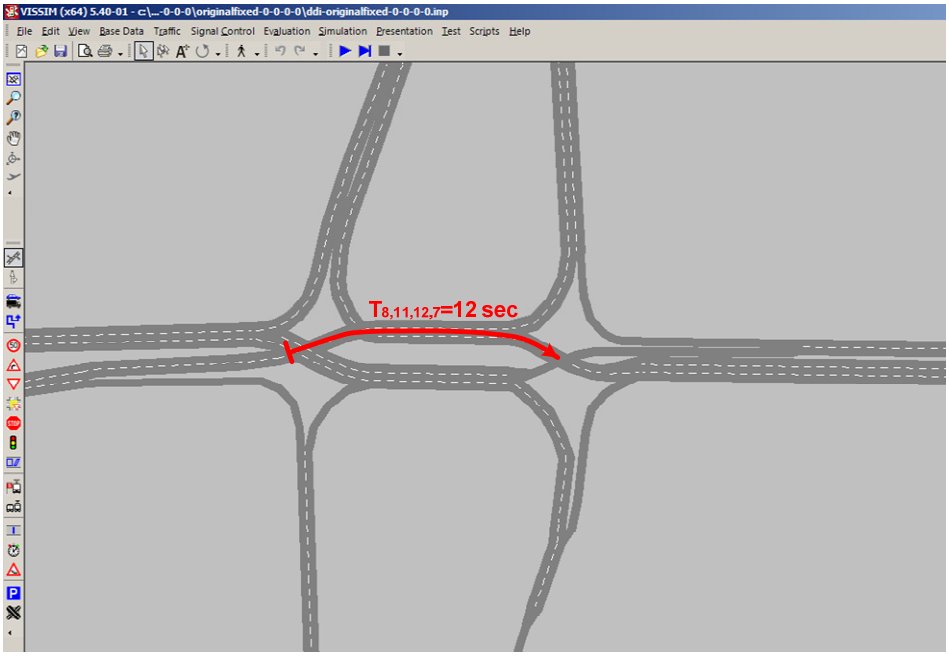

Figure 6-48 Configuration of the Simulation Models When $T_{8,11,12,7}$=12 Sec

Table 6-20 Effects of Route Distribution Generated from Nodes 3 and 4

	Pre-timed	Fully Actuated
Scenario	Average Delay of All (sec/veh)	Average Delay of All (sec/veh)
0-0-0-0-Original	19.3	19.5
0-0-50-50-Original	18.8	19.4
0-0-100-100-Original	19.3	19.2
Minimum	18.8	19.2
Maximum	19.3	19.5
Range	0.5	0.3
Range Percentage	2.7%	1.6%
100-100-0-0-Original	27.4	29.1
100-100-50-50-Original	22.2	23.1
100-100-100-100-Original	22.1	22.6
Minimum	22.1	22.6
Maximum	27.4	29.1
Range	5.3	6.5
Range (%)	24.0%	28.8%

The range of average delays of all vehicles among 15 route distribution scenarios under original pre-timed control is 9.3 sec/veh, or 51.4%. The pertinent range by original fully

actuated control is 10.9 sec/veh, or 59.9% (Table 6 25). Excluding the distribution scenario "100-100-0-0-Original," the range of average delay of all vehicles by pre-timed control is 5.1 sec/veh, or 28.2%. The pertinent range under original fully actuated control is 4.9 sec/veh, or 26.9%. These results indicate that the original pre-timed and fully actuated controls have nearly same range of variability for these distribution scenarios. Overall, the fully actuated control had almost the same average delays compared with pre-timed control with only a 0.2-sec/veh difference between mean average delays.

Table 6-21 Effects of Route Distribution on Original Methods

Scenario	Pre-timed Average Delay of All (sec/veh)	Fully Actuated Average Delay of All (sec/veh)	Difference	Difference (%)
0-0-0-0-Original	19.3	19.5	0.2	1.0%
0-0-50-50-Original	18.8	19.4	0.6	3.2%
0-0-100-100-Original	19.3	19.2	-0.1	-0.5%
100-100-0-0-Original	27.4	29.1	1.7	6.2%
100-100-50-50-Original	22.2	23.1	0.9	4.1%
100-100-100-100-Original	22.1	22.6	0.5	2.3%
0-0-50-100-Original	19.3	19.3	0.0	0.0%
0-50-50-100-Original	18.1	18.2	0.1	0.6%
0-100-50-100-Original	18.5	18.7	0.2	1.1%
50-0-50-100-Original	19.8	20.7	0.9	4.5%
50-50-50-100-Original	19.0	19.3	0.3	1.6%
50-100-50-100-Original	19.1	19.7	0.6	3.1%
100-0-50-100-Original	23.2	22.8	-0.4	-1.7%
100-50-50-100-Original	21.8	19.2	-2.6	-11.9%
100-100-50-100-Original	22.0	22.6	0.6	2.7%
Minimum	18.1	18.2	0.1	0.6%
Maximum	27.4	29.1	1.7	6.2%
Mean	20.7	20.9	0.2	1.1%
Range	9.3	10.9	1.6	17.2%
Range (%)	51.4%	59.9%	0.1	16.6%

According to the data in Table 6-22, the mean average delay of adjusted pre-timed control and fully actuated control was 21.0 and 21.2 sec/veh, respectively. The change of

average delay under adjusted pre-timed control is 8.6 sec/veh, or 45.7%, while the change for adjusted fully actuated control is within 10.6 sec/veh, or 57.3%. These results indicate that the adjusted fully actuated control has greater range of variability for the change of route distribution than pre-timed control given the same other conditions. The 45.7% and 57.3% values in Table 6-22 explain the effects of adjusted phase splits based on route distributions, in comparison to the 51.4% and 55.9% values shown in Table 6-21 for original methods. However, the efficiency performance of adjusting signal operations is not major.

Table 6-22 Effects of Traffic Distribution on Adjusted Methods

	Pre-timed	Fully Actuated		
Scenario	Average Delay of All (sec/veh)	Average Delay of All (sec/veh)	Difference	Difference (%)
0-0-0-0-Adjusted	19.3	19.5	0.2	1.0%
0-0-50-50-Adjusted	18.8	19.4	0.6	3.2%
0-0-100-100-Adjusted	19.3	19.2	-0.1	-0.5%
100-100-0-0-Adjusted	27.4	29.1	1.7	6.2%
100-100-50-50-Adjusted	22.2	23.1	0.9	4.1%
100-100-100-100-Adjusted	22.1	22.6	0.5	2.3%
0-0-50-100-Adjusted	19.3	19.3	0.0	0.0%
0-50-50-100-Adjusted	19.0	19.0	0.0	0.0%
0-100-50-100-Adjusted	20.6	20.6	0.0	0.0%
50-0-50-100-Adjusted	19.6	19.9	0.3	1.5%
50-50-50-100-Adjusted	19.0	18.5	-0.5	-2.6%
50-100-50-100-Adjusted	20.3	20.6	0.3	1.5%
100-0-50-100-Adjusted	23.1	22.6	-0.5	-2.2%
100-50-50-100-Adjusted	22.4	21.5	-0.9	-4.0%
100-100-50-100-Adjusted	23.3	23.0	-0.3	-1.3%
Minimum	18.8	18.5	-0.3	-1.6%
Maximum	27.4	29.1	1.7	6.2%
Mean	21.0	21.2	0.1	0.7%
Range	8.6	10.6	2.0	23.3%
Range (%)	45.7%	57.3%	0.1	25.3%

Overall, the adjusted traffic signal plans, both pre-timed and fully actuated control, brought about an almost equitable mean average delay compared with the original traffic signal plans, according to the results shown in Table 6-23. The original pre-timed control with the average delay of 0.4 sec/veh outperformed the adjusted pre-timed control. Original fully actuated signal plans had less average delay by 0.3 sec/veh than adjusted fully actuated plans (Table 6-23). One possible reason for these results is that the cycle lengths of these scenarios are in the same range of optimal cycle lengths discussed in the "Cycle Length" section ofthis chapter.

Table 6-23 Comparison between Original and Adjusted Methodologies

	Pre-timed	Fully Actuated
Scenario	Average Delay of All (sec/veh)	Average Delay of All (sec/veh)
0-0-0-0	0	0
0-0-50-50	0	0
0-0-100-100	0	0
100-100-0-0	0	0
100-100-50-50	0	0
100-100-100-100	0	0
0-0-50-100	0	0
0-50-50-100	0.9	0.8
0-100-50-100	2.1	1.9
50-0-50-100	-0.2	-0.8
50-50-50-100	0	-0.8
50-100-50-100	1.2	0.9
100-0-50-100	-0.1	-0.2
100-50-50-100	0.6	2.3
100-100-50-100	1.3	0.4
Minimum	-0.2	-0.8
Maximum	2.1	2.3
Mean	0.4	0.3
Range	2.3	3.1
Range (%)	11.1%	14.8%

6.4.2 *Simulations When $T_{8,11,12,7}$=22 sec*

Similar to the simulations where $T_{8,11,12,7}$=12 sec, the VISSIM model was run for each scenario with ten simulations using randomly generated seeds. The warm-up time in the simulation models was 300 seconds, and 900 seconds of simulation data were compiled for each traffic movement and the entire road system at the DDI. The configuration of the simulation models when $T_{8,11,12,7}$=22 sec is demonstrated in Figure 6-49. In Chapter 5, the route distribution percentage in front of nodes 3 and 4 were not included in defining the value of extensional green time. Different from the simulation results when $T_{8,11,12,7}$=12 sec, the methodology of adding extension is reasonable based on the results shown in Table 6-24 when $T_{8,11,12,7}$=22 sec. The ranges of average delay of all vehicles in the network are not greater than 4.5% for different route distribution scenarios related to nodes 3 and 4.

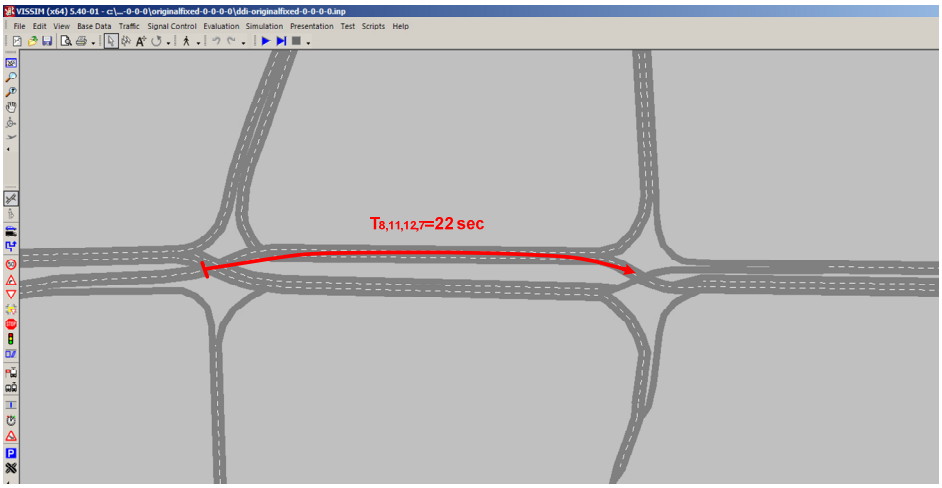

Figure 6-49 Configuration of the Simulation Models When $T_{8,11,12,7}$=22 Sec

Table 6-24 Effects of Route Distribution Related to Nodes 3 and 4

	Pre-timed	Fully Actuated
Scenario	Average Delay of All (sec/veh)	Average Delay of All (sec/veh)
0-0-0-0-Original	17.3	19.13
0-0-50-50-Original	17.2	18.83
0-0-100-100-Original	17.2	18.57
Minimum	17.2	18.6
Maximum	17.3	19.1
Range	0.1	0.6
Range Percentage	0.7%	3.0%
100-100-0-0-Original	22.7	25.1
100-100-50-50-Original	22.3	24.9
100-100-100-100-Original	21.7	24.3
Minimum	21.7	24.3
Maximum	22.7	25.1
Range	1.0	0.8
Range (%)	4.5%	3.4%

The range of average delays of all vehicles among 15 route distribution scenarios by pre-timed control is 5.5 sec/veh, or 32.1%. The pertinent range by fully actuated control is 6.5 sec/veh, or 35.1% (Table 6-25). Overall, fully actuated control increased average delay by 10.9% compared with pre-timed control. The major reason for this result is that vehicles that pass through the first signal needs more time to travel through the second signal, compared to the corresponding scenarios when $T_{8,11,12,7}$=12 sec. Fully actuated control operation can terminate or "gap out" earlier, so the remaining parts of a platoon might not pass through the second signal smoothly. However, the pre-timed signal operation can hold the green time on at the two crossover signals to guarantee most vehicles in a platoon pass through the second signal without encountering early "gap out".

Table 6-25 Effects of Route Distributions by Original Methods

Scenario	Pre-timed Average Delay of All (sec/veh)	Fully Actuated Average Delay of All (sec/veh)	Difference	Difference (%)
0-0-0-0-Original	17.3	19.1	1.8	10.5%
0-0-50-50-Original	17.2	18.8	1.6	9.5%
0-0-100-100-Original	17.2	18.6	1.4	8.0%
00-100-0-0-Original	22.7	25.1	2.4	10.4%
100-100-50-50-Original	22.3	24.9	2.5	11.4%
100-100-100-100-Original	21.7	24.3	2.5	11.6%
0-0-50-100-Original	17.3	18.6	1.3	7.6%
0-50-50-100-Original	18.5	19.8	1.3	7.2%
0-100-50-100-Original	19.7	21.1	1.4	7.1%
50-0-50-100-Original	17.8	20.5	2.6	14.7%
50-50-50-100-Original	19.0	21.7	2.7	14.0%
50-100-50-100-Original	20.5	22.8	2.3	11.4%
100-0-50-100-Original	19.2	22.0	2.8	14.6%
100-50-50-100-Original	20.4	23.1	2.7	13.1%
100-100-50-100-Original	21.8	24.3	2.5	11.5%
Minimum	17.2	18.6	1.4	8.0%
Maximum	22.7	25.1	2.4	10.4%
Mean	19.5	21.6	2.1	10.9%
Range	5.5	6.5	1.0	17.9%
Range (%)	32.1%	35.1%	0.0	9.2%

Overall, the adjusted traffic signal plans underperformed compared to the original traffic signal plans, according to the results shown in Table 6-26. The average delays of adjusted pre-timed control increased from 19.5 sec/veh to 20.9 sec/veh in simulations controlled by the original pre-timed type. However, the adjusted fully actuated control brought about the average total delay of 21.0 sec/veh, which is less than the 21.6 sec/veh under the original fully actuated control. The range of average delays by adjusted pre-timed control is within7.8 sec/veh, or 45.2%. The range of average delays by adjusted fully actuated control is within 6.5 sec/veh, or 35.8%. Dissimilar to original traffic signal

control plans, the adjusted fully actuated control had less range of the average delays by 20.7% than adjusted pre-timed control in other similar conditions.

Table 6-26 Effects of Route Distribution by Adjusted Methods

Scenario	Pre-timed Average Delay of All (sec/veh)	Fully Actuated Average Delay of All (sec/veh)	Difference	Difference (%)
0-0-0-0-Adjusted	17.3	19.1	1.8	10.5%
0-0-50-50-Adjusted	17.2	18.8	1.6	9.5%
0-0-100-100-Adjusted	17.2	18.6	1.4	8.0%
100-100-0-0-Adjusted	24.8	24.0	-0.8	-3.2%
100-100-50-50-Adjusted	24.1	23.7	-0.4	-1.7%
100-100-100-100-Adjusted	23.9	23.5	-0.4	-1.7%
0-0-50-100-Adjusted	17.3	18.6	1.3	7.6%
0-50-50-100-Adjusted	22.2	21.0	-1.2	-5.6%
0-100-50-100-Adjusted	25.0	24.5	-0.4	-1.7%
50-0-50-100-Adjusted	18.3	18.1	-0.2	-1.0%
50-50-50-100-Adjusted	20.6	20.4	-0.2	-1.0%
50-100-50-100-Adjusted	21.4	21.3	-0.1	-0.4%
100-0-50-100-Adjusted	19.1	19.4	0.2	1.2%
100-50-50-100-Adjusted	21.2	21.1	-0.1	-0.3%
100-100-50-100-Adjusted	23.9	23.5	-0.4	-1.7%
Minimum	17.2	18.1	0.9	5.1%
Maximum	25.0	24.5	-0.4	-1.7%
Mean	20.9	21.0	0.1	0.7%
Range	7.8	6.5	-1.3	-16.7%
Range (%)	45.2%	35.8%	-0.1	-20.7%

The original pre-timed control outperformed with the average delay of 1.4 sec/veh compared to adjusted pre-timed control. However, adjusted signal plans had an average delay of 0.6 sec/veh less than original plans when under fully actuated control (Table 6-27). In addition, the adjusted signal plans did not reduce the variance of delays among various route distribution scenarios, since the percentage of ranges are 45.2% for pre-

timed and 35.8% for fully actuated control, as shown in Table 6-26, as compared to the 32.1% and 35.1% shown in Table 6-25.

Table 6-27 Comparison between Original and Adjusted Methodologies

	Pre-timed	Fully Actuated
Scenario	Average Delay of All (sec/veh)	Average Delay of All (sec/veh)
0-0-0-0	0	0
0-0-50-50	0	0
0-0-100-100	0	0
100-100-0-0	2.05	-1.1
100-100-50-50	1.73	-1.21
100-100-100-100	2.13	-0.81
0-0-50-100	0	0
0-50-50-100	3.77	1.2
0-100-50-100	5.22	3.39
50-0-50-100	0.42	-2.39
50-50-50-100	1.57	-1.3
50-100-50-100	0.91	-1.5
100-0-50-100	-0.04	-2.61
100-50-50-100	0.78	-1.97
100-100-50-100	2.12	-0.79
Minimum	0.0	-2.6
Maximum	5.2	3.4
Mean	1.4	-0.6
Range	5.3	6.0
Range (%)	27.0%	27.7%

6.4.3 All Simulations

The mean average delay and range of the average delays in all scenarios are summarized in Table 6-28 to Table 6-31. Table 6-28 illustrates that the mean average delay of scenarios controlled by original pre-timed type changes slightly (-1.2 or -5.8%) when travel time between the two crossovers increased from 12 sec to 22 sec. The average delays of variable route distributions in a wider DDI vary less than a narrow DDI for pre-timed control. Similar conclusions were observed under the original fully actuated control.

In addition, the scenarios controlled by original fully actuated control had an almost equivalent mean average delay with the pre-timed control scenarios when $T_{8,11,12,7}$=12 sec. However, the mean average delays of original fully actuated control increased from 19.5 to 21.6 sec sec under pre-timed control when $T_{8,11,12,7}$=22 sec. These results indicate that a larger space between crossovers at a DDI causes fully actuated control to operate less efficiently.

Table 6-28 Original Pre-timed and Fully Actuated Control

		Pre-timed (Original)	Fully Actuated (Original)	Difference	Difference (%)
$T_{8,11,12,7}$=12 sec	Mean	20.7	20.9	0.2	1.0%
	Range (%)	51.4%	59.9%	8.5%	16.5%
$T_{8,11,12,7}$=22 sec	Mean	19.5	21.6	2.1	10.8%
	Range (%)	32.1%	35.1%	3.0%	9.3%
Difference	Mean	-1.2	0.7		
Difference (%)	Mean	-5.8%	3.3%		
Difference	Range	-19.3%	-24.8%		
Difference (%)	Range	-37.5%	-41.4%		

Table 6-29 shows no reduction of average delay when comparing adjusted pre-timed control to the original pre-timed control for scenarios with different spaces between the crossovers Adjusted pre-timed control also did not reduce much (not greater than 0.5%) the variability of average delays for a variety of traffic distributions. However, the original pre-timed control reduces the range of average delays by 19.3% when the DDI spacing increases.

Table 6-29 Original Pre-timed and Adjusted Pre-timed Control

		Pre-timed (Original)	Pre-timed (Adjusted)	Difference	Difference (%)
$T_{8,11,12,7}$=12 sec	Mean	20.7	21.0	0.3	1.4%
	Range (%)	51.4%	45.7%	-5.7%	-11.1%
$T_{8,11,12,7}$=22 sec	Mean	19.5	20.9	1.4	7.2%
	Range (%)	32.1%	45.2%	13.1%	40.8%
Difference	Mean	-1.2	-0.1		
Difference (%)	Mean	-5.8%	-0.5%		
Difference	Range	-19.3%	-0.5%		
Difference (%)	Range	-37.5%	-1.1%		

Based on the results in Table 6-30, both original fully actuated and adjusted fully actuated control brings about nearly equivalent average delays among all route distribution scenarios under scenarios with different spaces between the two crossovers of the DDI. In addition, both controls caused less variability of average delays in widely spaced DDI crossovers than tightly spaced crossovers.

Table 6-30 Original Fully Actuated and Adjusted Fully Actuated Control

		Fully Actuated (Original)	Fully Actuated (Adjusted)	Difference	Difference (%)
$T_{8,11,12,7}$=12 sec	Mean	20.9	21.2	0.3	1.4%
	Range (%)	59.9%	57.3%	-2.6%	-4.3%
$T_{8,11,12,7}$=22 sec	Mean	21.6	21.0	-0.6	-2.8%
	Range (%)	35.1%	35.8%	0.7%	2.0%
Difference	Mean	0.7	-0.2		
Difference (%)	Mean	3.3%	-0.9%		
Difference	Range	-24.8%	-21.5%		
Difference (%)	Range	-41.4%	-37.5%		

Table 6-31 confirms that the average delay did not change very much when route distributions and the DDI spacing varies. The range of average delays in different route distribution scenarios for the DDI under a larger space was less than the DDI with a compact space.

Table 6-31 Adjusted Pre-timed and Adjusted Fully Actuated Control

		Pre-timed (Adjusted)	Fully Actuated (Adjusted)	Difference	Difference (%)
$T_{8,11,12,7}$=12 sec	Mean	21.0	21.2	0.2	1.0%
	Range (%)	45.7%	57.3%	11.6%	25.4%
$T_{8,11,12,7}$=22 sec	Mean	20.9	21.0	0.1	0.5%
	Range (%)	45.2%	35.8%	-9.4%	-20.8%
Difference	Mean	-0.1	-0.2		
Difference (%)	Mean	-0.5%	-0.9%		
Difference	Range	-0.5%	-21.5%		
Difference (%)	Range	-1.1%	-37.5%		

6.5 SPACE BETWEEN CROSSOVERS

Table 6-32 and Table 6-33 illustrate the difference of average delays caused by the space between DDI crossovers for each scenario. The data in the column "Difference of Average Delay" of these tables is calculated by subtracting average delays when travel time between the two crossovers is 22 sec and 12 sec. According to the results shown in these two tables, the DDI crossover spacing does not bring about evident differences in the mean average delays among original fully actuated, adjusted pre-timed, and adjusted fully actuated controls. Adjusted pre-timed control had the smallest range of average delays out of all the route distribution scenarios under both spacing-related cases. Other traffic controls for the larger DDI spacing reduced the range of average delays of the all route distribution scenarios compared to the tighter-spaced DDI. The mean of average delays for original pre-timed control when travel time is 22 sec fell by 1.1 sec/veh. The mean of average delays for adjusted pre-timed control has fewer variances with increasing DDI spacing, but with a greater vibration compared to the original pre-timed

control (Table 6-32). Similar conclusions are realized with the fully actuated control results shown in Table 6-33.

Table 6-32 Difference of Average Delays of Pre-timed Control Caused by Spaces

Scenario	Difference of Average Delay (sec/veh)	Scenario	Difference of Average Delay (sec/veh)
0-0-0-0-Original	-2.0	0-0-0-0-Adjusted	-2.0
0-0-50-50-Original	-1.6	0-0-50-50-Adjusted	-1.6
0-0-100-100-Original	-2.1	0-0-100-100-Adjusted	-2.1
100-100-0-0-Original	-4.7	100-100-0-0-Adjusted	-2.6
100-100-50-50-Original	0.1	100-100-50-50-Adjusted	1.9
100-100-100-100-Original	-0.4	100-100-100-100-Adjusted	1.8
0-0-50-100-Original	-2.0	0-0-50-100-Adjusted	-2.0
0-50-50-100-Original	0.3	0-50-50-100-Adjusted	3.2
0-100-50-100-Original	1.2	0-100-50-100-Adjusted	4.4
50-0-50-100-Original	-2.0	50-0-50-100-Adjusted	-1.4
50-50-50-100-Original	0.0	50-50-50-100-Adjusted	1.6
50-100-50-100-Original	1.4	50-100-50-100-Adjusted	1.1
100-0-50-100-Original	-4.0	100-0-50-100-Adjusted	-4.0
100-50-50-100-Original	-1.4	100-50-50-100-Adjusted	-1.2
100-100-50-100-Original	-0.2	100-100-50-100-Adjusted	0.6
Minimum	-4.7	Minimum	-4.0
Maximum	1.4	Maximum	4.4
Mean	-1.1	Mean	-0.2
Range	6.1	Range	8.3

Table 6-33 Difference of Average Delays of Fully Actuated Control Caused by Spaces

Scenario	Difference of Average Delay (sec/veh)	Scenario	Difference of Average Delay (sec/veh)
0-0-0-0-Original	-0.4	0-0-0-0-Adjusted	-0.4
0-0-50-50-Original	-0.6	0-0-50-50-Adjusted	-0.6
0-0-100-100-Original	-0.6	0-0-100-100-Adjusted	-0.6
100-100-0-0-Original	-4.0	100-100-0-0-Adjusted	-5.1
100-100-50-50-Original	1.8	100-100-50-50-Adjusted	0.6
100-100-100-100-Original	1.7	100-100-100-100-Adjusted	0.8
0-0-50-100-Original	-0.7	0-0-50-100-Adjusted	-0.7
0-50-50-100-Original	1.6	0-50-50-100-Adjusted	2.0
0-100-50-100-Original	2.4	0-100-50-100-Adjusted	3.9
50-0-50-100-Original	-0.3	50-0-50-100-Adjusted	-1.8
50-50-50-100-Original	2.4	50-50-50-100-Adjusted	1.9
50-100-50-100-Original	3.1	50-100-50-100-Adjusted	0.7
100-0-50-100-Original	-0.8	100-0-50-100-Adjusted	-3.3
100-50-50-100-Original	3.9	100-50-50-100-Adjusted	-0.4
100-100-50-100-Original	1.7	100-100-50-100-Adjusted	0.5
Minimum	-4.0	Minimum	-5.1
Maximum	3.9	Maximum	3.9
Mean	0.7	Mean	-0.2
Range	7.9	Range	9.0

6.6 SUMMARY

This chapter thoroughly examined a case study in the city of Reno, NV. First, the feasibility of proposed operation 2 was tested through setting up parameters in a real traffic signal controller. Then, a coordinated actuated control based on proposed operation 2-b and a coordinated actuated control of the current operation 5 were applied to the Moana DDI. The simulation results proved that the coordinated actuated control based on proposed operation 2 outperformed the control based on current operation 5. In addition, the relationship between average delay of all vehicles and cycle length at the

Moana DDI was thoroughly studied for three traffic control types: pre-timed control, fully actuated control, and coordinated actuated control. Then, 120 scenarios were evaluated to test the differences of average delays for a variety of route distributions when the travel time between the two crossovers of the DDI was 12 sec and 22 sec respectively. Similarly, the effects of DDI crossover spacing was also tested, and the results indicated that the average delays varied with few differences when the space between DDI crossovers is changed. Further detailed information about average delays and average maximum queues for each scenario is presented in Appendix C.

CHAPTER 7. CONCLUSIONS

7.1 CONTRUBUTIONS

The diverging diamond interchange is a significant improvement in safety and operational efficiency of an interchange. Many professionals have compared the operational performance between DDIs and CDIs. However, no standards or methodologies exist for developing signal timing plans for DDIs. Most traffic signal timing plans are decided manually based on the practical experience of traffic professionals. This research comprehensively studied specific features of DDIs and developed three major methodologies for use in finding the optimal traffic signal operations for DDIs. Compared to previous studies on DDIs, this research makes the following major contributions:

1. This research comprehensively reviewed previous studies pertaining to traffic signal operations at DDIs. This review also briefly summarized the advantages and disadvantages of DDIs compared to CDIs. In addition, it made a summary of the major results of these studies.
2. This research pointed out the advantages and disadvantages of traffic signal operations for five current operations applied to DDIs.
3. A three-phase traffic signal phasing (proposed operation 1-a) was presented for situations where the off-ramp left turn traffic is relatively low and controlled by "yield" signs. Also, a methodology similar to Webster's method was developed for determining cycle length and phase splits of a DDI based on their relative critical

movement volumes. Unlike Webster's method, this methodology includes the travel time between the two crossovers of a DDI into its calculation. This research also recommended a methodology for selecting phasing sequences according to critical traffic volumes and saturation flow rates. A modified methodology, proposed operation 1-b, based on traffic distributions among origins and destinations, was presented through adding an extensional green time for two phases. The extension was determined by the travel time between the two crossovers and route distributions among the origins and destinations of a DDI. Finally, a method for getting route distribution data was studied. This study theoretically proved that route distribution data can be derived by the traffic data of all movements, which can be easily collected at each approach at a DDI.

4. A more complex traffic signal operation, proposed operation 2, for a DDI was provided. This research also presented the methodologies for deciding cycle length, phase splits, extension, phasing sequence, and a strategy for collecting route distribution data for a DDI. Different from proposed operation 1, proposed operation 2 employed the eight National Electrical Manufacturers Association (NEMA) phases skillfully. This operation applies to situations where left-turn off-ramp traffic is heavy and controlled by signals.
5. This research also recommended applying genetic algorithms (GA) to searching for optimal solutions to DDI traffic control based on the above phasing schemes of the proposed operations. It also proved that the traffic signal unknown variables can be exactly explained by the chromosomes from a GA. This may dramatically improve GA performance in seeking acceptable optimal solutions for DDIs traffic operations,

compared to the limited performance of GA applications on traffic signal coordination operations for several intersections. Unfortunately, this study did not combine the GA with a traffic simulation tool, such as VISSIM, to find out the optimal solutions for DDI based on the schemes of proposed operations 1 and 2. If a simulation tool can output the average total delay faster and allow users to easily access and modify its signal timing parameters by programming software such as C++ and Matlab directly, GA can possibly be applied to finding optimal traffic operations for DDIs.

6. All proposed operations in this research can be implemented through the use of one singular controller. They can be suitable for all traffic signal control types such as pre-timed, fully actuated, and coordinated actuated control. Fully actuated control settings in a real controller were provided through this research in Appendix A. Traffic engineers and professionals can adjust the parameter settings for their specific cases.
7. Finally, this research proposed a case study at the Moana DDI located in the city of Reno, NV. This case study first compared the operational efficiency of proposed operation 2with an operation recommended by the City of Reno. The results indicated that proposed operation 2-b outperformed the operation from the City of Reno when comparing average delays. Then, the optimal cycle length of this case was studied and the results indicated the relationship between average delay and cycle length is consistent with the relationship presented in highway capacity manual 2010 (HCM 2010). The effects of origin-destination (O-D) distributions and the travel time between the two crossovers were comprehensively studied.

7.2 FINDINGS

The key findings through the case study are provided below:

1. The signal settings in a NAZTEC NEMA traffic controller were successfully tested in this research. These settings can be used for practical recommendations for traffic engineers and professionals.
2. The proposed operation 2-b reduced average total delays by 17% and 28% during AM and PM peak hours, respectively, compared to the current operation 5 developed by the City of Reno.
3. When the sum of critical saturation flow ratios is less than 0.51 at the DDI, the pre-timed operation with a shorter cycle length, between 60 sec and 150 sec, incurred the least average total delay. If the sum of critical saturation flow ratios was between approximately 0.64 and 0.73, the optimal cycle lengths of pre-timed operation were between 80 sec and 100 sec. When the sum of critical saturation flow ratios was 0.85, the optimal cycle lengths were found between around 85 sec and 130 sec. The results also confirm that proposed operation 2-b in Chapter 5 is applied well when the sum of critical saturation flow ratios is between around 0.73 and 0.85.
4. When the sum of critical saturation flow ratios is less than 0.51 at the DDI, the fully actuated operation with a shorter cycle length (the sum of critical maximum recalls set in a controller), between 60 sec and 150 sec, incurred the least average total delay. When the sum of a scenario's critical saturation flow ratios was 0.64, the average total delays decreased with the decrease of its cycle length from 150 sec to 70 sec, except for the 60-sec cycle length. Overall, the cycle length of fully actuated control

did not cause apparent differences of average total delays when the sum of critical saturation flow ratios was not greater than 0.64. If the sum of critical saturation flow ratios was around between 0.73 and 0.85, the optimal cycle lengths of fully actuated operation were between 80 sec and 100 sec.

5. If the sum of critical saturation flow ratios was less than 0.51 at the DDI, the coordinated actuated operation with a shorter cycle length, between 60 sec and 150 sec, brought about the least average total delay. When the sum of critical saturation flow ratios for a scenario was 0.64, the average total delays decreased with the decrease of its cycle length from 150 sec to 70 sec, but this was not applicable for the cycle length of 60 sec. Overall, the actuated coordinated control caused the average total delays to increase with the cycle lengths from around 10 sec/veh for a 60-sec cycle to nearly 20 sec/veh for a 150–sec cycle. If the sum of critical saturation flow ratios was around 0.73, the optimal cycle lengths of coordinated actuated operation were between 75 sec and 110 sec. If the sum of critical saturation flow ratios was around 0.85, the optimal cycle lengths of coordinated actuated operation were between 85 sec and 130 sec.
6. The average total delays of pre-timed control and fully actuated control did not vary much when the cycle length changed from 60 sec to 150 sec and the sum of saturation flow ratios was less than 0.51. Both control types outperformed coordinated actuated control under these conditions. Not many differences in the average total delays occurred under pre-timed control, fully-actuated control, and coordinated actuated control when the cycle length changed from 60 sec to 150 sec and the sum of saturation flow ratios were around between 0.64 and 0.85. In addition, the average

total delays of these controls had similar trends: decreased at the beginning, kept stable in the middle, and increased at the end as the cycle length increased from 60 sec to 150 sec.

7. Proposed operations 1 and 2 need to be adjusted for route distributions among O-D pairs of a DDI, since the average delay of each route distribution scenario is different. Only pre-timed and fully actuated control of proposed operation 2 were analyzed in this study. The range of average delay among all route distribution scenarios in this study is 51.4% for original pre-timed control and 59.9% for original fully actuated control when travel time is 12 sec. The range of average delay among the same route distribution scenarios reduced to 32.1% for original pre-timed control and 35.5% for original fully actuated control when the travel time between crossovers increases to 22 sec. These results indicate that the differences of average delays on different route distribution scenarios decrease when the space between two crossovers of a DDI increases.
8. Different from the expectations, the adjusted pre-timed, adjusted fully actuated control did not improve the traffic signal operations when travel time is 12 sec or 22 sec. These results can be explained by two reasons: the first is that the original proposed operations have included the travel time between the two crossovers in their calculation process to seek the phase splits; the second is that the optimal cycle is around between 80 sec to 110 sec based on the study in this research. The original cycle length is 86 sec for both cases when travel times are 12 sec and 22 sec. However, the maximum cycle length for adjusted cycle length is 108 sec and 128 sec respectively when travel times are 12 sec and 22 sec, respectively. The benefits of

adding additional green times to phases 2, 3, and 4 were counteracted by increasing cycle lengths.

7.3 FUTURE STUDIES

Although this research made a thorough study on DDIs traffic signal operations, several areas can be further studied. Some areas for further research are outlined below:

1. This research presented signal operations for selecting the cycle length, phase splits, and phasing sequence. However, this study did not comprehensively examine all the scenarios with pertinent performance by applying these proposed operations.
2. In theory, the extension for proposed operations is reasonable and necessary. However, the study case's results show that the adjusted signal timing plans did not outperform the original signal operations that were not added by an extension. Whether this conclusion is only applied for this case or also applied for other cases should be thoroughly studied. How to determine the parameters in the methodology for extension, or whether some other methodologies may exist to better depict the effects of traffic distribution on traffic signal operations at DDIs should be thoroughly researched in the future.
3. This research only proposed a methodology for finding the optimal solutions for DDIs by combing GA and proposed phasing schemes. Whether GAs can successfully discover the optimal timing solution for DDIs should be tested through further studies. In addition, the parameters in GA should be thoroughly studied. These parameters

include initial population size, population size, crossover rate, mutation methodologies etc.

4. Pedestrian phases were not included in this research. The mutual effects of pedestrians and vehicular traffic should also be examined.
5. This study only researched the relationship between average delay and cycle length for one crossover spacing scenario. The relationship between average delay and cycle length in other DDIs with different spaces should be thoroughly researched.
6. Although traffic O-D distribution and travel time between the two crossovers were researched in this study, more comprehensive research needs to proceed.
7. The effects of traffic composition' on signal operations at a DDI also need to study.
8. This study focused on an isolated DDI without considering its adjacent intersections. A more general optimal methodology should be developed for coordinating traffic flow with several intersections including a DDI.
9. There are many interchanges in use such as single-point urban interchanges (SPUIs), CDIs, and roundabout diamond interchanges. An economic cost and benefit analysis is necessary for making a recommendation to an agency whether it should replace a current interchange with a DDI.

REFERENCES

1. Missouri Department of Transportation. *Missouri's Experience with a Diverging Diamond Interchange*. Jefferson, MO, 2010, pp. 4–22.
2. Bared, J. *Double Crossover Diamond Interchange*. McLean, VA, 2009, pp. 1–4.
3. Bared, J. G., T. Granda, and A. Zineddin. *Drivers' Evaluation of the Diverging Diamond Interchange*. McLean, VA, 2009, p. 11.
4. Rasband, E., T. Forbush, and K. Ash. *UDOT Diverging Diamond Interchange (DDI) Observations & Experience*. Salt Lake City, UT, 2012, p. 23.
5. Chlewicki, G. *New Interchange and Intersection Designs : The Synchronized Split-Phasing Intersection and the Diverging Diamond Interchange*. Anaheim, CA, 2003, pp. 3–16.
6. Hughes, W., R. Jagannathan, D. Sengupta, and J. H. Hummer. *Alternative Intersections/Interchanges: Informational Report (AIIR)*. Washington, DC, 2010.
7. Bared, J., P. Edara, and R. Jagannathan. Design and Operational Performance of Double Crossover Intersection and Diverging Diamond Interchange. *Transportation Research Record*, Vol. 1912, No. 1, Jan. 2005, pp. 31–38.
8. Sharma, S., and L. Hall. Performance Evaluation of the Diverging Diamond Interchange in Comparison with the Conventional Diamond Interchange. 2007.
9. Siromaskul, S., and S. B. Speth. A Comparative Analysis of Diverging Diamond Interchange Operations. 2008.
10. Siromaskul, S. Diverging Diamond Interchange Design 101 : Things to Know Before You Start. 2010.
11. Chilukuri, V., S. Siromaskul, M. Trueblood, and T. Ryan. *Diverging Diamond Interchange Performance Evaluation*. St. Louis, MO, 2011, pp. 34–35.
12. Regenold, M. *From Waving Arms to LED's A Brief History of Traffic Signals Tech Transfer*. Center for Transportation Research and Education, Iowa State University, Ames, IA, 2007.
13. Bullock, D., and Montasir M. Abbas. A Real-Time Offset Transitioning Algorithm for Coordinating Traffic Signals. 2001, pp. 4–5.
14. Gordon, R., W. Tighe, and I. Siemens. *Traffic Control Systems Handbook*. Washington, D.C., 2005.
15. Webster, F., and B. Cobbe. *Traffic signals*. London, UK, Nov. 1966.
16. *Highway Capacity Manual*. Transportation Research Board, Washington, D.C., 2010.
17. Pline, J. L. Traffic Engineering Handbook. *Institute of Transportation Engineers*, 2000.

18. *Manual on Uniform Traffic Control Devices*. U.S. Department of Transportation, Washington, D.C., 2009.

19. Husch, D., and J. Albeck. *Synchro 6 User Guide*. Trafficware, Albany, CA, 2004.

20. *Traffic Signal Design Guidelines*. Georgia Department of Transportation, Atlanta, GA, 2003.

21. Hu, P., and Z. Tian. A New Approach to Variable-Bandwidth Progression Optimization. 2010.

22. Chang, A. Synchronization of Traffic Signals in Grid Networks. *IBM Journal of Research and Development*, Vol. 11, No. 4, Jul. 1967, pp. 436–441.

23. Robertson, D. I. TRANSYT: Traffic Network Study Tool. *Fourth International Symposium on the Theory of Traffic Flow*, 1968.

24. Wallace, C., K. Courage, and D. Reaves. *TRANSYT-7F User's Manual (Release 11)*. McTrans Center, University of Florida, Gainesville, FL.

25. *Traffic Software Integrated System*. Department of Transportation, Federal Highway Admnistration, 1997.

26. Chaudhary, N. A., and C. J. Messer. *PASSER IV-96, Version 2.1: User/Reference Manual*. Texas Transportation Institute, Texas A&M University System, Huston, TX, 1996.

27. *TEAPAC Complete 2010 Tutorial / Reference Manual*. Strong Concepts, Northbrook, IL, 2011.

28. Bleyl, R. A Practical Computer Program for Designing Traffic Signal System Timing Plans. *Highway Research Record*, 1967, pp. 19–33.

29. *VISSIM 5.4 User Manual*. PTV Planung Transport Verkehr AG, 2012.

30. Wallace, C. *Development of a Forward link Opportunities Model for Optimization of Traffic Signal Progression on Arterial Highways*. University of Florida, 1979.

31. Orcutt, F. L. *The Traffic Signal Book*. Prentice Hall, 1993.

32. Koonce, P., L. Rodegerdts, K. Lee, and S. Quayle. *Traffic Signal Timing Manual*. Federal Highway Administration, Washington, D.C., 2008.

33. *NTCIP 1202 - Object Definitions for Actuated Traffic Signal Controller Units*. Rosslyn, VA, 2005.

34. Skabardonis, A. Development and Application of Control Strategies for Signalized Intersections in Coordinated Systems. *Transportation Research Record*, Vol. 1634, No. 1, Jan. 1998, pp. 110–117.

35. Hunt, P. B., D. I. Robertson, R. D. Bretherton, and M. C. Royle. The SCOOT on-line Traffic Signal Optimisation Technique. *Traffic Engineering and Control*, Vol. 23, No. 4, 1982, pp. 190–192.

36. Shelby, S. Single-Intersection Evaluation of Real-Time Adaptive Traffic Signal Control Algorithms. *Transportation Research Record*, Vol. 1867, No. 1, Jan. 2004, pp. 183–192.

37. Sims, A. G., and K. W. Dobinson. The Sydney coordinated adaptive traffic (SCAT) system philosophy and benefits. *IEEE Transactions on Vehicular Technology*, Vol. 29, No. 2, May 1980, pp. 130–137.

38. Lowrie, P. The Sydney Coordinated Adaptive Traffic System – Principles, Methodology, Algorithms. 1982.

39. Luk, J. Two Traffic-responsive Area Traffic Control Methods: SCAT and SCOOT. *Traffic engineering & control*, Vol. 25, No. 1, 1984, pp. 14.

40. Dutta, U., and D. McAvoy. Comparative Performance Evaluation of SCATS and Pre-timed Control Systems. *Transportation Research Forum*, 2010.

41. Hu, P., Z. Tian, A.-A. Dayem, and F. Yang. *Field Evaluation of SCATS Control System in Las Vegas*. 3963–3973.

42. Petrella, M., and J. Lappin. *Measuring Driver Satisfaction with an Urban Arterial Before and After Deployment of an Adaptive Timing Signal System*. FHWA, Washington, D.C., 2007.

43. Gartner, N. Development and Testing of a Demand-Responsive Strategy for Traffic Signal Control. 1982.

44. Gartner, N. OPAC: A Demand-Responsive Strategy for Traffic Signal Control. *Transportation Research Record*, No. 906, 1983, pp. 75–81.

45. Gartner, N. H., C. Stamatiadis, and C. S. Zhou. *Outline of the VFC-OPAC Model*. Lowell, MA, 1998.

46. Gartner, N. H. Implementation of the OPAC Adaptive Control Strategy in a Traffic Signal Network. 2001.

47. Head, K., P. B. Mirchandani, and D. Sheppard. Hierarchical Framework For Real-Time Traffic Control. *Transportation Research Record*, No. 1360, 1992, pp. 82–88.

48. Dell'Olmo, P., and P. Mirchandani. REALBAND: An Approach for Real-Time Coordination of Traffic Flows on A Network. *Transportation Research Record*, No. 1494, 1995, pp. 106–116.

49. Dell'Olmo, P., and P. Mirchandani. A Model for Real-Time Coordination Using Simulation Based Optimization. *Advanced Methods in Transportation Analysis*, 1996, pp. 525–546.

50. Sen, S., and K. L. Head. Controlled Optimization of Phases at an Intersection. *Transportation Science*, Vol. 31, No. 1, Feb. 1997, pp. 5–17.

51. Webster, F. Traffic signal settings. *Road research technical paper No. 39*, 1958.

52. Cheng, D., Z. Tian, and C. Messer. Modification of Webster's Minimum Delay Cycle Length Equation Based on HCM 2000. *Transportation Research Board*, 2003.

53. Brooks, W. Vehicular Traffic Control: Designing Arterial Progressions Using A Digital Computer. *IBM Corporation*, 1965.

54. Morgan, J. T., and J. D. C. Little. Synchronizing Traffic Signals for Maximal Bandwidth. *Operations Research*, Vol. 12, No. 6, Nov. 1964, pp. 896–912.

55. Morgan, J., J. Little, J. T. Morgan, and R. V. Martin. Synchronizing Traffic Signals for Maximal Bandwidth. *Highway Research Record 118*, 1966, pp. 21–47.

56. Gartner, N., J. Little, and H. Gabbay. Optimization of Traffic Signal Settings in Networks by Mixed-Integer Linear Programming. *Transportation Science*, Vol. 9, 1974, pp. 321–343.

57. Little, J., M. Kelson, and N. Gartner. MAXBAND: A Program for Setting Signals on Arteries and Triangular Networks. *Transportation Research Record*, No. 795, 1981, pp. 40–46.

58. Messer, C., R. Whitson, C. L. Dudek, and E. J. Romano. A Variable Sequence Multiphase Progression Optimization Program. *Highway Research Record*, No. 445, 1973, pp. 24–33.

59. Cohen, S., and J. Mekemson. Optimization of Left-turn Phase Sequence on Signalized Arterials. *Transportation Research Record*, No. 1021, 1985, pp. 53–58.

60. Chang, E.-P., S. L. Cohen, C. Liu, N. A. Chaudhary, and C. Messer. MAXBAND-86: Program for Optimizing Left-Turn Phase Sequence in Multi-Arterial Closed Networks. *Transportation Research Record*, No. 1181, 1988, pp. 61–67.

61. Carvell, J. D. *Dallas Corridor Study: Final Report*. Washington, D.C., 1976.

62. Chang, E., and C. Messer. *Arterial Signal Timing Optimization using PASSER II-90-Program User's Manual*. Arlington, TX, 1991.

63. Wagner, F., D. Gerlough, and F. Barnes. *Improved Criteria for Traffic Signal Systems on Urban Arterials*. Washington, D.C., 1969.

64. Venglar, S., P. Koonce, and T. Urbanik. *PASSER IIITM-98: Application and User's Guide*. College Station, TX, 1998.

65. Chu, C., N. Chaudhary, J. Johnson, and S. Sunkari. *Enhancements to PASSER V Signal Timing Optimization Program*. Austin, TX, 2008.

66. Kovvali, V. *Development of a Robust Arterial Signal Coordination Software*. College Station, TX, 2001.

67. Robertson, D. TRANSYT: A Traffic Network Study Tool. *Road Research Laboratory*, Vol. 253, 1969.

68. Wallace, C., K. Courage, and M. Hadi. *TRANSYT-7F Users Manual-Volume 4 of Methodology for Optimizing Signal*. Center for Microcomputers in Transportation, University of Florida, Gainesville, FL, 1998.

69. Dantzig, G. B., and M. N. Thapa. *Linear Programming 2: Theory and Extensions*. Springer, 2003.

70. Schrijver, A. *Theory of linear and integer programming*. John Wiley & Sons, 1998.

71. Nocedal, J., and S. Wright. *Numerical optimization*. Springer Berlin Heidelberg, 2006.

72. Boyd, S., and L. Vandenberghe. *Convex optimization*. Cambridge University Press, 2004.

73. Denardo, E. *Dynamic Programming: Models and Applications*. Courier Dover Publications, Mineola, NY, 2003.

74. Luenberger, D. *Optimization by Vector Space Methods*. John Wiley & Sons, 1997.

75. Simon, H. *The Sciences of the Artificial*. MIT Press, Cambridge, MA, 1969.

76. Ashby, W. R. *Design for A Brain*. New York, Wiley, 1960.

77. Traill, R. *Molecular Explanation for Intelligence - Including Its Growth, Maintenance, and Failings*. 1978.

78. Hu, P., Z. Tian, Z. Yuan, and S. Jia. Variable-Bandwidth Progression Optimization in Traffic Operation. *Journal of Transportation Systems Engineering and Information Technology*, Vol. 11, No. 1, Feb. 2011, pp. 61–72.

79. Dantzig, G. B., and M. N. Thapa. *Linear Programming 1: Introduction*. Springer, 1997.

80. Vanderbei, R. J. *Linear Programming: Foundations and Extensions*. Springer, 2007.

81. Ahuja, R. K., homas L. Magnanti, and J. B. Orlin. *Network Flows: Theory, Algorithms and Applications*. Prentice Hall, 1993.

82. Tsay, H.-S., and L.-T. Lin. *A New Algorithm for Solving the Maximum Progression Bandwidth*. National Research Council, Transportation Research Board, 1988.

83. Snyman, J. *Practical Mathematical Optimization: An Introduction to Basic Optimization Theory and Classical and New Gradient-Based Algorithms*. Springer, 2005.

84. Press, W., S. Teukolsky, W. Vetterling, and B. Flannery. *Numerical Recipes in C: The Art of Scientific Computing*. Cambridge University Press, 1992.

85. Newell, A., and H. Simon. *An Example of Human Chess Play in the Light of Chess Playing Programs*. 1964, pp. 19–75.

86. Newell, A., and H. a. Simon. Computer Science as Empirical Inquiry: Symbols and Search. *Communications of the ACM*, Vol. 19, No. 3, Mar. 1976, pp. 113–126.

87. Rechenberg, I. *Evolutionsstrategie: Optimierung technischer Systeme nach Prinzipien der biologischen Evolution*. Frommann-Holzboog, 1973.

88. John, H. *Holland, Adaptation in Natural and Artificial Systems*. University of Michigan, Ann Arbor, 1975.

89. Markoff, J. What's the Best Answer? It's Survival of The Fittest. *New York Times*, Oct. 1990.

90. Holland, J. Genetic Algorithms. *Scientific American*, 1992, pp. 66–72.

91. Gotshall, S., and B. Rylander. Optimal Population Size and the Genetic Algorithm. *Citeseer*, 2008.

92. Goldberg, D. *Optimal Initial Population Size for Binary-coded Genetic Algorithms*. 1985.

93. Goldberg, D., K. Deb, and J. Clark. Genetic Algorithms, Noise, and the Sizing of Populations. 1987.

94. Fitzpatrick, J., and J. Grefenstette. Genetic Algorithms in Noisy Environments. *Machine learning*, Vol. 3, No. 2-3, Oct. 1988, pp. 101–120.

95. Haupt, R., and S. Haupt. *Practical Genetic Algorithms*. John Wiley & Sons, Hoboken, NJ, 2004.

96. Kenneth, A. An Analysis of the Behavior of a Class of Genetic Adaptive Systems. *University of Michigan*, 1975.

97. Baker, J. E. Reducing Bias and Inefficiency in the Selection Algorithm. 1987.

98. Bethke, A. *Genetic Algorithms as Function Optimizers*. ACM Press, New York, New York, USA, 1981.

99. Rabinovich, Y., and A. Wigderson. An Analysis of a Simple Genetic Algorithm. 1991.

100. Dueck, G., and T. Scheuer. Threshold Accepting: a General Purpose Optimization Algorithm Appearing Superior to Simulated Annealing. *Journal of computational physics*, Vol. 90, No. 1, Sep. 1990, pp. 161–175.

101. Lei, Y. J., S. W. Zhang, X. W. Li, and C. M. Zhou. *Genetic Algorithm Tool Box and Its Application in MATLAB (Chinese Version)*. Xidian University Press, Xi'an, China, 2004.

102. Ting, C.-K. On the Mean Convergence Time of Multi-parent Genetic Algorithms Without Selection. 2005.

103. Melanie Michell. *An Introduction to Genetic Algorithms*. MIT Press, 1998.

APPENDIX A.

FULLY ACTUATED CONTROL SETTINGS

The controller parameters of fully actuated control for proposed operation 2 are provided below as an example. All the symbols and abbreviations are consistent with what are in the Naztec controller Manual.

1. Basic Parameters

a. Phase Times (MM->1->1->1)

Table A-1 shows the phase time parameters in the controller. All the "Yel Clr" and "Red Clr" are calculated based on the ITE guidelines and extensive simulation results. Phase 8's minimum green is set to 0 sec which will allow releasing phases 1 and 2 as early as possible when there is no traffic in phases 4 and 3.

Table A-1 Phase Time Parameters in Naztec Controller

Phase	**1**	**2**	**3**	**4**	**5**	**6**	**7**	**8**
Min Grn	3	8	5	12	5	10	5	0
Gap Ext	1.5	1.5	1.5	1.5	1.5	1.5	1.5	1.5
Max 1	3	22	26	53	5	24	7	3
Max 2	50	50	50	60	50	50	50	50
Yel Clr	3.5	3.5	3.5	3.5	3.5	3.5	3.5	3.0
Red Clr	3.5	3.5	2.5	2.5	1.5	1.5	1.5	0

b. Phase Options (MM->1->1->2)

Set up the parameters in the controller as shown in Table A-2 following MM->1->1->2.

Table A-2 Phase Option Parameters in the Naztec Controller

Phase	1	2	3	4	5	6	7	8
Enable	×	×	×	×	×	×	×	×
Min Recall				×			×	×
Max Recall	×				×		×	
…								
Dual Entry		×				×		

2. *Overlaps*
   a. Overlap Program Selection and Configuration (MM->1->5->2)

   Each overlap is created separately from MM->1->5->2.

   The overlap of phases 2, 4, and 6 is created by entering "1," then another "1," and selecting phases 2, 4, and 6 in the screen as shown in Table A-3.

Table A-3 Overlap of Phases 2, 4, and 6 in the Naztec Controller

Ovrlp A	Φs	Φs	Φs	Φs	Φs	Φs	Φs	Φs
Included Ps	0	2	0	4	0	6	0	0
Modifier Ps	0	0	0	0	0	0	0	0
Type: NORMAL		Grn:	0	Yel:	3.5	Red:	1.5	

The overlap of phases 1, 2 and 3 is created by entering "2," then another "1," and selecting phases 1, 2, and 3 in the screen as shown in Table A-4.

Table A-4 Overlap of Phases 1, 2, and 3 in the Naztec Controller

Ovrlp B	Φs	Φs	Φs	Φs	Φs	Φs	Φs	Φs
Included Ps	1	2	3	0	0	0	0	0
Modifier Ps	0	0	0	0	0	0	0	0
Type: NORMAL		Grn:	0	Yel:	3.5	Red:	1.5	

The overlap of phases 1 and 3 is created by entering "3," then "1," at last selecting phases 1 and 3 in the screen as shown in Table A-5.

Table A-5 Overlap of Phases 1 and 3 in the Naztec Controller

Ovrlp C	**Φs**	**Φs**	**Φs**	**Φs**	**Φs**	**Φs**	**Φs**	**Φs**
Included Ps	1	0	3	0	0	0	0	0
Modifier Ps	0	0	0	0	0	0	0	0
Type: NORMAL		Grn:	0	Yel:	3.5	Red:	1.5	

The overlap of phases 5 and 6 is created by first entering "4," then "1," in the end selecting phases 5 and 6 in the screen as shown in Table A-6.

Table A-6 Overlap of Phases 5 and 6 in the Naztec Controller

Ovrlp D	**Φs**	**Φs**	**Φs**	**Φs**	**Φs**	**Φs**	**Φs**	**Φs**
Included Ps	0	0	0	0	5	6	0	0
Modifier Ps	0	0	0	0	0	0	0	0
Type: NORMAL		Grn:	0	Yel:	3.5	Red:	1.5	

The overlap of phases 2 and 7 is created by entering "5," then "1," and selecting phases 2 and 7 in the screen as shown in Table A-7.

Table A-7 Overlap of Phases 2 and 7 in the Naztec Controller

Ovrlp E	**Φs**	**Φs**	**Φs**	**Φs**	**Φs**	**Φs**	**Φs**	**Φs**
Included Ps	0	2	0	0	0	0	7	0
Modifier Ps	0	0	0	0	0	0	0	0
Type: NORMAL		Grn:	0	Yel:	3.5	Red:	1.5	

After MM->1->5->2, setup parameters for conflicting phases 3 and 4 by entering "3," then "2," and selecting phases 4 in the screen as shown in Table A-8.

Table A-8 Parameters for Conflicting Phases 3 and 4 in the Naztec Controller

Ovrlp C	**Φs**	**Φs**	**Φs**	**Φs**	**Φs**	**Φs**	**Φs**	**Φs**
Confl Φs	0	0	0	4	0	0	0	0
…								

b. General Overlap Parameters (MM->1->5->1)

The following general overlap parameters are selected in the controller from MM->1->5->1:

Lock Inhibit: ON Confl Lock Enable: ON Parent ϕ Clrncs : ON

3. *Ring Sequence (MM->1->2->4)*

After MM->1->2->4, select the phase sequence # "9" in the 16 default phase sequences for STD8.

4. *Operational Mode (MM->2)*

a. Coordination Mode (MM->2->1)

After MM->2->1, select the parameters in the controller as follow:

Test OPMode: "0" Force-off: Float Correction: Long

Maximum: MAX_1 Flashmode: Channel

b. Split Table (MM->2->7)

After MM->2->7, enter "1," then select "1," input the splits of proposed operation 2 in year 2015 PM peak hour as shown in

Table A-9 as an example.

Table A-9 Phase Splits in the Naztec Controller

Phase	**1**	**2**	**3**	**4**	**5**	**6**	**7**	**8**
Time	10	29	32	59	10	29	12	79
Coor-Φ				×				×
Mode	NON	NON	NON	NON	NON	NON	NON	NON

c. Patten Table (MM->2->4)

Following MM->2->4, enter the parameters as shown in Table A-10. The offset value of "10" is for demonstration only and it should be corrected based on the adjacent traffic signal control parameters and the pertinent requirements.

Table A-10 Pattern Parameters in the Naztec Controller

Pat #	**Cycle**	**Offset**	**Split**	**Seqnc**
1	130	10	1	9
2				
…				

d. Check Coordination (MM->2->8->5)

Selecting MM->2->8->5 step by step, the results from the controller are as below.

Table A-11 Coordination Diagnostic Status in the Naztec Controller

Coordination Diagnostic Status			
Cycle	130	Pattrn 1	Fault: OK
Offset	10	Source Test Data:	OK

Coord FREEFreeStat Failed

5. *Scheduler (MM->4)*
   a. Action Table (MM->4->5)

      Following MM->4->5, select the parameters as indicated in Table A-12.

Table A-12 Action Parameters in the Naztec Controller

Actn	**Patrn**	**…**
1	1	…
…	…	…

   b. Day Plan Table (MM->4->4)

      After MM->4->4, choose the parameters as presented in Table A-13.

Table A-13 Day Plan Parameters in the Naztec Controller

Plan-1	**Evt**	**Time**	**Actn**	**Evt**	**Time**	**Actn**
Link 0	1	00:00	1	2	23:59	1
…	…	…	…	…	…	…

APPENDIX B.

CYCLE LENGTH

The VISSIM simulation model ran each scenario 10 times using random simulation seeds and 300 sec warm-up time. The compiled data between 301 sec and 1200 sec were collected and summarized in this section. Figure B-1 presents an example of original node evaluation files from one VISSIM model. The values on the line of "All" in these and other similar figures are the maximum queues of all the movements in the road network. The maximum queue of each traffic movement is limited to the maximum length of the pertinent link in VISSIM simulation models. The values shown in Table B-1 to Table B-10 are the average results of 10 simulation runs of pre-timed control. The values shown in Table B-11 to Table 6-20 are the average results of 10 simulation runs of fully actuated control. The values shown in Table B-21 to Table B-30 are the average results of 10 simulation runs of coordinated actuated control.

```
Node evaluation

File:     C:\Patrick\C70\C70-FixedTime\DDI-C70-FixedTime.inp
Comment:  ;Demand Ratio=170%    ; Random Seed = 2
Date:     Tuesday, October 09, 2012 10:58:57 AM
VISSIM:   5.40-01 [31360]

Node 1
Node 2

Node: Node Number
Movement: Movement (Bearing from-to)
veh(All): Number of Vehicles, All Vehicle Types
Delay(All): Average delay per vehicle [s], All Vehicle Types
maxQueue: Maximum Queue Length [ft]

Node; Movement; veh(All); Delay(All); maxQueue;
   1;       N-W;       32;       16.5;     81.0;
   1;      N-SE;       16;       13.6;     41.1;
   1;       W-E;       96;       74.5;    564.7;
   1;       W-S;        0;        0.0;      0.0;
   1;       W-S;       29;        8.5;    295.2;
   1;       E-W;       91;        8.9;    124.4;
   1;       E-S;       31;        0.4;    107.1;
   1;       All;      295;       30.4;    564.7;
   2;       E-N;       22;        9.4;      0.0;
   2;       E-W;       31;      190.3;    866.4;
   2;       S-E;       12;        3.0;      0.0;
   2;       S-W;       92;       18.2;    240.4;
   2;       W-N;       74;        2.1;      0.0;
   2;       W-E;       36;        8.6;    123.0;
   2;       All;      267;       31.0;    866.4;
   0;       All;      562;       30.7;    866.4;
```

Figure B-1 A Node Evaluation File (*.kna) from One VISSIM Model

1. Pre-timed Control

Table B-1 Simulation Results When Cycle Length is 60 sec

Link	Average Delay (sec/veh)					Average Maximum Queue (ft)				
	S1	S2	S3	S4	S5	S1	S2	S3	S4	S5
10->9	18.1	19.7	22.7	25.9	32.9	110.7	147.9	180.6	214.4	314.2
10->11	10.8	11.1	11.9	11.9	12.0	71.3	84.8	103.1	101.5	123.4
1->8	21.0	26.0	47.0	85.4	128.5	192.9	261.6	488.4	868.3	1165.6
3->8	4.7	4.4	4.4	5.1	5.3	56.4	71.6	76.2	90.4	93.4
14->7	26.7	31.0	41.0	69.1	127.4	150.1	173.9	260.7	440.8	787.9
5->4	10.2	10.5	11.2	11.2	12.0	89.7	107.2	144.5	158.3	179.8
12->7	6.0	6.0	7.4	7.3	7.1	73.3	91.2	112.3	150.2	139.0
All	10.3	11.7	16.8	25.7	37.2	202.1	261.6	511.4	909.3	1165.6

Notes: S1: Scenario 1; S2: Scenario 2; S3: Scenario 3; S4: Scenario 4; and S5: Scenario 5.

Table B-2 Simulation Results When Cycle Length is 70 sec

Link	Average Delay (sec/veh)					Average Maximum Queue (ft)				
	S1	S2	S3	S4	S5	S1	S2	S3	S4	S5
10->9	21.8	22.4	25.1	26.0	29.3	133.5	157.2	190.5	233.9	295.5
10->11	13.0	12.4	13.7	14.2	13.9	75.8	92.4	113.1	112.5	137.2
1->8	24.0	27.4	37.5	60.7	106.3	224.1	286.1	425.6	663.4	1120.6
3->8	4.2	4.3	4.7	5.1	5.4	59.8	56.1	76.2	84.0	94.0
14->7	32.3	35.2	47.9	74.2	133.3	159.5	195.8	299.0	451.6	763.4
5->4	12.5	13.0	13.3	13.4	14.7	105.9	117.9	167.5	172.6	203.7
12->7	4.0	4.8	6.3	7.0	6.6	65.6	99.3	115.4	170.5	173.8
All	11.6	12.6	15.8	21.9	34.1	224.8	289.5	444.1	732.9	1129.3

Notes: S1: Scenario 1; S2: Scenario 2; S3: Scenario 3; S4: Scenario 4; and S5: Scenario 5.

Table B-3 Simulation Results When Cycle Length is 80 sec

Link	Average Delay (sec/veh)					Average Maximum Queue (ft)				
	S1	S2	S3	S4	S5	S1	S2	S3	S4	S5
10->9	19.9	21.0	22.8	24.1	27.1	143.4	158.4	189.3	226.7	292.7
10->11	15.1	16.4	17.7	18.2	18.2	85.5	100.4	111.5	123.7	159.7
1->8	21.5	23.4	28.7	38.8	85.2	213.7	271.5	368.6	522.0	1025.5
3->8	4.0	4.8	5.3	5.4	6.0	48.4	58.6	73.2	76.8	85.6
14->7	27.0	31.1	35.2	43.1	76.5	156.4	193.1	251.9	336.3	563.4
5->4	13.9	15.6	16.6	17.6	18.5	104.9	137.0	169.1	187.3	249.0
12->7	4.0	4.1	5.1	6.2	6.5	46.5	75.5	111.9	130.0	195.1
All	11.0	12.0	13.9	16.6	28.3	215.8	271.5	382.0	541.4	1027.5

Notes: S1: Scenario 1; S2: Scenario 2; S3: Scenario 3; S4: Scenario 4; and S5: Scenario 5.

Table B-4 Simulation Results When Cycle Length is 90 sec

Link	Average Delay (sec/veh)					Average Maximum Queue (ft)				
	S1	S2	S3	S4	S5	S1	S2	S3	S4	S5
10->9	20.3	21.0	23.1	24.9	27.4	138.7	165.9	214.9	226.8	305.2
10->11	16.4	19.0	20.4	20.5	20.8	82.7	105.8	138.7	150.2	166.0
1->8	22.5	23.0	28.3	33.8	64.6	210.4	285.4	381.0	489.8	887.2
3->8	3.8	5.3	5.8	5.8	6.2	53.6	59.0	65.2	82.8	87.2
14->7	26.4	32.0	36.3	47.0	83.2	159.4	198.9	247.3	341.7	595.6
5->4	15.7	16.8	18.5	20.5	21.9	122.5	153.6	195.2	220.4	266.3
12->7	3.5	3.6	3.5	4.9	5.8	73.2	87.4	130.1	155.6	189.5
All	11.4	12.3	14.2	16.5	25.4	210.9	288.1	392.4	510.4	946.1

Notes: S1: Scenario 1; S2: Scenario 2; S3: Scenario 3; S4: Scenario 4; and S5: Scenario 5.

Table B-5 Simulation Results When Cycle Length is 100 sec

Link	Average Delay (sec/veh)					Average Maximum Queue (ft)				
	S1	S2	S3	S4	S5	S1	S2	S3	S4	S5
10->9	21.1	22.1	24.6	25.3	29.5	136.4	179.2	213.4	246.1	331.0
10->11	16.7	20.7	22.7	23.3	23.4	89.3	113.3	148.4	171.2	185.6
1->8	23.4	23.1	28.1	34.8	70.2	230.8	284.8	410.0	507.3	916.5
3->8	4.2	4.9	5.4	5.1	7.0	53.3	51.7	66.8	76.2	92.2
14->7	28.1	31.5	38.6	41.2	67.5	170.3	194.6	279.0	326.2	531.5
5->4	17.5	18.1	22.7	23.7	24.3	128.9	156.5	204.6	242.0	300.8
12->7	3.5	3.2	3.6	4.8	5.2	53.9	59.2	96.6	108.2	194.8
All	11.9	12.6	15.0	16.7	26.2	235.1	284.8	410.0	510.0	934.2

Notes: S1: Scenario 1; S2: Scenario 2; S3: Scenario 3; S4: Scenario 4; and S5: Scenario 5.

Table B-6 Simulation Results When Cycle Length is 110 sec

Link	Average Delay (sec/veh)					Average Maximum Queue (ft)				
	S1	S2	S3	S4	S5	S1	S2	S3	S4	S5
10->9	21.1	21.6	26.1	27.7	30.6	126.4	167.0	230.7	269.3	349.7
10->11	19.1	20.6	25.5	25.4	27.1	97.2	117.7	148.2	171.8	190.6
1->8	22.4	24.8	29.5	35.4	68.9	221.4	313.3	418.8	524.0	927.0
3->8	4.0	5.1	5.5	5.4	6.2	50.2	50.3	66.9	66.6	83.5
14->7	28.5	32.4	37.8	44.6	58.5	168.3	204.4	276.9	353.8	507.5
5->4	18.9	21.1	25.3	26.6	28.7	150.1	164.5	221.2	271.8	342.3
12->7	3.1	2.8	3.0	4.4	5.0	72.5	69.6	87.9	132.6	201.9
All	12.0	13.2	15.8	17.7	26.2	229.3	313.3	435.6	533.0	935.4

Notes: S1: Scenario 1; S2: Scenario 2; S3: Scenario 3; S4: Scenario 4; and S5: Scenario 5.

Table B-7 Simulation Results When Cycle Length is 120 sec

Link	Average Delay (sec/veh)					Average Maximum Queue (ft)				
	S1	S2	S3	S4	S5	S1	S2	S3	S4	S5
10->9	20.4	22.1	25.7	28.0	31.3	123.1	179.7	222.8	299.5	377.3
10->11	18.8	22.3	28.3	28.7	30.4	93.5	127.8	164.1	179.5	214.3
1->8	23.1	24.5	30.2	34.6	60.1	230.1	294.6	443.4	544.3	855.3
3->8	4.3	4.8	6.0	5.9	7.5	53.8	46.3	68.2	74.2	84.4
14->7	27.3	32.3	40.3	45.6	62.7	162.3	207.5	308.2	359.2	516.4
5->4	18.8	21.9	26.9	29.0	31.6	135.9	170.0	244.3	270.2	396.9
12->7	2.9	3.0	3.1	3.9	4.6	47.7	70.5	83.5	147.1	244.6
All	12.0	13.3	16.3	18.2	25.6	235.7	294.6	448.0	545.5	880.5

Notes: S1: Scenario 1; S2: Scenario 2; S3: Scenario 3; S4: Scenario 4; and S5: Scenario 5.

Table B-8 Simulation Results When Cycle Length is 130 sec

Link	Average Delay (sec/veh)					Average Maximum Queue (ft)				
	S1	S2	S3	S4	S5	S1	S2	S3	S4	S5
10->9	20.1	22.6	27.9	30.6	33.0	125.2	170.4	242.0	292.1	393.0
10->11	19.3	22.0	29.4	32.2	33.3	96.2	122.2	165.5	189.4	225.3
1->8	21.9	26.2	30.7	35.3	58.0	217.0	303.4	456.6	564.4	815.6
3->8	4.4	4.5	5.3	5.9	7.1	56.0	52.4	65.7	66.4	81.7
14->7	28.0	30.9	41.6	48.8	64.2	164.7	202.7	307.9	398.8	541.9
5->4	18.8	22.7	28.5	30.8	34.6	151.0	171.0	236.3	306.1	372.5
12->7	2.9	3.3	3.0	3.7	4.7	54.1	111.9	111.9	128.4	152.3
All	11.8	13.8	16.9	19.2	25.9	221.5	313.1	469.4	578.0	832.5

Notes: S1: Scenario 1; S2: Scenario 2; S3: Scenario 3; S4: Scenario 4; and S5: Scenario 5.

Table B-9 Simulation Results When Cycle Length is 140 sec

Link	Average Delay (sec/veh)					Average Maximum Queue (ft)				
	S1	S2	S3	S4	S5	S1	S2	S3	S4	S5
10->9	20.6	22.2	28.6	30.8	37.7	130.6	174.5	257.7	294.8	424.9
10->11	18.3	21.3	30.4	34.3	35.6	95.1	119.4	164.9	201.4	249.7
1->8	23.2	25.9	32.1	37.6	63.3	239.4	303.4	493.0	600.4	897.5
3->8	3.9	4.5	5.5	5.6	6.3	49.4	49.3	57.2	66.0	87.8
14->7	28.6	31.2	42.3	52.3	63.1	171.5	207.2	310.4	397.3	534.7
5->4	18.6	23.3	29.6	35.4	39.2	137.9	175.0	256.1	330.4	560.5
12->7	3.2	3.2	2.5	3.5	4.5	50.3	82.8	82.8	132.8	174.2
All	12.0	13.7	17.4	20.4	28.1	242.3	303.5	493.4	611.1	918.2

Notes: S1: Scenario 1; S2: Scenario 2; S3: Scenario 3; S4: Scenario 4; and S5: Scenario 5.

Table B-10 Simulation Results When Cycle Length is 150 sec

Link	Average Delay (sec/veh)					Average Maximum Queue (ft)				
	S1	S2	S3	S4	S5	S1	S2	S3	S4	S5
10->9	20.1	22.3	28.6	30.4	35.7	126.7	178.5	259.0	315.6	414.4
10->11	19.2	22.8	31.7	36.4	37.8	95.1	119.8	182.0	222.3	258.4
1->8	22.5	25.5	31.0	37.1	58.8	227.5	312.9	451.4	624.1	862.2
3->8	3.9	4.9	5.0	6.1	6.5	51.5	55.0	57.2	73.7	90.6
14->7	27.5	33.1	42.0	50.4	69.0	172.9	217.0	341.1	397.4	558.2
5->4	19.5	23.4	31.6	36.9	41.4	144.9	178.7	270.2	326.1	500.4
12->7	3.2	3.0	2.9	3.2	4.7	55.8	81.9	98.3	114.1	214.2
All	11.9	13.8	17.4	20.4	27.4	230.6	312.9	468.1	640.0	882.3

Notes: S1: Scenario 1; S2: Scenario 2; S3: Scenario 3; S4: Scenario 4; and S5: Scenario 5.

2. Fully Actuated Control

Table B-11 Simulation Results When Cycle Length is 60 sec

Link	Average Delay (sec/veh)					Average Maximum Queue (ft)				
	S1	S2	S3	S4	S5	S1	S2	S3	S4	S5
10->9	18.4	20.7	23.4	24.4	32.0	119.0	144.1	178.3	207.2	299.0
10->11	11.4	11.8	11.8	11.5	11.7	71.3	78.4	91.7	101.7	117.7
1->8	21.8	25.6	47.6	89.0	131.4	210.1	266.1	494.1	919.7	1165.5
3->8	4.6	4.1	4.8	4.9	5.1	59.0	66.5	68.9	86.0	97.6
14->7	28.0	30.6	42.2	69.5	133.6	157.8	172.9	281.0	450.5	796.1
5->4	9.5	10.5	10.7	11.1	12.1	91.0	107.6	129.9	159.1	177.6
12->7	6.0	6.4	7.3	7.6	7.2	79.2	94.0	133.2	162.4	148.0
All	10.5	11.9	17.0	26.3	37.8	214.6	266.2	519.2	953.2	1165.5

Notes: S1: Scenario 1; S2: Scenario 2; S3: Scenario 3; S4: Scenario 4; and S5: Scenario 5.

Table B-12 Simulation Results When Cycle Length is 70 sec

Link	Average Delay (sec/veh)					Average Maximum Queue (ft)				
	S1	S2	S3	S4	S5	S1	S2	S3	S4	S5
10->9	18.9	19.0	21.9	23.6	28.1	116.5	151.5	175.0	219.8	289.4
10->11	13.1	13.8	13.7	14.4	15.0	81.9	106.8	108.1	123.0	137.0
1->8	20.8	23.1	28.8	49.1	94.3	204.1	273.3	334.3	599.0	1090.0
3->8	4.9	4.7	5.4	5.3	5.8	56.1	55.7	78.9	85.2	101.9
14->7	26.3	29.1	37.8	59.7	113.9	134.2	178.9	266.8	393.6	695.1
5->4	12.0	12.9	13.5	13.7	14.3	102.7	136.7	153.1	170.9	194.7
12->7	4.2	4.9	5.6	6.4	6.7	69.8	101.8	97.9	154.3	155.4
All	10.5	11.4	13.5	18.9	31.6	204.1	273.3	358.9	646.2	1104.3

Notes: S1: Scenario 1; S2: Scenario 2; S3: Scenario 3; S4: Scenario 4; and S5: Scenario 5.

Table B-13 Simulation Results When Cycle Length is 80 sec

Link	Average Delay (sec/veh)					Average Maximum Queue (ft)				
	S1	S2	S3	S4	S5	S1	S2	S3	S4	S5
10->9	19.4	21.1	22.6	25.5	28.5	132.5	159.2	195.8	234.2	299.0
10->11	15.9	16.6	18.7	18.5	18.4	86.3	98.7	122.4	141.5	164.6
1->8	21.7	23.8	30.4	42.0	86.8	210.0	269.1	398.6	545.0	1024.7
3->8	4.3	4.7	5.0	5.0	6.2	49.8	50.8	72.5	75.8	94.4
14->7	26.5	30.1	32.5	43.6	81.7	150.9	194.3	239.7	326.8	592.9
5->4	13.9	15.2	16.2	17.7	17.4	104.3	135.0	181.5	197.9	236.8
12->7	3.9	4.0	4.9	6.4	6.7	59.9	90.0	113.8	136.9	174.9
All	11.0	12.1	14.0	17.4	29.1	212.2	269.2	405.9	568.7	1048.1

Notes: S1: Scenario 1; S2: Scenario 2; S3: Scenario 3; S4: Scenario 4; and S5: Scenario 5.

Table B-14 Simulation Results When Cycle Length is 90 sec

Link	Average Delay (sec/veh)					Average Maximum Queue (ft)				
	S1	S2	S3	S4	S5	S1	S2	S3	S4	S5
10->9	19.7	20.1	23.1	25.1	27.7	132.1	148.2	207.8	241.0	325.4
10->11	15.9	17.7	19.7	20.1	20.5	84.2	110.6	123.6	145.2	165.2
1->8	22.7	23.2	27.6	33.3	65.7	230.2	262.4	386.0	471.0	868.3
3->8	4.7	5.2	5.5	6.0	6.6	53.6	58.2	69.3	86.3	96.2
14->7	26.2	30.2	38.7	46.9	76.1	147.3	202.2	270.6	354.2	586.6
5->4	14.9	17.6	20.5	19.9	21.9	119.9	151.8	198.0	229.9	273.4
12->7	3.4	3.7	3.7	4.5	6.1	73.0	72.4	103.4	144.2	182.2
All	11.4	12.2	14.3	16.2	25.3	231.5	262.6	401.5	494.6	922.1

Notes: S1: Scenario 1; S2: Scenario 2; S3: Scenario 3; S4: Scenario 4; and S5: Scenario 5.

Table B-15 Simulation Results When Cycle Length is 100 sec

Link	Average Delay (sec/veh)					Average Maximum Queue (ft)				
	S1	S2	S3	S4	S5	S1	S2	S3	S4	S5
10->9	21.0	21.9	23.5	25.6	29.2	134.8	165.3	206.1	257.1	316.6
10->11	16.3	18.9	23.6	22.8	24.3	82.7	112.9	143.2	146.4	189.4
1->8	23.0	24.5	28.8	34.7	66.6	231.2	288.2	403.6	499.8	898.2
3->8	4.0	5.0	5.4	6.6	6.0	49.9	56.5	62.8	75.6	86.5
14->7	28.6	32.4	36.1	43.9	69.5	163.2	204.8	285.1	351.0	520.5
5->4	15.8	18.8	23.6	22.8	24.0	125.2	161.0	213.2	241.7	291.4
12->7	3.8	2.8	3.4	4.9	4.8	60.4	52.4	113.1	214.1	183.3
All	11.7	12.8	15.0	17.1	25.5	231.2	288.2	416.2	512.0	925.6

Notes: S1: Scenario 1; S2: Scenario 2; S3: Scenario 3; S4: Scenario 4; and S5: Scenario 5.

Table B-16 Simulation Results When Cycle Length is 110 sec

Link	Average Delay (sec/veh)					Average Maximum Queue (ft)				
	S1	S2	S3	S4	S5	S1	S2	S3	S4	S5
10->9	21.3	21.9	26.0	27.2	30.8	139.3	172.4	223.8	282.9	359.5
10->11	19.4	22.0	24.5	26.2	27.2	95.2	129.2	144.1	162.2	193.1
1->8	22.7	25.2	30.3	34.4	68.5	214.7	319.2	432.0	522.2	911.4
3->8	4.1	4.8	5.1	5.4	6.5	50.5	56.2	60.1	61.2	87.2
14->7	29.8	31.9	37.4	42.2	59.0	166.9	215.0	303.9	334.2	481.5
5->4	17.7	20.8	24.8	26.6	28.9	143.7	162.5	220.6	256.7	315.4
12->7	3.1	3.1	3.3	4.2	5.7	56.3	68.6	87.1	152.6	174.8
All	12.1	13.4	15.8	17.5	26.4	225.7	319.2	438.2	529.2	916.5

Notes: S1: Scenario 1; S2: Scenario 2; S3: Scenario 3; S4: Scenario 4; and S5: Scenario 5.

Table B-17 Simulation Results When Cycle Length is 120 sec

Link	Average Delay (sec/veh)					Average Maximum Queue (ft)				
	S1	S2	S3	S4	S5	S1	S2	S3	S4	S5
10->9	20.2	21.7	26.2	29.0	32.0	135.1	171.6	221.6	274.0	364.1
10->11	20.0	22.7	27.1	29.2	29.6	100.3	122.4	159.2	189.8	219.2
1->8	22.8	24.9	29.2	33.9	58.0	228.9	304.2	421.6	509.2	810.9
3->8	4.0	4.7	5.4	5.6	6.7	50.7	53.8	59.6	71.6	86.6
14->7	30.2	33.4	40.4	44.6	64.9	165.4	212.5	323.3	355.3	527.3
5->4	17.9	22.4	27.2	29.0	32.2	137.3	168.9	231.5	274.2	367.7
12->7	3.3	3.0	3.4	3.4	4.7	64.2	67.4	113.9	110.2	186.4
All	12.1	13.5	16.2	18.0	25.0	233.2	304.2	424.4	517.0	847.6

Notes: S1: Scenario 1; S2: Scenario 2; S3: Scenario 3; S4: Scenario 4; and S5: Scenario 5.

Table B-18 Simulation Results When Cycle Length is 130 sec

Link	Average Delay (sec/veh)					Average Maximum Queue (ft)				
	S1	S2	S3	S4	S5	S1	S2	S3	S4	S5
10->9	19.9	22.3	27.0	31.0	33.7	133.9	168.7	248.3	318.3	387.0
10->11	20.8	23.6	29.3	32.7	33.3	106.9	121.3	179.1	200.2	237.8
1->8	22.1	25.3	31.5	36.6	63.5	218.7	328.5	463.3	539.0	867.6
3->8	4.2	4.7	5.2	5.8	7.1	52.7	61.8	59.5	58.5	101.3
14->7	29.4	32.6	39.8	48.2	59.9	169.8	206.4	299.1	386.2	548.6
5->4	18.0	22.6	29.9	32.0	35.1	139.5	171.1	239.2	302.4	392.4
12->7	3.5	2.9	3.4	3.4	4.7	71.5	56.4	111.9	175.4	164.3
All	12.0	13.6	17.1	19.6	26.7	223.1	328.5	463.3	542.2	878.4

Notes: S1: Scenario 1; S2: Scenario 2; S3: Scenario 3; S4: Scenario 4; and S5: Scenario 5.

Table B-19 Simulation Results When Cycle Length is 140 sec

Link	Average Delay (sec/veh)					Average Maximum Queue (ft)				
	S1	S2	S3	S4	S5	S1	S2	S3	S4	S5
10->9	20.5	22.3	27.0	30.3	34.0	133.8	168.8	239.9	304.1	405.6
10->11	20.8	24.7	30.3	35.6	37.8	100.0	127.6	185.0	188.1	257.2
1->8	23.1	25.1	30.7	37.3	59.7	228.8	313.5	474.7	569.0	859.4
3->8	4.2	4.8	5.4	5.1	7.3	50.9	57.2	55.8	64.9	91.2
14->7	29.8	31.7	40.7	50.8	62.2	169.7	209.6	322.0	396.5	534.6
5->4	17.8	22.6	30.4	34.7	41.0	135.0	172.0	267.6	297.2	533.6
12->7	3.4	3.0	2.5	3.2	4.8	74.3	100.9	79.7	148.1	232.0
All	12.3	13.7	16.9	20.1	27.0	231.1	323.2	482.2	573.5	899.9

Notes: S1: Scenario 1; S2: Scenario 2; S3: Scenario 3; S4: Scenario 4; and S5: Scenario 5.

Table B-20 Simulation Results When Cycle Length is 150 sec

Link	Average Delay (sec/veh)					Average Maximum Queue (ft)				
	S1	S2	S3	S4	S5	S1	S2	S3	S4	S5
10->9	20.2	22.3	26.9	32.2	35.6	131.4	177.6	242.2	310.5	448.3
10->11	20.9	24.3	31.7	37.1	38.5	101.9	119.2	177.6	215.3	263.5
1->8	23.2	25.5	30.8	39.2	65.8	233.7	310.7	455.2	617.5	926.4
3->8	4.2	4.9	5.6	5.6	7.0	50.8	57.3	65.7	79.8	87.3
14->7	29.4	31.3	40.3	49.7	64.0	167.9	205.7	328.0	399.7	559.3
5->4	18.0	22.4	31.3	36.7	42.0	136.6	170.1	284.3	330.6	556.6
12->7	3.3	2.7	2.7	3.2	4.2	74.3	90.5	84.2	122.3	239.4
All	12.3	13.7	17.2	20.9	28.9	235.9	320.3	472.6	617.5	940.2

Notes: S1: Scenario 1; S2: Scenario 2; S3: Scenario 3; S4: Scenario 4; and S5: Scenario 5.

3. Coordinated Actuated Control

Table B-21 Simulation Results When Cycle Length is 60 sec

Link	Average Delay (sec/veh)					Average Maximum Queue (ft)				
	S1	S2	S3	S4	S5	S1	S2	S3	S4	S5
10->9	15.4	17.9	20.5	23.4	29.1	110.5	136.6	178.5	216.8	286.3
10->11	13.5	12.6	13.1	12.6	13.3	78.6	88.3	99.9	110.7	131.9
1->8	18.5	22.0	33.0	61.3	111.3	179.0	243.8	360.5	699.8	1136.4
3->8	5.2	5.4	5.7	5.5	6.0	57.1	62.7	83.1	84.9	88.9
14->7	28.3	30.1	42.2	70.3	133.2	148.3	172.7	270.4	427.2	773.5
5->4	13.2	12.0	11.5	11.8	12.3	113.2	128.6	149.1	158.0	186.0
12->7	4.5	5.3	6.2	7.4	7.2	70.8	88.8	107.0	148.6	152.0
All	10.0	11.0	14.2	21.4	34.7	184.9	243.9	386.6	770.8	1136.4

Notes: S1: Scenario 1; S2: Scenario 2; S3: Scenario 3; S4: Scenario 4; and S5: Scenario 5.

Table B-22 Simulation Results When Cycle Length is 70 sec

Link	Average Delay (sec/veh)					Average Maximum Queue (ft)				
	S1	S2	S3	S4	S5	S1	S2	S3	S4	S5
10->9	17.1	18.8	19.9	22.1	25.5	126.2	142.5	179.6	211.9	289.9
10->11	16.1	15.8	15.3	16.5	15.8	84.4	92.8	114.5	125.3	145.1
1->8	18.2	21.1	26.1	40.6	83.9	189.7	246.1	320.0	489.3	1006.1
3->8	5.5	5.3	5.7	5.5	6.4	51.4	61.6	71.9	76.6	108.1
14->7	29.0	32.3	42.9	62.0	110.3	161.4	200.4	267.8	411.1	713.0
5->4	15.1	15.2	15.2	15.1	15.9	118.4	130.5	161.4	188.8	209.2
12->7	3.3	3.9	5.3	6.0	6.8	51.9	97.0	97.2	133.8	162.7
All	10.4	11.4	13.2	17.3	29.0	197.8	248.4	342.5	568.2	1060.4

Notes: S1: Scenario 1; S2: Scenario 2; S3: Scenario 3; S4: Scenario 4; and S5: Scenario 5.

Table B-23 Simulation Results When Cycle Length is 80 sec

Link	Average Delay (sec/veh)					Average Maximum Queue (ft)				
	S1	S2	S3	S4	S5	S1	S2	S3	S4	S5
10->9	17.0	18.1	21.8	22.4	25.9	127.9	151.5	199.1	213.4	297.6
10->11	21.1	18.8	20.0	18.9	19.1	96.9	106.7	127.6	138.7	159.8
1->8	19.3	21.6	26.0	35.6	74.1	218.4	265.5	356.9	500.6	957.1
3->8	5.6	5.6	5.2	5.3	5.5	52.0	64.6	58.0	83.0	91.5
14->7	33.2	33.2	37.1	47.6	82.7	172.4	208.5	256.7	360.3	604.0
5->4	19.5	19.1	18.0	18.5	19.6	145.5	167.8	191.3	222.6	242.9
12->7	2.7	2.9	4.5	5.5	6.7	40.2	63.4	93.7	125.5	178.7
All	11.5	11.9	13.5	16.1	26.5	223.1	265.5	365.3	534.1	1010.1

Notes: S1: Scenario 1; S2: Scenario 2; S3: Scenario 3; S4: Scenario 4; and S5: Scenario 5.

Table B-24 Simulation Results When Cycle Length is 90 sec

Link	Average Delay (sec/veh)					Average Maximum Queue (ft)				
	S1	S2	S3	S4	S5	S1	S2	S3	S4	S5
10->9	17.0	19.3	20.5	23.5	26.6	134.9	164.9	189.7	228.7	309.0
10->11	24.8	23.1	22.9	21.4	22.0	102.7	109.4	136.8	148.7	164.3
1->8	18.0	21.6	24.9	30.5	56.5	196.1	257.8	360.7	463.8	774.7
3->8	6.6	5.9	6.0	6.1	7.2	57.8	50.0	77.6	87.2	90.1
14->7	35.1	37.9	39.6	47.7	78.5	185.3	211.8	275.9	355.5	584.2
5->4	23.0	21.4	22.4	23.0	22.4	145.8	165.3	214.6	246.5	276.3
12->7	2.0	2.8	3.3	3.9	5.3	58.6	78.5	88.8	129.5	201.2
All	12.1	12.9	14.0	16.0	23.5	203.8	257.9	371.8	498.0	826.2

Notes: S1: Scenario 1; S2: Scenario 2; S3: Scenario 3; S4: Scenario 4; and S5: Scenario 5.

Table B-25 Simulation Results When Cycle Length is 100 sec

Link	Average Delay (sec/veh)					Average Maximum Queue (ft)				
	S1	S2	S3	S4	S5	S1	S2	S3	S4	S5
10->9	17.3	19.4	23.4	24.5	27.8	137.1	177.3	224.0	229.7	312.1
10->11	28.9	27.3	25.2	26.8	24.2	111.2	118.6	155.8	166.4	202.4
1->8	20.3	22.1	26.8	30.8	58.1	234.5	272.5	377.5	494.0	816.9
3->8	6.2	6.1	5.7	6.2	6.8	47.8	54.1	66.1	70.9	83.6
14->7	37.6	40.5	41.6	45.2	70.1	173.5	225.1	296.7	354.1	528.2
5->4	28.3	25.8	26.3	25.5	26.5	163.5	184.4	232.9	254.4	331.1
12->7	1.8	2.5	3.2	3.6	5.6	44.8	61.6	111.2	123.0	166.1
All	13.4	13.9	15.3	16.6	24.1	234.5	272.9	385.6	513.5	834.7

Notes: S1: Scenario 1; S2: Scenario 2; S3: Scenario 3; S4: Scenario 4; and S5: Scenario 5.

Table B-26 Simulation Results When Cycle Length is 110 sec

Link	Average Delay (sec/veh)					Average Maximum Queue (ft)				
	S1	S2	S3	S4	S5	S1	S2	S3	S4	S5
10->9	19.4	20.1	25.1	27.3	30.0	146.5	163.7	227.4	280.5	339.0
10->11	34.7	31.6	28.2	28.2	27.7	125.3	138.5	157.3	183.8	199.7
1->8	19.2	23.4	28.6	34.4	62.0	229.4	289.5	420.6	533.8	874.9
3->8	5.4	7.0	5.9	5.8	6.6	43.9	56.5	52.6	69.3	90.9
14->7	41.0	41.7	45.6	48.0	62.1	204.6	225.8	318.2	363.6	488.5
5->4	32.5	30.4	28.9	29.3	29.8	169.6	208.1	249.2	271.2	326.8
12->7	2.5	2.1	3.0	3.7	5.1	44.0	43.2	124.3	117.2	208.5
All	14.4	15.0	16.4	18.1	25.0	237.2	289.7	437.2	534.9	885.0

Notes: S1: Scenario 1; S2: Scenario 2; S3: Scenario 3; S4: Scenario 4; and S5: Scenario 5.

Table B-27 Simulation Results When Cycle Length is 120 sec

Link	Average Delay (sec/veh)					Average Maximum Queue (ft)				
	S1	S2	S3	S4	S5	S1	S2	S3	S4	S5
10->9	18.2	21.4	24.3	27.0	30.9	146.3	195.4	256.2	266.7	363.7
10->11	37.4	34.0	35.2	33.5	32.0	132.0	144.7	175.7	190.5	231.1
1->8	19.8	23.0	28.6	32.3	47.0	238.8	322.0	438.8	538.1	740.2
3->8	7.5	6.8	7.2	6.5	7.2	40.3	52.9	66.6	87.8	78.7
14->7	47.1	42.9	46.4	50.2	63.5	225.9	246.6	316.1	377.3	519.9
5->4	35.5	35.2	34.9	32.9	34.9	194.0	212.1	279.9	300.2	400.3
12->7	1.8	2.4	2.6	3.2	4.8	34.0	45.9	67.1	140.1	154.4
All	15.6	16.0	17.7	18.6	23.0	250.1	323.7	447.9	553.8	762.1

Notes: S1: Scenario 1; S2: Scenario 2; S3: Scenario 3; S4: Scenario 4; and S5: Scenario 5.

Table B-28 Simulation Results When Cycle Length is 130 sec

Link	Average Delay (sec/veh)					Average Maximum Queue (ft)				
	S1	S2	S3	S4	S5	S1	S2	S3	S4	S5
10->9	19.5	22.8	25.8	29.3	31.9	144.6	205.0	244.7	303.3	399.8
10->11	43.0	39.2	37.5	36.0	35.7	139.2	164.3	189.3	200.5	230.7
1->8	19.8	23.7	31.1	35.8	55.6	253.4	320.3	478.1	564.7	805.5
3->8	7.4	7.3	6.9	6.4	7.4	54.0	55.8	66.9	84.0	92.8
14->7	47.6	50.3	48.2	53.7	62.6	216.5	260.1	314.3	390.7	531.9
5->4	41.9	39.1	38.0	36.8	37.1	217.4	237.0	313.3	357.0	403.0
12->7	1.7	1.8	2.6	3.2	4.8	31.5	55.8	95.5	156.5	222.7
All	16.5	17.3	18.8	20.3	25.6	260.7	326.1	478.7	575.6	815.7

Notes: S1: Scenario 1; S2: Scenario 2; S3: Scenario 3; S4: Scenario 4; and S5: Scenario 5.

Table B-29 Simulation Results When Cycle Length is 140 sec

Link	Average Delay (sec/veh)					Average Maximum Queue (ft)				
	S1	S2	S3	S4	S5	S1	S2	S3	S4	S5
10->9	18.0	21.8	25.7	30.5	33.3	144.8	187.0	260.3	321.3	414.9
10->11	45.2	42.5	42.2	38.1	38.4	140.6	168.1	189.0	234.6	254.3
1->8	20.6	24.2	28.6	36.1	57.4	280.1	357.6	448.2	596.9	867.8
3->8	8.0	7.0	7.0	7.7	8.7	43.9	48.0	65.4	67.3	87.8
14->7	52.6	51.9	54.3	55.7	67.1	228.5	260.1	383.7	418.6	540.1
5->4	43.9	41.4	39.4	39.4	42.2	205.9	254.4	284.4	340.8	636.6
12->7	2.1	1.8	2.5	2.7	4.1	42.3	50.6	88.5	132.7	159.1
All	17.1	17.6	18.8	20.9	27.2	286.2	357.6	478.3	619.8	942.0

Notes: S1: Scenario 1; S2: Scenario 2; S3: Scenario 3; S4: Scenario 4; and S5: Scenario 5.

Table B-30 Simulation Results When Cycle Length is 150 sec

Link	Average Delay (sec/veh)					Average Maximum Queue (ft)				
	S1	S2	S3	S4	S5	S1	S2	S3	S4	S5
10->9	20.1	23.6	29.4	28.5	35.3	163.1	209.6	281.1	330.0	454.2
10->11	50.3	45.6	43.2	45.1	39.6	154.1	160.5	197.0	229.1	278.6
1->8	21.6	26.9	31.6	35.6	57.7	254.1	356.9	492.8	608.8	885.6
3->8	8.1	8.4	6.2	6.9	7.8	51.5	63.6	61.1	77.1	82.9
14->7	55.3	55.3	58.6	57.3	70.3	250.8	283.6	383.5	424.1	571.6
5->4	50.0	45.2	45.0	46.1	46.5	234.8	260.4	353.0	390.9	575.6
12->7	1.9	2.3	2.3	2.8	4.2	52.8	71.0	93.4	148.5	201.3
All	18.7	19.3	20.7	21.8	28.1	283.1	365.7	515.3	618.0	904.0

Notes: S1: Scenario 1; S2: Scenario 2; S3: Scenario 3; S4: Scenario 4; and S5: Scenario 5.

APPENDIX C.

DISTRIBUTION OF TRAFFIC

The VISSIM simulation model ran each scenario 10 times using random simulation seeds and 300 sec warm-up time. Each run's simulation data between 301 sec to 1200 sec were compiled and presented in this appendix. Figure B-1 presents an example of node evaluation files from one VISSIM model. Figure C-1 to Figure C-16 provide the average delays of 10 simulation runs for each scenario when travel time between the two crossovers is 12 sec. Figure C-17 to Figure C-32 provide the average maximum queues of 10 simulation runs for each scenario when travel time between the two crossovers is 12 sec. Figure C-33 to Figure C-48 provide the average delays of 10 simulation runs for each scenario when travel time between the two crossovers is 22 sec. Figure C-49 to Figure C-64 provide the average maximum queues of 10 simulation runs for each scenario when travel time between the two crossovers is 22 sec. The values on the line of "All" in these and other similar figures are the maximum queues of all the movements in the road network. The maximum queue of each traffic movement is limited to the maximum length of the pertinent link in VISSIM simulation models. For example, the maximum queue is around 1300 feet at turning movement "5->4" in Figure C-17 means the queue reached at the maximum length of the link in the VISSIM simulation model.

1. **Average Delay When Travel Time between the Two Crossovers is 12 Sec**

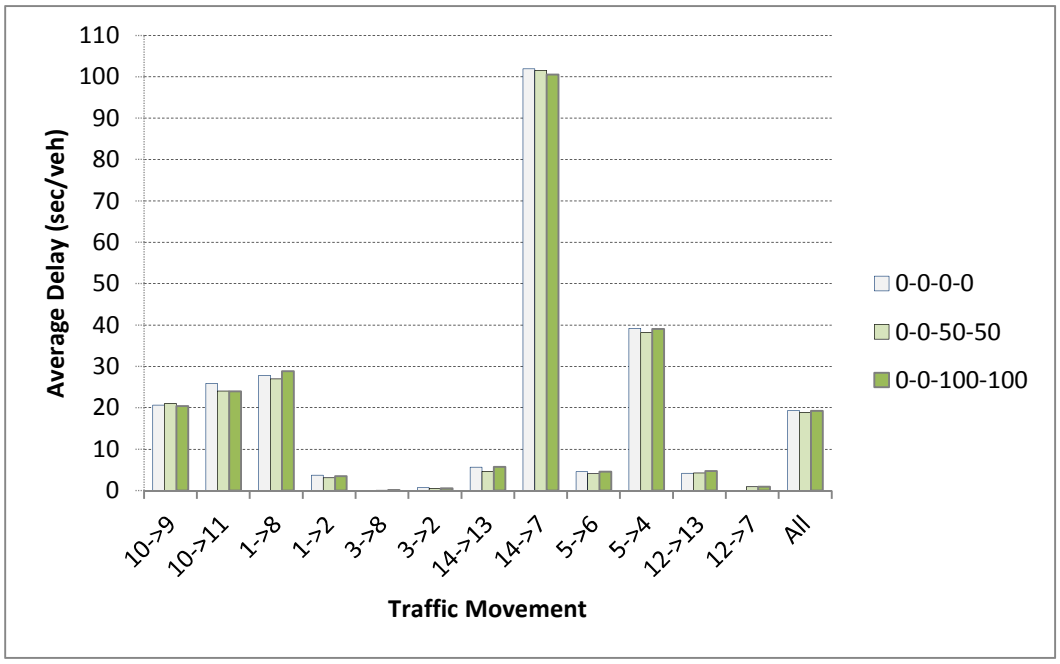

Figure C-1 Average Delay of Pre-Timed Control

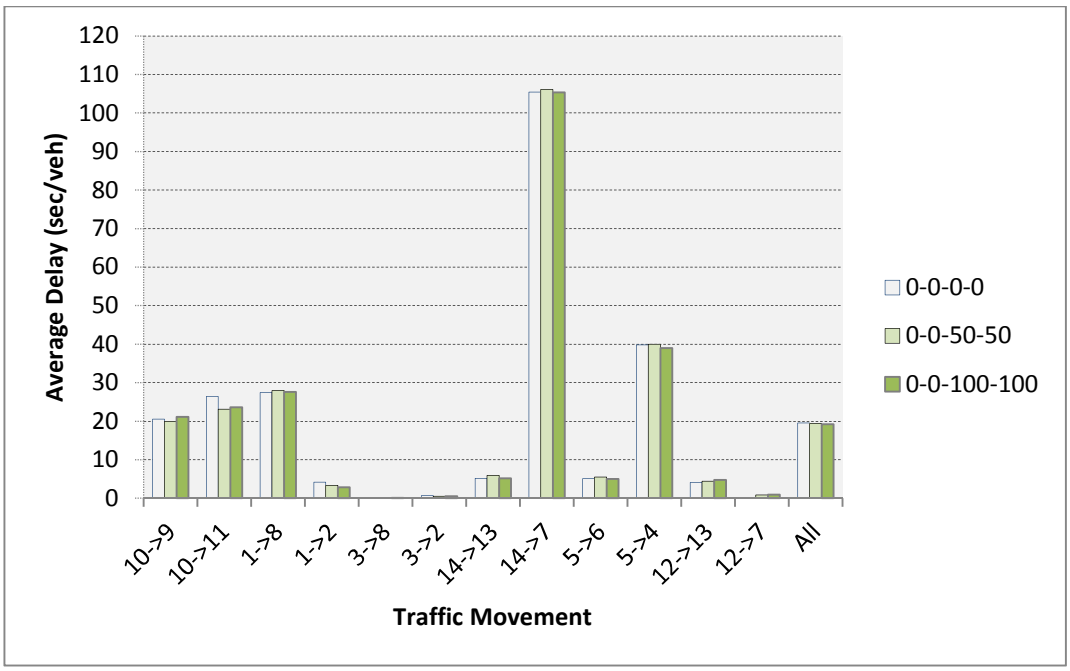

Figure C-2 Average Delay of Fully Actuated Control

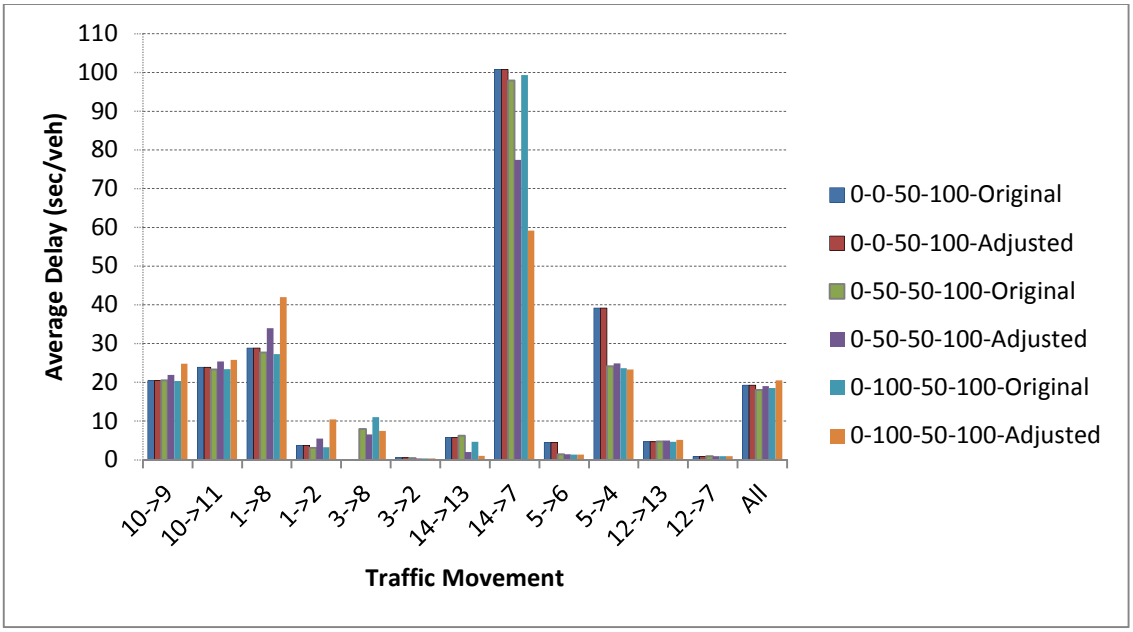

Figure C-3 Average Delay of Pre-Timed Control

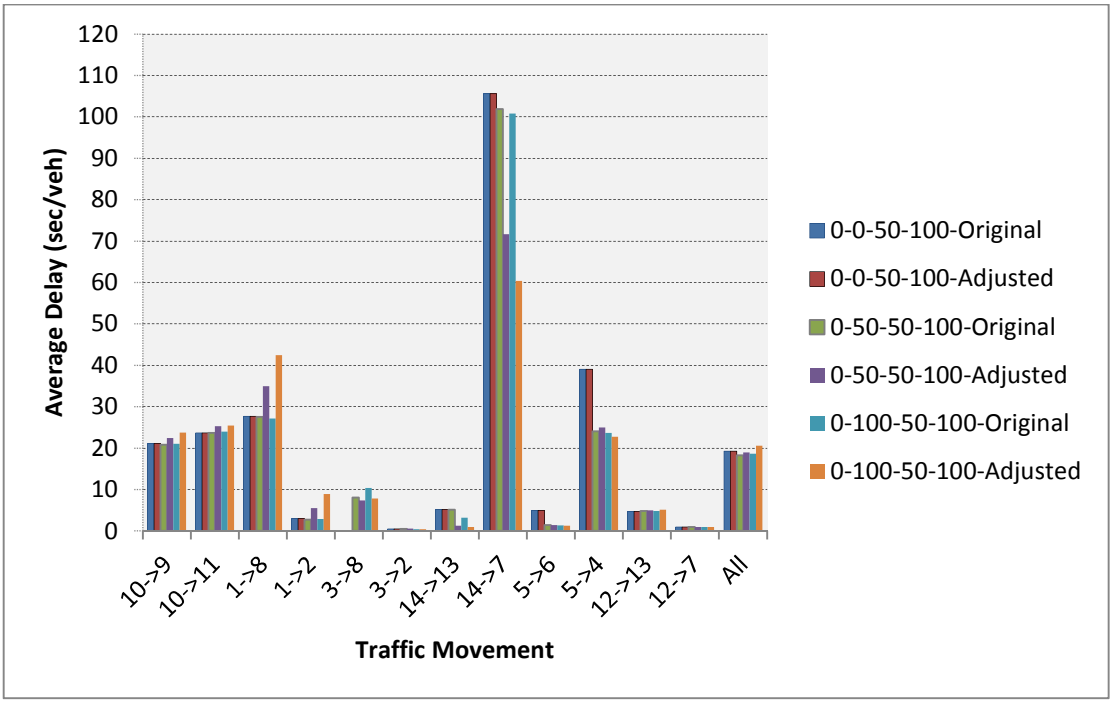

Figure C-4 Average Delay of Fully Actuated Control

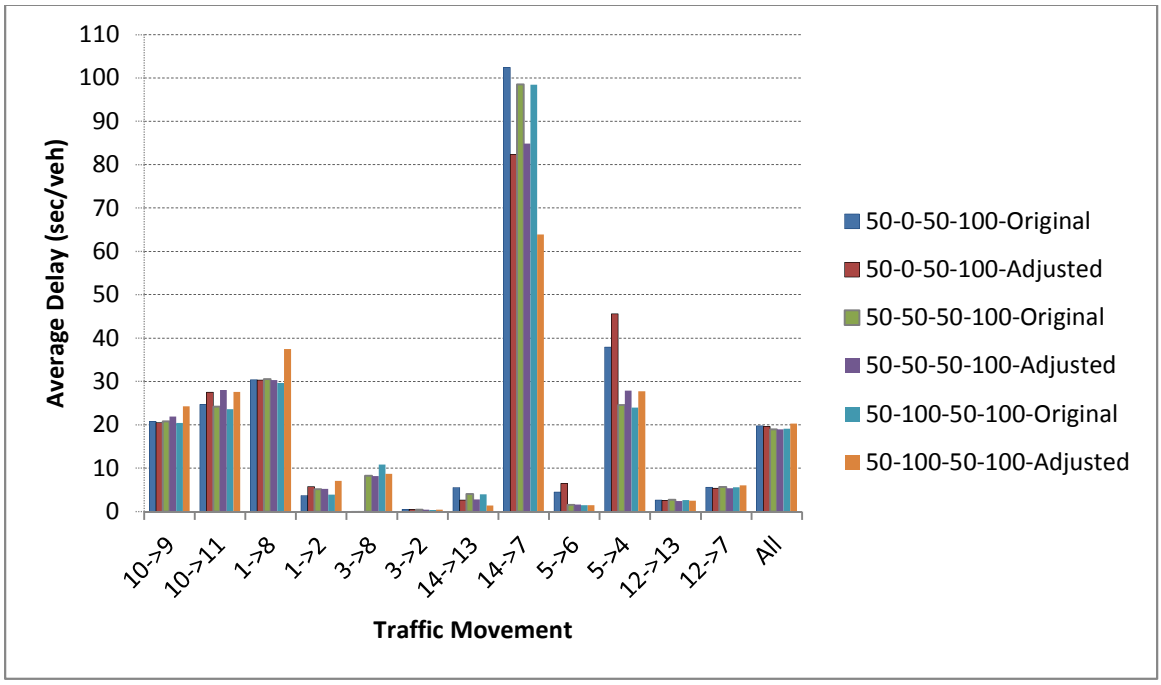

Figure C-5 Average Delay of Pre-Timed Control

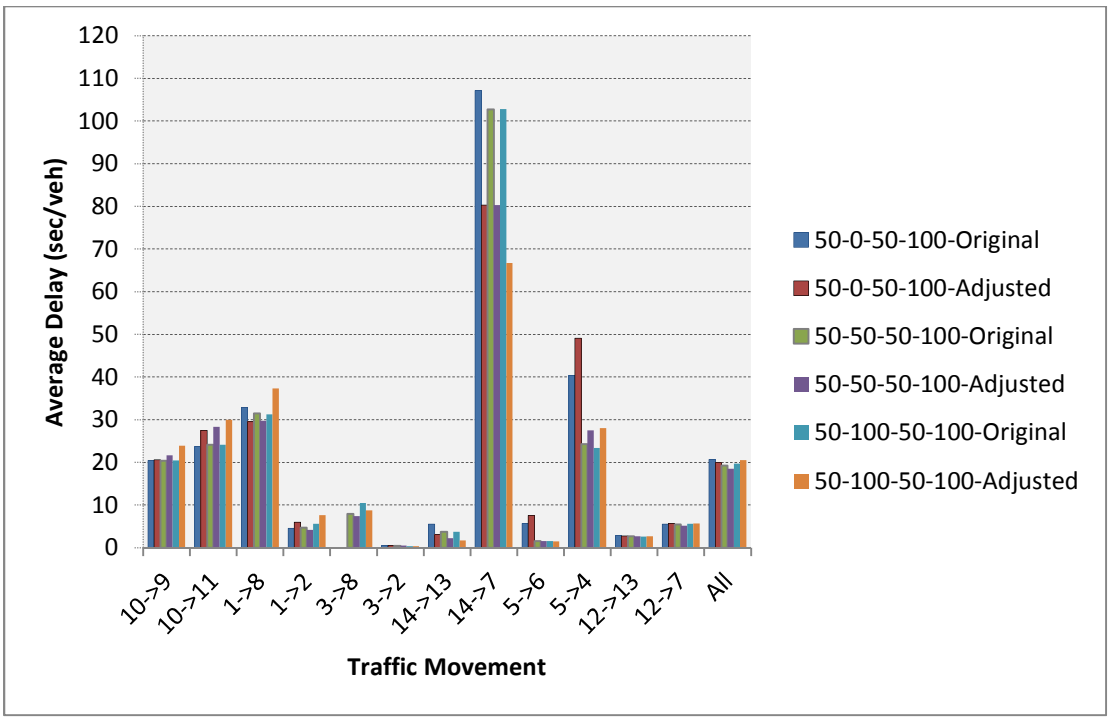

Figure C-6 Average Delay of Fully Actuated Control

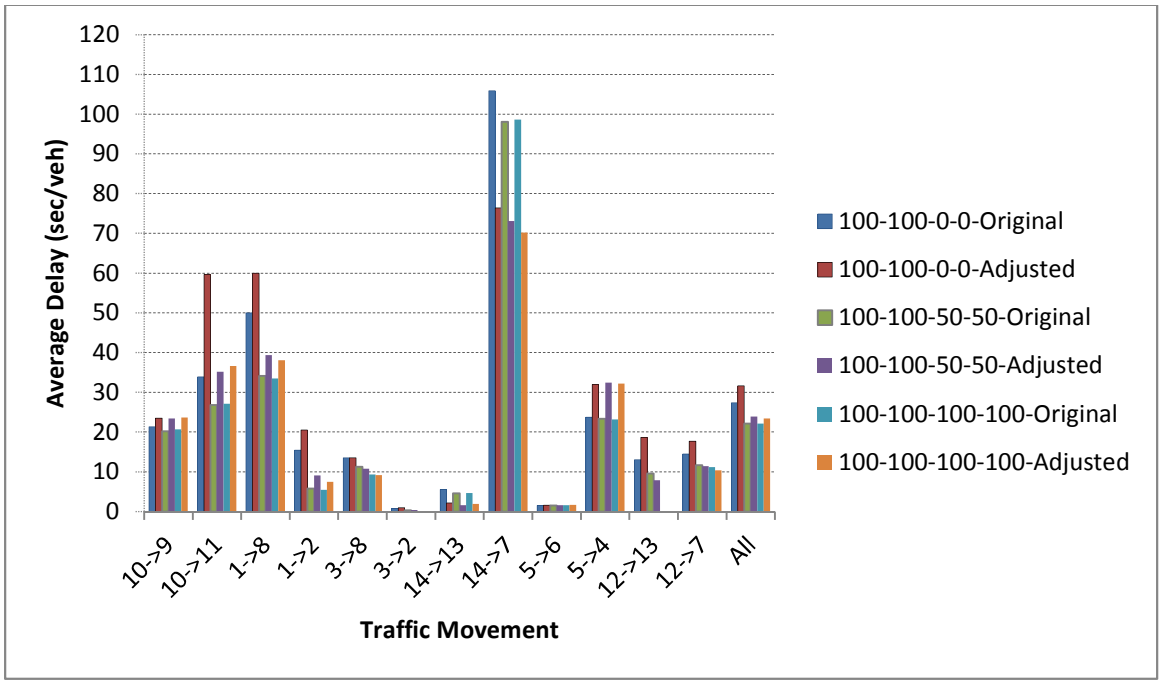

Figure C-7 Average Delay of Pre-Timed Control

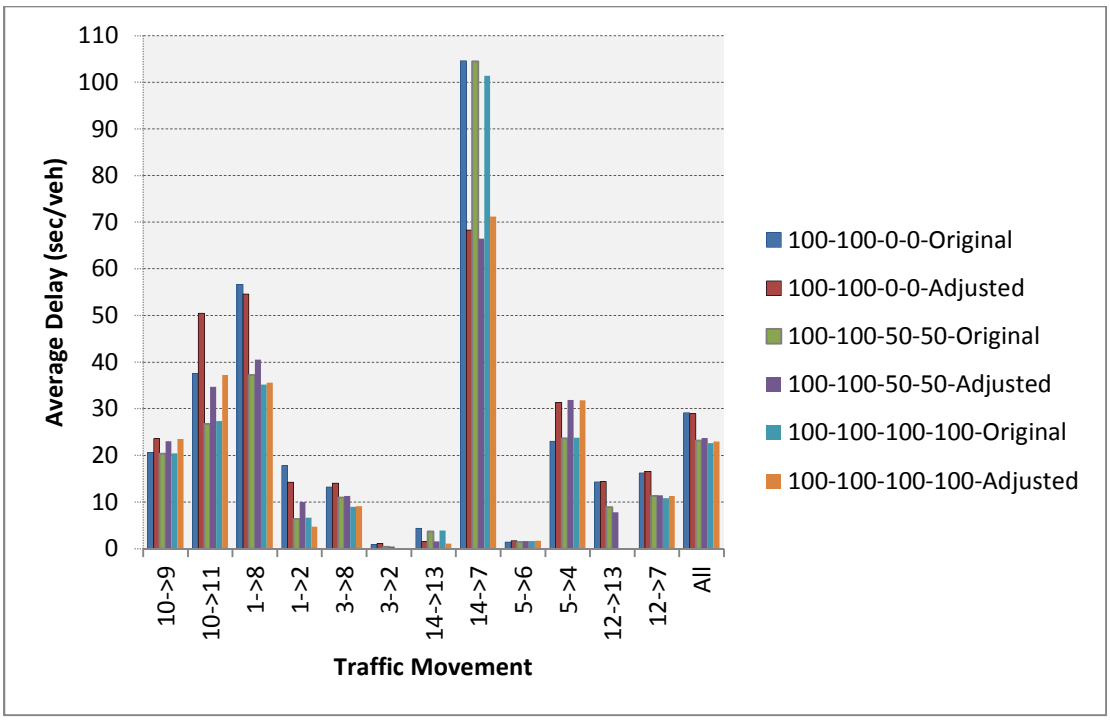

Figure C-8 Average Delay of Fully Actuated Control

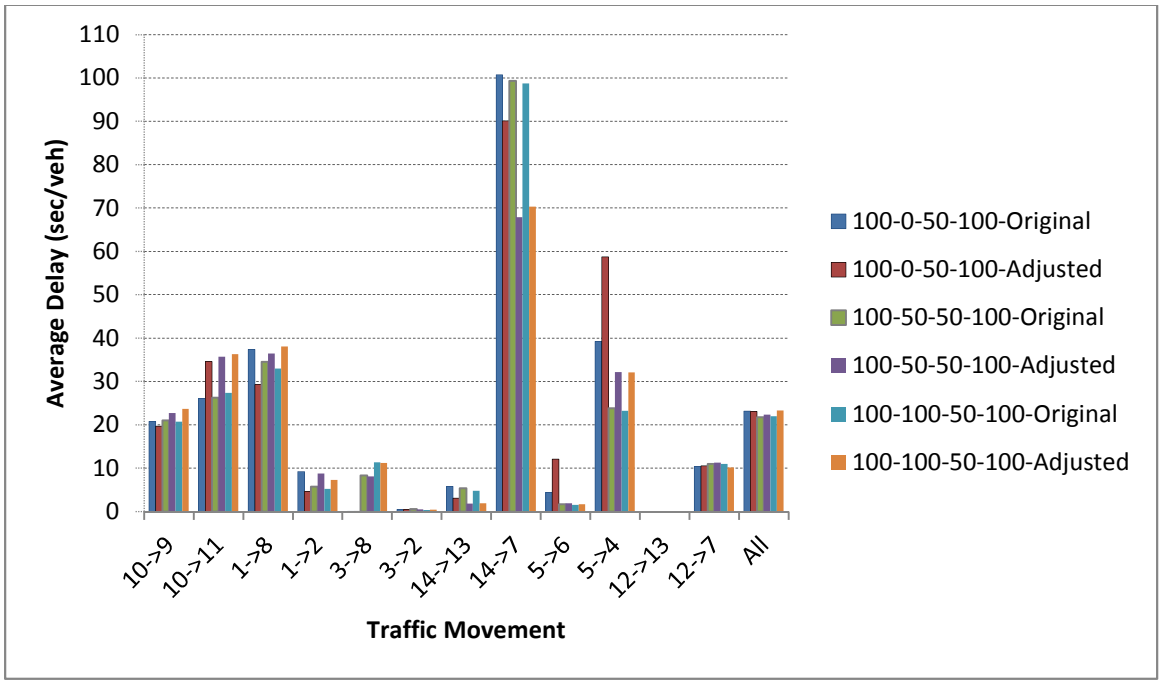

Figure C-9 Average Delay of Pre-Timed Control

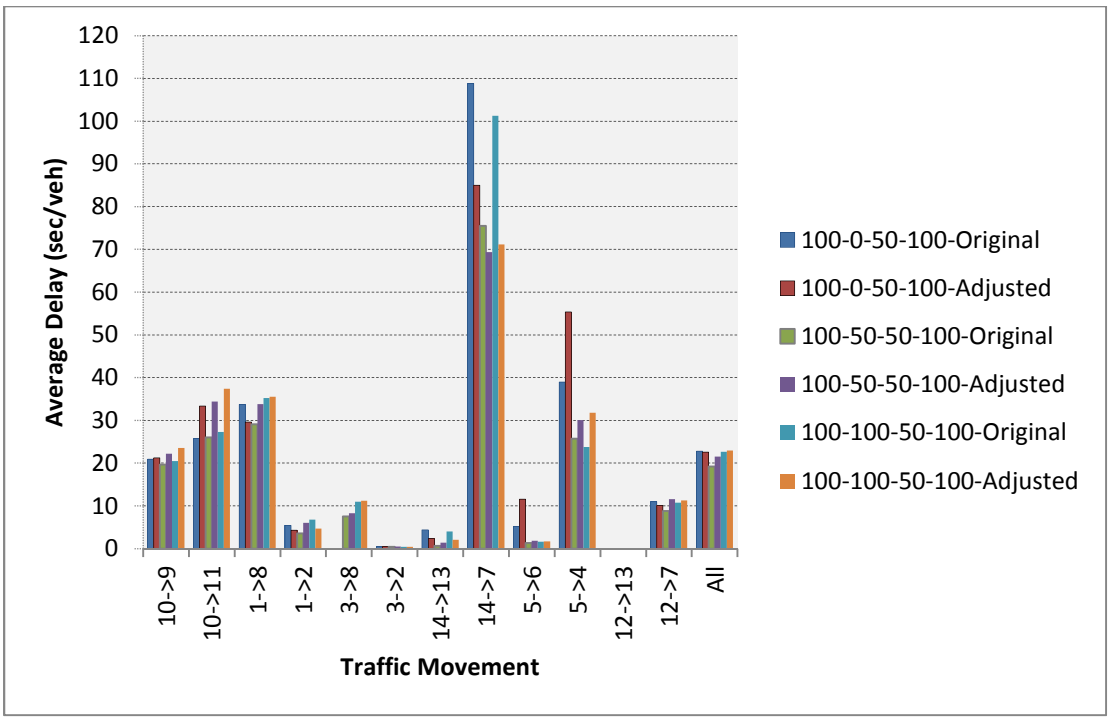

Figure C-10 Average Delay of Fully Actuated Control

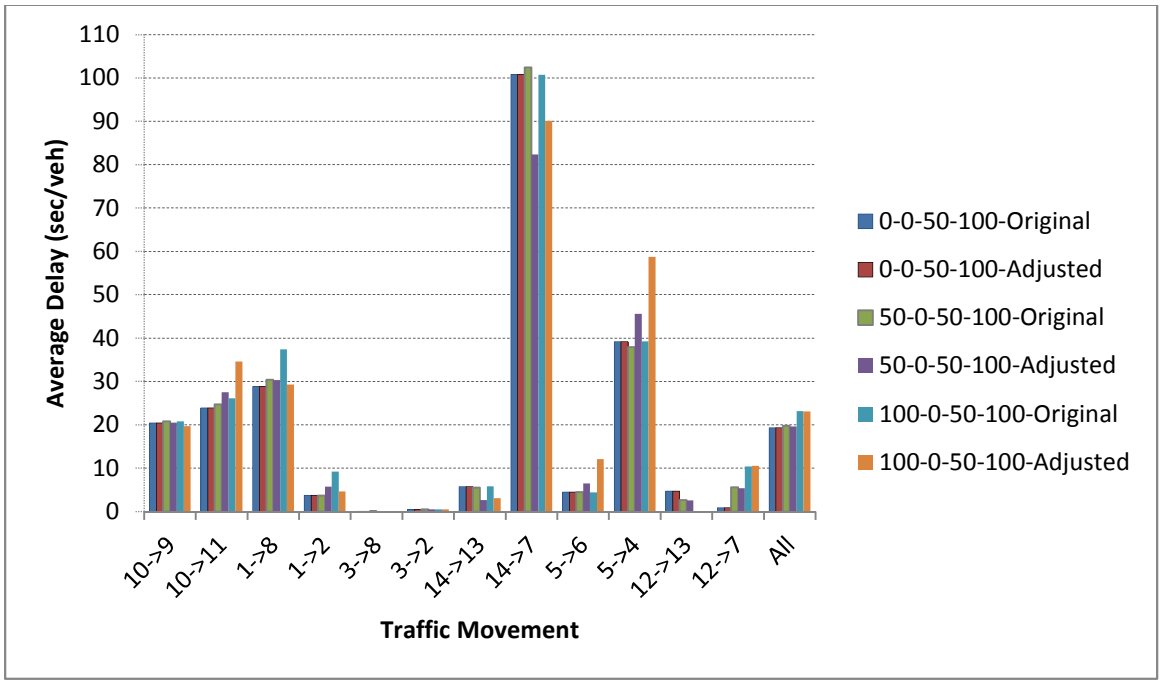

Figure C-11 Average Delay of Pre-Timed Control

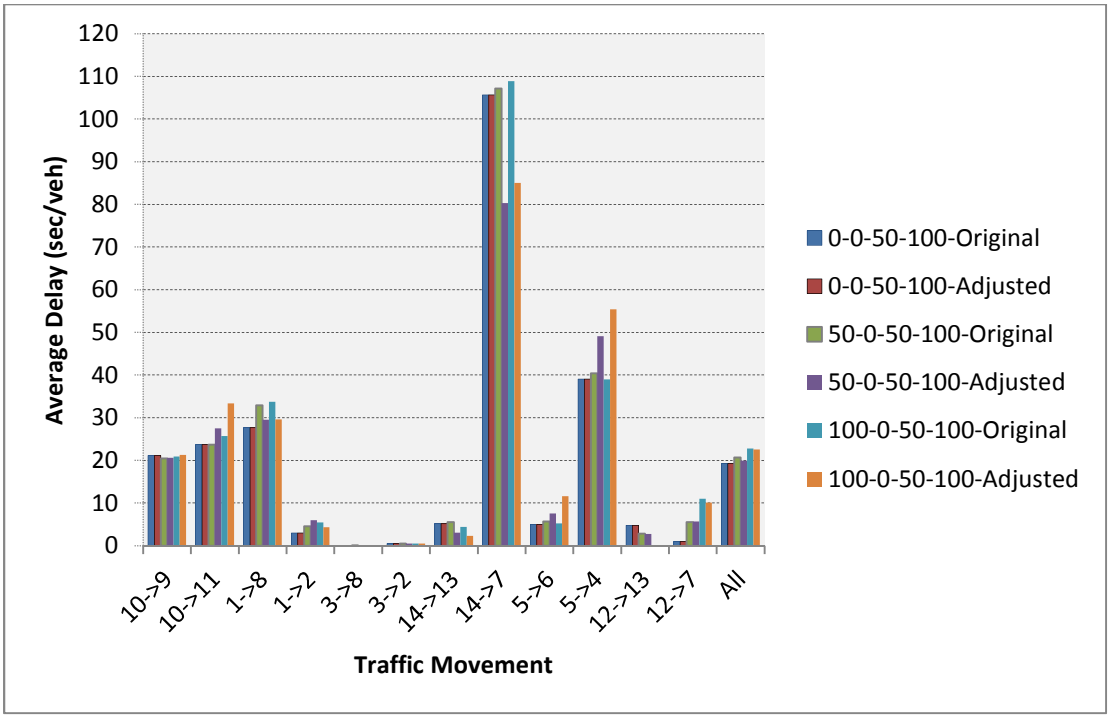

Figure C-12 Average Delay of Fully Actuated Control

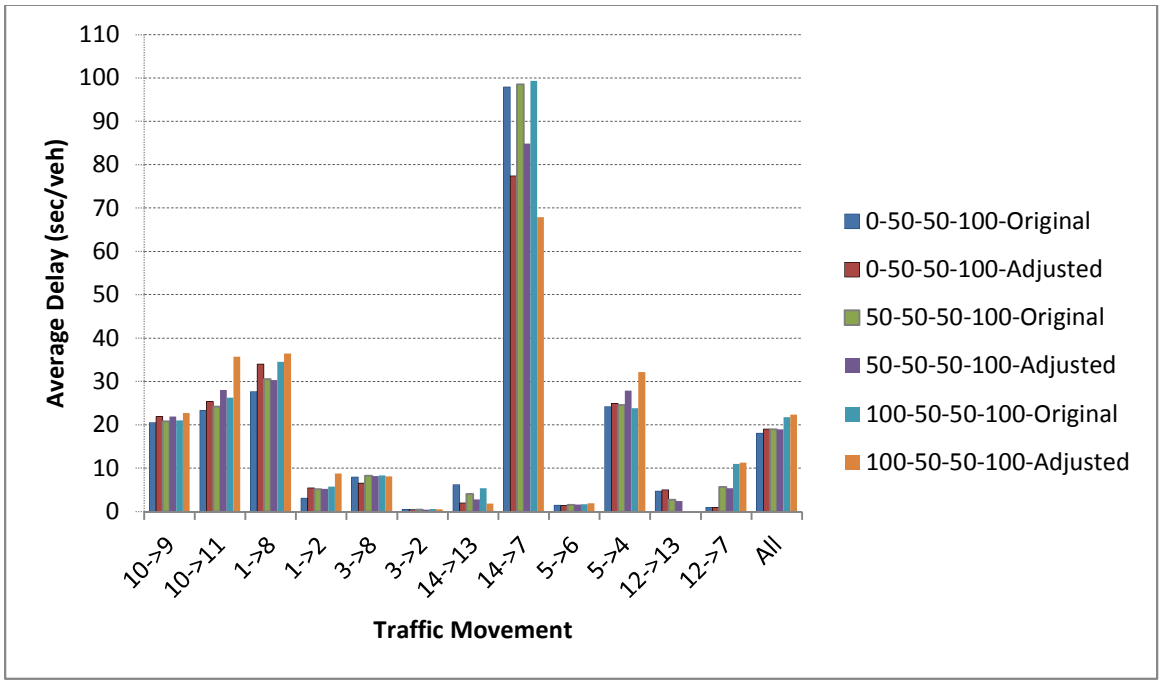

Figure C-13 Average Delay of Pre-Timed Control

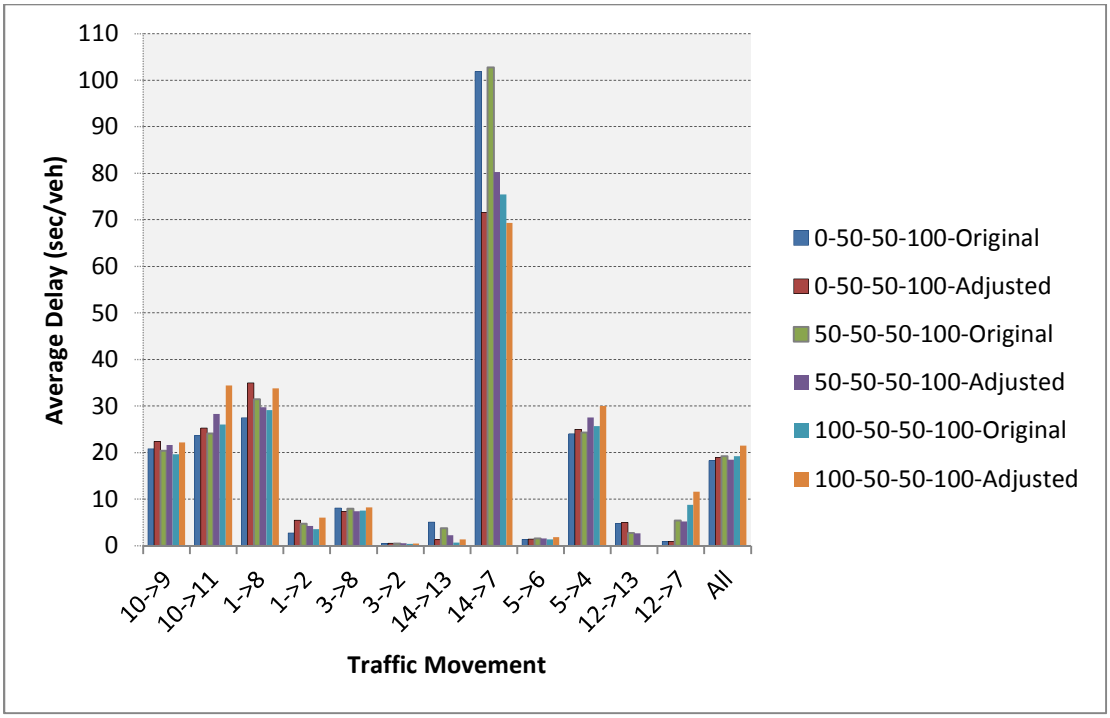

Figure C-14 Average Delay of Fully Actuated Control

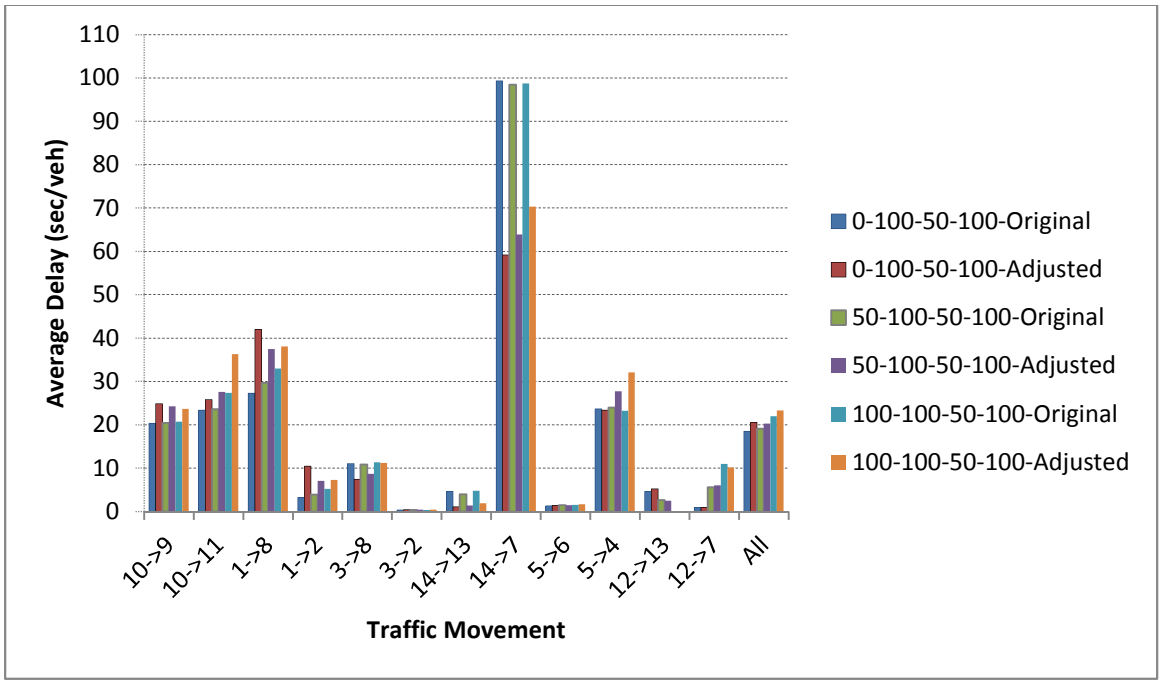

Figure C-15 Average Delay of Pre-Timed Control

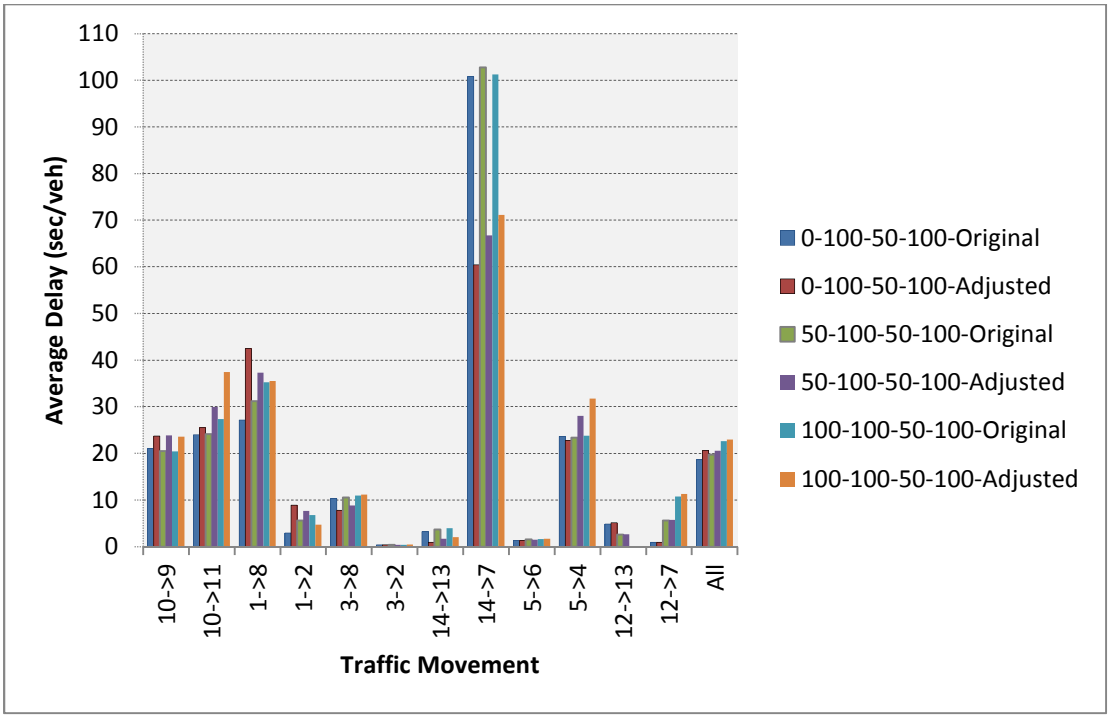

Figure C-16 Average Delay of Fully Actuated Control

2. Average Maximum Queue When Travel Time between the Two Crossovers is 12 Sec

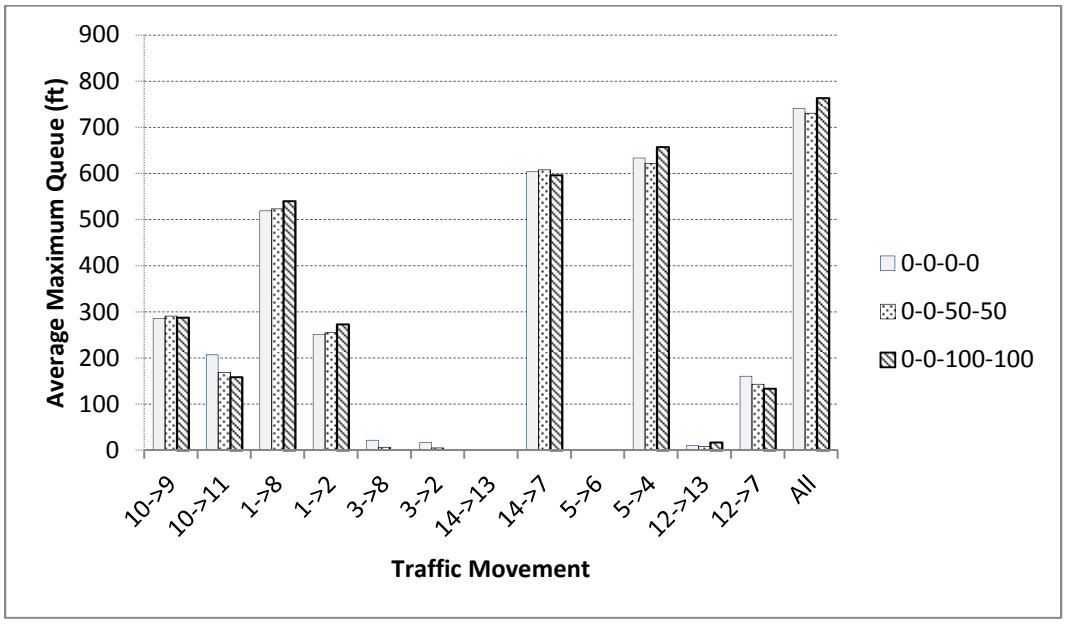

Figure C-17 Average Maximum Queue of Pre-Timed Control

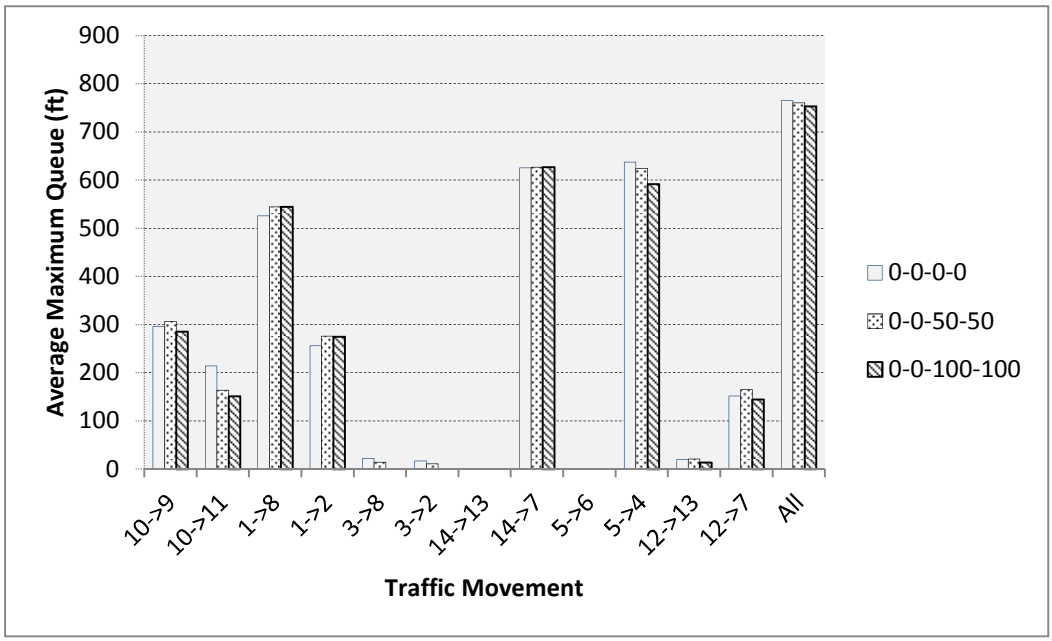

Figure C-18 Average Maximum Queue of Fully Actuated Control

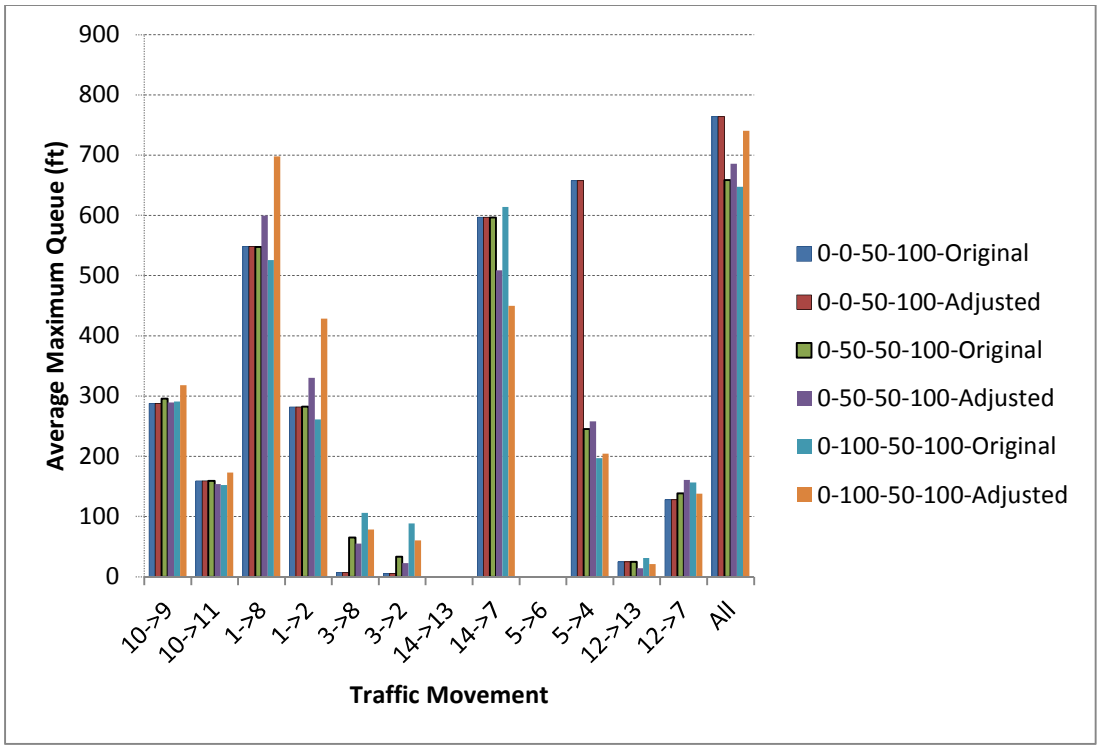

Figure C-19 Average Maximum Queue of Pre-Timed Control

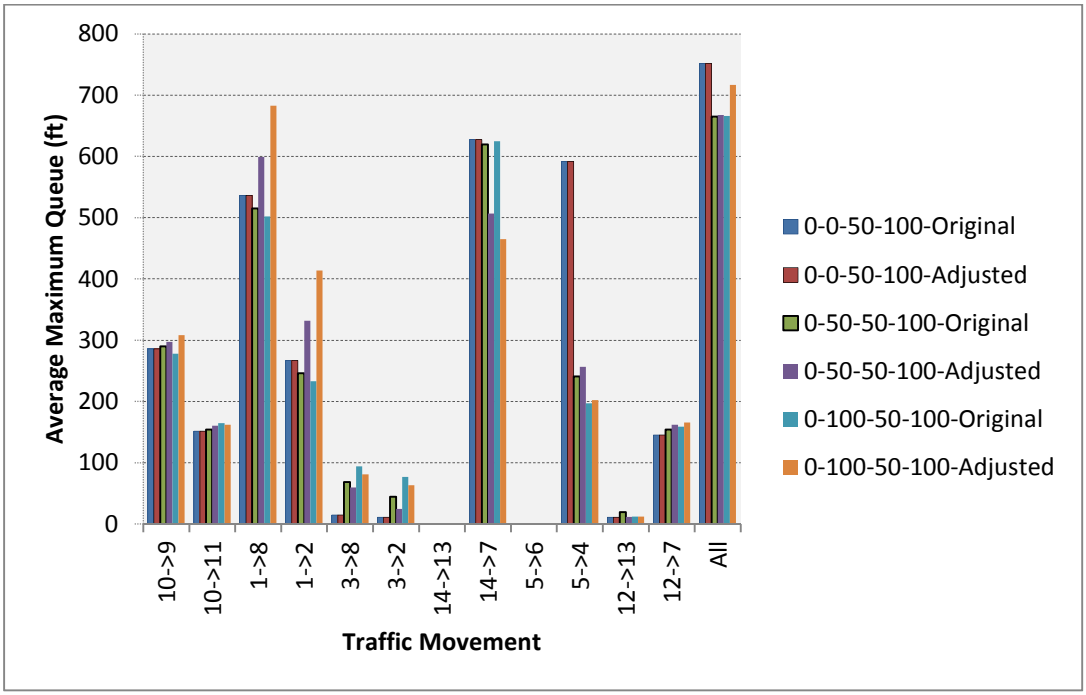

Figure C-20 Average Maximum Queue of Fully Actuated Control

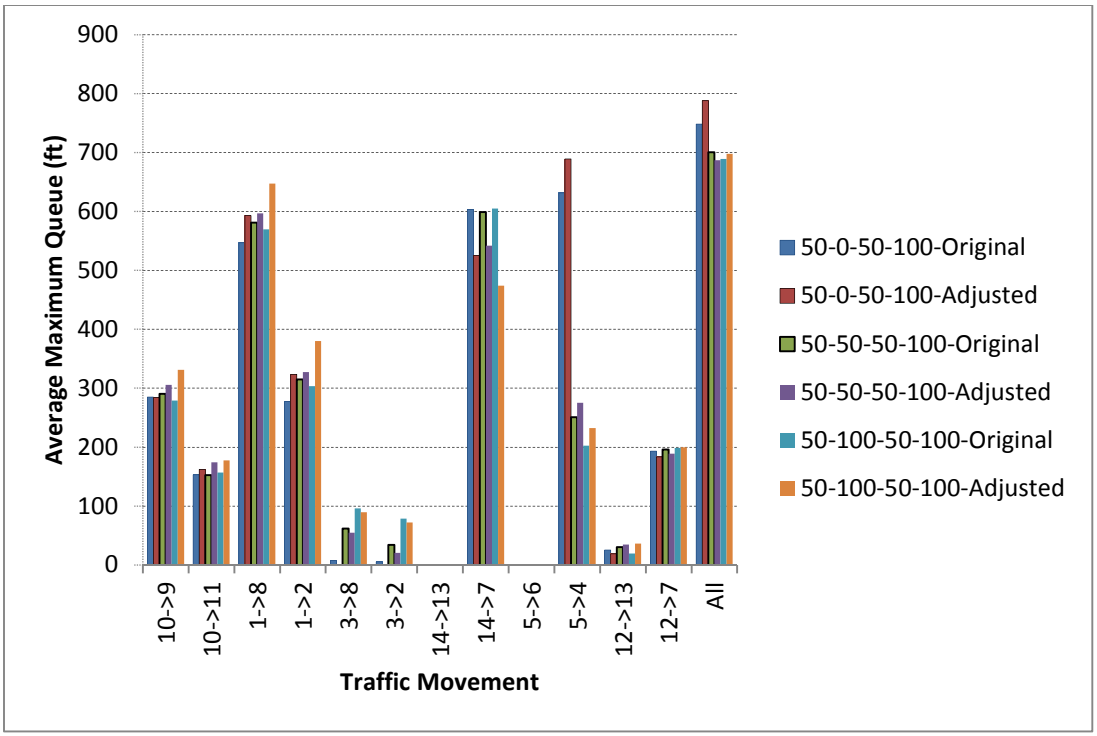

Figure C-21 Average Maximum Queue of Pre-Timed Control

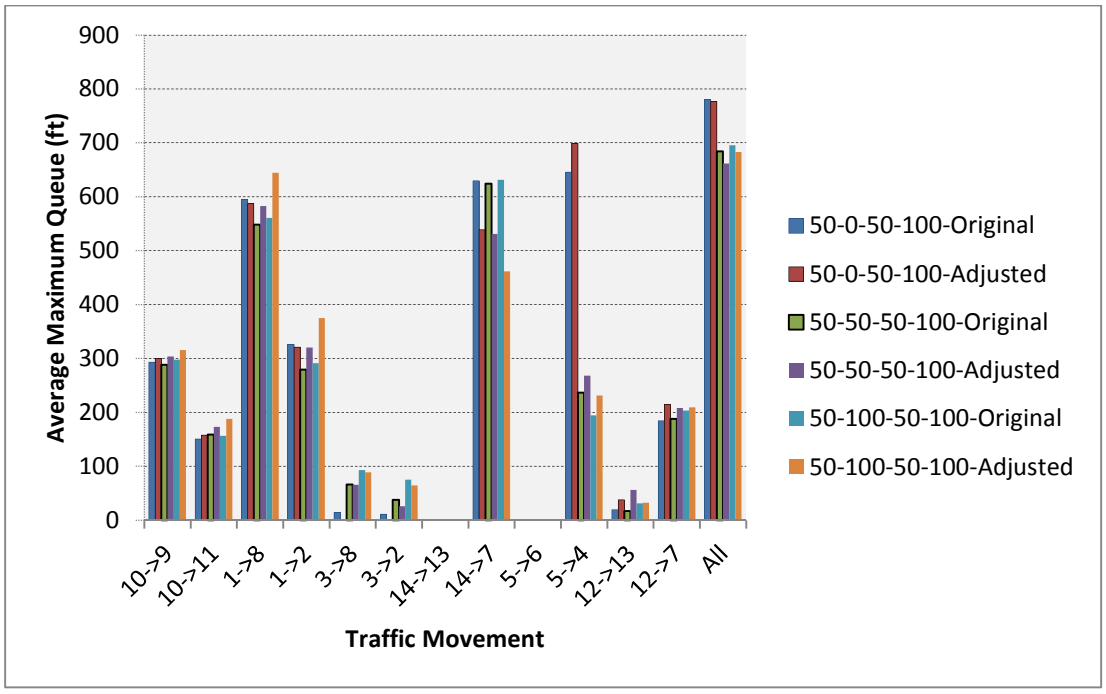

Figure C-22 Average Maximum Queue of Fully Actuated Control

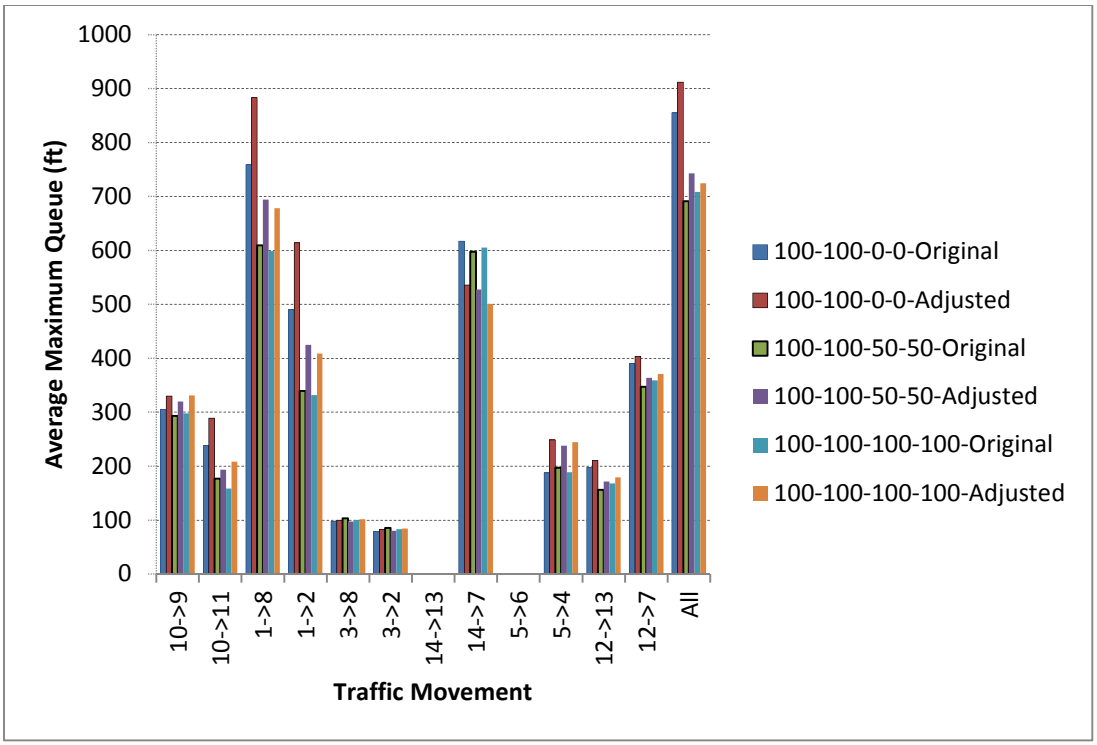

Figure C-23 Average Maximum Queue of Pre-Timed Control

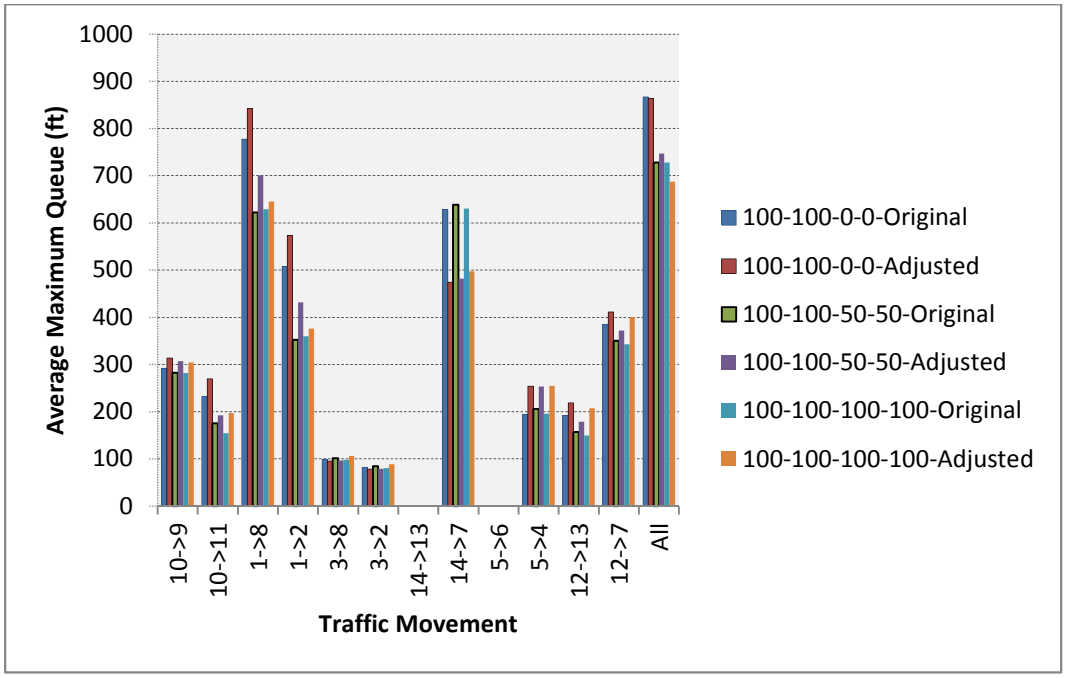

Figure C-24 Average Maximum Queue of Fully Actuated Control

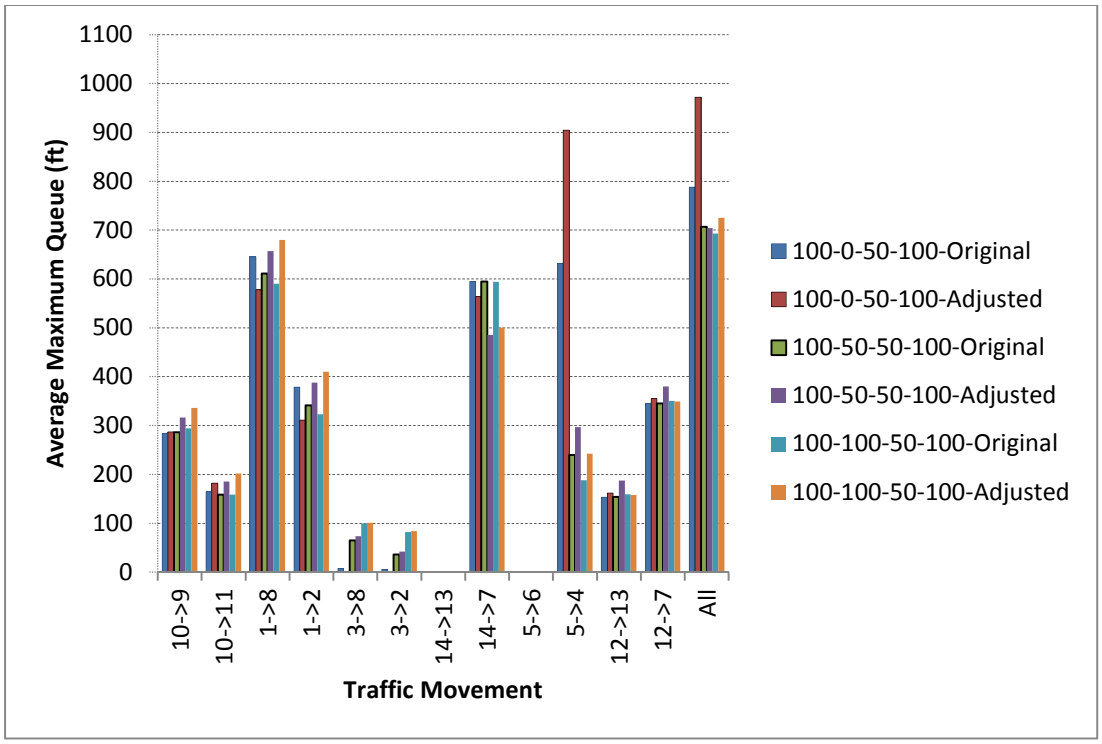

Figure C-25 Average Maximum Queue of Pre-Timed Control

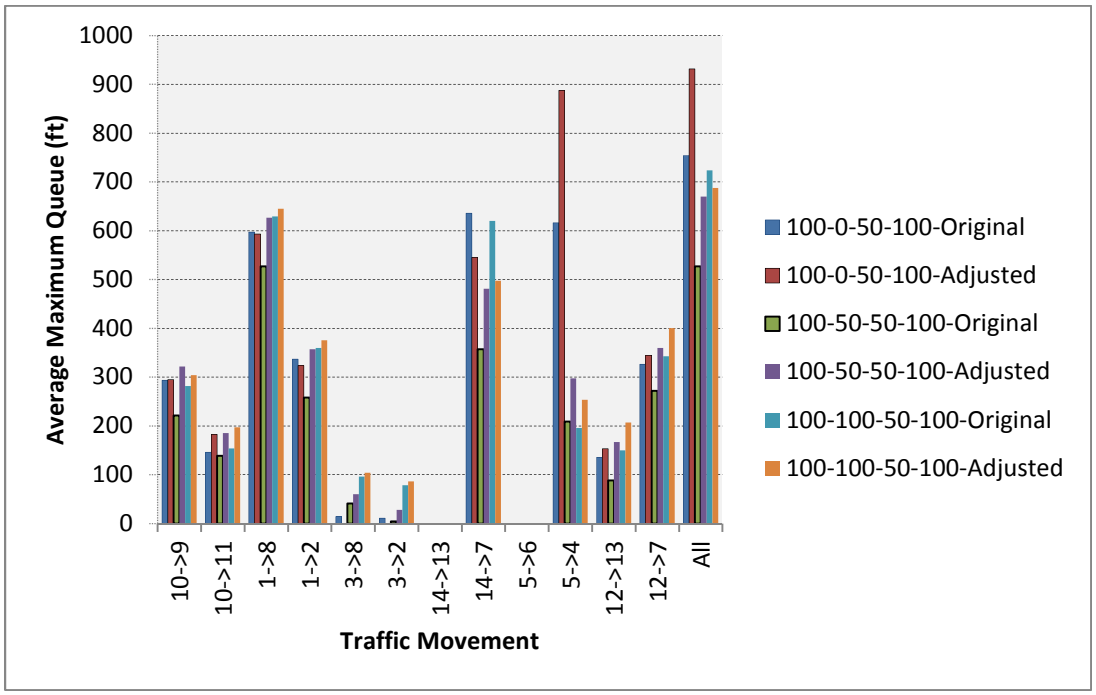

Figure C-26 Average Maximum Queue of Fully Actuated Control

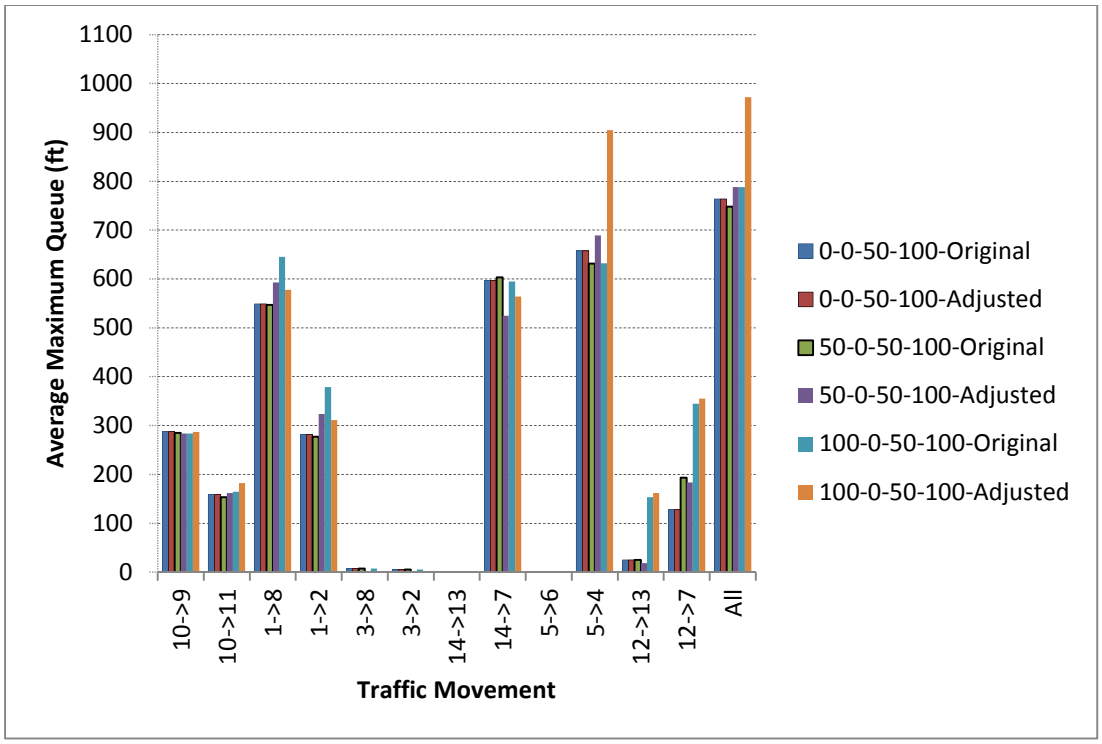

Figure C-27 Average Maximum Queue of Pre-Timed Control

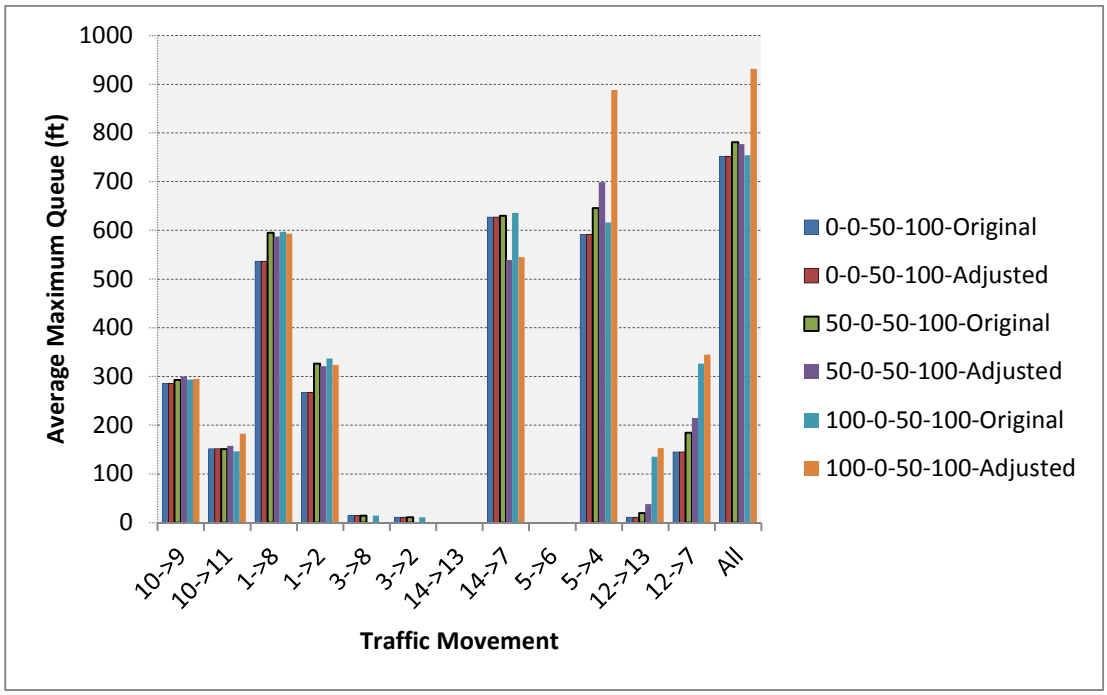

Figure C-28 Average Maximum Queue of Fully Actuated Control

Figure C-29 Average Maximum Queue of Pre-Timed Control

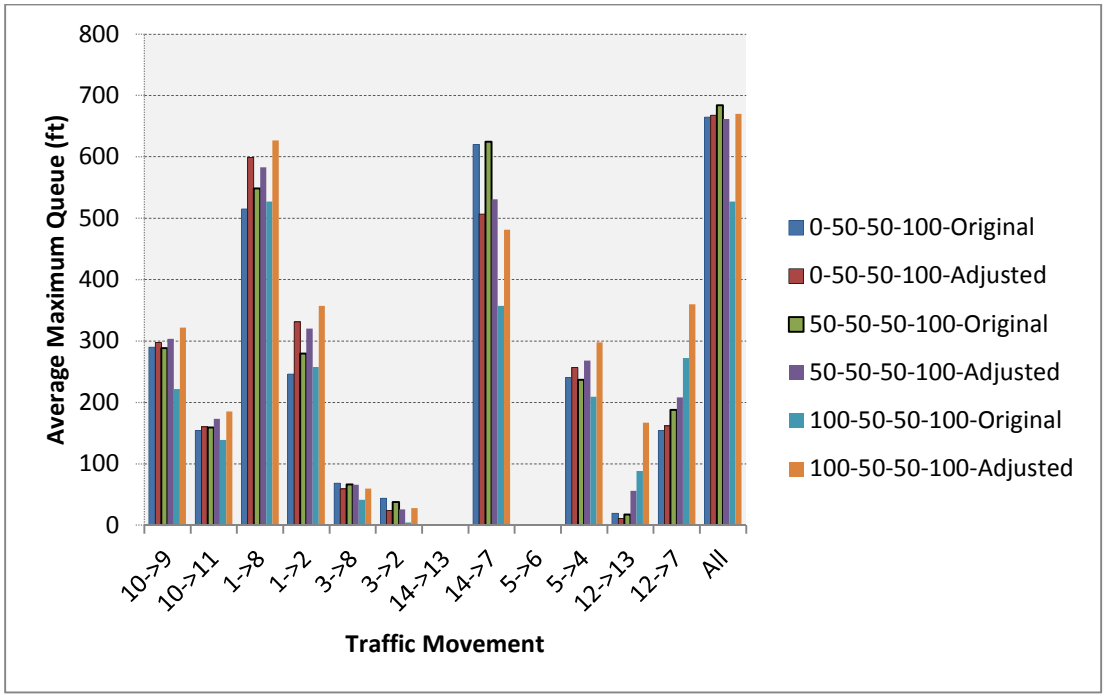

Figure C-30 Average Maximum Queue of Fully Actuated Control

Figure C-31 Average Maximum Queue of Pre-Timed Control

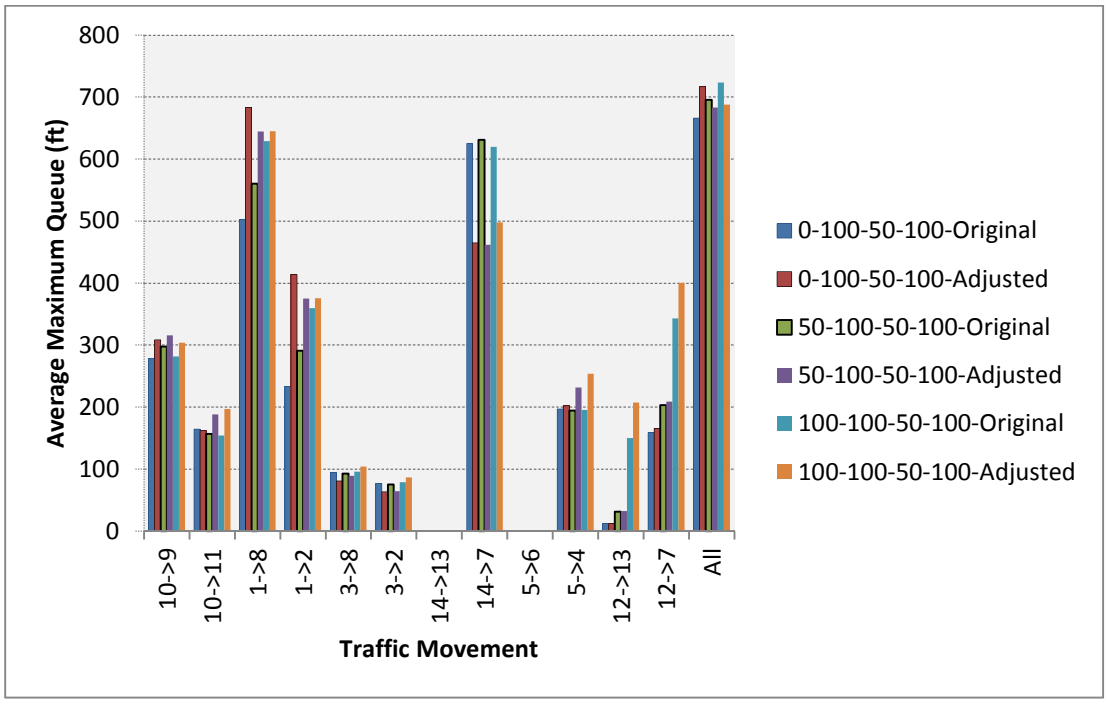

Figure C-32 Average Maximum Queue of Fully Actuated Control

3. Average Delay When Travel Time between the Two Crossovers is 22 Sec

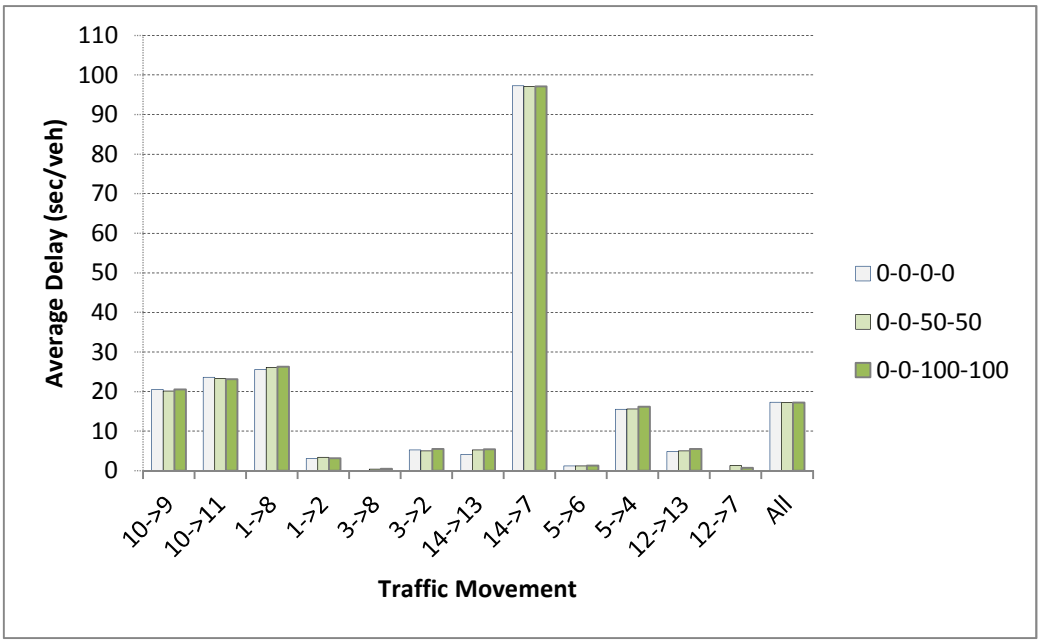

Figure C-33 Average Delay of Pre-Timed Control

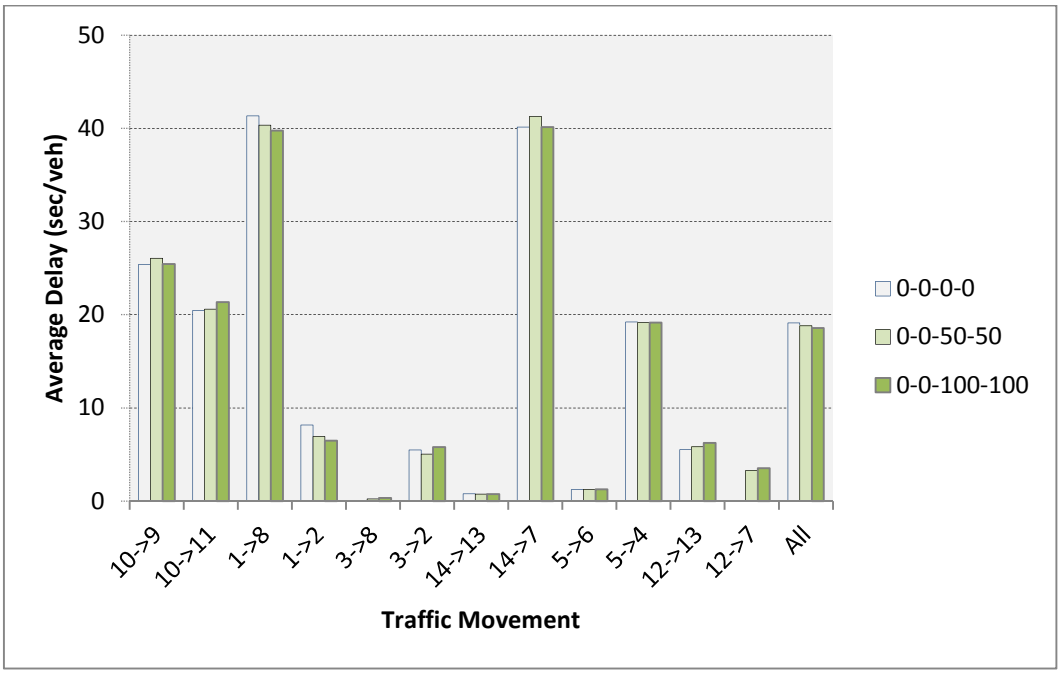

Figure C-34 Average Delay of Fully Actuated Control

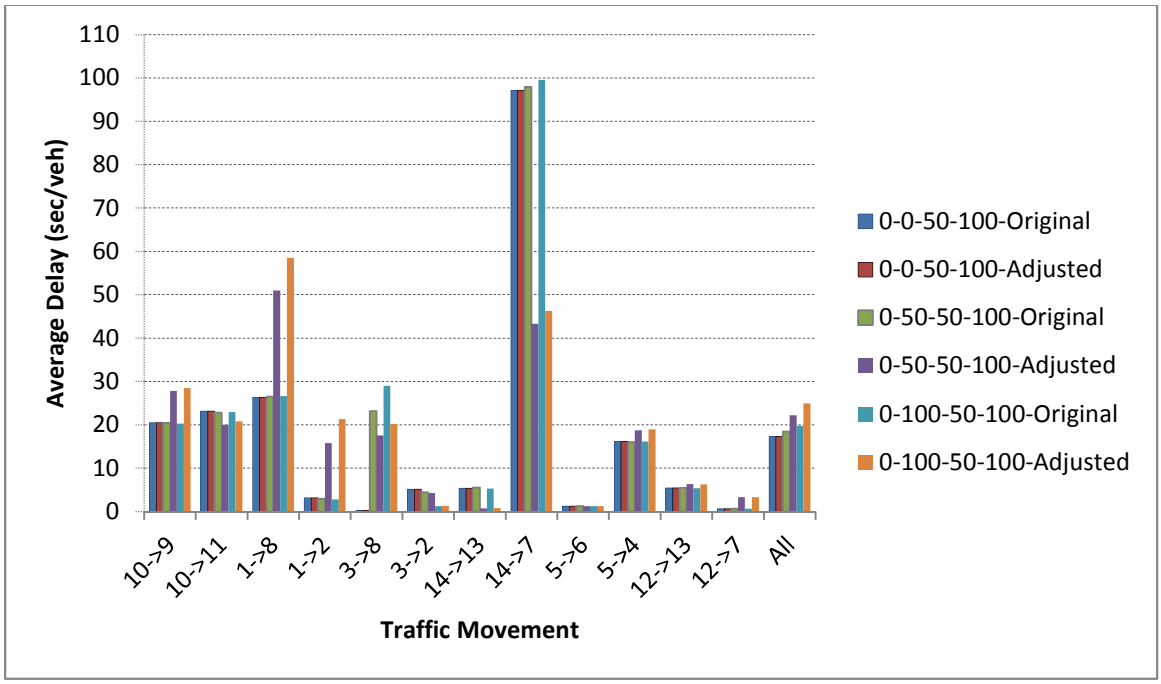

Figure C-35 Average Delay of Pre-Timed Control

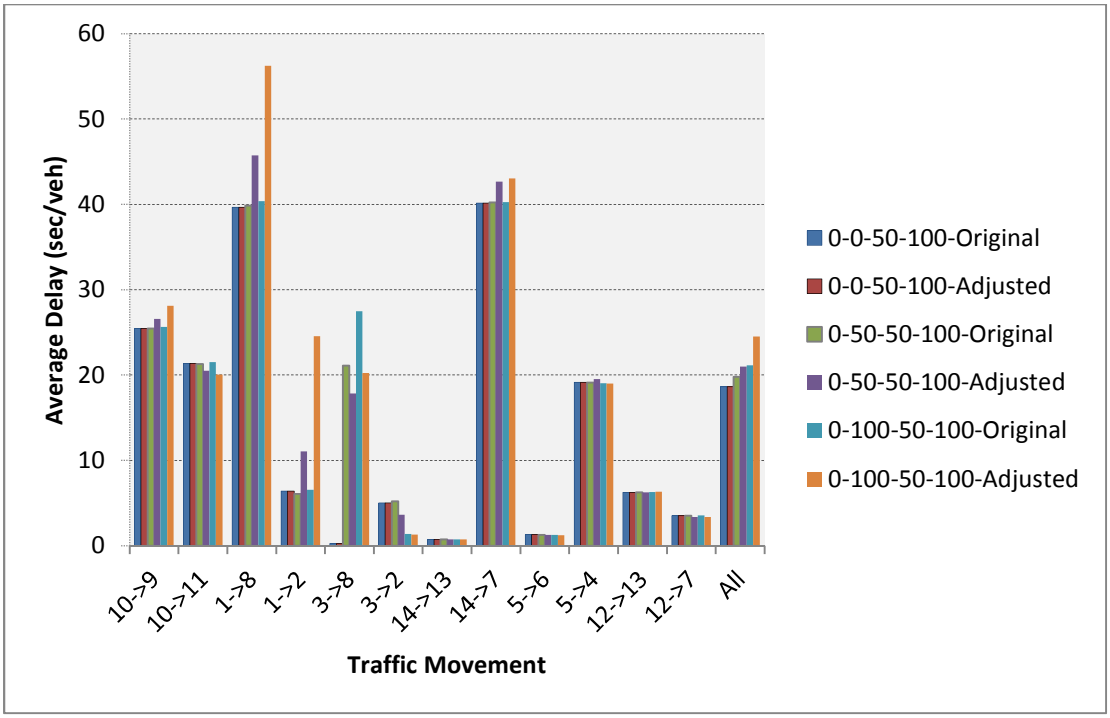

Figure C-36 Average Delay of Fully Actuated Control

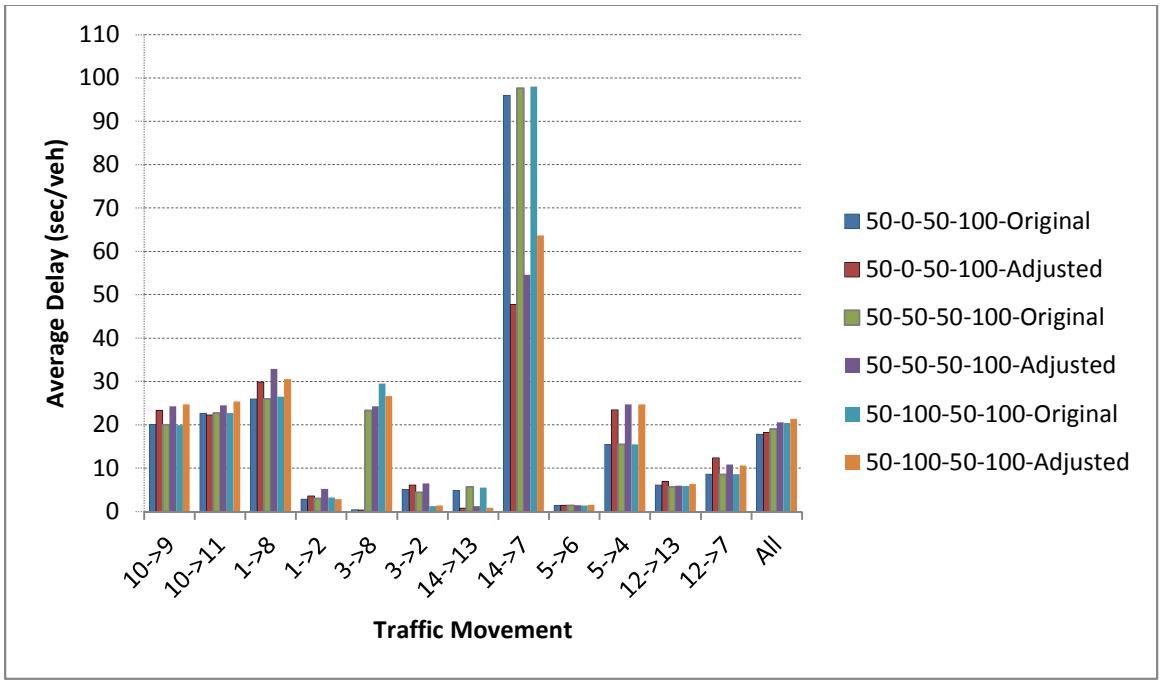

Figure C-37 Average Delay of Pre-Timed Control

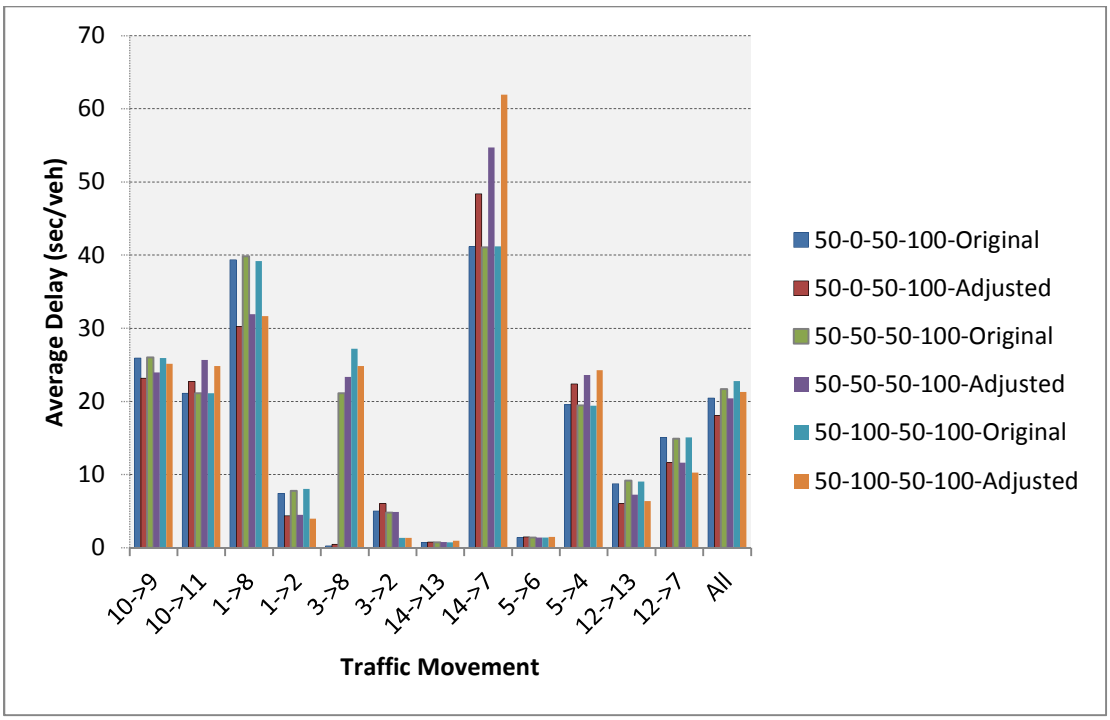

Figure C-38 Average Delay of Fully Actuated Control

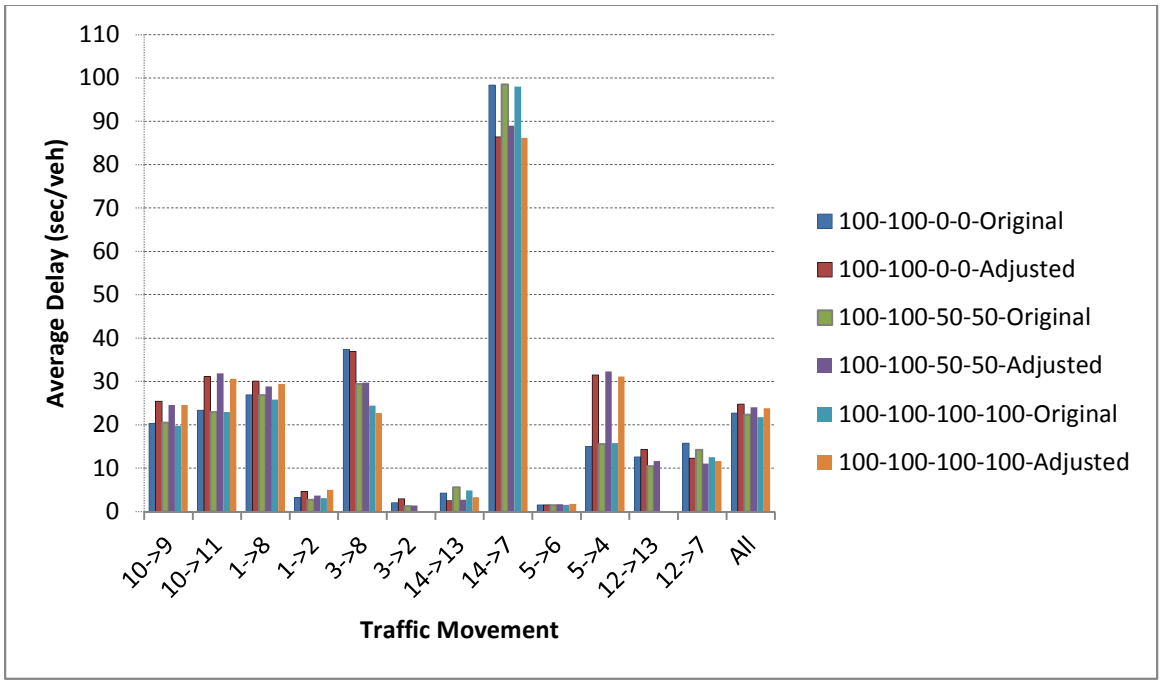

Figure C-39 Average Delay of Pre-Timed Control

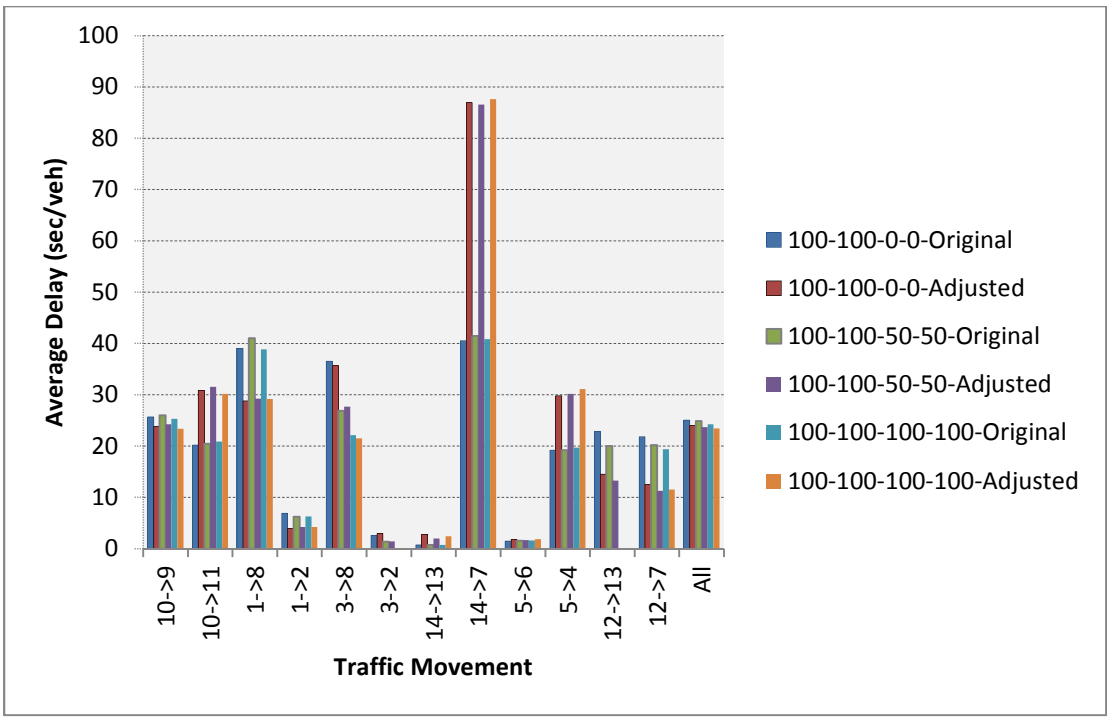

Figure C-40 Average Delay of Fully Actuated Control

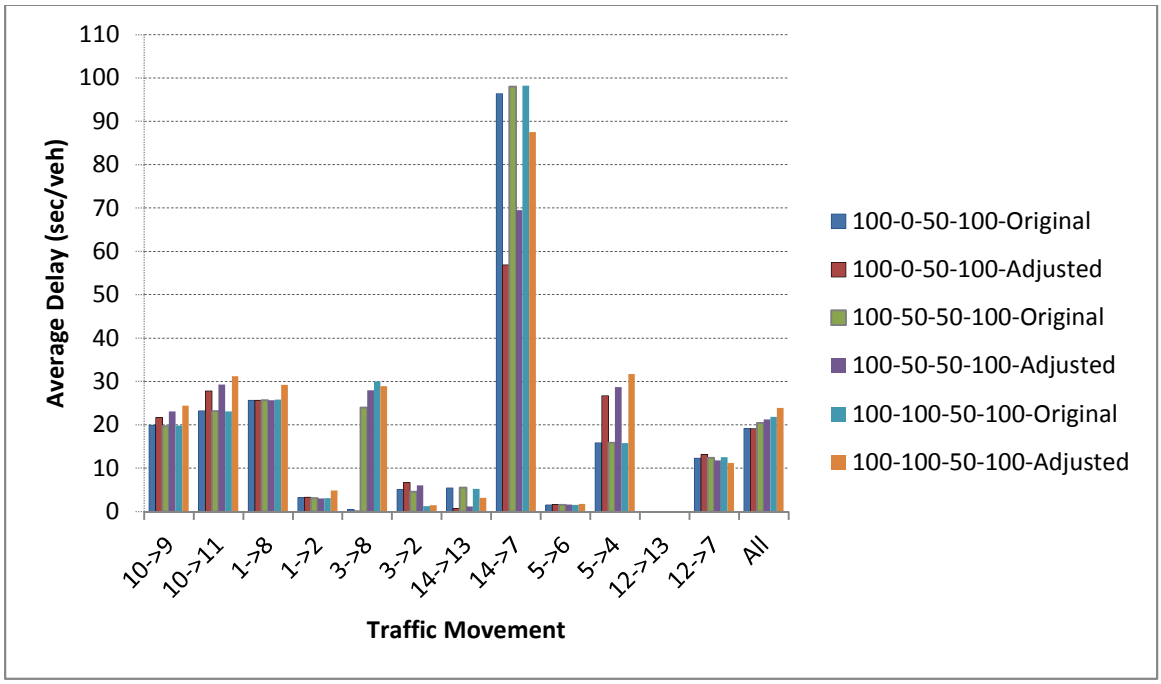

Figure C-41 Average Delay of Pre-Timed Control

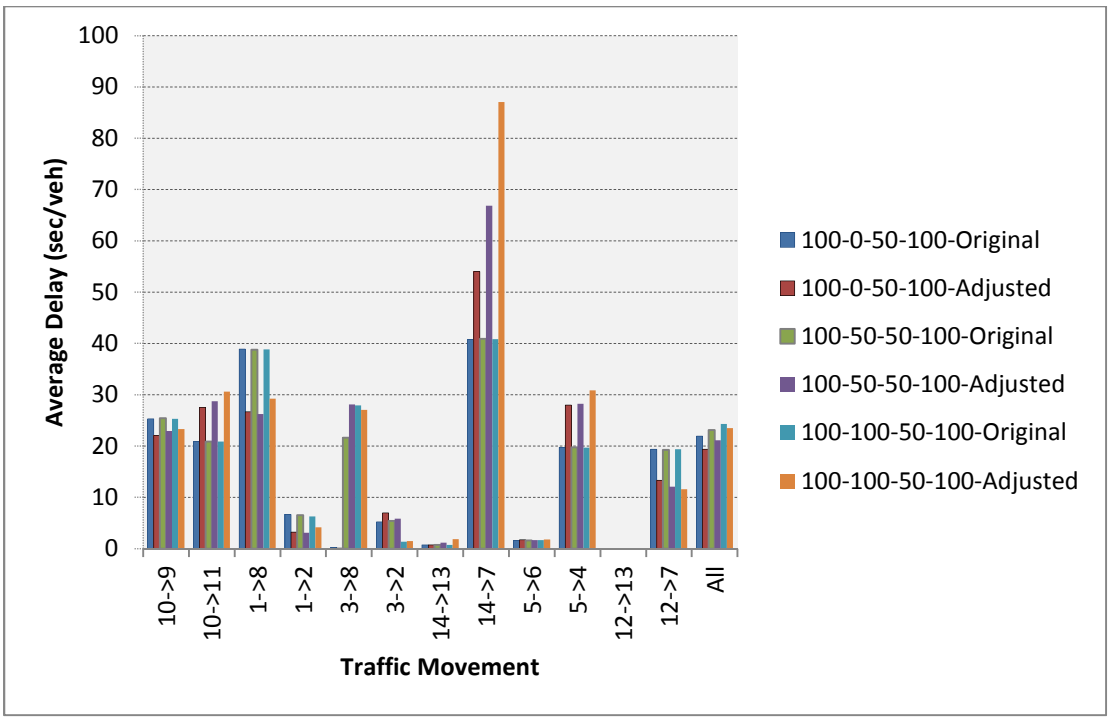

Figure C-42 Average Delay of Fully Actuated Control

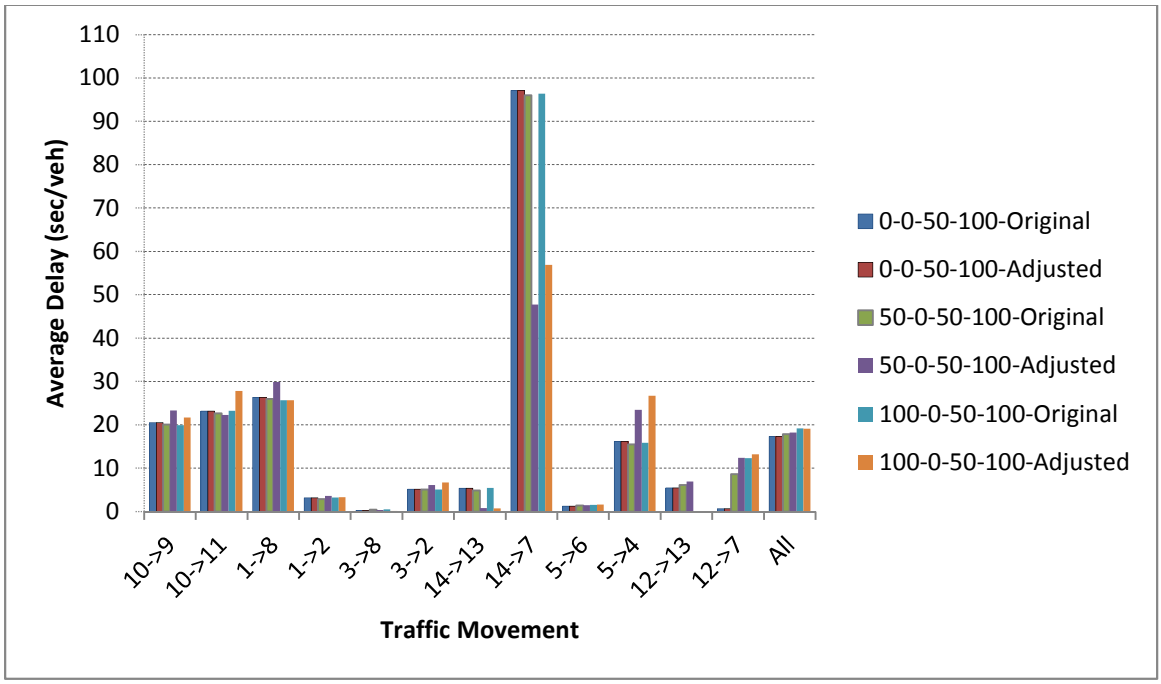

Figure C-43 Average Delay of Pre-Timed Control

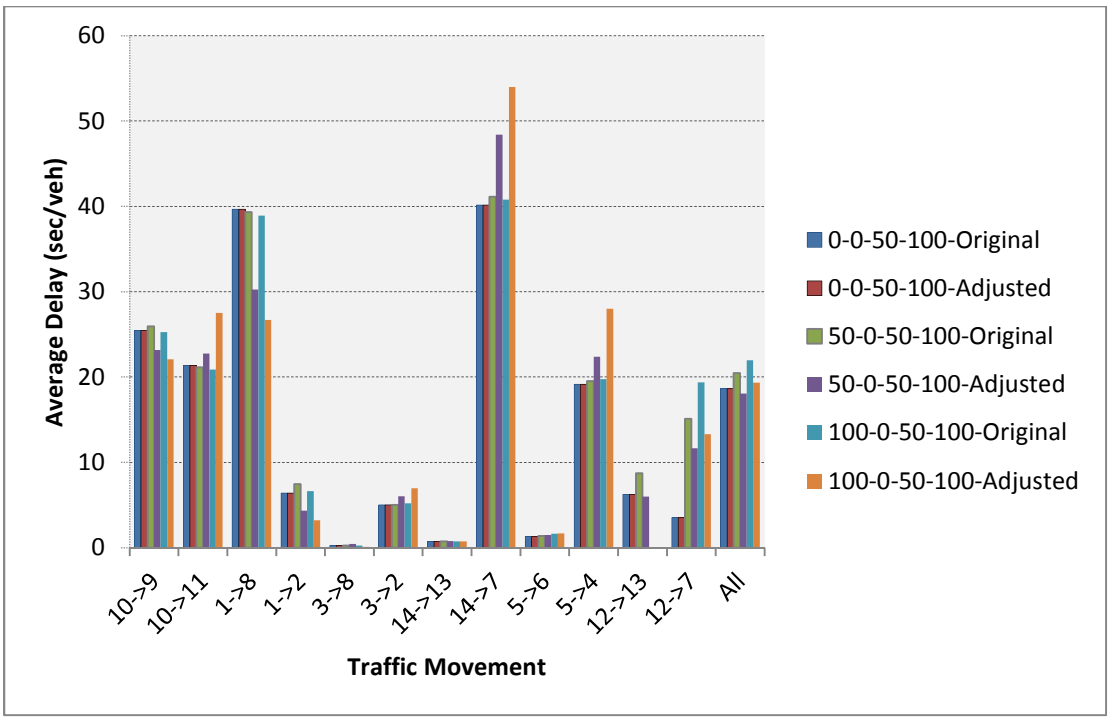

Figure C-44 Average Delay of Fully Actuated Control

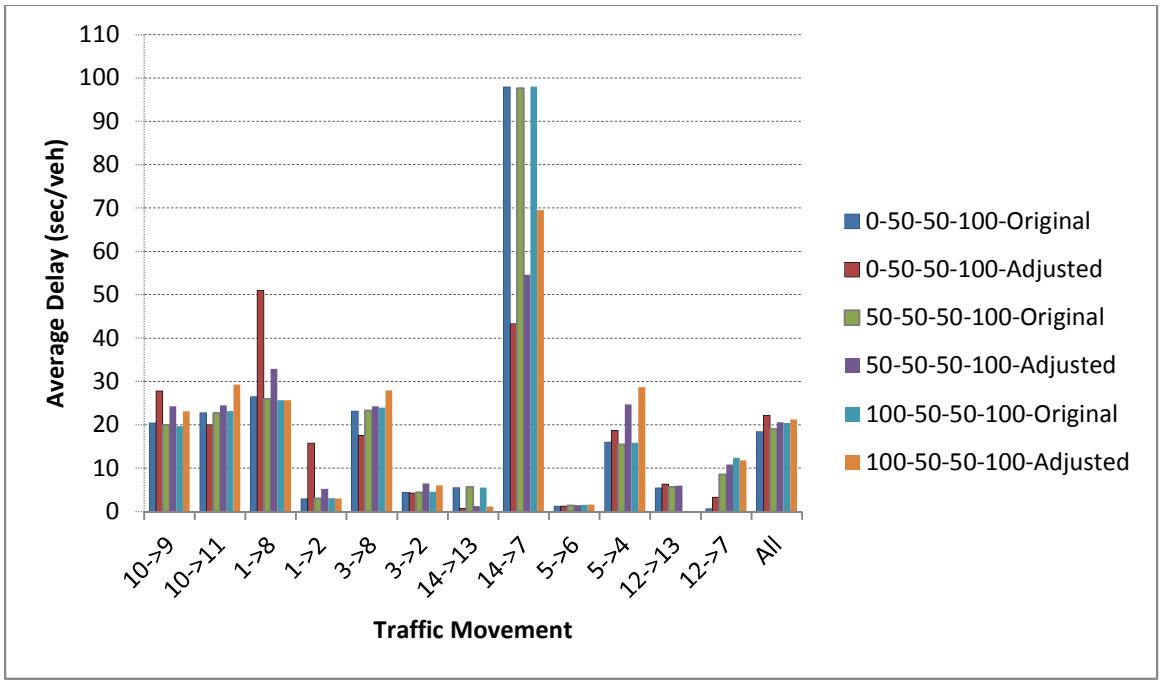

Figure C-45 Average Delay of Pre-Timed Control

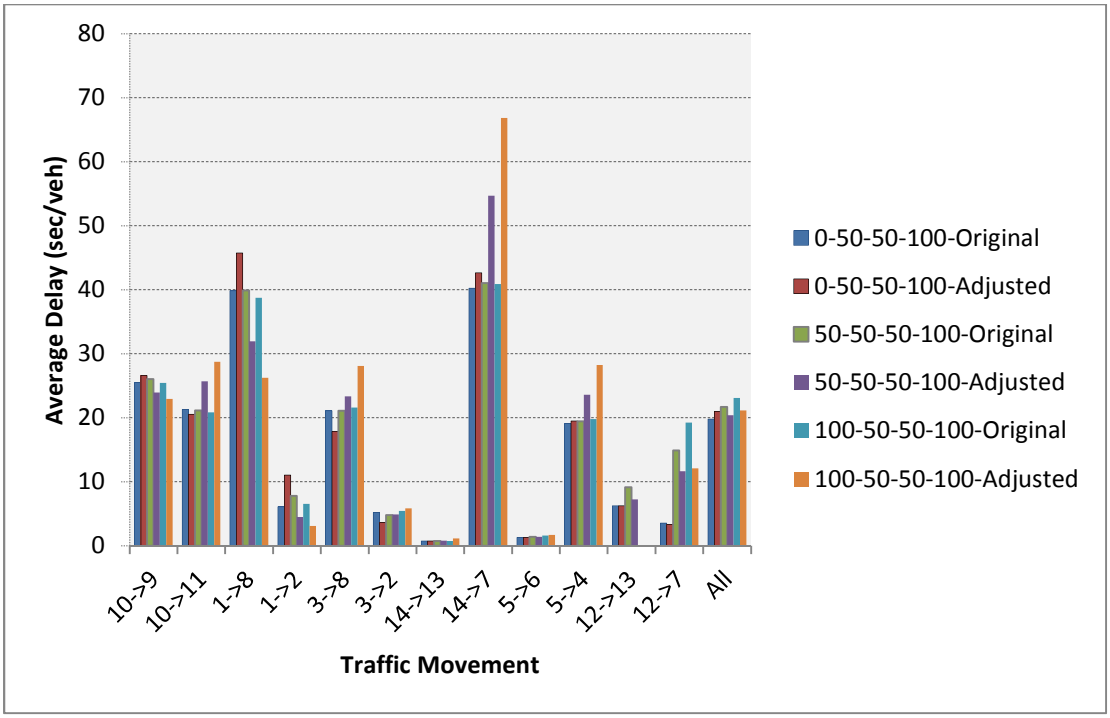

Figure C-46 Average Delay of Fully Actuated Control

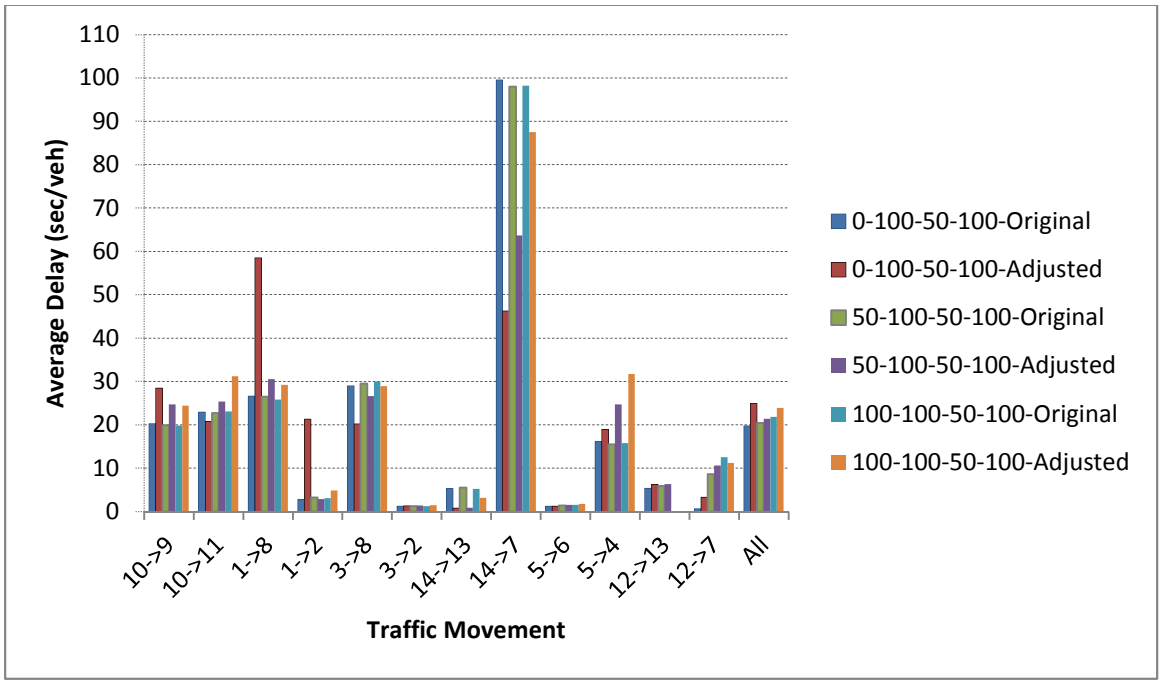

Figure C-47 Average Delay of Pre-Timed Control

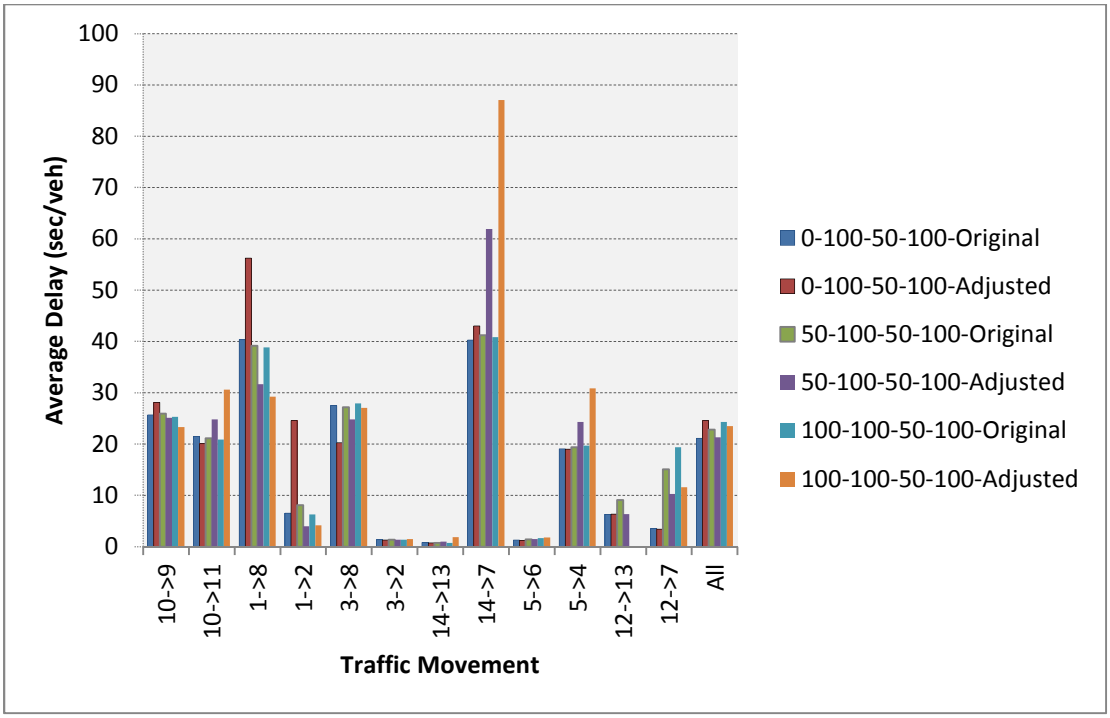

Figure C-48 Average Delay of Fully Actuated Control

4. Average Maximum Queue When Travel Time between the Two Crossovers is 22 Sec

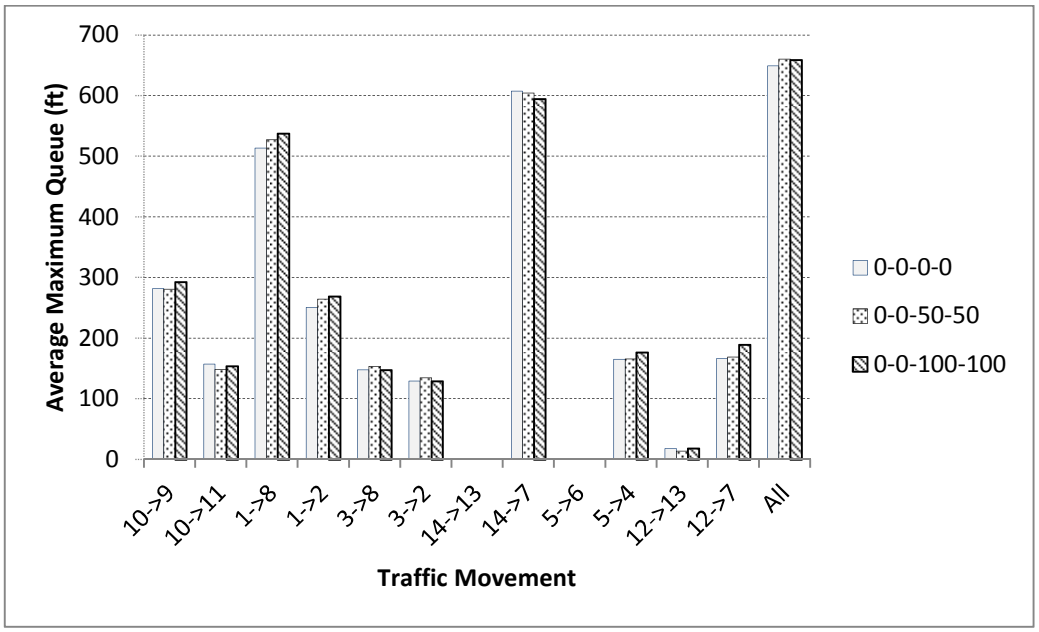

Figure C-49 Average Maximum Queue of Pre-Timed Control

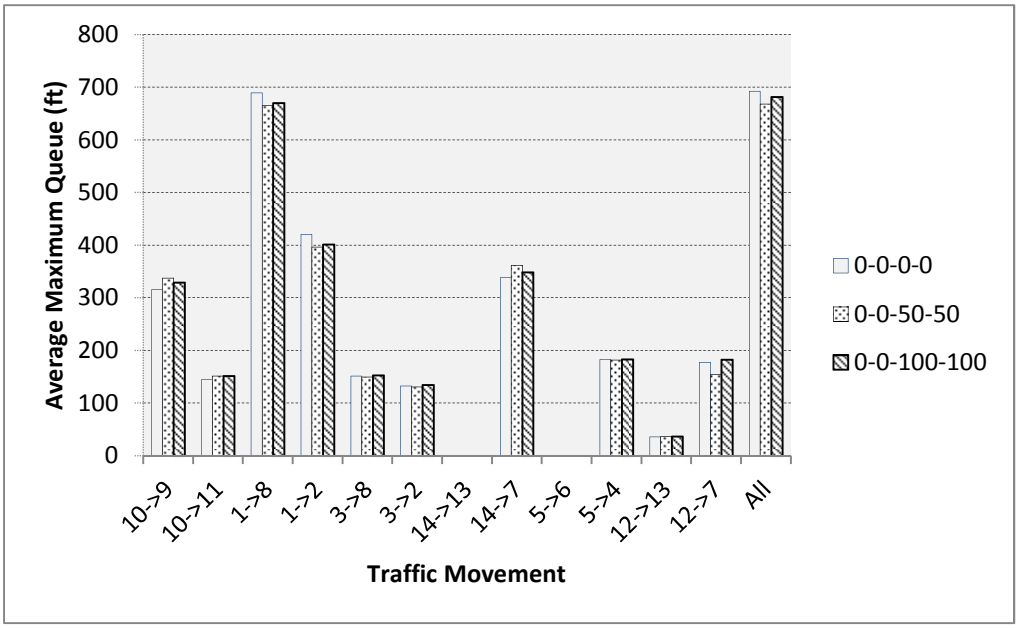

Figure C-50 Average Maximum Queue of Fully Actuated Control

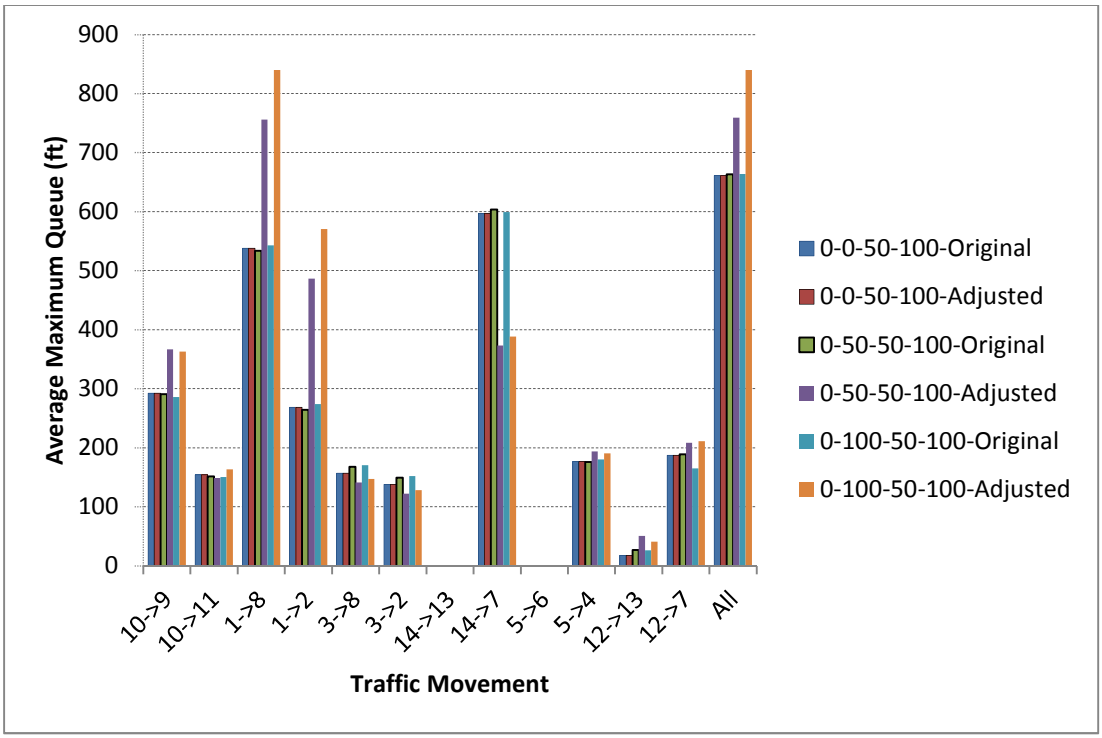

Figure C-51 Average Maximum Queue of Pre-Timed Control

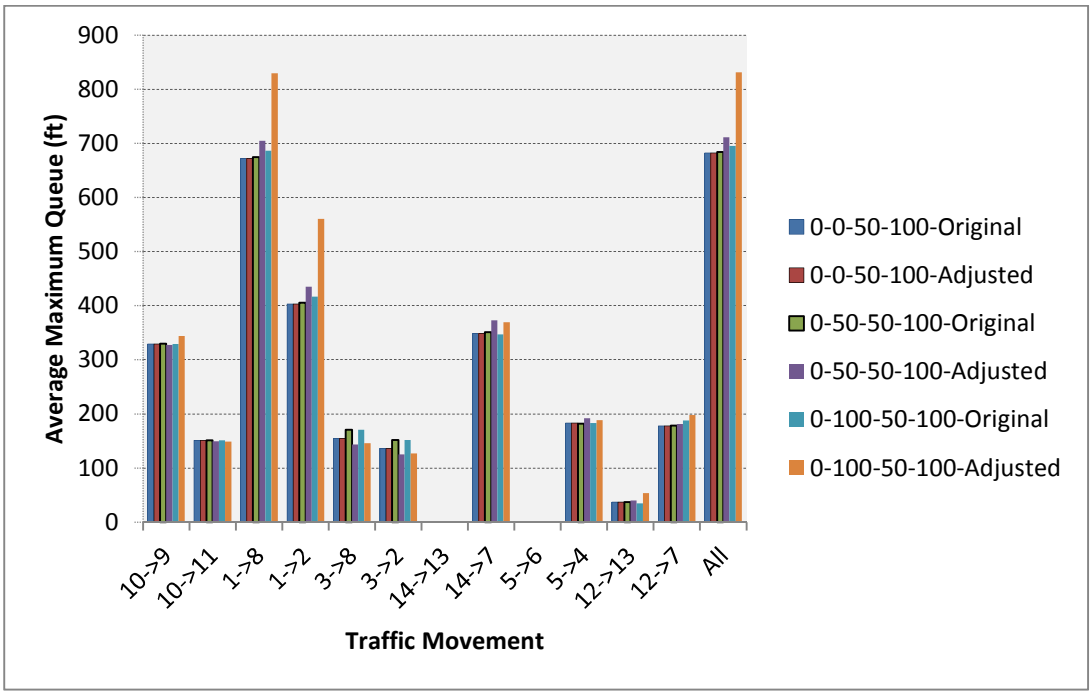

Figure C-52 Average Maximum Queue of Fully Actuated Control

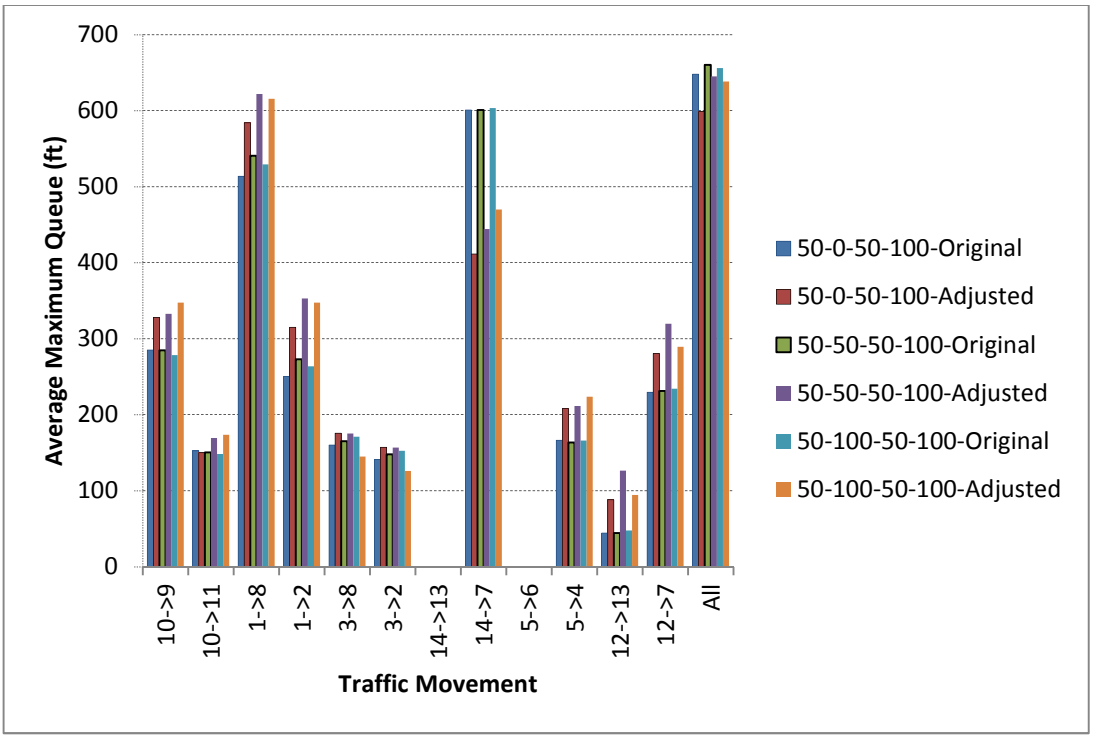

Figure C-53 Average Maximum Queue of Pre-Timed Control

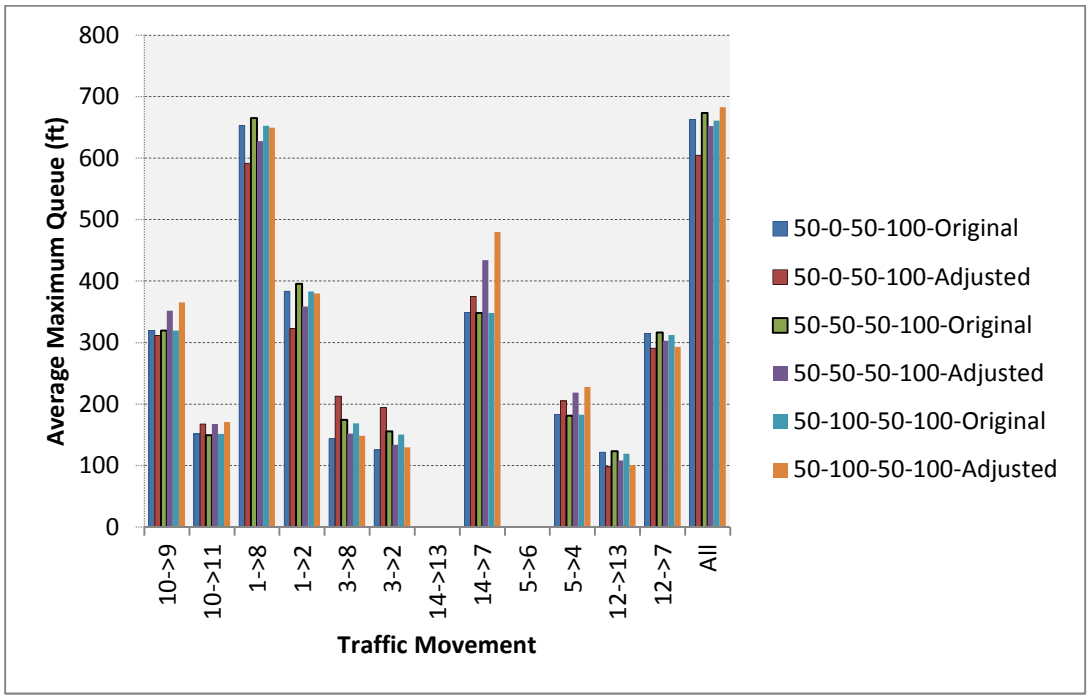

Figure C-54 Average Maximum Queue of Fully Actuated Control

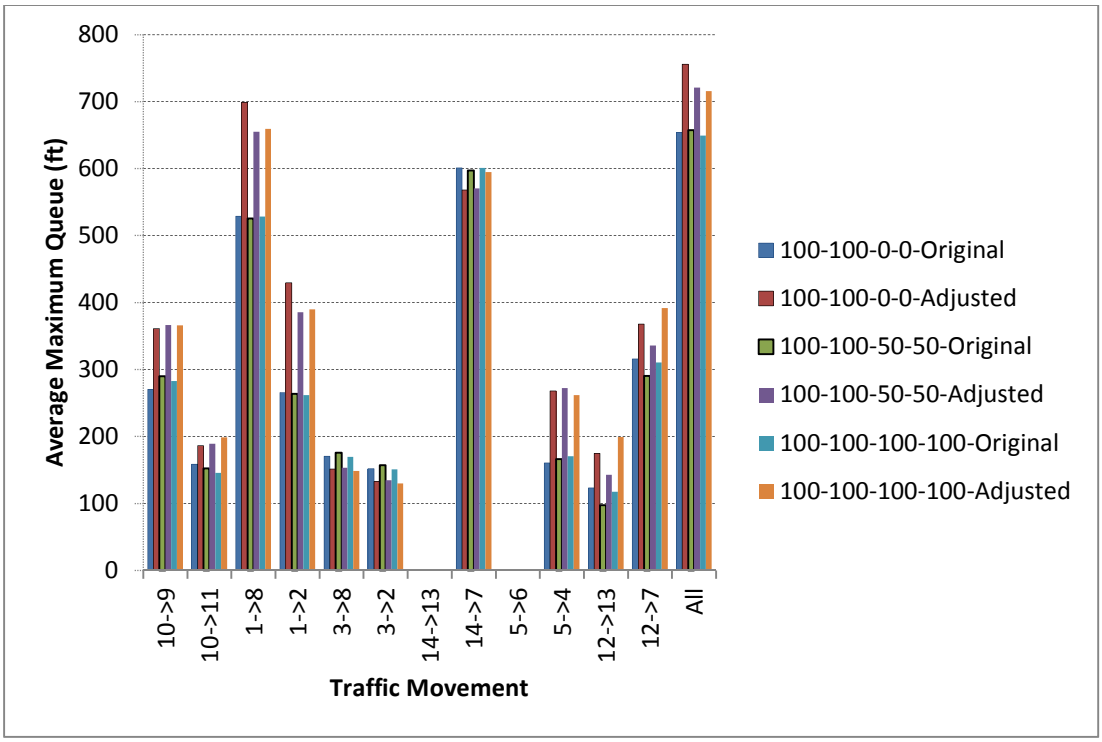

Figure C-55 Average Maximum Queue of Pre-Timed Control

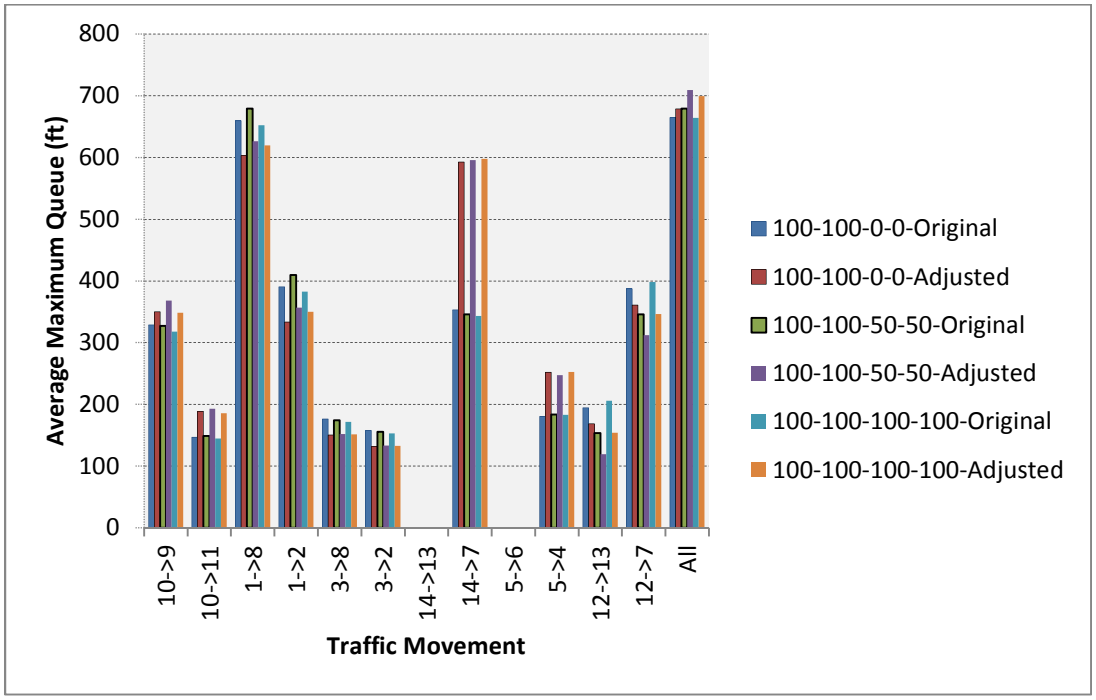

Figure C-56 Average Maximum Queue of Fully Actuated Control

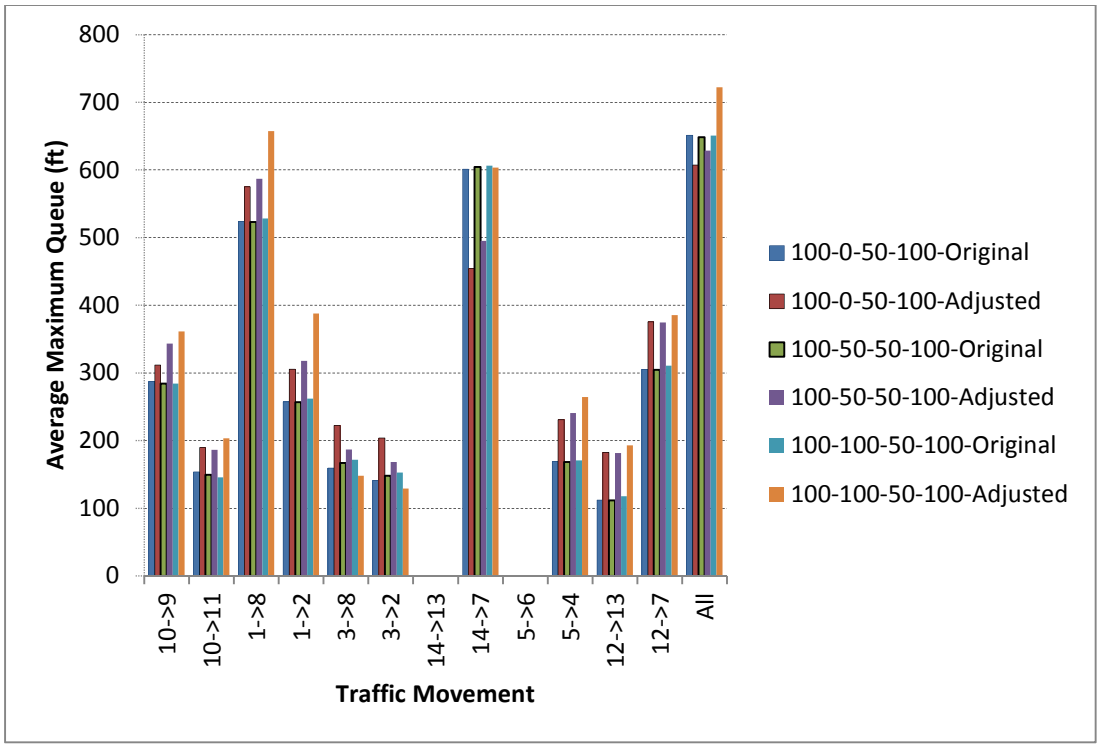

Figure C-57 Average Maximum Queue of Pre-Timed Control

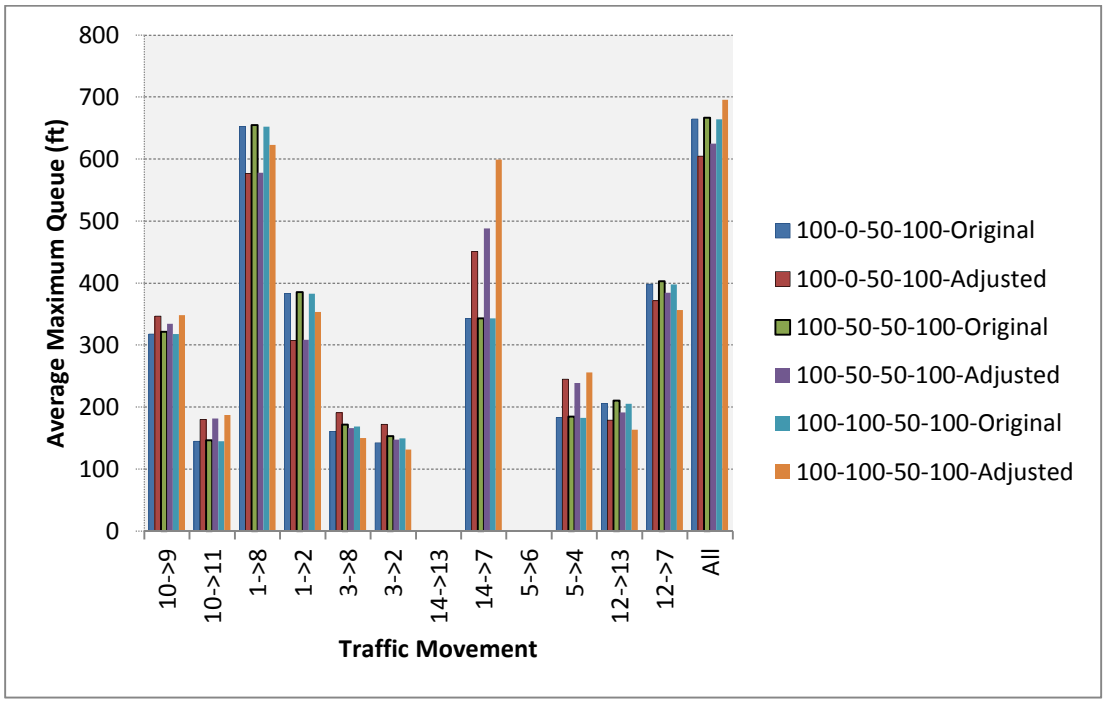

Figure C-58 Average Maximum Queue of Fully Actuated Control

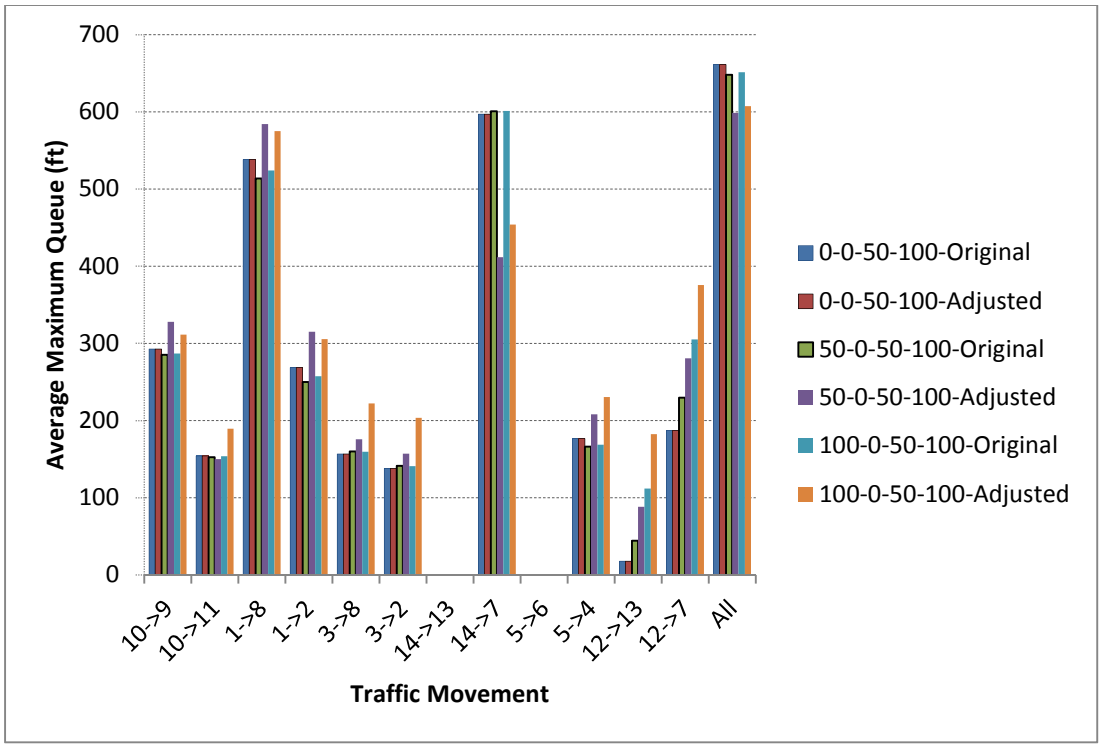

Figure C-59 Average Maximum Queue of Pre-Timed Control

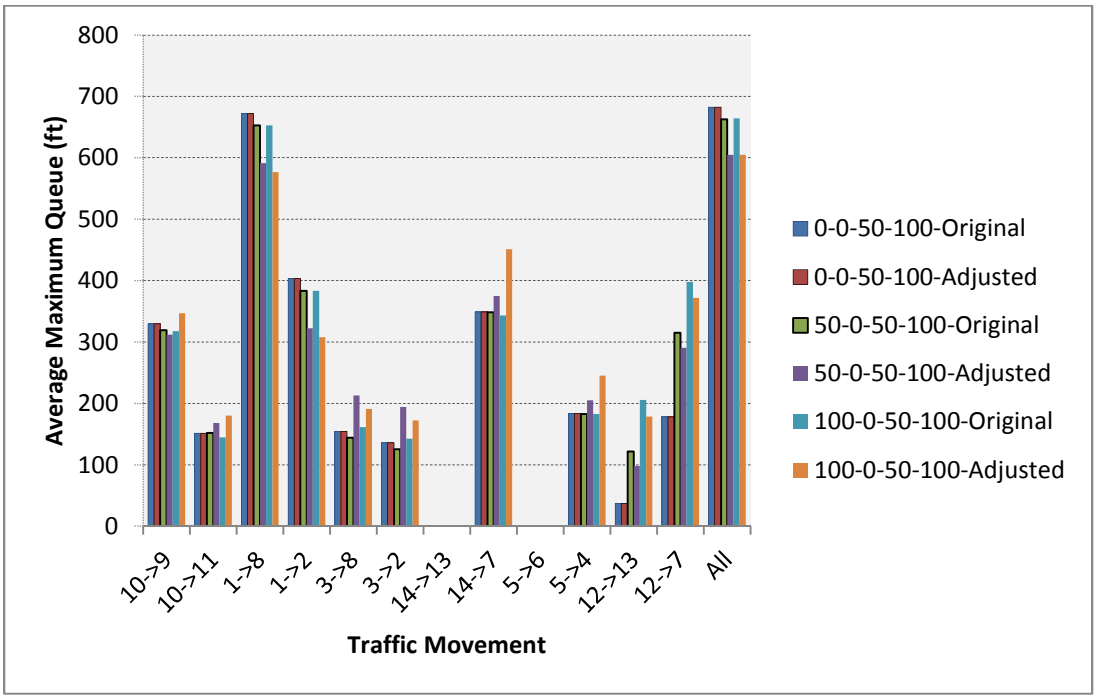

Figure C-60 Average Maximum Queue of Fully Actuated Control

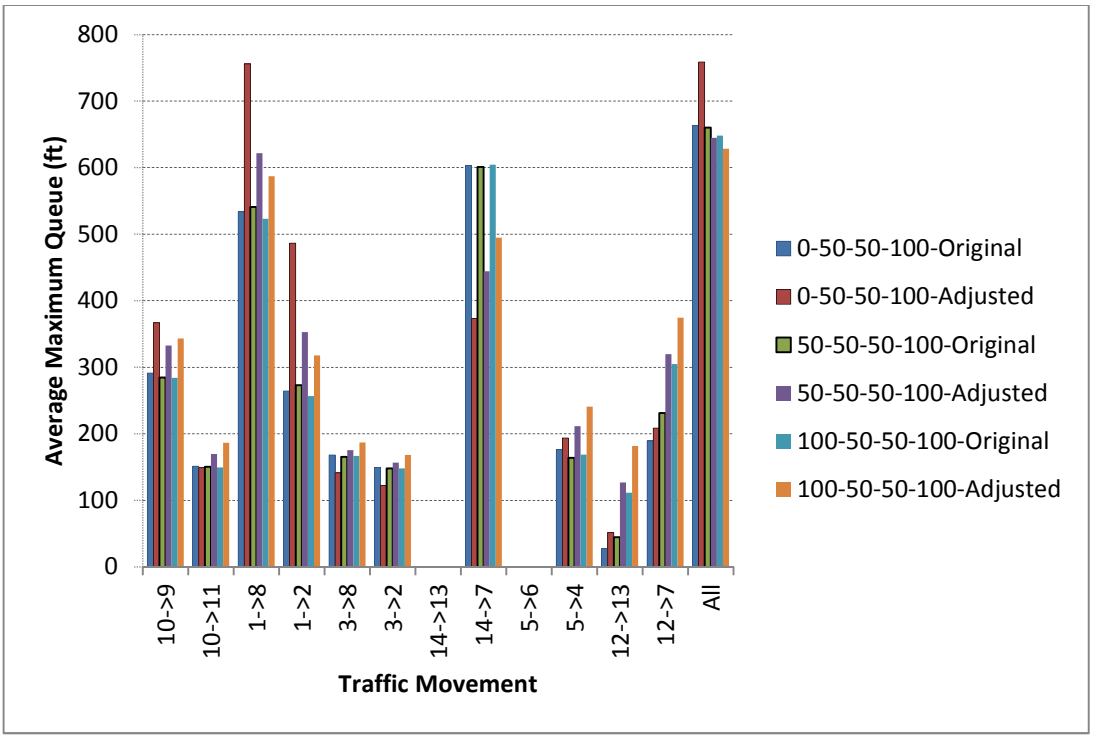

Figure C-61 Average Maximum Queue of Pre-Timed Control

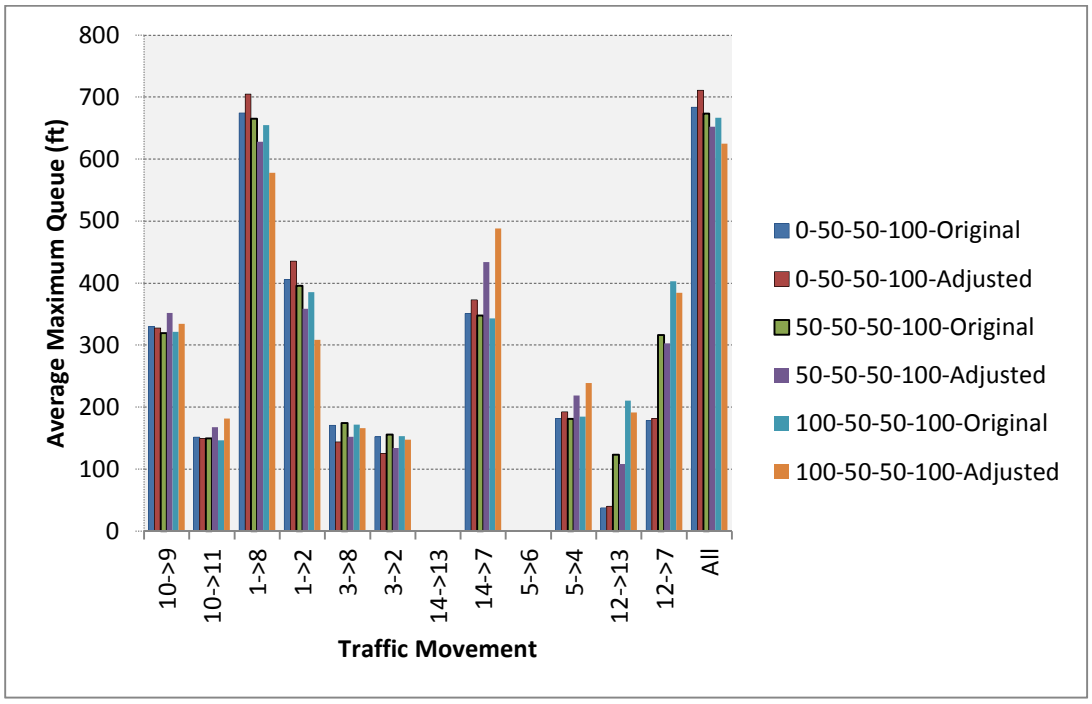

Figure C-62 Average Maximum Queue of Fully Actuated Control

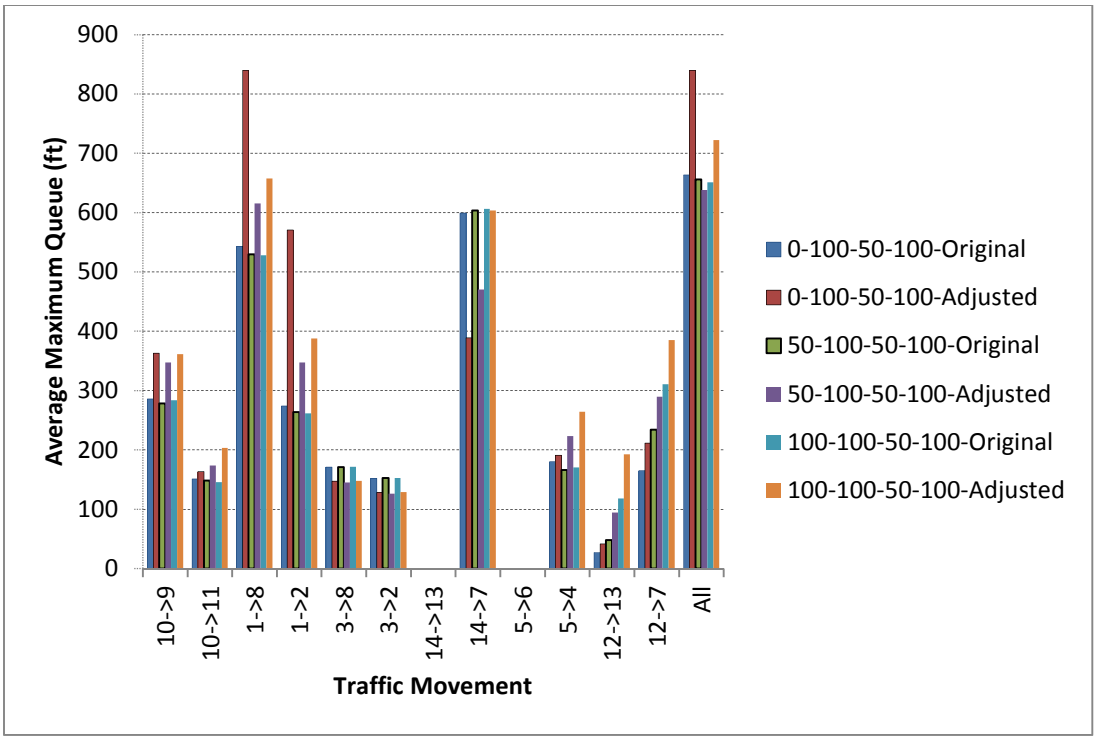

Figure C-63 Average Maximum Queue of Pre-Timed Control

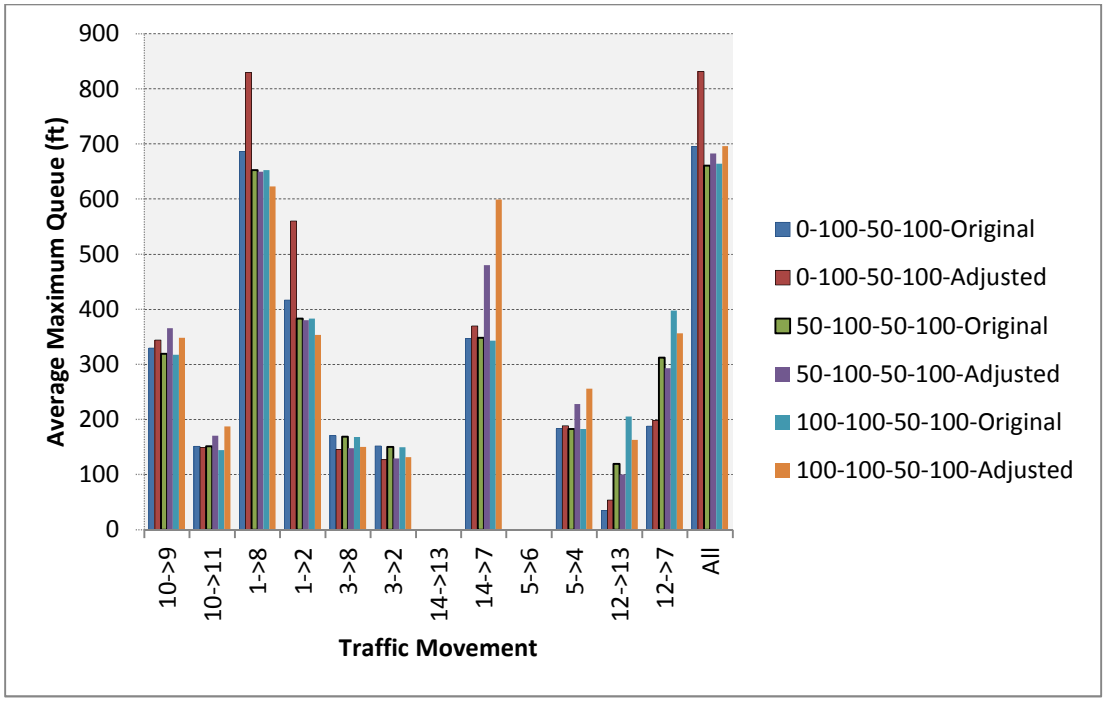

Figure C-64 Average Maximum Queue of Fully Actuated Control

VITA

Name: Peifeng Hu

Address: University of Nevada, Reno, MS 258

Reno, NV 89557

Email Address: hupeifeng1981@gmail.com

Education: Ph.D., Civil Engineering, University of Nevada, Reno, NV, U.S., 2013

M.B.A., Business Administration, University of Nevada, Reno, NV, U.S., 2013

M.S., Transportation Planning and Management, Beijing Jiaotong University, Beijing, China, 2007

B.S., Mathematics, Inner Mongolia University, Hohhot, China, 2004